Departament de Geografia
Universitat Autònoma de Barcelona

Efectes de la compressió amb pèrdua en les imatges de teledetecció i la cartografia resultant

Lossy compression effects on remote sensing images and resulting cartography

Tesi Doctoral
Doctorat en Geografia

Facultat de Filosofia i Lletres
Universitat Autònoma de Barcelona

Doctoranda: Alaitz Zabala Torres
Director: Dr. Xavier Pons
Octubre de 2010

A mamá y a aita.

I a tots els *tallarines*
que m'endolceixen el camí.

AGRAÏMENTS / ACKNOWLEDGEMENTS

Una Tesi Doctoral és una camí llarg i costerut, però, per sort, també molt interessant i divertit.

Camines de la mà d'altres camins (o projectes) en alguns trams i en d'altres la solitud (o la sensació de caminar a poc a poc... que et sembla que recules i tot!) omple les hores o els dies. Crec que tinc sort d'haver tingut poques estones de solitud. Gràcies a tots els que m'heu ajudat a evitar-ho. És molt difícil no deixar-se ningú de tots el que m'heu acompanyat i ajudat, ni que sigui a fer algunes passes petites... però faré l'esforç. I les meves disculpes d'entrada per si no ho aconsegueixo del tot.

En primer lloc gràcies a en Xavier, per estar al costat (a vegades més a prop, altres més lluny) i donar consells i ànims en tot aquest temps, especialment en els moments més durs (professionalment i personal).

Després, al grup de recerca. Sento GRUMETS com un grup treballador i entusiasta, que intenta portar el vaixell sempre a nous horitzons. Cadascú fa la seva feina (i sort!) i a vegades sembla que siguin tan diferents... però en el fons totes intenten mantenir el vaixell surant... i avançant. Molts de vosaltres m'heu ajudat en l'elaboració d'aquesta Tesi, permetent-me aprendre del vostre treball o col·laborant directament amb ell en la meva recerca: en Gerard per les classificacions de zones forestals (i l'ajuda amb l'anàlisi discriminant, l'R,...); en Pere pels conreus; en Jordi i en Miquel per les regressions de models climàtics; en José Àngel, la Charo, en Joan Pino i en Sirio per les fotointerpretacions. Jordi, Cristina C. i Paula, merci per aguantar-me al despatx; i Cristina D., Òscar, Víctor i Anna per aguantar-me dinant! :). Gràcies Joan i Lluís per deixar-me el despatx quan vinc al CREAF ;), i Núria per les estones compartides. Gràcies a tots.

No puc deixar d'agrair la col·laboració i ajuda de tots els companys de grup GICI (*Group on Interactive Coding of Images*), del Departament d'Enginyeria de la Informació i de les Comunicacions (dEIC) de la UAB. A tots ells gràcies per les hores dedicades a ajudar-me en els aspectes més de fons de la compressió i les seves implicacions, així com pel treball conjunt d'aquests anys. Especialment a en Joan Serra, en Francesc Aulí i en Jorge González, pel suport més continuat i per permetre'm utilitzar les publicacions conjuntes com a part d'aquesta Tesi.

Dels companys del Departament de Geografia de la UAB, voldria agrair a l'Antoni F. Tulla que, com a director del mateix, sempre intenta que tothom hi tingui cabuda i s'hi senti a gust. També voldria agrair especialment a tots aquells companys que, gràcies als canvis en la vostra docència, em vareu permetre concentrar la meva i, al curs passat, fer l'estada de recerca a l'Agència Europea de l'Espai.

Those six months at European Space Agency (ESTEC) were a great experience. I was able to learn a lot from my colleagues from the On-Board Payload Data Processing Section, Data Systems Division, Electrical Engineering Department (TEC-EDP) at ESA/ESTEC. The research I developed would had not been possible without the help of my supervisor Raffaele Vitulli and the whole SENTINEL-2 team. I would like to sincerely thank all of them for their time, help and the contributions they made to this research.

Des del punt de vista de finançament, la recerca ha estat parcialment finançada gràcies als projectes TSI2006-14005-C02, TIN2009-14426-C02-02 (Ministerio de Ciencia y Innovación i fons FEDER), SGR 2009-1511 (Agència de Gestió d'Ajuts Universitaris i de Recerca, Generalitat de Catalunya) i FP7-242390-GEO-PICTURES (FP7-SPACE-2009-1, Comissió Europea). A més, la beca de mobilitat de l'AGAUR (Comissionat per a Universitats i Recerca del Departament d'Innovació, Universitats i Empresa de la Generalitat de Catalunya, expedient 2009 BE2 00426) m'ha permès anar a l'Agència Europea de l'Espai (ESA) a Holanda a fer una estada de sis mesos, una part dels fruits de la qual contribueixen a aquesta Tesi.

Moreover, I would like to thank to all the members of the committee that will evaluate this research because I am sure that their considerations and suggestions will allow me to improve my future research. I feel the same gratitude for those who read this Thesis and make a report of it, to allow me to apply for the European Doctorate Mention. Thanks for your time and ideas.

I per acabar (però com sempre, no per això menys important), GRÀCIES als que m'acompanyen al camí gran, el de tots els dies, que inclou la Tesi, la feina, l'oci i els problemes. Especialment l'Arnau, per moltes coses.... per les muntanyes, els quilòmetres de bici, les castanyes i, sobretot, el "clavell blanc" i tot el que vindrà. Gracias por estar siempre aquí. Gràcies per compartir-ho amb mi... i per cantar:

"Yo teeeeeengooooo....."

ÍNDEX

RESUM / SUMMARY

1. RESUM (CATALÀ)

La teledetecció proporciona, probablement, la més enorme font de dades de la qual la humanitat disposa sobre el planeta. I aquesta generació de dades continua creixent a un ritme vertiginós, no només perquè els satèl·lits existents segueixen enviant imatges, sinó també perquè es llancen nous satèl·lits, en molts casos capaços de generar encara més informació. Com resulta fàcil intuir, aquest procés comporta enormes possibilitats d'aplicació, però també una important problemàtica de maneig de tota aquesta informació i una creixent necessitat de formats de compressió que permetin disminuir el volum de dades emmagatzemades sense disminuir significativament la qualitat de les imatges per a aplicacions posteriors.

A més a més, el nou paradigma de les Infraestructures de Dades Espacials (IDE), desenvolupat en els darrers anys, promou l'establiment de serveis de dades web, habitualment en termes dels estàndards definits per l'Open Geospatial Consortium. L'establiment d'aquests serveis requereix de l'ús d'estratègies de compressió (i sovint de transmissió interactiva) per a transferir imatges (que poden ser molt grans en alguns casos) de manera repetitiva a entorns d'ample de banda potser restringit. La problemàtica associada a la restricció de l'ample de banda és especialment crítica en situacions d'emergència en les quals els dispositius mòbils amb poc ample de banda són generalment l'única opció possible.

L'objectiu principal d'aquesta Tesi doctoral és estudiar i quantificar els efectes de diferents tècniques de compressió amb pèrdua en la cartografia generada a través d'imatges de teledetecció, considerant diferents tipus d'imatges, diferents escenaris geogràfics, diversos mètodes de generació de cartografia i diverses opcions de compressió (estàndard emprat: JPEG, JPEG 2000 o CCSDS; moment en què es realitza la compressió: a bord o usuari; i diversos nivells de compressió).

Entre les principals aportacions s'ha descobert que l'efecte de la compressió depèn de la metodologia emprada per a obtenir la cartografia desitjada, de l'estàndard de compressió emprat, del moment en què la compressió s'ha realitzat i de la fragmentació de la zona a cartografiar. Les zones més fragmentades accepten menys compressió, especialment si s'usen els estàndards menys eficients. JPEG 2000 obté millors resultats que JPEG clàssic quan s'aplica a nivell d'usuari, especialment si s'empra compressió 3D en JPEG 2000. CCSDS obté millors resultats que JPEG 2000 quan s'utilitza a bord a raons de compressió baixes (les desitjades en aquest entorn) i si el rang dinàmic de la imatge és petit baix (fins a 1000). Finalment, l'adaptació de l'estàndard JPEG 2000 per a codificar les zones de NODATA és factible emprant

tècniques de codificació que milloren la fidelitat de la compressió evitant codificar la zona definida com a NODATA, i permetent mantenir la seva definició, de gran utilitat per als usuaris de teledetecció.

Des d'un punt de vista més quantitatiu, els resultats de la tesi mostren que quan s'utilitzen tècniques de fotointerpretació sobre ortoimatges per a obtenir un mapa categòric d'usos del sòl, una compressió JPEG 2000 del 5:1 pot ser aplicada sense obtenir efectes en la cartografia obtinguda, més enllà dels propis deguts a la subjectivitat del fotointèrpret. Quan s'usen models de regressió per a obtenir variables quantitatives com la temperatura mitjana o mínima anual, a partir de dades de teledetecció (temperatura de superfície terrestre i NDVI) i/o variables geogràfiques (altitud, latitud, continentalitat, etc.), la compressió JPEG 2000 no afecta a la regressió fins a raons de compressió molt elevades (25:1 o 5:1 segons si s'usen només variables climàtiques o també variables de teledetecció). Si l'objectiu és la classificació píxel a píxel multitemporal d'imatges de satèl·lit per a obtenir mapes d'usos del sòl, la compressió aplicada pot ser diferent en funció del tipus de paisatge (zona de boscos o de conreus) i la fragmentació de la zona. El rang de compressions JPEG 2000 admeses varien des del 3.33:1 o 5:1 en el pitjor dels casos (zones de boscos fragmentades) fins l'100:1 (zones de conreus menys fragmentades). Si la classificació s'obté a través de tècniques de segmentació (grups de píxels), les conclusions indiquen que fins a compressions JPEG 2000 de 20:1 (depenent de la fragmentació de la zona), la classificació obtinguda és similar a la classificació original.

2. SUMMARY (ENGLISH)

Remote sensing is probably the largest source of data about the Earth that humanity has. Data are continually generated, and the amount of information we are acquiring is growing. This is not only because the currently existing satellites keep sending images, but also because new satellites that generally generate more information are being launched. This process clearly provides enormous application potential, but there is also an important handling problem and a growing need for compression formats that allow the volume of stored data to be decreased without significantly reducing the quality of the images used in applications.

The new Spatial Data Infrastructures (SDI) paradigm developed over recent years promotes the establishment of web data services, usually in terms of the Open Geospatial Consortium. These services require compression and interactive transmission strategies in order to transfer images (which may be very large) repetitively to environments with restricted bandwidth. The problems related to restricted bandwidth are especially critical in emergency situations in which mobile devices with low bandwidth are usually the only option.

The main aim of this PhD Thesis was to study and quantify the effects of several lossy compression techniques on the cartography resulting from remote sensing images, taking into account several image types, geographical scenarios and compression options (standards: JPEG, JPEG 2000 or CCSDS, using on board compression or user compression).

Among the main contributions of the thesis, we found that the effect of compression depends on the methodology used to obtain the cartography, on the compression standard employed and on the fragmentation of the study area. More fragmented areas cannot be compressed as much as less fragmented areas, especially if less efficient standards are used. JPEG 2000 obtains better results than the classic JPEG, especially if 3D JPEG 2000 is used. CCSDS obtains better results than JPEG 2000 when on board compression is used at low compression ratios (which are enough in this environment) and if the dynamic range of the image is low (up to 1000). Finally it is possible to use a JPEG 2000 modification to code NODATA areas with coding techniques that improve compression fidelity, avoid coding NODATA areas and allow them to be defined, which is very useful for remote sensing users.

From a quantitative point of view, these results show that when photointerpretation techniques are used on orthoimages to obtain a land cover map, JPEG 2000 compression can be applied at 5:1 with fewer effects on the resulting cartography than those introduced by the subjectivity of the photointerpreter. When regression models are applied to obtain quantitative variables, such

as mean or minimum annual temperature, from remote sensing data (land surface temperature and NDVI) and/or geographical variables (altitude, latitude, continentality, etc.), JPEG 2000 compression does not affect regression up to very high compression ratios (25:1 or 5:1 depending on whether only climatic data or remote sensing data are also used). If the aim is a pixel by pixel classification of a multitemporal satellite image series to obtain land cover maps, the compression applied may be different depending on the landscape type (crops or forest areas) and the fragmentation of the area. The JPEG 2000 compression ratios varied from 3.33:1 or 5:1 in the worst case (fragmented forest areas) to 100:1 (less fragmented crop areas). If object-based classification is the objective, our results show that classifications of JPEG 2000 compressions up to 20:1 (depending on the area fragmentation) obtain similar results as classifications of non-compressed images.

1. INTRODUCCIÓ

1.1. MOTIVACIÓ DE LA TESI

1.1.1 IMATGES DE TELEDETECCIÓ I SIG

Des del inici de la seva utilització, el 1915, la fotografia aèria es va convertir en una molt benvinguda font de dades per a totes les activitats relacionades amb el coneixement o la gestió del territori. Més tard, i gràcies als avenços en les telecomunicacions, l'aeronàutica i els sistemes sensors, va aparèixer l'observació espacial, que des d'inicis de la dècada de 1970 proporciona imatges periòdiques de la superfície terrestre. Els programes espacials de diferents països i agències internacionals han ajudat sens dubte a fer evolucionar la tecnologia fins al que avui es coneix com a teledetecció (*Remote Sensing* en anglès), una poderosa eina per al control i seguiment del territori i els recursos naturals, entre moltes altres aplicacions pràctiques (Chuvieco 2010).

En essència, la teledetecció consisteix en l'extracció d'informació d'una àrea mitjançant sensors que capten la radiació emesa o reflectida en diferents longituds d'ona o bandes espectrals, i en el posterior tractament d'aquestes bandes. Aquestes bandes constitueixen un patró o signatura espectral del material que ha emès o reflectit la radiació que les ha formades i permeten l'identificació de les entitats o dels fenòmens d'aquell territori a través de sistemes de reconeixement de patrons radiomètrics o espacials. Depenent del nombre de bandes disponibles, es parla d'imatges multispectrals (nombre per sota d'una desena) i d'imatges hiperspectrals (amb un nombre de bandes de l'ordre de desenes o centenars però també aquelles imatge en les quals la resolució espectral és molt gran, per exemple 10 nm o inferior).

La teledetecció proporciona, probablement, la més enorme font de dades de la qual la humanitat disposa sobre el planeta. I aquesta generació de dades continua creixent a un ritme vertiginós, no només perquè els satèl·lits existents segueixen enviant imatges, sinó també perquè es llancen nous satèl·lits, en molts casos capaços de generar encara més informació. Com resulta fàcil intuir, aquest procés comporta enormes possibilitats d'aplicació, però també una important problemàtica de maneig de tota aquesta informació i una creixent necessitat de formats de compressió que permetin disminuir el volum de dades emmagatzemades sense disminuir significativament la qualitat de les imatges per a aplicacions posteriors. Per a més detalls sobre els conceptes i les bases de la teledetecció (que no tenen cabuda en aquesta introducció) el lector pot consultar algun manual de la matèria (Jensen 2004, Richards & Xia 2005, Campbell 2008, Chuvieco 2010).

A l'arrel de l'augment de generació i consum d'imatges no només es troba l'extraordinari camp d'aplicació de la teledetecció en meteorologia, oceanografia, control de recursos naturals, etc., sinó que es troba també l'enorme explosió de l'ús de Sistemes d'Informació Geogràfica (SIG o GIS). En efecte, encara que continua havent un actiu camp d'investigació teòrica al voltant dels SIG, la seva utilització pràctica ha passat a ser totalment habitual en molts àmbits, fins al punt d'haver-se convertit en una eina imprescindible per a molts científics, planificadors i gestors dels diversos camps relacionats d'una manera o altra amb el territori (cartografia, ordenació del territori, gestió ambiental, etc.). Aquests usuaris de SIG utilitzen contínuament imatges, bé sigui de forma directa (per exemple com fons de referència en forma d'ortoimatges, o com base de processos de fotointerpretació per a generar cartografia temàtica) o indirecta (utilitzen mapes temàtics que en molts casos han estat obtinguts com resultat de processar les imatges de molt diverses maneres). En aquest context existeix una avidesa de disponibilitat d'imatges de teledetecció (percebudes, en molts casos, com superiors per la seva actualitat i detall a la cartografia convencional), amb creixents demandes quant a resolució espacial, radiomètrica, espectral i temporal. La integració i sinèrgia teledetecció-SIG s'ha d'entendre tant per l'aproximació als SIG de les tècniques de teledetecció (per exemple amb una creixent exigència d'una georeferenciació de les imatges cada vegada més rigorosa –ús de models orbitals i/o del relleu en els processos– que pràcticament no estava present en manuals de teledetecció de fa més d'una dècada), com per l'ús de dades SIG en els processos de teledetecció (obtenció de punts de control, veritat terreny per a validacions, etc., que anteriorment s'introduïen en el context de l'aplicació de teledetecció sense extreure'ls de forma integrada de bases SIG).

1.1.2 PROBLEMÀTIQUES ASSOCIADES A L'ÚS DE LES IMATGES DE TELEDETECCIÓ

Com s'ha apuntat, un dels desafiaments de la teledetecció és l'emmagatzematge i tractament de les imatges multi i hiperspectrals, majoritàriament a causa del gran volum de dades que representen. Per exemple, una zona de només 10 km d'ample per 10 km de llarg que hagi estat adquirida amb un sensor amb resolució d'1 m, utilitzant un total de 10 bandes amb una profunditat de 8 bits per banda suposa un total d'1 Gigabyte, és a dir, prop de dos CD-ROM d'emmagatzematge. Si estenem el nostre exemple de només 100 km^2 a la província de Lleida (12167 km^2), les necessitats es tornen unes 120 vegades majors, i si demanem una resolució temporal mensual de les dades es tornen unes 1460 vegades majors per a un sol any. Encara que existeixen dispositius d'emmagatzematge de gran capacitat, l'accés a tals volums de dades és lent i costós. Evidentment, només el cost d'emmagatzematge d'una seqüència d'aquestes imatges suposa una inversió molt elevada en maquinari, tant per capacitat com per velocitat, i fa gairebé impracticable el seu intercanvi o difusió a través de la xarxa Internet actual.

A més a més, el nou paradigma de les Infraestructures de Dades Espacials (IDE), desenvolupat en els darrers anys, promou l'establiment de serveis de dades web, habitualment en termes dels estàndards definits per l'Open Geospatial Consortium, com el Web Map Service (WMS), Web Coverage Service (WCS) (Maguire & Longley 2005) o el recent Web Map Tile Service (WMTS, Masó *et al.* 2010). L'establiment d'aquests serveis requereix de l'ús d'estratègies de compressió (i sovint de transmissió interactiva) per a transferir imatges (que poden ser molt grans en el cas de servidors WCS) de manera repetitiva a entorns d'ample de banda potser restringit. La problemàtica associada a la restricció de l'ample de banda és especialment crítica en situacions d'emergència en les quals els dispositius mòbils amb ample de banda restringit són generalment l'única opció possible. Malgrat la cada vegada més inevitable necessitat de compressió en el context del SIG i la teledetecció en general, i dels serveis web en particular, no es pot sacrificar la necessitat d'emprar formats de compressió estàndards, encara que les variacions dels estàndards recentment publicades a la literatura puguin permetre obtenir raons de compressió superiors (però usant formats no estàndards, i per tant inadmissibles al context de les IDE). De fet, cal destacar que molts d'aquests serveis web estan emprant alguns estàndards de compressió, especialment JPEG (ISO JTC 1/SC 29 1994).

Fins al moment, però, no ha estat gaire habitual en la comunitat científica de la teledetecció l'ús de tècniques de reducció de dades a causa del temor de descartar informació que pugui resultar important per a processos posteriors. Aquesta lògica preocupació de no perdre informació ha fet que l'Anàlisi de Components Principals (PCA) probablement sigui el mètode més utilitzat donat que la selecció d'informació es produeix sobre la base d'un criteri estadístic de retenció de variància (Lee *et al.* 1990). No obstant això, i donat el gran volum d'informació actualment disponible, sembla raonable insistir en la investigació en tècniques que permetin la reducció d'aquest volum i alhora combinar-ho amb estudis que avaluïn adequadament les implicacions en la qualitat de la informació extreta i no només sobre la base d'una simple valoració subjectiva del seu aspecte visual.

1.1.3 ESTAT ACTUAL

La compressió amb pèrdua (també anomenada "degradativa" o "no conservativa") és una de les tècniques de reducció de dades més potents, exitosament aplicada a la compressió d'imatges. A partir de la seva aparició, el format JPEG (Wallace 1991, Pennebaker & Mitchell 1993, ISO JTC 1/SC 29 1994) es va convertir en l'estàndard de facto per a la compressió d'imatges amb pèrdua. Aquest mètode, que en la seva codificació habitual només permet compressió amb pèrdua (fins i tot sol·licitant el 100% de qualitat), s'ha utilitzat durant més d'una dècada. Però

l'aparició de noves tècniques, la majoria d'elles basades en la transformada *wavelet* (ECW, SPIHT), han generat la necessitat de definir i implementar un nou estàndard de compressió, el JPEG 2000 (Taubman & Marcellin 2002, ISO JTC 1/SC 29 2004), també basat en transformada *wavelet* i d'introducció relativament recent en teledetecció. Cal destacar que, a diferència del format JPEG clàssic, el format JPEG 2000 incorpora també la possibilitat de realitzar compressió sense pèrdua, tot i que aquesta opció, com és d'esperar, no pot assolir raons de compressió tan elevades com en la compressió amb pèrdua.

El format JPEG 2000 ofereix nombrosos avantatges sobre el format JPEG clàssic (Aboufadel 2001 i Adams 2001): aquest estàndard suporta compressió amb i sense pèrdua d'una component (imatges en escala de grisos) o de diverses components (imatges en color o multispectrals, per exemple). D'altra banda, permet assolir raons de compressió força més elevades amb qualitats similars i, a més, permet recuperar imatges a diferents resolucions i mides a partir del mateix fitxer comprimit (JPEG només pot recuperar imatges a la resolució fixada i descomprimint tot el fitxer). Un altre avantatge de JPEG 2000 és la seva capacitat de definir àrees d'interès (ROI, *region of interest*) que es comprimeixen en menor grau.

Més enllà de la pròpia definició d'un format que comprimeixi amb o sense pèrdua, no són gaire abundants les investigacions encaminades a definir numèricament la qualitat dels resultats basats en imatges comprimides i, encara menys, en un entorn de teledetecció i SIG.

En referència a la qualitat geomètrica i visual de la imatge després d'aplicar compressió amb pèrdua, Li *et al.* 2002 conclouen que amb compressions menors a 10:1 en format JPEG (raó de compressió de 0.10) la qualitat visual de la imatge és encara excel·lent i per això la pèrdua de qualitat és acceptable per a la majoria d'aplicacions fotogramètriques. En relació a aquesta línia d'investigació, els articles que avaluen l'efecte de la compressió amb pèrdua sobre la generació automàtica de Models Digitals d'Elevacions (MDE) arriben a conclusions similars. Lam *et al.* 2001 conclouen també que és possible utilitzar raons de compressió 0.10 en format JPEG sense efectes en la generació dels MDE i que la degradació de qualitat de la imatge és major com més gran és la riquesa textural de la imatge. D'altra banda, Shih & Liu, 2005 realitzen un estudi similar a l'anterior però usant alhora el format JPEG i el JPEG 2000. Per una part conclouen que aquesta pèrdua en la qualitat relacionada amb l'augment en la riquesa textural de la imatge és més acusada en el format JPEG que en el format JPEG 2000. Per una altra banda, observen que en totes les mesures de qualitat de la imatge, el format JPEG 2000 obté millors resultats que el format JPEG clàssic, especialment a elevades raons de compressió.

Respecte a la qualitat temàtica de les classificacions obtingudes després d'aplicar compressió amb pèrdua, els resultats de les encara poques investigacions realitzades són relativament dispars. Així, Paola & Schowengerdt 1995 suggereixen que es poden obtenir classificacions de qualitat (al voltant de 83% d'encert de la classificació a partir de la imatge comprimida respecte la classificació a partir de la imatge original) amb imatges comprimides amb una raó de 7.1:1 (raó de compressió de 0.14) o fins i tot major depenent del tipus d'imatge i del mètode de classificació emprat i usant el format de compressió JPEG clàssic. En la mateixa línia, Tintrup *et al.* 1998 obtenen un encert de 95% per a compressions menors, de 2.5:1 (raó de compressió de 0.4).

D'altra banda, el mateix estudi de Paola & Schowengerdt 1995 admet que encara que les classificacions mantenen l'aparença global, l'efecte de suavització (*smoothing effect*) té tendència a eliminar la majoria de detalls píxel a píxel. En la mateixa línia de resultats, les conclusions de l'estudi de Pérez *et al.* 2003 desaconsellen l'ús d'imatges amb compressió amb pèrdua en mètodes de classificació ja que comproven que s'obté un encert de només un 70%, en el millor dels casos i per a compressions de 6.16:1 (raó de compressió de 0.16).

Per la seva banda, l'extracció d'objectes homogenis a partir de les imatges (segmentació) és una tècnica molt menys estesa que la classificació però ja va ser proposada fa molts anys i respon a una interessant estratègia en l'obtenció de mapes categòrics (Kettig & Landgrebe 1975). La idea consisteix a realitzar una pre-classificació de la imatge en objectes espectralment homogenis abans d'abordar la classificació en si o bé usar una segmentació derivada d'una font externa com un cadastre; una vegada realitzat el procés, la classificació s'aborda sobre la base d'aquests objectes en lloc de sobre la base de píxels. Els processos de compressió *wavelet* consideren el context espacial, pel que sembla interessant investigar els problemes i sinèrgies que puguin trobar-se quan s'apliqui segmentació a imatges sotmeses a compressió amb pèrdua. Kiema 2000 sosté que és possible comprimir les imatges fins una raó de 20:1 sense afectar negativament els resultats de la segmentació.

Així, el nombre de treballs que permeten contrastar la hipòtesi de si pot es utilitzar compressió amb pèrdua sense efectes importants sobre l'anàlisi visual o digital és encara massa escàs. Sovint els treballs presenten llacunes metodològiques importants. Com a exemple, l'estudi de Xu *et al.* 2003 utilitza una sola imatge pancromàtica d'Ikonos per a establir una classificació de només 9 categories i suggereix que és possible reduir el nombre de nivells de gris de la imatge fins 16 sense perjudicar el resultat de la classificació. No obstant això, com els propis autors apunten, aquestes conclusions estan basades en una situació molt simplificada (1 banda i 1

data) i són prematures, ja que encara és necessari realitzar estudis amb un major nombre de bandes espectrals i amb imatges de diferents dates, diferents estratègies d'obtenció de la cartografia, etc. En molts dels altres treballs, les limitacions es refereixen a la mida o quantitat de les imatges usades.

Des del punt de vista de la literatura també existeixen un seguit de treballs que exploren modificacions en els estàndards de compressió per tal de millorar-los (Qian *et al.* 2005, Penna *et al.* 2006, Penna *et al.* 2007, Du & Fowler 2007, Wang *et al.* 2007, Carvajal *et al.* 2008, Choi *et al.* 2008, Chou & Liu 2008). Malauradament, només alguns d'aquests estudis comproven l'efecte de la compressió sobre les aplicacions posteriors de les imatges (Qian *et al.* 2005, Penna *et al.* 2007, Carvajal *et al.* 2008, Choi *et al.* 2008). D'altra banda, aquests estudis que realitzen aquesta avaluació d'efectes en les aplicacions usen imatges petites (màxim 512*512 píxels) i estudis aplicats senzills, sense considerar escenaris de generació de cartografia de manera sistemàtica, en el context de gestió territorial (ús d'imatges multitemporals per a la gestió de l'agricultura o els boscos, etc.).

1.1.4 COMPRESSIÓ A NIVELL D'USUARI I COMPRESSIÓ A BORD

Els estudis presentats anteriorment, se centren en dos grans aspectes: els efectes de la compressió sobre les imatges i les seves aplicacions, i les millores dels formats de compressió (només en alguns casos avaluen també els seus efectes). En tots els casos, l'avaluació de la compressió i/o els seus efectes es realitza en el context de que aquesta compressió és realitzada a nivell d'usuari, és a dir, al final de la cadena de processat de les imatges.

Per altra banda, les agències responsables del disseny i llançament dels satèl·lits que capten les imatges estan cada vegada més interesades en la possible incorporació de compressió a bord (*on-board*) de les pròpies plataformes. El motiu és evitar sobrepassar la capacitat de descarrega a terra (*downlink*) degut al major volum de dades captades pels nous sensors (Yu *et al.* 2009). En aquest entorn, la compressió de les dades és necessària per a permetre descarregar-les al segment terra usant el mínim ample de banda possible, donat el límit en aquest recurs i la quantitat de les dades generades pels sensors.

L'any 2005, el Consell del Comitè Consultiu per Sistemes de Dades Espacials (*Consultative Committee for Space Data Systems, CCSDS*) va aprovar una recomanació per a compressió de dades a plataformes espacials (CCSDS 2005). Aquesta recomanació defineix un algorisme de compressió basat en la transformada *wavelet* que satisfà les necessitats d'una plataforma de compressió en temps real a bord d'un satèl·lit.

Alguns treballs de la literatura investiguen definint o millorant sistemes de compressió especialment dissenyats per a ser emprats a bord (Qian *et al.* 2005, García-Vílchez & Serra-Sagristà 2009) i permetre operar en entorns on la càrrega i el temps de procés en comprimir (a bord de la plataforma) és molt limitant.

En aquest context, es fa també palesa la necessitat d'investigar l'impacte de la compressió sobre les imatges (i les seves aplicacions), quan aquesta compressió és efectuada al propi sistema sensor (a bord), abans de la descàrrega de les dades a terra i del seu processament (previ o posterior a la distribució de les imatges). Per a poder estudiar l'efecte de la possible compressió a bord, es possible aprofitar els simuladors desenvolupats per les agències per a dissenyar i optimitzar els requeriments de les noves missions, com per exemple el *Sentinel-2 Image Performance Simulator* (Sentinel-2 2007) desenvolupat per EADS Astrium i emprat per l'Agència Europea de l'Espai (*European Space Agency*, ESA) per a l'ajust del sensor a bord del nou satèl·lit òptic Sentinel-2 (Sentinel-2 2010).

1.2. OBJECTIUS DE LA TESI

L'objectiu principal d'aquesta Tesi doctoral és estudiar i quantificar els efectes de diferents tècniques de compressió amb pèrdua en la cartografia generada a través d'imatges de teledetecció, considerant diferents escenaris geogràfics i diferents nivells de compressió.

Per tal de poder complir aquest estudi tant ampli, la Tesi se centra en l'anàlisi dels efectes de la compressió utilitzant:

- diversos mètodes de generació de cartografia:
  - a través d'anàlisi visual: fotointerpretació
  - a través d'anàlisi digital: classificacions i regressions
- diversos estàndards de compressió: JPEG, JPEG 2000 i CCSDS
- diversos punts de la cadena de processament de les imatges en els quals aplicar aquesta compressió: a nivell d'usuari i a bord de les plataformes

L'anàlisi combinada dels diferents factors presentats ha permès cobrir les principals metodologies de generació de cartografia, generant així un estudi raonablement complet respecte les necessitats dels gestors del territori (que el poden estudiar usant les diverses tècniques de generació de cartografia). D'altra banda, l'ús de diversos mètodes de compressió en les seves diverses configuracions (JPEG clàssic, JPEG 2000 2-D i 3-D i CCSDS) també permet

acostar als experts en teledetecció i gestió del territori el coneixement sobre les diverses opcions de compressió i llur impacte en els usos posteriors que realitzen amb aquestes. Finalment, el fet de realitzar estudis respecte l'efecte de la compressió segons on s'efectua, aporta informació rellevant tant als usuaris de les imatges com a les agències que dissenyen els satèl·lits i que poden usar les conclusions per al disseny de missions futures.

També cal destacar que la diversitat d'imatges emprades en els estudis realitzats també ha cobert el major ventall possible, donant també un altre punt de valor afegit a aquesta Tesi, per tal com permet obtenir conclusions també en diversos escenaris de treball (des del punt de vista de les diverses resolucions –espacial, espectral i temporal- de les imatges). Des del punt de vista de la resolució temporal s'ha treballat amb escenaris en els quals es disposada d'una única data per a realitzar la cartografia desitjada (una ortoimatge per a realitzar una mapa d'usos del sòl a través de fotointerpretació), així com escenaris multitemporals amb ús de diverses imatges per a la obtenció d'una única cartografia (per exemple cinc dates Landsat per a classificar zones forestals). La resolució espacial coberta ha estat també diversa, des de resolucions de 0.5 i 1 m per a les ortoimatges emprades en els estudis de fotointerpretació i segmentació (respectivament), fins als productes TERRA-MODIS d'1 km emprats per a la regressió de variables climàtiques. La resolució espectral de les imatges utilitzades en la recerca és també molt variada: des de les ortoimatges en color (3 bandes) per la fotointerpretació o segmentació, fins a imatges multiespectrals Landsat, SPOT o Sentinel-2 (simulades) per als diversos escenaris de classificació, o les imatges hiperspectrals AVIRIS utilitzades per a la classificació de zones de conreus (en el context de l'article sobre la codificació del NODATA).

1.3. MÈTODES GENERALS

1.3.1 COMPRESSIÓ

1.3.1.1 Introducció

La recerca de la Tesi ha avaluat diversos estàndards de compressió per a estudiar el seu efecte en la generació de cartografia. Com s'ha presentat anteriorment, JPEG clàssic (Wallace 1991, Pennebaker & Mitchell 1993 i ISO JTC 1/SC 29 1994) i JPEG 2000 (Taubman & Marcellin 2002 i ISO JTC 1/SC 29 2004) són els dos estàndards de compressió que s'han estudiat quan la compressió és aplicada a nivell d'usuari. Per tal de considerar l'efecte quan la compressió és realitzada a bord, s'ha utilitzat l'estàndard CCSDS (CCSDS 2005).

Els algorismes de compressió/descompressió utilitzats han estat la implementació de JPEG clàssic de MiraMon 5.2 i posteriors (mòdul JPEGIMG, Pons 2008) basada en les llibreries públiques de JPEG de l'*Independent JPEG Group* (IJG 1998), la implementació BOÍ de l'estàndard JPEG 2000 (del departament d'Enginyeria de la Informació i de les Comunicacions, dEIC, de la Universitat Autònoma de Barcelona, Aulí-Llinàs *et al.* 2005), la implementació Kakadu de l'estàndard JPEG 2000 (per a la compressió 3D, Taubman 2008), així com les implementacions de l'Agència Europea de l'Espai (Cabral 2009) i de la University of Nebraska-Lincoln (Wang 2008) de l'estàndard CCSDS.

La mesura de la compressió s'ha realitzat sobre la base de les raons de compressió (CR) i no de la qualitat de la compressió, habitual en JPEG, ja que aquella ha semblat més rellevant donada l'evident aplicació pràctica de la investigació d'aquesta Tesi. S'ha de tenir en compte que una mateixa raó de compressió pot suposar diversos graus de qualitat en funció del tipus d'imatge (fragmentació espacial, tipus de dades, etc.) però també és veritat que no hi ha un índex de qualitat nítidament admès com a universal i representatiu (tot i l'àmplia utilització del PSRN[1]). La raó de compressió es defineix com la relació entre la grandària del fitxer comprimit i l'original, és a dir:

$$CR = \frac{\text{Mida Fitxer Comprimit}}{\text{Mida Fitxer Original}}$$

Generalment s'expressa en tant per u, o en tant per cent, multiplicant CR per 100. En molts dels articles de la literatura s'expressa de la forma "<Mida fitxer original>:<Mida fitxer comprimit>". Així per exemple si un fitxer de 10 Mb es comprimeix fins a 2 Mb la seva raó de compressió serà de 0.20, 20% o 5:1.

1.3.1.2 Valor NODATA

La majoria de les imatges emprades en els diferents estudis presenten zones sense dades (NODATA) degut a diversos dels processaments realitzats sobre elles. Les correccions geomètriques, radiomètriques i la presència d'alguns núvols (i les seves ombres) són els principals motius que fan necessari l'ús d'un valor particular per a marcar aquestes zones i diferenciar-les de les zones amb valors vàlids (vegeu Figura 1a).

No tots els programes de compressió i descompressió utilitzats disposen de la consideració d'aquests valors NODATA. A més, utilitzar-los directament a la compressió pot generar

[1] *Peak signal-to-noise ratio*: raó entre la màxima potència d'una senyal i la potència del soroll que afecta la fidelitat de la seva representació. Com que molts senyals tenen un rang dinàmic molt ampli generalment s'expressa en decibels.

problemes greus en les imatges generades (especialment si el valor utilitzat per a marcar les zones sense dades és un valor extrem del rang que permet la imatge).

En els primers estudis realitzats es va usar una estratègia per eliminar el valor NODATA de les imatges i evitar el seu impacte negatiu en la compressió. Aquesta eliminació es va realitzar mitjançant el mòdul FagoVal del MiraMon, que elimina (fagocita) selectivament un valor donat a fitxers ràster, substituint-lo, en aquest cas, per la mitjana aritmètica dels valors adjacents (vegeu el resultat d'aquesta fagocitosi a la Figura 1b).

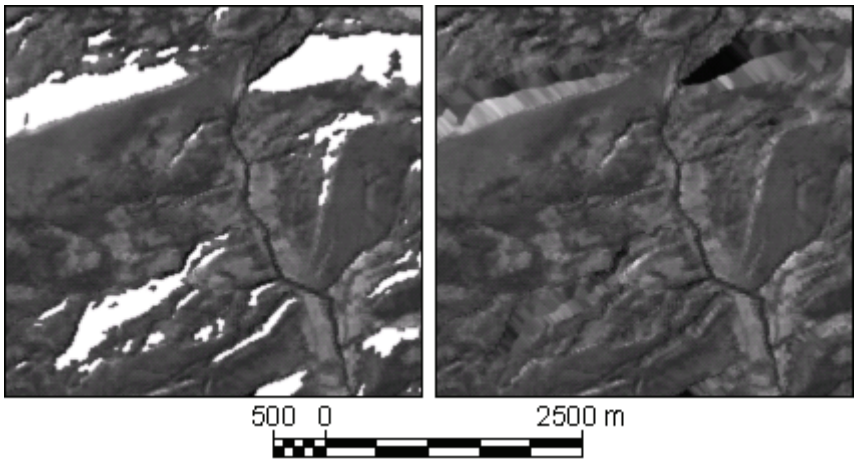

Figura 1: Banda IR proper (banda 4, sensor TM, satèl·lit Landsat-5; 12-03-2003) sobre la zona de la Garrotxa-Ripollès: a) Imatge original amb valors NODATA en blanc (esquerra). b) Imatge sense valors NODATA, fagocitats (dreta).

La recerca posterior realitzada (corresponent al cinquè capítol d'aquesta Tesi), ha portat a concloure que la millor estratègia per a codificar el NODATA en el marc de l'estàndard JPEG 2000 és substituir el valor NODATA per la mitjana de la imatge.

1.3.1.3 Compressió JPEG clàssica

El format JPEG permet comprimir una o tres bandes, generant un fitxer de grisos o de color (així com generar un fitxer de grisos a partir de tres bandes). El format de compressió JPEG es basa en una transformada discreta del cosinus (DCT) com primer pas del sistema de compressió; en segon lloc es duu a terme una quantització escalar uniforme i, finalment, una codificació per entropia mitjançant l'algorisme de Huffman. L'algorisme DCT comprimeix la imatge en blocs de 8x8 píxels i els desa de manera consecutiva al fitxer. Cada bloc es comprimeix de manera independent sense cap referència als blocs adjacents, de manera que a elevades raons de compressió l'efecte en blocs esdevé força visible.

Al format JPEG clàssic se sol establir la qualitat del fitxer JPEG resultant. Generalment, i encara que es modifiqui la qualitat sol·licitada, no és possible generar de forma directa un fitxer JPEG amb una mida determinada (és a dir la raó de compressió del qual sigui un valor determinat). Per aquest motiu, per cada escenari de compressió s'ha escollit el fitxer JPEG la mida del qual és més aproximada a la necessària per obtenir aquella raó de compressió (per excés o per defecte, i obtingut per aproximacions successives).

1.3.1.4 Compressió JPEG 2000

JPEG 2000 és l'últim estàndard de compressió d'imatges dissenyat després dels requisits posats pel *JPEG 2000 Working Group* (ISO/IEC 15444-1 2000) (suport a components múltiples, bits per píxel variable per a cada component, diferent tipus de progressió, suport a regions d'interès, correcció d'errors, etc.). Aquests requisits es van tenir en compte per desenvolupar un esquema de codificació nou amb un grau de flexibilitat que permet una molt bona parametrització de cada etapa de compressió, que encaixa dins diversos escenaris de treball, com per exemple per als usuaris de teledetecció i SIG.

Aquesta elevada flexibilitat no només és relativa al format de compressió sinó també a la possibilitat d'accés a la imatge comprimida. El format de compressió té mecanismes per a accedir i extraure porcions de la "tira de bits" (*bitstream*) sense haver de descodificar tota la imatge, a diferència del que passa amb JPEG clàssic.

Com es mostra a la Figura 2, l'esquema general de la compressió consta dels següents passos:

1. Pre-processament (*multi-component transform*): La codificació espera rebre un conjunt de dades aproximadament centrades en el zero i el pre-processament s'assegura que això sigui cert. En cas de dades sense signe es resta a cada valor 2^{P-1} on P és el nombre de bytes per píxel de la imatge (per exemple a les imatges en format byte es resta el valor 128 (2^6) a cada píxel). En els casos en què les tres primeres components de la imatge es corresponen a les bandes RGB es realitza una transformada de color (reversible o irreversible) per a passar a l'espai de color YCbCr (irreversible) o YUB (reversible).

2. Transformada *wavelet* (*wavelet transform*): La transformada *wavelet* s'aplica sobre cada component generant un conjunt de subbandes de freqüència. El nombre de subbandes obtingudes depèn del nombre de nivells de transformada realitzats. Si es fa un sol nivell de transformada s'obtenen quatre subbandes. Per les seves propietats estadístiques, aquestes subbandes es poden codificar de manera més eficient que les dades originals. L'estàndard

defineix una transformada reversible (que treballa amb enters) i una irreversible (que treballa en reals, no es pot desfer de manera exacta i per això és irreversible), que són les usades per a generar imatges comprimides sense o amb pèrdua (respectivament).

3. Quantització de coeficients (*quantization*): Quan la transformada ha estat irreversible els valors obtinguts són reals i han de ser convertits a enters per a ser codificats. En cas de transformada reversible no és necessari realitzar aquesta quantització.

4. Codificació de les dades 1 (*tier 1 encoding*): Codificació dels valors de les subbandes per a generar petits *codestreams*.

5. Codificació de les dades 2 (*tier 2 encoding*): Generació del les capçaleres principals i de paquets i escriptura del fitxer comprimit. Cada paquet consta d'una capçalera (*header*) i de les dades codificades (*body*).

6. Control de distorsió (*rate control*): Aquest procés necessita informació de la quantització, i els dos passos de codificació per a permetre escollir els millors *codestreams* per a ser classificats i ordenats a les capes de qualitat (i permetre la transmissió o recuperació de la imatge a diferents nivell de qualitat).

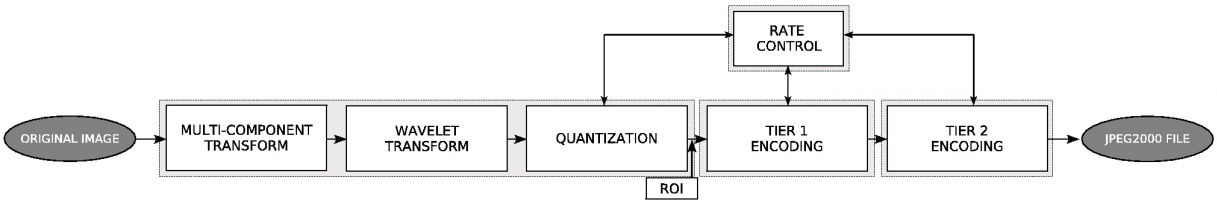

Figura 2: Esquema de compressió de l'estàndard JPEG 2000 (Font: Dept. d'Enginyeria de la Informació i de les Comunicacions (dEIC) de la Universitat Autònoma de Barcelona)

L'estàndard tracta sobre tres dominis diferenciats: el domini espacial (són les mostres, els píxels de les imatges d'entrada), el domini de la transformada (són els coeficients obtinguts després d'aplicar la transformada) i el domini de la imatge comprimida.

Durant l'evolució de la recerca també s'ha emprat diverses parametritzacions d'aquest estàndard. En els primers estudis s'ha realitzat compressió JPEG 2000 banda a banda (per a obtenir resultats comparables a JPEG clàssic). Posteriorment s'ha anat incorporant altres característiques d'aquest estàndard per a aprofitar al màxim les seves possibilitats: compressió multibanda (amb transformada *wavelet* en les dues dimensions espacials) i compressió 3D (amb transformada *wavelet* en les dues dimensions espacials i també en la dimensió espectral).

Finalment, és important destacar que l'estàndard contempla la possibilitat de generar una imatge resultant amb una mida determinada. Per tant, a diferència del que passa amb la compressió JPEG, és senzill generar les imatges comprimides que compleixin una determinada raó de compressió.

1.3.1.5 Compressió CCSDS

Durant la darrera dècada, el Consell del Comitè Consultiu per Sistemes de Dades Espacials (*Consultative Committee for Space Data Systems, CCSDS*) ha aprovat dos estàndards relacionats amb la compressió d'imatges: CCSDS 121.0-B-1 (CCSDS 1997) i CCSDS 122.0-B-1 (CCSDS 2005). El primer és un estàndard de compressió sense pèrdua (aprovat el 1997), i el segon defineix l'estàndard per la compressió d'imatges (*Image Data Compression, IDC*) que contempla la compressió amb i sense pèrdua, i que va ser aprovat el 2005. El llibre verd (tutorial) d'aquest segon estàndard es va aprovar el 2007 (CCSDS 2007), el mateix any que el comitè va crear el grup de treball *Multispectral Hyperspectral Data Compression (MHDC) Working Group* (CCSDS 2007b) per a definir un estàndard que consideri la compressió de dades multi i hiperspectrals a bord, que encara no ha estat aprovat.

La recomanació IDC defineix un algorisme de compressió basat en la transformada *wavelet* que satisfà les necessitats d'una plataforma de compressió en temps real a bord d'un satèl·lit. Alguns d'aquests requeriments són: 1/ ha de permetre treballar tant en instruments que captin les dades per escenes com en tipus *push-broom*, 2/ la qualitat de les dades ha de ser variable (sense i amb pèrdua), 3/ les dades d'entrada han d'admetre des de 4 a 16 bits per píxel, 4/ ha de permetre processat en temps real, 5/ ha de requerir el mínim processat en el segment de terra i 6/ ha de limitar els efectes de la compressió amb pèrdua a zones petites de la imatge (paquets de compressió de mida variable). El CCSDS permet menys parametritzacions que JPEG 2000 i, per tant, menys complexitat, el que comporta disminuir el cost computacional de la compressió a bord.

1.3.1.6 Descompressió i posterior tractament

Les imatges després de la compressió i descompressió han de ser tractades per a reaplicar-hi la màscara de les zones NODATA (que s'han eliminat abans de la compressió com s'ha explicat a l'apartat 1.3.1.2). La màscara és diferent per a cada una de les imatges o altres variables.

Finalment es recuperen les metadades de les imatges (conservades només per algunes eines de compressió i descompressió) com el sistema de referència, les dimensions de la imatge, la seva

descripció, etc. Es mantenen o documenten les metadades referides als processos realitzats sobre les imatges: eliminació del valor NODATA, compressió, descompressió, reclassificació del valor 255, etc. En tot el procés de documentació se segueix l'estàndard de metadades per a la informació geogràfica ISO TC 211 2003 i les ampliacions d'aquest estàndard contemplades pel perfil d'aquesta estàndard implementat al Gestor de Metadades del MiraMon. Aquest perfil amplia l'estàndard per a considerar algunes metadades sobre imatges no considerades a l'estàndard i altres aportacions pròpies (Zabala & Pons 2002, Julià *et al.* 2005), així com un model per a definir i heretar metadades de sèries i capes cartogràfiques (Zabala & Masó 2005).

1.3.2 GENERACIÓ DE CARTOGRAFIA

1.3.2.1 Introducció

Al llarg de la recerca realitzada s'ha aprofundit en l'efecte de la compressió sobre diversos mètodes de generació de cartografia. Aquest és, a més, el fil organitzatiu de la Tesi, com es comenta a l'apartat 1.5, sobre l'organització de la Tesi.

En la resta d'aquest apartat es descriuran breument els principals mètodes d'anàlisi i de generació de cartografia emprats en la recerca realitzada.

1.3.2.2 Fotointerpretació

L'anàlisi visual o fotointerpretació de les imatges permet al fotointèrpret considerar diversos elements (i no només el valor radiomètric de cada píxel) per tal de decidir la classe a què ha d'assignar cada zona de la imatge; entre aquests elements es pot esmentar la textura, l'estructura o la ubicació i distribució dels objectes. Aquest és un dels seus principals avantatges (les categories complexes són més fàcilment cartografiables amb aquestes metodologies) i motiu pel qual és el mètode de realització de diverses cartografies de detall d'usos i coberts del sòl.

Una d'aquestes cartografies realitzades per fotointerpretació és el Mapa de Cobertes del Sòl del Catalunya (MCSC, Burriel *et al.* 2005), una cartografia temàtica d'alta resolució dels principals tipus de cobertes del sòl del país (boscos, conreus, zones urbanitzades, etc.). El MCSC, degut al seu elevat detall, és de gran interès per al coneixement del territori, però també per a la valoració de l'ocupació del sòl en cada lloc, tant des del punt de vista ecològic com econòmic. Amb el MCSC es pot obtenir la superfície forestal o de conreus a nivell comarcal, municipal, de parc natural, etc, i extreure'n els mapes corresponents, planificar el disseny de mostrejos de camp (com el de l'Inventari Ecològic i Forestal de Catalunya), connectors entre espais naturals,

estudis per als planejaments urbanístic i territorial, infraestructures (distribució de xarxa elèctrica, traçat de vies de comunicació, etc.), plans de regadiu, avaluacions d'impacte ambiental, etc.

En l'estudi de l'efecte de la compressió sobre la fotointerpretació s'ha emprat la mateixa informació de base i la metodologia que les emprades al MCSC (Burriel *et al.* 2005), generant un mapa categòric d'usos del sòl amb una llegenda de 15 categories. En el disseny de l'experiment es va tenir en compte la participació d'un sol fotointèrpret per minimitzar les diferències produïdes per diferents criteris entre persones (Mann & Rothley 2006) i la valoració de la seva subjectivitat realitzant dues vegades la fotointerpretació sobre les imatges sense comprimir (amb un temps de pausa enmig per evitar efectes de record). Els detalls d'aquesta recerca es presenten al capítol 2.

1.3.2.3 Regressió

Aprofitar l'elevada resolució temporal d'alguns sensors per a caracteritzar el territori és també una de les metodologies més utilitzades en teledetecció. Les eines de regressió poden ajudar a obtenir una variable quantitativa a tot el territori a través d'altres variables relacionades.

Des del punt de vista de la modelització climàtica, una de les metodologies habituals consisteix en l'obtenció de la temperatura de l'aire a partir de variables geogràfiques (continentalitat, elevació, latitud, etc.) com a variables independents, i variables climàtiques com a variables dependents, i posteriorment ajustant un model de regressió (Ninyerola *et al.* 2007). D'altra banda, alguns estudis usen només imatges de satèl·lit o variables derivades de teledetecció (temperatura de la superfície terrestre, NDVI o albedo), per a modelitzar la temperatura de l'aire (Prihodko & Goward 1997, Recondo & Pérez-Morandeiram 2002 i Sun *et al.* 2005). Finalment alguns estudis combinen ambdós tipus de variables (SIG i teledetecció) per a obtenir, sovint, millors resultants en l'obtenció de la temperatura de l'aire (Cristóbal *et al.* 2005, Cristóbal *et al.* 2006).

Seguint les tendències de la literatura, en el capítol 3 se segueixen les metodologies habituals per a l'estimació de la temperatura de l'aire a partir només de variables geogràfiques (Ninyerola *et al.* 2007) o d'ambdós tipus de variables (Cristóbal *et al.* 2006). La metodologia usa mètodes que combinen la regressió múltiple i la interpolació local dels residus de la primera a partir de dades d'estacions meteorològiques.

L'anàlisi estadística s'utilitza per a explicar la relació climàtica entre les variables desitjades (temperatura, etc) i les variables independents. Una part de les dades d'estacions meteorològiques s'utilitzen per obtenir el model de regressió i la resta per a validar el model amb dades independents. A partir de diverses variables independents es permet definir diversos models de regressió (usant totes les variables o un subconjunt de les mateixes), el millor dels quals (segons la Cp de Mallows) és seleccionat com a model que més s'apropa a les dades climàtiques reals. El segon pas és obtenir els residuals, és a dir la diferència entre els valors reals de les dades d'entrenament i els valors predits pel model en aquells punts. Aquests residus s'interpolen espacialment usant mètodes d'interpolació local (inversa ponderada de la distància, *splines*, etc) per a obtenir una superfície contínua de residus que permet corregir (millorar) el model obtingut per la regressió. Aquesta regressió és útil per a reduir el nivell d'error global produït pel fet que les variables independents no expliquen tota la variància climàtica espacial. Finalment, el model de regressió és validat, emprant les dades independent reservades, a través d'una regressió simple entre els valors independents observats i els predits.

1.3.2.4 Classificació

Els mètodes d'anàlisi digital basats en classificació de les dades per a la generació d'una cartografia temàtica són els mètodes més estudiats en la Tesi, per tal de cobrir el gran ventall d'opcions disponibles.

En primer lloc, els mètodes de classificació es poden separar en dos grans grups segons l'element de la imatge a classificar: els píxels o grups de píxels (segments).

a) Classificació píxel a píxel

En el primer dels grups, els diversos aspectes de la Tesi han treballat diferents mètodes de classificació píxel a píxel d'entre els mètodes de classificació supervisada i mixta. Dins els mètodes clàssics de classificació supervisada s'ha estudiat l'efecte de la compressió sobre els classificadors de mínima distància i màxima versemblança (implementats a l'aplicació ENVI, ITTVIS 2006) per la classificació de zones de conreus, de l'annex 1. D'altra banda, un mètode de classificació híbrida (HybCls, implementat a l'aplicació MiraMon, Serra *et al.* 2003, Serra *et al.* 2009) ha estat emprat per a classificar les zones de boscos i les zones de conreus (capítol 2 i annex 1).

La classificació híbrida realitzada es basa en un primer pas no supervisat (IsoMM) i un segons pas supervisat en què les classes estadístiques s'assignen a classes temàtiques (ClsMix). IsoMM

es una implementació de l'algorisme IsoData (Duda & Hart 1973). IsoData típicament agrupa píxels d'una escena a un centre de classe prèviament especificat i ho fa amb criteri de mínima distància a través d'un procés iteratiu. Es calculen nous centres de classe segons els píxels incorporats a la fase anterior. El procés es repeteix fins que les assignacions de píxels a centres de classes són suficientment constants o fins que s'arriba a un nombre predeterminat (màxim) d'iteracions. El resultat és un ràster que agrupa els píxels de la imatge original en classes estadístiques i un fitxer per cada categoria estadística amb les seves característiques. La segona part de la classificació híbrida està basada en el mòdul ClsMix de MiraMon, que reclassifica cada classe estadística (d'una imatge classificada no supervisada) en classes temàtiques. Aquestes classes temàtiques són definides a partir d'un conjunt d'àrees d'entrenament (vegeu punt anterior per a descripció de la seva obtenció). ClsMix utilitza bàsicament dos paràmetres per a realitzar la reclassificació. D'una banda, la fidelitat de la classe estadística a la classe temàtica, que és la mínima proporció amb què una classe espectral es troba dins de la classe temàtica a què finalment s'assignarà i que s'expressa en funció de la classe estadística. D'altra banda la representativitat de la classe estadística a la classe temàtica, que és la proporció de la classe estadística dins la classe temàtica en relació a la classe temàtica. El paràmetre fidelitat està relacionat directament amb els errors d'omissió de la classificació. La majoria de píxels que una categoria omet no es confonen amb altres categories sinó que romanen sense classificar. Com més alt és aquest paràmetre, més difícil és que un píxel es classifiqui a una determinada categoria i, per tant, més segurs s'està de l'elecció, aconseguint menors errors de comissió (això sí, a costa de classificat més àrea).

b) Classificació per segments

La classificació d'imatges es realitza tradicionalment caracteritzant amb mesures estadístiques els píxels individuals amb els classificadors supervisats i no supervisats (Xiaoxia *et al.* 2005). D'altra banda, i amb la millora de la resolució espacial de les imatges (com les derivades de sensors aeroportats o satel·litaris d'alta resolució), el nombre d'articles basats tècniques de classificació de grups de píxels o segments (GEOBIA, *GEographic Object-Based Image Analysis*) ha crescut als darrers anys (Blaschke 2010). De fet, un signe d'aquest augment és que el nombre de conferències internacionals i de publicacions a les revistes sobre aquestes tècniques ha augmentat considerablement en els darrers anys. Aquesta metodologia es basa a seleccionar grups de píxels com a objectes per a ser classificats, de manera que és necessari realitzar un procés de segmentació de la imatge previ a la classificació per tal d'obtenir aquests objectes (Conchedda *et al.* 2008 i Ke *et al.* 2010). Hi ha diverses aproximacions a la segmentació, i en aquest cas s'han utilitzat algorismes implementats a l'aplicació Definiens (Baatz *et al.* 2004).

Definiens Professional v.5 té 4 mètodes de segmentació. Una gran part de la literatura suggereix utilitzar l'algorisme de multiresolució (Baatz & Shäpe 2006) com el primer pas de la segmentació per a obtenir objectes homogenis al primer nivell de segmentació. Diversos paràmetres ajustats a cada imatge s'han de definir en aquest nivell: pes de les diferents capes (o imatges), mida d'objectes desitjada, pes del color i la forma i pes de la compacitat i la suavitat (*smoothness*). Després d'establir el primer nivell de segmentació, s'usa l'algorisme de segmentació basat en la diferència espectral per tal de fusionar diversos objectes en un mateix (si és inferior a un llindar definit). La literatura demostra que diferents nivells de segmentació són necessaris per tal d'extreure els límits dels objectes a diferents escales.

c) Avaluació de les classificacions

L'encert de les classificacions obtingudes es realitza a partir de la generació de matrius de confusió (Foody 2002) en relació als encerts i errors de la classificació respecte a un conjunt de dades veritat terreny. La matriu de confusió permet calcular per a cada classificació l'encert global, l'índex Kappa, i els encerts del productor i de l'usuari per cada classe (Campbell 2008). Per a tots els estudis que avaluen els efectes de la compressió (així com també per la majoria dels estudis de canvis d'usos dels sòl) és important ser capaços d'avaluar les classificacions amb la màxima fiabilitat possible.

La millor opció és avaluar la classificació respecte una veritat terreny absoluta el màxim propera en el temps a la data de captació de la imatge. Aquesta aproximació no és molt utilitzada (de fet, si es disposa d'una veritat terreny absoluta actualitzada, per què es voldria obtenir el resultat de la classificació?) però permet avaluar com d'apropiat és el mètode proposat i, doncs, permet validar-lo. Malgrat ser, probablement, l'estratègia més acurada per a calcular els encerts de les classificacions, aquesta no és l'estratègia generalment utilitzada donada la dificultat d'obtenir un mapa de veritat absoluta de la zona d'estudi.

L'aproximació més habitual per al càlcul de l'encert és utilitzar àrees de test independents reservades amb aquest propòsit (com per exemple a Qian *et al.* 2005), ja que és el mètode d'avaluació on el temps de dedicació és més petit en relació a la capacitat d'avaluar els errors generats per la classificació.

Finalment, alguns estudis que avaluen els efecte de la compressió, empren la classificació obtinguda sobre les imatges sense compressió com a veritat terreny per a obtenir l'encert de les classificacions sobre imatges comprimides (com per exemple a Choi *et al.* 2008, Pérez *et al.* 2003). Aquest aproximació, malgrat que té certs avantatges com el fet que l'àrea de comparació

és gran (tota la classificació) i això evita problemes en el càlculs dels encerts (especialment de les categories amb menys representació espacial), té alguns inconvenients com ara el fet que suposa que la classificació sobre les imatges sense compressió no té errors (fet que es rebat fàcilment quan l'avaluació d'aquesta classificació es realitza usant una veritat terreny absoluta o àrees de test independents). Malgrat tot, el fet de ser una estratègia àmpliament utilitzada a la literatura, fa que sigui un mètode d'avaluació a considerar, només pel fet de permetre la comparació de la recerca realitzada amb la literatura prèvia.

En els diversos treballs realitzats s'ha emprat aquestes diverses estratègies d'avaluació. La majoria de treballs empren més d'una d'aquests opcions d'avaluació alhora, fet que enriqueix l'anàlisi de les dades en permetre comparar els resultats obtinguts pels diversos mètodes d'avaluació, que aporten informació complementària.

1.4. CONTRIBUCIONS ESPERADES DE LA TESI

Per a poder donar indicacions sobre els nivells de compressió que hom pot aplicar en cada situació on aquesta pot ser necessària o recomanable, l'impacte de la compressió amb pèrdua sobre les imatges de teledetecció i, en conseqüència, sobre els usos que els científics i tècnics fan d'aquestes imatges és de gran importància. Aquesta compressió, a més, serà en breu aplicada per les pròpies agències en el tractament de les imatges previ a la seva distribució (segment de processament de terra) i fins i tot en els instruments a bord de nous satèl·lits que s'estan dissenyant (per exemple Sentinel-2, Proba-V, SeoSat, etc). Totes aquestes previsions fan necessària l'existència d'informacions, com les aportades per les publicacions presentades, que permetin acotar els efectes de la compressió a diversos escenaris i, d'aquesta manera, definir protocols optimitzats de compressió en relació al punt d'equilibri entre el guany (en espai de disc, ample de banda necessari per les transmissions, etc) i l'impacte de la compressió sobre les imatges i els usos que se'n fan.

1.5. ORGANITZACIÓ DE LA TESI

Els objectius de la Tesi pretenien cobrir diversos escenaris de compressió i generació de cartografia, i això ha donat lloc a diverses publicacions que investiguen l'efecte de la compressió en un cert tipus de mètode de generació de cartografia (usant diversos mètodes de compressió). Aquesta Tesi es presenta com a compendi de publicacions, i està formada per

quatre articles que formen els capítols principals (part fonamental) de la mateixa i per tres articles addicionals (annexos).

L'organització dels capítols s'ha realitzat principalment en funció del mètode emprat per a la obtenció de cartografia. En primer lloc es presenten els treballs que avaluen l'efecte de la compressió quan aquesta és realitzada a **nivell d'usuari**. Dins aquest, l'ordre dels articles presentats és:

- **Anàlisi visual**: El capítol 2 de la Tesi correspon a l'anàlisi de l'efecte de la compressió en la fotointerpretació per a generar cartografia temàtica d'usos del sòl. Aquest article forma part dels *Proceedings* del congrés internacional organitzat el 2008 per la *Society of Photo-optical Instrumentation Engineers* (SPIE, Zabala *et al.* 2008).

- **Anàlisi digital**:

  - Regressió: El capítol 3 de la Tesi avalua l'efecte de la compressió sobre la regressió emprada per a produir dades climàtiques a través de dades de teledetecció i SIG. Aquest article també forma part dels *Proceedings* del congrés internacional organitzat el 2007 per la SPIE (Zabala *et al.* 2007).

  - Classificació: S'ha estudiat dues estratègies de classificació: píxel a píxel i per segments.

    - El capítol 4 de la Tesi estudia l'efecte de la classificació píxel a píxel sobre zones forestals, i ha estat publicat a la revista internacional indexada al JCR-SCI *International Journal of Applied Earth Observation and Geoinformation* (JAG) (Zabala & Pons 2010).

    - El capítol 5 presenta un mètode de codificació del NODATA dins el marc de l'estàndard JPEG 2000 que permet millorar la compressió de les imatges si s'empren les modificacions proposades. L'avaluació de les tècniques de compressió codificades s'ha realitzat usant eines de classificació píxel a píxel per a detectar la coberta d'aigua en una zona de conreus d'arròs i classificar zones de conreus i ha estat publicat a la revista indexada al JCR-SCI *Journal of Applied Remote Sensing (JARS)* (Zabala *et al.* 2010).

    - L'annex 1 presenta l'article sotmès a la revista internacional indexada al JCR-SCI *International Journal of Remote Sensing*, que també avalua l'efecte de la

compressió sobre classificacions realitzades píxel a píxel, en aquest cas en zones de conreus (Zabala & Pons 2010b).

- L'annex 2 presenta un article de l'efecte de la compressió quan el mètode de classificació emprat és aplicat a grups de píxels (prèvia segmentació de la imatge). Una primera versió breu de l'article va ser publicada arrel de la seva presentació al congrés internacional *Geobia'10*, i una versió estesa del mateix ha estat sotmesa per a ser publicada al *Special Issue: Geobia'10* de la revista internacional indexada al JCR-SCI *International Journal of Applied Earth Observation and Geoinformation* (JAG) (Zabala *et al.* 2010b).

D'altra banda, la darrera publicació és en relació a la línia de recerca sobre l'estudi dels efectes de la **compressió** quan aquesta és realitzada **a bord** de la plataforma. Aquesta línia de recerca es va iniciar a principis de 2010 durant l'estada pre-doctoral de sis mesos al centre ESTEC de l'Agència Europea de l'Espai (ESA) a Holanda. Els primers fruits d'aquesta línia de recerca han estat presentats al *2nd International Workshop on On-Board Payload Data Compression (OBPDC)* i són presentat a l'annex 3 (Zabala *et al.* 2010c).

2. IMAGE COMPRESSION EFFECTS IN VISUAL ANALYSIS

Image compression effects in visual analysis

A. Zabala*[a], X. Pons[a,b], F. Aulí-Llinàs[c], Joan Serra-Sagristà[c]
[a] Geography Department
[b] Centre de Recerca Ecològica i Aplicacions Forestals (CREAF)
[c] Dept. of Information and Communications Engineering
Universitat Autònoma Barcelona, 08193, Cerdanyola del Vallès, Barcelona, Spain

ABSTRACT

This study deals with the effects of lossy image compression in the visual analysis of remotely sensed images. The experiments consider two factors with interaction: the type of landscape and the degree of lossy compression. Three landscapes and two areas for each landscape (with different homogeneity) have been selected. For every of the six study area, color 1:5000 orthoimages have been submitted to a JPEG2000 lossy compression algorithm at five different compression ratios. The image of every area and compression ratio has been submitted to on-screen photographic interpretation, generating 30 polygon layers. Maps obtained using compressed images with a high compression ratio present high structural differences regarding to maps obtained with the original images. On the other hand, the compression of 20% obtains values only slightly different from those of the original photographic interpretation, but these differences seem owed to the subjectivity of the photographic interpretation. Therefore, this compression ratio seems to be the optimum since it implies an important reduction of the image size without determining changes neither in the topological variables of the generated vector nor in the obtained thematic quality.

Keywords: image compression, JPEG2000, visual analysis, photointerpretation.

1. INTRODUCTION

In the last years, the increasing number of sensors launched and the higher resolution of these instruments leads to an enormous (and increasing) amount of new data produced. Therefore, data compression has become a habitual processing before producing final products, especially those bound to visual exploitation. Lossy compression, *i.e.* the one sacrificing part of the data in order to achieve more compression ratio, is one of the most powerful data compression techniques. In 1991 JPEG first appeared [1],[2], proposed by the *Joint Photographic Experts Group*. This compression standard was a revolution because it achieved compression ratios of 20% of the image without substantial visual differences. Further on, compression schemes based on wavelet transform achieved even higher compression levels for similar visual quality. Among those, last years SID, ECW and JPEG2000 [3],[4] compression standards have been used on Remote Sensing (RS) and Geographic Information System (GIS) communities'.

In spite of these compression results, few studies have been carried out to evaluate quantitatively the effects of compression on image applications. Referring to geometric and visual analysis image quality, [5] conclude that JPEG compression ratios of 10% maintained an excellent visual quality and thus the images are useful for many photogrammetric applications. The same JPEG compression ratio can be applied to images before using them to generate a Digital Elevation Model (DEM) [6], even though the more texture richness the more image degradation at he same compression ratio. [7] compare JPEG and JPEG2000 and conclude that this loss of quality related to image texture is less prominent using JPEG2000 compression standard, and that in all quality image measures JPEG2000 obtains better results than JPEG, specially at higher compression levels.

According to literature results [7],[8],[9], JPEG2000 compression standard is used due to its better results and its higher compression capacity. This paper evaluates the influence of JPEG2000 compression format on image photointerpretation to generate land cover maps.

*alaitz.zabala@uab.cat; phone +34 935 814 343.

Satellite Data Compression, Communication, and Processing IV
edited by Bormin Huang, Roger W. Heymann, Joan Serra-Sagrista
Proc. of SPIE Vol. 7084, 70840I, (2008) · 0277-786X/08/$18 · doi: 10.1117/12.798572

2. METHODOLOGY

2.1 Experimental Design

Digital 1:5000 color orthoimages (pixel of 0.5 m) produced by *Catalan Cartographic Institute* on 2000 are used to generate land cover maps of six study areas, each over a different landscape and fragmentation. Chosen areas represent next landscapes: homogeneous agricultural, heterogeneous agricultural, homogeneous forest, heterogeneous forest, homogeneous urban and heterogeneous urban.

Images are subjected to a photointerpretation process in the same way that the used to produce second edition of *Soil Land Cover Map of Catalonia* (MCSC-2) [10]. This photointerpretation is repeated six times over each area, because it has been executed once for each of the five compression ratios studied and once for the original images.

Compression ratio is generally expressed as a percentage or a per unit quantity. Sometimes the expression "1/CR : 1" is also used (where CR is the compression ratio per unit). On this paper image compression has been computed as compression ratios (CR), defined as size of the compressed file and the original file, and hereafter it will always be used in percentage:

$$CR = \frac{Compressed \quad file \quad size}{Original \quad file \quad size} x100$$

For example if a 10 Mb file is compressed to a 2 Mb file, the compression ratio achieved is 20% (used in this paper), 0.20 or 5:1.

It is necessary to bear in mind that the same compression ratio can imply different image quality, depending on image type and content (*e.g.* spatial fragmentation). This is the reason why three landscapes have been chosen with two different areas for each landscape, with different spatial fragmentation.

2.2 Study areas

Six study areas, representative of three selected landscapes have been selected. All areas are on Catalonia, a region at NE of Spain (see Fig. 1) and each area covers a region of about 850 ha.

Areas have been chosen using the advice of the MCSC-2 team, who has an expert knowledge of the Catalan area and its landscapes. For all the selected areas, the photointerpretation over the original images on the homogeneous area has fewer polygons than the photointerpretation of the heterogeneous area. The homogeneous agricultural has 284 polygons and the heterogeneous has 457. The homogeneous forest has 102 polygons and the heterogeneous has 510. Finally, the homogeneous urban has 192 polygons and the heterogeneous has 307.

The homogeneous agricultural area (in yellow and with left oblique lines in Fig. 1) is centered in the region of Alt Penedès, focusing on the towns of Vilobí del Penedès, Sant Martí Sarroca and Font-Rubí. The original image has 7002 columns and 4914 rows of 0.5 m pixel size making a total of 860.2 ha. 80% of the image is covered by crops, 6% by shrubs, 5% by urban areas, 4% by dense forests and 2% by riparian forests. Other minority land covers present in the study area are: urban bare soil, mining areas, water bodies, open forests, communication ways, sport and leisure facilities and bare rocks (all of them less than 1%). Heterogeneous agricultural area (in orange and with horizontal lines in Fig. 1) is focused on the region of Bages, focusing on the towns of Sant Fruitós de Bages, Manresa and Sant Joan de Vilatorrada. The original image is 7014 columns and 4970 rows of 0.5 m pixel size making a total of 871.5 ha. 63% of the area is covered by crops, 13% by shrubs, 12% by urban areas, 6% by dense forests, 1% by urban bare soil and 1% by communication ways. Other minority classes, covering less than a 1% each, are sport and leisure facilities, water bodies, natural bare soil, riparian forests, meadows, open forests and bare rocks. The 1:5000 orthoimages over agricultural selected areas are shown in Fig. 2.

The homogeneous forest area (in light green and with horizontal and vertical lines in Fig. 1) is located south of the Osona county, focusing on the towns of El Brull, Tagamanent and Viladrau. This area is located entirely within the protected space of PEIN Massís del Montseny. The original image is 7096 columns and 5045 rows of 0.5 m pixel size making a total of 895.0 ha. 88% of the image is covered by dense forests, 9% by shrubs, 1% by open forests and 1% by bare rocks. Classes covering less than 1% each are: crops, urban bare soil, natural bare soil, burned areas and urban areas. The heterogeneous forest area (in dark green and with right oblique lines in Fig. 1) is located north of the county of Vallès Occidental, particularly over the municipalities of Terrassa, Vacarisses and Matadepera. This area is almost entirely within the protected space of PEIN Sant Llorenç del Munt i l'Obac. The original image is 7050 columns and 4994 rows

of 0.5 m pixel size making a total of 880.2 ha. 80% of the study area is covered by dense forests, 10% by shrubs, 4% by bare rocks, 3% by urban areas and 1% by open forests. Minority land covers are: natural bare soil, urban bare soil and crops. The 1:5000 orthoimages over forest selected areas are shown in Fig. 3.

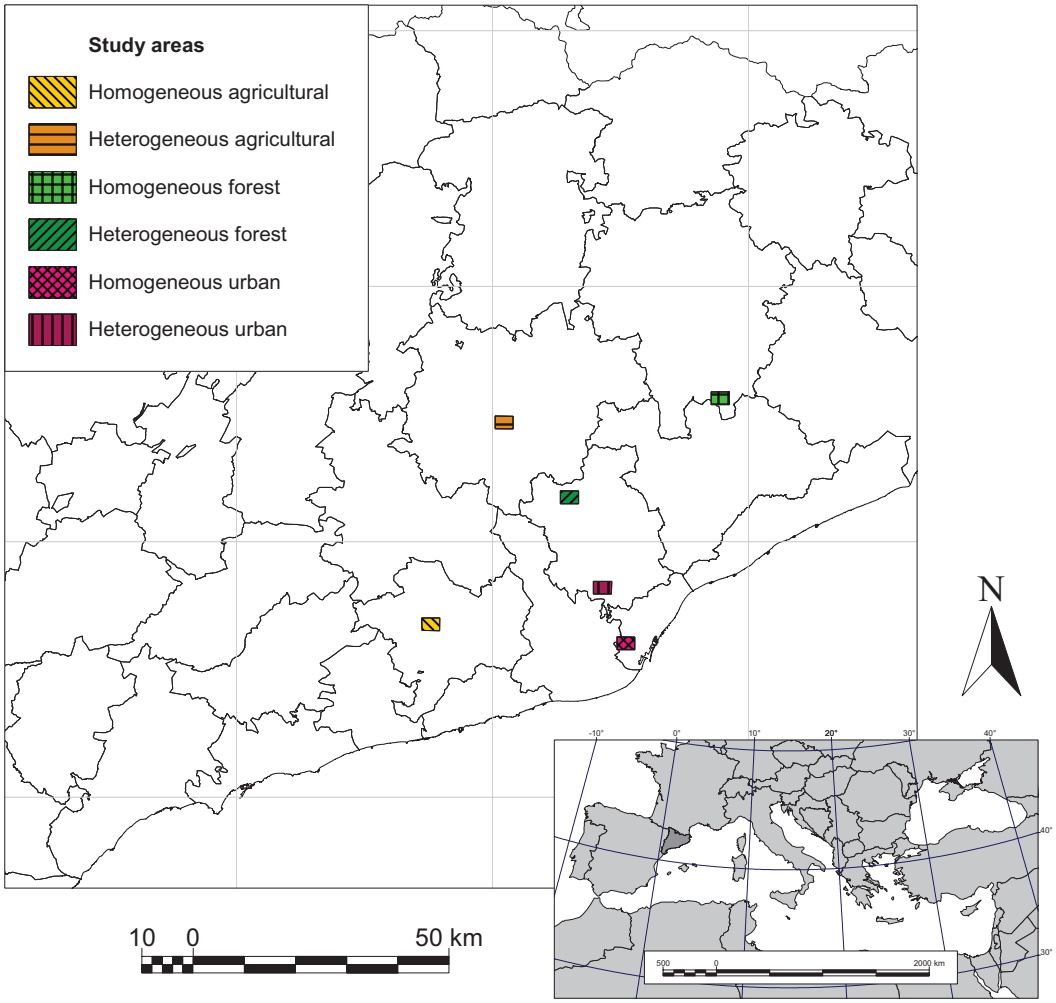

Fig. 1. Situation of the study areas in the context of the Catalan region (NE of Spain).

Fig. 2. 1:5000 orthoimages of the agricultural areas: homogeneous (left) and heterogeneous (right).

The homogeneous urban area (in pink and with left and right oblique lines in Fig. 1) is located mainly in the southwest of the county of Barcelona, in the municipality of Barcelona, and also contains a small portion of the municipalities of L'Hospitalet de Llobregat and Esplugues de Llobregat in the Baix Llobregat county. The original image is 7002 columns and 4976 rows of 0.5 m pixel size making a total of 871.0 ha. 84% of the image is covered by urban areas, 5% by urban bare soil, 4% by shrubs, 3% by communication ways, 1% by sport and leisure facilities and 1% by dense forests. Crops, meadows, *Platanus spp.* plantations and open forests are only slightly represented on this area. Finally, the heterogeneous urban area (in purple and with vertical lines in Fig. 1) is located south of the county of Vallès Occidental, specifically on the town of Sant Cugat del Vallès. The original image is 7107 columns and 5034 rows of 0.5 m pixel size making a total of 894.34 hectares. 61% of the area is covered by urban areas, 15% by shrubs, 13% by dense forests, 3% by sport and leisure facilities, 3% by crops, 3% by urban bare soil and 1% by communication ways. Less represented land covers are: riparian forests, *Platanus spp.* plantations, open forests and natural bare soil. The 1:5000 orthoimages over urban selected areas are shown in Fig. 4.

Fig. 3. 1:5000 orthoimages of the forest areas: homogeneous (left) and heterogeneous (right).

Fig. 4. 1:5000 orthoimages of the urban areas: homogeneous (left) and heterogeneous (right).

2.3 Preparation of orthoimagery

To obtain orthoimagery of selected areas (Fig. 2, Fig. 3 and Fig. 4) it has been necessary to make a mosaic from the original orthoimagery produced by *Catalan Cartographic Institute*. In most cases, the mosaic has not introduced difficult to the photointerpretation, only sometimes a change of tone between adjacent images. In some cases, due to various orientations on image acquisition and generally in urban areas, mismatch areas are visible between adjacent images because they are not vertical at all points (true ortho). These imbalances can be also easily solved by the photointerpreter.

2.4 Image compression

JPEG2000 is a compression format designed following the requirements defined in the JPEG2000 Working Group [3]. These requirements were taken into account to develop a new coding system with greater flexibility, allowing the user to

parameterize all stages of compression and decompression. Some of its features are support to multi-components, variable bits per pixel for each component, regions of interest support, error correction, etc.

The compression and decompression application used was BOÍ (previously called J2K), an implementation developed by the Department of Information and Communications Engineering (dICE) from the Autonomous University of Barcelona [11] that implements Part 1 of JPEG2000 standard.

For each of those areas of study the 3 bands of color orthoimage (R, G and B) have been compressed to generate a single JPEG2000 compressed file. This jointly compression benefits of preserving as much information from the three bands together, allowing to keep more information of any of the color components if necessary. A lossy compression has been realized over original images, defining the desired size of the compressed file to reach some predefined compression ratios. The compression ratios studied are 20%, 10%, 5% and 1%. A lossless compression, hereafter WL (that stands for without loss), is also done over the images. Photointerpretation has been carried out over recovered files.

2.5 Photointerpretation

The photointerpretation process is identical to that used in the second edition of *Soil Land Cover Map of Catalonia* (MCSC-2) [10]. The photointerpretation and digitization of the areas has been done on a computer screen, allowing the use of other digital cartographic elements as direct support to the process. 1:5000 orthoimages and its compressed versions (at defined compression ratios) have been use as the base material for the photointerpretation. In this task the GIS and RS software MiraMon has been used [12].

Working scale is around 1:1500, possible by the high resolution orthoimagery (0.5 m pixel). The minimum digitization area is 500 m^2. These features give the MCSC-2 and maps generated following the same methodology, as presented in this article, a high level of detail and high planimetric precision [10].

MCSC-2 has three different levels of thematic resolution, similar to other land cover maps as *Corine Land Cover map* [13] of the European Environment Agency. For purposes of this study, the intermediate legend level (level 2), with 24 thematic categories, was selected. Table 1 shows the categories defined in levels 1 and 2 of the MCSC-2.

Table 1: MCSC-2 legend categories (levels 1 and 2).

Level 1	Level 2
Forest land	Dense forests
	Riparian forests
	Reforested areas
	Populus spp. plantations
	Platanus spp. plantations
	Open forests
	Burned areas
	Shrubs
	Wetland vegetation
	Meadows
	Bare rocks
	Sloppy rocky ground
Forest land	Natural bare soil
	Beaches
	Glaciers and perpetuals snowfiels
Water bodies	Water bodies
Crops	Crops
	Agricultural canals and ponds
Unproductive artificial	Urban areas
	Urban ponds
	Communication ways
	Sport and leisure facilities
	Mining areas
	Urban bare soil

The photointerpretation process has been made by one person to minimize differences that might be introduced by difference in criterion among different photointerpreters. In a study comparing baseline data produced by different photointerpreters [14], the greatest similarity is among data produced by the same photointerpreter. To minimize the effect of "remembrance", the six study areas were photointerpreted alternatively. The order followed on photointerpretation has considered first homogeneous and secondly heterogeneous areas. Forest landscape has been the first photointerpreted, followed by agricultural area and, finally, urban area. Therefore, the final photointerpretation order has been: homogeneous forest, homogeneous agricultural, homogeneous urban, heterogeneous forest, heterogeneous agricultural and heterogeneous urban.

Regarding compression, photointerpretation has been initiated with the more compressed images, to avoid that the memory of "more detailed" images (less compression) masked possible errors with images of higher compression. Therefore, the photointerpretation has been done first of all with the images compressed at a 1% compression ratio

(following the landscapes order stated above), and then for other compression ration in increasing order (5%, 10% and 20%) to end with the images compressed without loss (WL images).

Attempts have been made to assess the subjectivity of the photointerpreter itself, *i.e.*, changes produced when digitizing the same area twice for the same photointerpreter. To get a measure of this subjectivity, and be able to differentiate these changes from those introduced by the compression, a second photointerpretion has been done using WL images. This photointerpretation was made one month and a half after finishing the previous ones, to be as independent as possible with the previous ones, and it is indicated in the results as "WLb".

These processes have generated a set of 36 polygon layers, one for every area and compression ratio (WL photointerpreted twice).

2.6 Parameters analyzed

The first set of parameters has been used to assess the impact of compression on the geometry and topology vectors obtained at different compression ratios (CR). Three parameters have been chosen: vertices number, polygons number and the total length of arcs of the digitized vector (arcs length).

Secondly the effect of compression on the thematic vectors accuracy has been evaluated. The measure used for this evaluation is the success percentage, regarding the vector layer obtained on images compressed without loss (WL). Besides of the general thematic quality, comparative analyses have been also carried out on the effects of the compression on the different categories of the legend. The parameter used to evaluate this per-category thematic accuracy is the percentage of each category that is maintained on the vector generated from the compressed images, thus if all the dense forests of the reference vector is present on the evaluated vector, a 100% will be computed without considering that the evaluated vector may have some other densely forested areas.

3. RESULTS

The objective of this study is to assess the effect of compression in the photointerpretation, and that is why it has been deemed sufficient to make comparisons on landscape structure and thematic quality taking layer vector obtained from the images compressed without loss (WL) as the value pattern.

3.1 Parameters assessing geometric and topological structure of the obtained vectors

Table 2 and Fig. 5 show different parameters relating to the structure or complexity of landscape. For each of these parameters Table 2 shows, in columns, the values calculated with the vector layers obtained from the images compressed at different CRs. Fig. 5 shows, for each of these three parameters, the percentage of the value of the parameter regarding the value of the layer used as a pattern (WL). All the parameters show the effort generating the layer and its structural complexity. As can be seen in Table 2, generally, the more compressed images, the less obtained landscape complexity.

Number of drawn vertices decreases at higher compression (lower CR). This trend can be observed for most landscapes as well as for the mean. Differences introduced by the photointerpreter subjectivity are, on average, around 6% (difference of WL and WLb). The change in vertices number of the image compressed at 20% is of the same order as this internal variability. By contrast, lower CRs (high compressions) imply a superior variation on this parameter, what it is supposed to be caused by changes in the image due to compression. With images compressed at 10% an average of 81% of the vertices are drawn, and in the case of the highest compressed images (0.1%), only a 67% of the vertices are drawn (in mean).

With regard to the number of polygons drawn the situation is similar. On average the number of polygons drawn decreased at higher compression. The variation in the number of polygons drawn with images compressed at 20% is in the same order than the number of polygons on WLb (photointerpreter subjectivity), in this case 5%. The highest compression scenario present accused differences with the reference vector layer (only 53% of polygons drawn).

Finally, the arcs length also presents a similar trend with a variation of only 4% of total length due to the photointerpreter subjectivity. The variation of the photointerpretation on the image compressed at 20% is, again, of the same order to that due to the subjectivity (4%) and, on the other hand, photointerpretations carried out over more compressed images have more diverting results up to 27% on the highest compression scenario.

The three studied parameters can be significantly adjusted using a quadratic model ($y = b_0 + b_1x + b_2x^2$) from CR. Table 3 shows the different parameters of these adjustments.

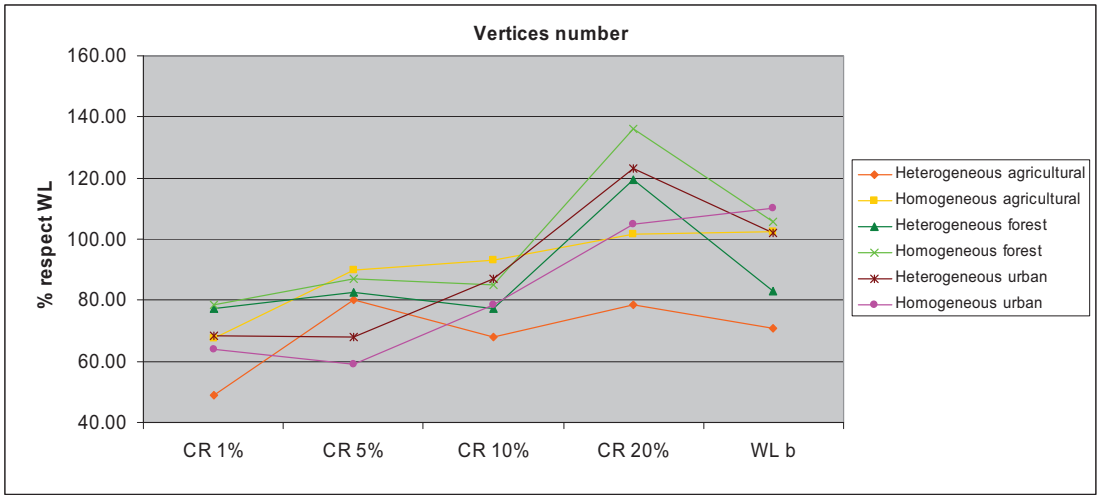

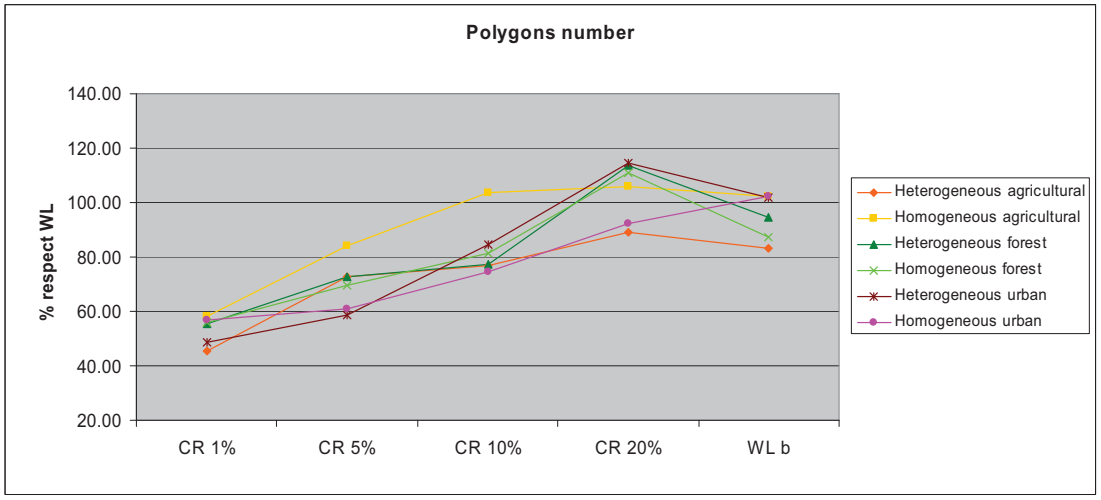

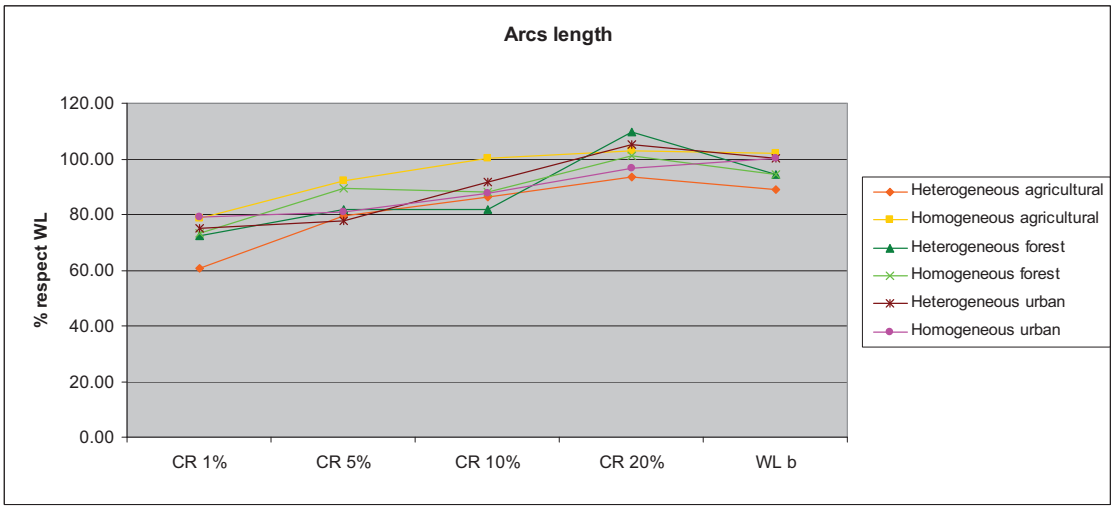

Fig. 5: Structure parameters.

Table 2: Structure parameters.

Vertices number	**CR 1%**	**CR 5%**	**CR 10%**	**CR 20%**	**WL**	**WLb**
Heterogeneous agricultural	5471	8982	7600	8786	11197	7941
Homogeneous agricultural	3966	5278	5472	5985	5886	6030
Heterogeneous forest	10543	11308	10593	16347	13673	11371
Homogeneous forest	2606	2887	2822	4518	3323	3507
Heterogeneous urban	3627	3620	4629	6555	5316	5424
Homogeneous urban	1805	1660	2212	2950	2817	3105
Mean	*4669.67*	*5622.5*	*5554.67*	*7523.5*	*7035.33*	*6229.67*
Polygons number	**CR 1%**	**CR 5%**	**CR 10%**	**CR 20%**	**WL**	**WLb**
Heterogeneous agricultural	207	332	351	408	457	380
Homogeneous agricultural	165	239	294	301	284	290
Heterogeneous forest	282	370	393	579	510	483
Homogeneous forest	57	71	83	113	102	89
Heterogeneous urban	150	180	260	351	307	312
Homogeneous urban	109	117	143	177	192	196
Mean	*161.67*	*218.17*	*254*	*321.5*	*308.67*	*291.67*
Arcs length (km)	**CR 1%**	**CR 5%**	**CR 10%**	**CR 20%**	**WL**	**WLb**
Heterogeneous agricultural	100.6138	132.5542	143.3636	155.5443	166.2873	147.7366
Homogeneous agricultural	81.2846	95.0097	103.2292	106.0115	103.1064	105.1882
Heterogeneous forest	127.9531	145.106	145.1853	194.2165	177.1139	167.3393
Homogeneous forest	44.8273	54.6195	53.7571	61.7569	61.1317	57.8230
Heterogeneous urban	102.8867	106.3192	125.1035	143.8422	136.7258	137.2872
Homogeneous urban	62.4976	64.1244	69.3053	76.3722	79.0698	79.3792
Mean	*86.67*	*99.62*	*106.66*	*122.96*	*120.57*	*115.79*

3.2 Thematic quality

To assess the thematic quality, it has been computed the confusion matrix of the analytical combination between the vector layer at each CR and the pattern vector layer. To calculate this confusion matrix, vectors are internally rasterized using a standard image pixel 0.5 m, because it is the resolution of the original images and consequently is the highest resolution expected in the vectors obtained.

a) Success percentage

Fig. 6 shows the success percentage for each scenario, computed as a percentage of the number of cells where the vector obtained from compressed images has the same category than the vector obtained from original images.

The variation of success percentage with compression presents a decreasing trend at higher compression (lower CR). Even though the change in the success produced by the subjectivity of photointerpreter (5.4%) is only slightly different that most of the observed changes in other compression ratios (6.1% to 11.4%), the trend to diminish the success at higher compression seems clear. This parameter can be significantly adjusted using a logarithmic model ($y = b_0 + b_1 \ln x$) from the compression ratio. Table 3 shows the different parameters of this adjustment.

Table 3: Regression adjustment parameters.

Indicator	**Model**	**R^2**	**df**	**F**	**P**
Vertices number	quadratic	0.953	2	20.13	0.047
Polygons number	quadratic	0.993	2	138.66	0.007
Arcs length (km)	quadratic	0.984	2	61.93	0.016
Success percentage	logarithmic	0.873	3	20.63	0.02

b) Maintained percentage of each category

Fig. 7 shows the maintained percentage of each category (in percentage referred to WL) for each type of landscape and CR. Only those categories with an area (at WL vectors) greater than 1% on the vectors from the original images are computed. The order of categories in each graphic of this figure is defined by the area of the category on the landscape (refer to section 2.2 for the area of each category on each landscape for WL vectors).

For all the pixels of the internally rasterized vector from the original images, it is computed if the pixel has the same category on the internally rasterized vector from the compressed images. Then the total percentage of each category on the vectors from original images is computed related to vectors from compressed images. Thus the 98.4% of crops on the homogeneous agricultural area on CR 20% (see Fig. 7, first graphic) means that there are 1.6% of pixels of the internally rasterized vector from the original images that are not crops on the internally rasterized vector from the compressed images.

A general trend can be observed on Fig. 7 that is consistent with the results of the previous subsection (success percentage): as CR decreases (more compressed images) all the categories on all the landscapes have a lower maintained percentage.

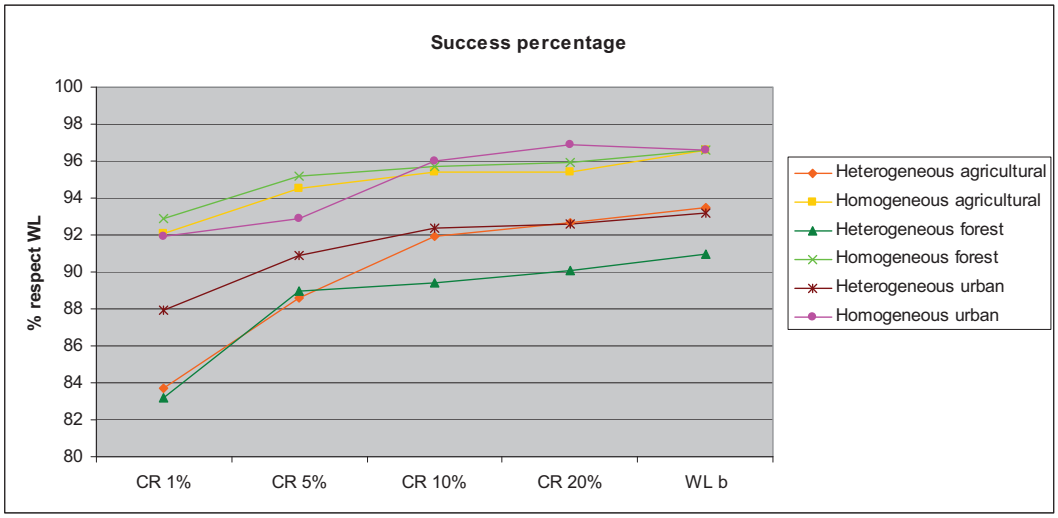

Fig. 6: Values of success percentage (in % referred to WL) for each type of landscape and compression ratio.

Table 4: Mean of loss of maintained percentage (100 – maintained percentage) of each category for all the landscapes (or groups of landscapes) ordered by the loss of maintained percentage on WLb.

	CR 1%	CR 5%	CR 10%	CR 20%	WLb
Crops (without urban landscapes)	1.9	1.7	2.1	2.0	1.6
Dense forests (only forest landscapes)	5.9	3.9	2.8	3.9	2.6
Urban areas (only urban landscapes)	2.1	1.5	2.1	2.8	2.8
Crops (all)	5.8	4.1	4.2	2.8	3.2
Crops (only urban landscapes)	13.8	9.0	8.4	4.5	6.5
Communication ways	11.0	8.4	6.6	7.0	6.7
Riparian forests	8.2	5.6	7.2	22.8	7.9
Urban areas (all)	13.8	7.7	9.5	9.8	10.1
Sport and leisure facilities	27.2	17.5	12.7	11.1	10.4
Dense forests (all)	22.9	27.0	18.9	11.8	12.6
Shrubs	45.4	29.1	22.4	16.8	14.9
Urban areas (without urban landscapes)	21.7	11.8	14.4	14.4	15.0
Urban bare soil (only urban landscapes)	34.7	26.0	20.4	16.3	16.7
Dense forests (without forest landscapes)	31.4	38.6	27.0	15.8	17.6
Bare rocks	25.8	18.1	24.4	15.4	20.2
Urban bare soil (all)	47.1	36.5	30.2	26.4	22.7
Urban bare soil (without urban landscapes)	72.0	57.5	50.0	46.6	34.8
Open forests	54.8	35.3	41.3	49.1	57.6

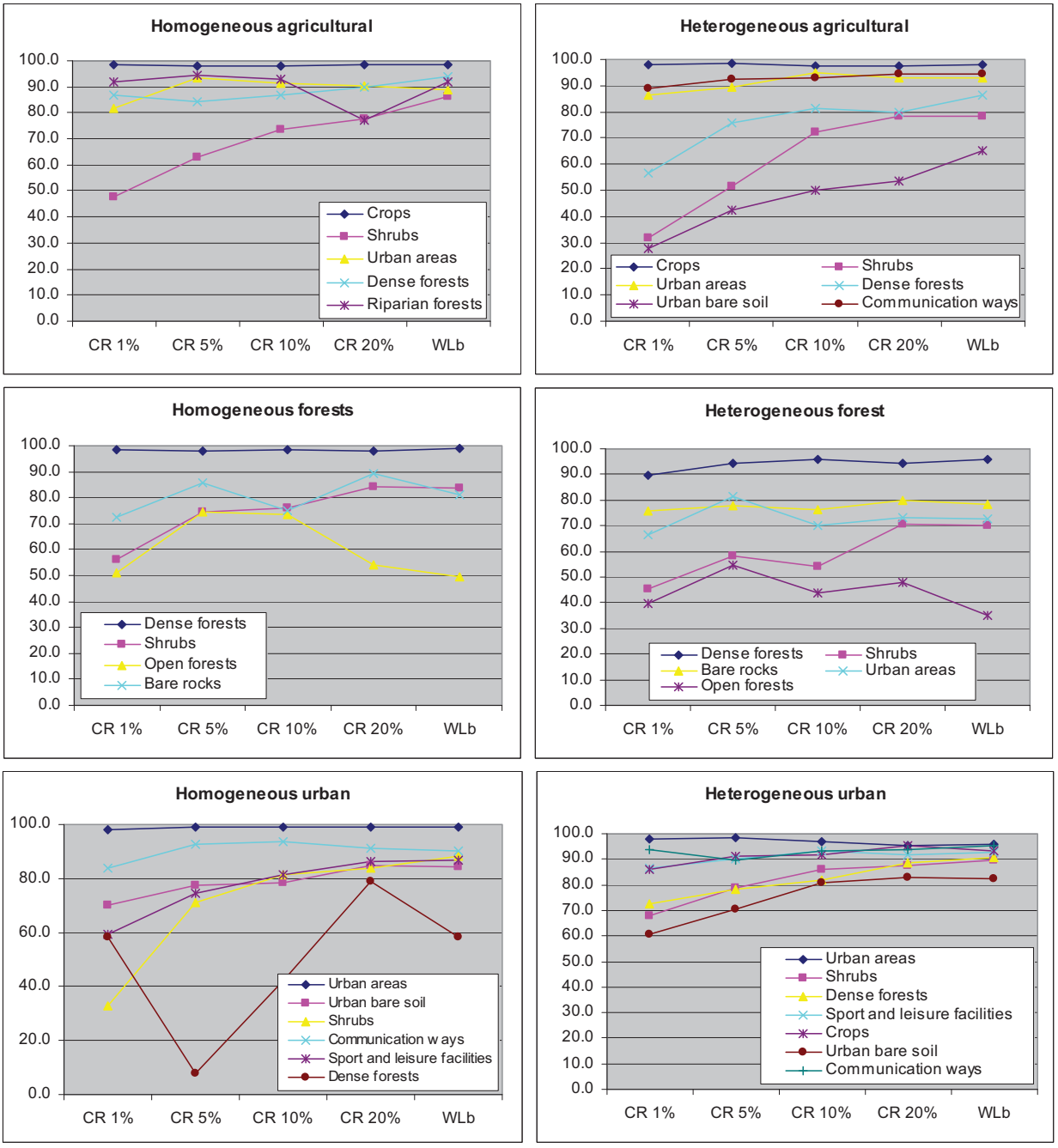

Fig. 7: Values of maintained percentage of each category (in % referred to WL) for each type of landscape and CR

Comparing different categories, it is worth to note that the capacity of the photointerpreter to recognize some categories is higher than for others categories. Observing WLb column of Table 4 it can be stated which categories are easily recognized on different landscapes. “Crops”, “Dense forests” (on forest landscapes) and “Urban areas” (on urban landscapes) are those categories easily photointerpreted. Among the hardest categories to be recognized for the photointerpreter there are “Bare rocks”, “Urban bare soil” and “Open forests”.

Regarding the effect of compression on the maintained percentage of each category, the difference between the lower and higher values of the maintained percentage at different CRs is computed (see Table 4). Thus, “Crops” category is the

less affected by the compression because the difference of maintained percentage for this category is only of 3 points. "Communication ways" and "Urban areas" categories are the next categories less affected by compression with a variation of only 4.4 and 6.2 points respectively of maintained percentage at different CR. Among the categories highly affected by compression "Open forests", "Urban bare soil" and "Shrubs" can be cited with a variation of 22.4, 24.4 and 30.5 points respectively.

4. CONCLUSIONS

At high compression levels (low CR) vectors obtained by photointerpretation present high differences on geometric and topological structure respect to the vectors obtained with the original images. Generated vectors at low CR have less vertices, polygons and arcs length. For each type of landscape, these differences are more pronounced in the heterogeneous areas. In general, and according to the structure of geometric and topological vectors obtained, the 20 % compression obtained values slightly different from the photointerpretation on the original images, but these differences seem due to the subjectivity of the photointerpreter. Therefore, this compression ratio seems to be the optimum since it implies an important reduction of the image size without determining changes neither in the topological variables of the generated vector nor in the obtained thematic quality. These results could be modified in other types of landscapes or using a legend with a larger number of categories.

It is worth to note that effects of compression on land cover classification is very different among several land covers as the capacity of the photointerpreter of recognizing some of them, *e.g.* crops, is slightly affected by compression and on the other hand, other categories are worse recognized at higher compression levels, *e.g.* shrubs.

Acknowledgments

This work has been partially supported by Spanish and Catalan Governments, by FEDER, through the research projects TIC2003-08604-C04-03 and TSI2006-14005-C02. We also want to thank our colleagues in CREAF for the help with the photointerpretation process, specially to Joan Pino, for his support on some of the design, execution and analysis of the research exposed on this paper .

REFERENCES

[1] ISO/IEC 10918-12 (1994): Digital compressing and coding for continuous-tone still images.

[2] Wallace G.K. (1991): "The JPEG still picture compression standard". *Communications of the ACM*, 34 (4):30-44.

[3] ISO/IEC 15444-1 (2000): JPEG2000 image coding system - Part 1: Core coding system.

[4] Taubman D.S., Marcellin M.W (2002): *JPEG2000: Image compression fundamentals, standards and practice*. Kluwer, Academic Publishers.

[5] Li, Z.L.; X.X. Yuan, W.K.K. Lam (2002): "Effects of JPEG compression on the accuracy of photogrammetric point determination". *Photogrammetric Engineering and Remote Sensing*, 68(8): 847-853.

[6] Lam, W.K.K; Z.L. Li, X.X. Yuan (2001): "Effects of JPEG compression on the accuracy of digital terrain models automatically derived from digital aerial images". *Photogrammetric Record*, 17 (98): 331-342.

[7] Shih, T.Y.; J.K. Liu (2005): "Effects of JPEG2000 compression on automated DSM extraction: Evidence from aerial photographs". *Photogrammetric Record*, 20 (112).

[8] Zabala, A.; X. Pons, J. Masó, F. García, F. Aulí, J. Serra (2005): "Evaluation of JPEG and JPEG2000 effects on remote sensing image classification for mapping natural areas". *WSEAS TRANSACTIONS on INFORMATION SCIENCE and APPLICATIONS*. 2 (6): 717-725. ISSN: 1790-0832.

[9] Zabala, A.; X. Pons, R. Díaz-Delgado, F. García, F. Aulí-Llinàs, J. Serra-Sagristà (2006): "Effects of JPEG and JPEG2000 Lossy Compression on Remote Sensing Image Classification for Mapping Crops and Forest areas", In: *26th International Geoscience and Remote Sensing Symposium. IEEE Press*, Denver, Colorado, USA, vol. II, 790-793, August 2006.

[10] Burriel, J.A., Ibáñez, J.J. & Pons, X. (2005): "Segunda edición del Mapa de Cubiertas del Suelo de Cataluña: herramienta para la gestión sostenible del territorio". *Actas del IV Congreso Forestal*.

[11] Aulí-Llinàs, F.; J.R. Paton, J. Bartrina-Rapesta, J.L. Monteagudo-Pereira, J. Serra-Sagristà (2005): "J2K: introducing a novel JPEG2000 coder". In: SPIE, IST (Ed.) *Visual Communications and Image Processing. Society of Photo-optical Instrumentation Engineers* (SPIE), Beijing, China.

[12] Pons, X. (2005): MiraMon. Sistema de Información Geográfica y software de Teledetección. Centre de Recerca Ecològica i Aplicacions Forestals, CREAF. Bellaterra. ISBN: 84-931323-5-7.

[13] European Environment Agency (1995): "CORINE land cover". Disponible en: http://www.eea.europa.eu.

[14] Mann, S and Rothley, K. D. (2006): "Sensitivity of Lansat/IKONOS accuracy comparison to errors in photointerpreted reference data and variations in test point sets*". International Journal of Remote Sensing*. Vol. 27, No 20, 5027-5036.

3. IMPLICATIONS OF JPEG 2000 LOSSY COMPRESSION ON MULTIPLE REGRESSION MODELLING

Implications of JPEG2000 lossy compression on multiple regression modelling

Alaitz Zabala*[a], Xavier Pons[a,b], Francesc Aulí-Llinàs[c], Joan Serra-Sagristà[c]
[a]Dep. of Geography, Universitat Autònoma de Barcelona;
[b]Center for Ecological Research and Applied Forestry;
[c]Dep. of Information and Communications Engineering
Universitat Autònoma de Barcelona - 08290 Cerdanyola del Vallès, SPAIN

ABSTRACT

Multiple regression is a common technique used when performing digital analysis on images to obtain continuous, quantitative, variables (as temperature, biomass, etc). In this scenario pixels are treated as samples from which several independent variables are known; when remote sensing images are available, the different spectral bands offered by a given sensor are often used as independent variables. The dependent variable is also a quantitative variable, such as a forest inventory variable or a climate variable (*e.g.*, temperature). This paper presents an evaluation of the implications of JPEG2000 lossy compression when applied to these regression processes. Annual minimum and annual mean air temperature are modelled using two methods according to the independent variables used: only geographical, and geographical and remote sensing images as independent variables. Raster matrix representing independent variables were compressed using compression ratios from 50% up to 0.01% of the original file size. Results have revealed that, even at high compression ratios, practically the same accuracy, measured with independent reference climatic stations, is obtained, so JPEG2000 seems an interesting technique not heavily affecting these common modelling approaches.

Keywords: JPEG2000, lossy compression, multiple regression.

1. INTRODUCTION

The increasing availability of a great number of Remote Sensing (RS) images (multi and hyperspectral), orthophotos, etc, and their use in Geographical Information Systems (GIS), is leading to perform research of compressing techniques in order to achieve appropriate compressing strategies of these images to be used in RS (classification, photo-interpretation, etc) and GIS (spatial analysis, modelling, etc). In 1991 the JPEG format[1,2], developed by the Joint Photographic Experts Group, appeared and revolutionized image compression due to the fact that it achieves very high compression ratios with no appreciable loss of image quality, at least for file sizes up to approximately 20 % of the original. Later on other compression techniques appeared based on wavelet transformations which permit even higher compression ratios with similar image quality. In recent years, SID, ECW and JPEG2000 formats[3] have become popular among the RS and SIG community. It is important to bear in mind that in every case we are dealing with lossy compression algorithms, which sacrifice part of the data in order to achieve a higher compression ratio.

In spite of the spectacular nature of the compression ratios achieved, there has been not much quantitative analysis of the implications of these compressions. Some studies have been carried out to obtain implications of lossy compression on geometrical and visual quality[4] and on Digital Elevation Model (DEM) generation[5,6]. Their general conclusion is that if the compressed imaged size is 10% of the original image size there is no influence on image quality or on the quality of the DEM generated. Regarding thematic quality, results obtained in classifications in previous studies where not conclusive[7,8,9,10] but recent ones conclude that a compression ratio of 0.4 can be used in the worse case[11].

Air temperature is an essential descriptor of Earth environmental conditions because it regulates important biogeochemical processes such as physiology of organisms, soil formation, atmospheric dynamics, etc. Meteorological stations provide data point measurements about air temperature, but to analyse such information upon a large and heterogeneous area it is necessary to use a continuous surface[12].

*alaitz.zabala@uab.cat; phone +34 935 813 273; fax +34 935 812 001.

Remote Sensing for Environmental Monitoring, GIS Applications, and Geology VII, edited by Manfred Ehlers, Ulrich Michel,
Proc. of SPIE Vol. 6749, 674918, (2007) · 0277-786X/07/$18 · doi: 10.1117/12.738028

An usual approach to air temperature mapping consist on multiple regression modelling using geographical variables such as latitude, elevation, continentality, etc. as independent variables, and climatic data (*e.g.*, air temperature coming from meteorological stations) as dependent variables[13]. On the other hand, some studies use only satellites images or remote sensing derived variables such as land surface temperature, NDVI or albedo[14,15,16] to model air temperature. A few studies combine geographical and remote sensing variables[17,18], obtaining better results on air temperature modelling than when using only geographical variables.

This study aims to assess the influence of image lossy compression on annual air temperature modelling based on the authors' own experience and on that cited studies. So that, it seemed interesting to study the case of maximum success (annual mean temperature) and the case of maximum difficulty (annual minimum temperature) to be modelled. These two climatic elements are modelled on this study to observe compression influence on these extreme modelling situations. On the other hand, and regarding to independent variables used on the modelling process, two approaches have been studied. First of all, modelling air temperature using only geographic variables has been chosen because is a widely used approach. Alternatively, combined models (using geographical and remote sensing variables) have also been tested.

2. STUDY AREA

Due to data available two study areas are used. Iberian Peninsula is in the south-west of Europe, between 10° 07' W and 2° 54' E (~1000 km) longitude, and between 35° 49' and 43° 42' N (~850 km) latitude. We used the Universal Transverse Mercator (UTM) projection in this study. Since the Iberian Peninsula is covered by 3 UTM zones (29, 30 and 31), we have selected the central zone (UTM-30N) as the reference system. The map from the Portuguese side has been reprojected from the Gauss-Krüger projection to the UTM projection using geodetic methods. Models using only geographic variables have available data for the whole Iberian Peninsula (see Fig. 1).

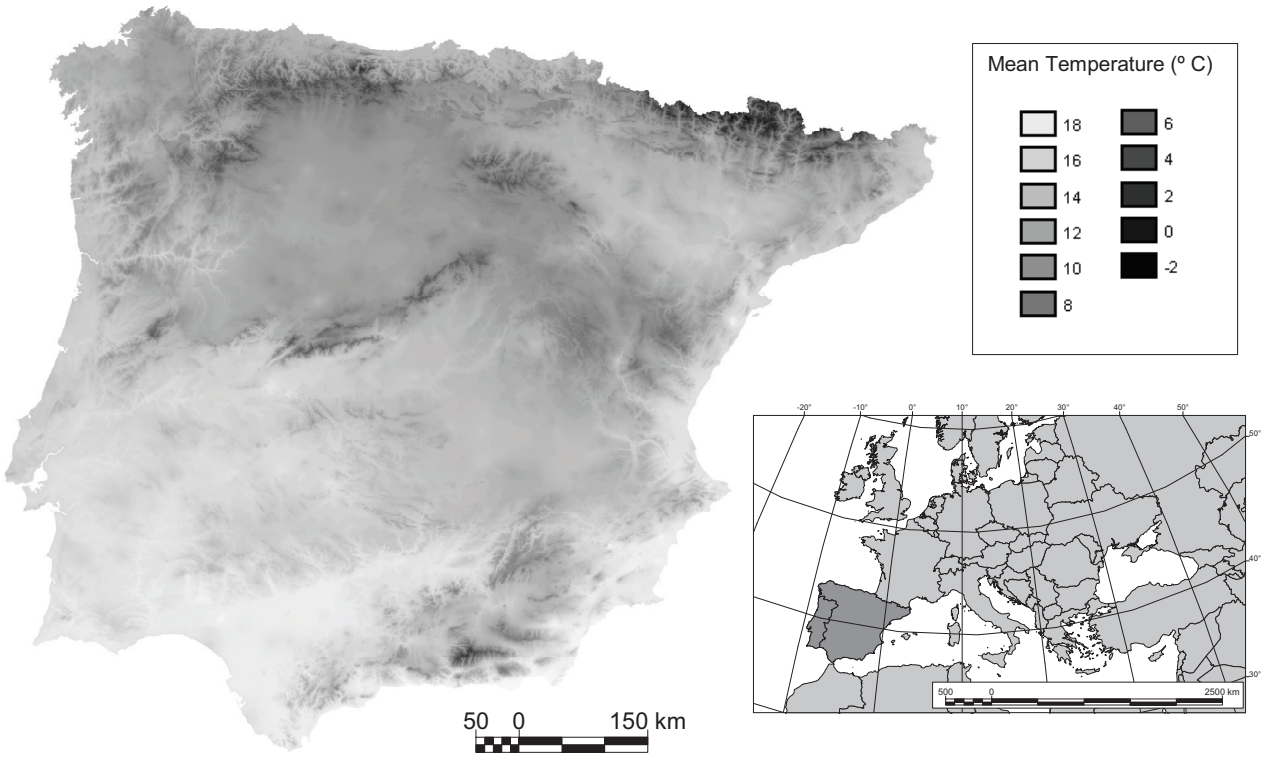

Fig. 1. Annual mean air temperature obtained from only geographical variables modelling over the Iberian Peninsula.

For combined models we have only available remote sensing variables are only available on Catalonia, in the north-east of the Iberian Peninsula, between 0° 4' W and 3° 19' W (~266 km) longitude, and between 40º 30' N and 42º 53' N

(~260 km) latitude (see Fig. 1). For Catalonia we have selected the UTM-31N zone as the reference system because it is the UTM zone that entirely covers the Catalan region.

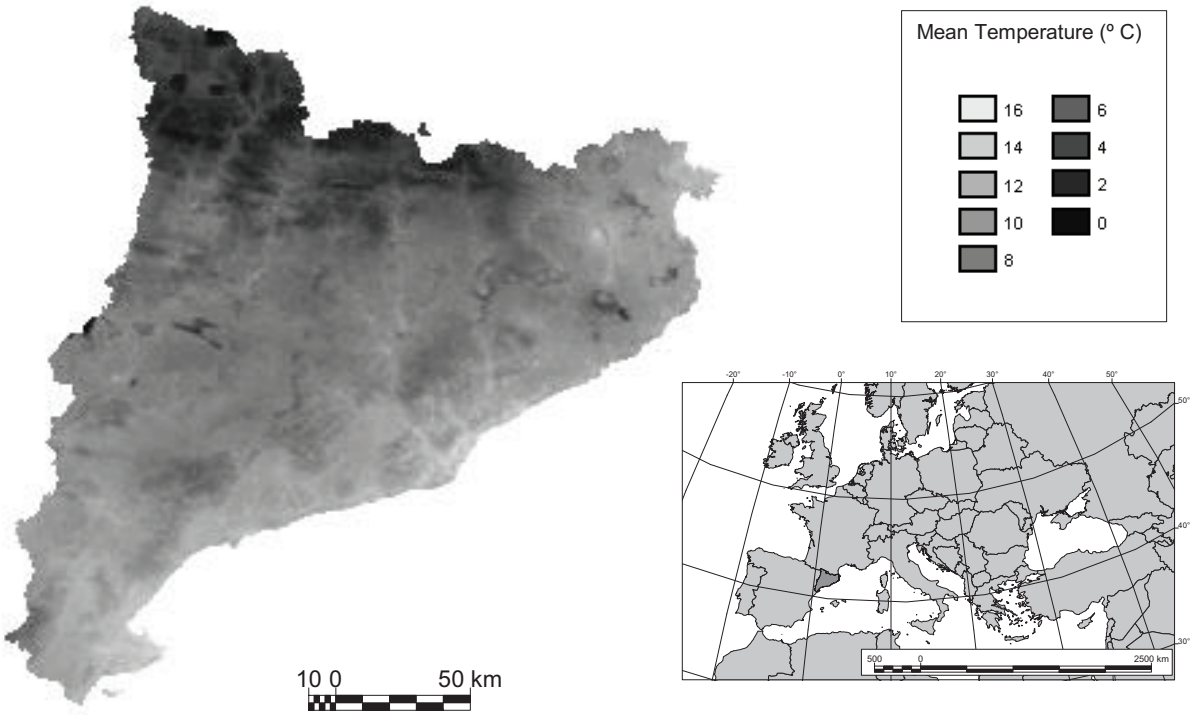

Fig. 2. Annual mean air temperature obtained from geographical and remote sensing variables modelling over Catalonia.

Study area for both modelling processes might be changed to be equal. Due to the fact that the main aim of this research is to evaluate effect of lossy compression on air temperature modelling, not the modelling process itself, the best modelling process for each situation has to be chosen and that means, for only geographical variables modelling, that the best choice is to use all data available over the Iberian Peninsula (more than one thousand meteorological stations).

3. MATERIAL

3.1 Only geographical variables modelling

a) Geographical data:

According to previous research[13], five geographical variables covering five climatic factors were used: altitude, latitude, continentality, solar radiation and terrain curvature. A continuous surface (*i.e.*, a raster matrix) was developed for each geographical variable to solve two problems: performing the regression analysis and mapping.

Altitude was obtained generating a 200 m spatial resolution DEM by digitizing and interpolating the contour lines of the 1:200 000 topographic map. Latitude was computed as lineal distances to Equator. Continentality was expressed as a logarithmic distance to the coast based on the idea that points placed far from the coast do not receive marine influence and therefore have similar continentality values. Coast line was split into three segments: Mediterranean, Atlantic and Cantabric coast. Solar radiation was modelled from a DEM and the sun position (detailed description of this modelling can be found on previous articles[19]). Terrain curvature was introduced to model local orography and was obtained from the second derivative of the immediate surrounding relief of each cell.

For the Iberian Peninsula, modelled using an only geographical variables model, a raster matrix of 5540 columns and 4425 rows was developed, with a pixel size of 200x200 m. Seven independent variables were used (one raster matrix for each of the five climatic factors except for the continentality which was represented by three raster matrices).

b) Climatic data:

Meteorological station data were obtained from the Spanish National Institute of Meteorology (INM) and from the literature in case of Portugal, using stations which series length is equal to or greater than 15 years. Details can be found in previous research[12,13].

3.2 Geographical and remote sensing variables modelling

a) Remote sensing data:

To model annual mean air temperature, TERRA-MODIS composites (each 8 and 16 days) were used. The product "Land Surface Temperature/Emissivity 8-Day L3 Global 1 km" (MOD11A2 or LST hereafter) contains daytime and nighttime land surface temperature each 8 days and has a spatial resolution of 1 km. The product "Vegetation Indices 16-Day L3 Global 500 m" (MOD13A1) contains Normalized Difference Vegetation Index (NDVI) and other vegetations indices, and has a spatial resolution of 500 m.

The study period comprises from 2000 to 2005. Within this period 235 LST products (470 bands taking into account that daytime and nigthtime land surface temperature are used on air temperature modelling) and 123 NDVI products were used. LST products have a dimension of 291x282, 1 km pixel. For NDVI products, a pixel size of 500 m (raster dimension 582x564) is obtained so it is necessary to resample that information to 1 km pixel size before the regression process. For both LST and NDVI, to model annual air temperature, map algebra[20] was used to obtain a mean daytime LST, mean nighttime LST and mean NDVI to feed the regression process.

b) Geographical data:

Continuous surfaces representing geographical variables had been obtained following a procedure similar to the one explained in the former section although only four variables are used, according to previous research[18]. Continentality has been expressed in this case using only a lineal distance to the Mediterranean coast because in this smaller area this approach is easier and effective. Resolution of the generated surfaces is 1 km to be equal to the lowest resolution of remote sensing variables used on regression modelling.

c) Climatic data:

Meteorological station data were obtained from the Catalan Meteorological Service (SMC), using stations which series length equal to or greater than 5 years, according to the length of image time series used. Using more restricted criterion to select meteorological stations (*i.e.*, larger series length) would result in large uncovered areas. At the end, 101 meteorological stations were selected to model annual minimum and mean air temperature.

4. METHODS

4.1 Spatial interpolation method

To model air temperature previous methodologies[18,13] are used for modelling with and without remote sensing images, respectively. Hereafter only geographical variables modelling will be named using the acronym "G" and geographical and remote sensing variables modelling with the acronym "GRS". These methods are based on multiple regression and local interpolation using meteorological station data.

Statistical analyses are used to explain the climatic relation between a climatic element (annual mean and minimum air temperature as dependent variable) and climatic factors and remote sensing images (as independent variables). 60% of meteorological stations are used to obtain the regression model and 40% to test it. When using many independent variables, many regression models may be tested using all combinations among variables. Mallows' C*p* best subsets is used to select the combination of independent variables that best describe data.

The second step is to obtain residuals, difference between real and predicted values, on meteorological stations used to adjust the model. These residuals are then interpolated using a local interpolation method (inverse distance weighting) to produce a residual continuous surface used to correct initial maps obtained by multiple regression. This correction is useful to reduce the error level because the independent variables cannot explain the entire climatic spatial variation.

Finally the regression model is validated using independent data (40% of meteorological station data set aside) trough a simple regression between independent observed values and predicted values. All process steps are implemented using batch processing and MiraMon GIS modules[21]).

Air temperature continuous surfaces are created trough map algebra[20] using continuous raster of independent variables.

4.2 Compression method

a) Compression measure:

The main aim of this paper is to asses on the use of lossy compression in order to reduce the great amount of data available nowadays without significantly reducing the information that can be extracted from this data. Lossless compression it is not considered because, even if it maintains exactly the values of original images, does not achieve as great compression ratios as lossy compression does.

On this paper, compression size is based on compression ratios (CR) since we considered it more relevant given the clearly practical applications of our research. Nevertheless, it should be borne in mind that the same compression ratio may produce different degrees of quality depending on the type of image. CR is computed as follows:

$$CR = \frac{Size\ \ of\ \ Compressed\ \ File}{Size\ \ of\ \ Original\ \ File}$$

In order to measure the effect of compression on the air temperature modelling, independent original images are compressed at different compression ratios to feed the regression model. Differences on regression fitting (R^2) and error (RMS) of obtained air temperature maps (from original and compressed variables) are used to evaluate these effects. See Fig. 3 for a general overview covering all the steps of the image compression/decompression process and of the air temperature modelling.

b) Compression algorithm and image types:

The compression/decompression algorithm used is the JPEG2000 implementation BOI software[22], developed by the Department of Information and Communications Engineering (dEIC) at the Autonomous University of Barcelona (UAB).

JPEG 2000 standard allows compressing both byte and integer formats. Part 10 of this standard, related to compressing float images, is not yet approved, so nowadays float compression can not be done with JPEG 2000 compression format. Anyway, BOI implementation has a non-standard process to proceed with float images lossy compression. Thus, we could compress original images maintaining its format.

Compression ratios studied vary from 0.50 (compressed file size is half that the original file size) to 0.0001 (compressed file size is a ten-one thousandth part of the original file size). BOI implementation allows the user to set the target bit-rate (file size) of the compressed code-stream. However, sometimes the real compressed file size differs from the required size due to the fact that the maximum compressed file size is smaller than the required size. Therefore, when presenting results intended and obtained CR is shown for each modelling method. On G method only seven raster matrices are used and, moreover, some of them are highly compressed so the obtained CR greatly varies from the intended one. On GRS method only five raster matrices representing geographical variables are used in front of 593 remote sensing bands used to produce the mean daytime LST, mean nighttime LST and mean NDVI to feed the regression process. Compression is applied to every of the 593 remote sensing bands and LST and NDVI means are computed using images after compression.

c) NODATA values treatment:

Original images display areas without data (NODATA) due to the radiometric corrections to which they have been subjected, the presence of a small number of clouds and regions were the model is not going to be applied (*e.g.*, over the sea). Not all the compression/decompression programs used are currently able to recognize these NODATA values. Using them as useful values when compressing will generate important errors in compressed images, especially if the NODATA value is an extreme value of the available rank, as usual it is.

It is therefore necessary to delete these values from the original images before compression. Elimination is carried out using the MiraMon FagoVal module, which selectively eliminates (phagocytes) a given value in raster files, replacing it (in this case) by the arithmetical mean of the adjacent values. Finally, it is necessary to create a mask with the NODATA areas in the original images in order to reapply it over the images after compression.

Images have to be decompressed to feed the regression process because it is still not prepared to deal with compressed images and because NODATA mask must be applied to images. Indeed, after decompression, the mask corresponding to

the zones that were NODATA in the original image is applied to it. The mask is different for each one of the images and other variables.

d) Metadata recover and documentation:

Finally, some metadata from original images such as spatial reference system, image size, band description, etc. is recovered. Metadata on processes carried over the images (NODATA elimination, compression, decompression, etc.) are maintained or documented (if necessary). Metadata created is compliant with ISO 19115[23], ISO 19139[24] and the GeMM Profile[25,26] which extend the previous cited standards to cover some image metadata and other contributions not included on those standards.

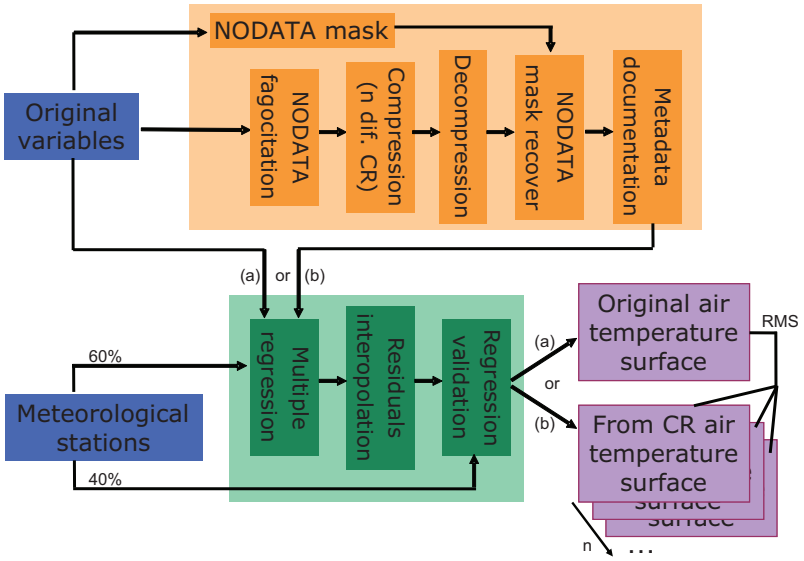

Fig. 3. General overview of image compression/decompression process and of air temperature modelling

5. RESULTS AND DISCUSSION

5.1 Regression validation

Results on regression validation are shown from Fig. 4 to Fig. 7 and from Table I to Table IV. In all of these figures lines and squares on blue depict annual minimum temperature and lines and red rhombuses depict annual mean temperature. Dashed lines depict results obtained with the original images.

Fig. 4 and Fig. 5 show, for G and GRS methods respectively, the coefficient of determination, R^2, of the multiple regressions between dependent and independent variables related to compression ratio (CR). Table I and II also display these determination coefficients.

Fig. 6 and Fig. 7 show, for G and GRS methods respectively, the root mean square (RMS) error (ºC) of the multiple regressions (obtained using independent meteorological stations) related to compression ratio (CR). Table III and IV also display these RMS.

Cited figures and tables represent how regression model explain dependent data, *i.e.*, air temperature. R^2 is the proportion of variability in a data set that is explained by a statistical model. Values of R^2 near to 1 represent that the produced model explain almost all data variability. This estimation is obtained using only data of points used to perform the regression method. Sometimes this indicator may sub-estimate the lack of adjustment between the model and real data. This is why a test with independent points is done to obtain the RMS error produced by the model.

On one hand, minimum air temperature is always worse explained with the regression model, both for G and GRS methods, as previous studies found. On the other hand, according to our results and contrary at that stated on the previous studies, GRS methods are not clearly better than G methods. GRS methods obtain lower RMS but also lower R^2. This situation may be produced by the less length of the series data used on G methods (forced by data availability).

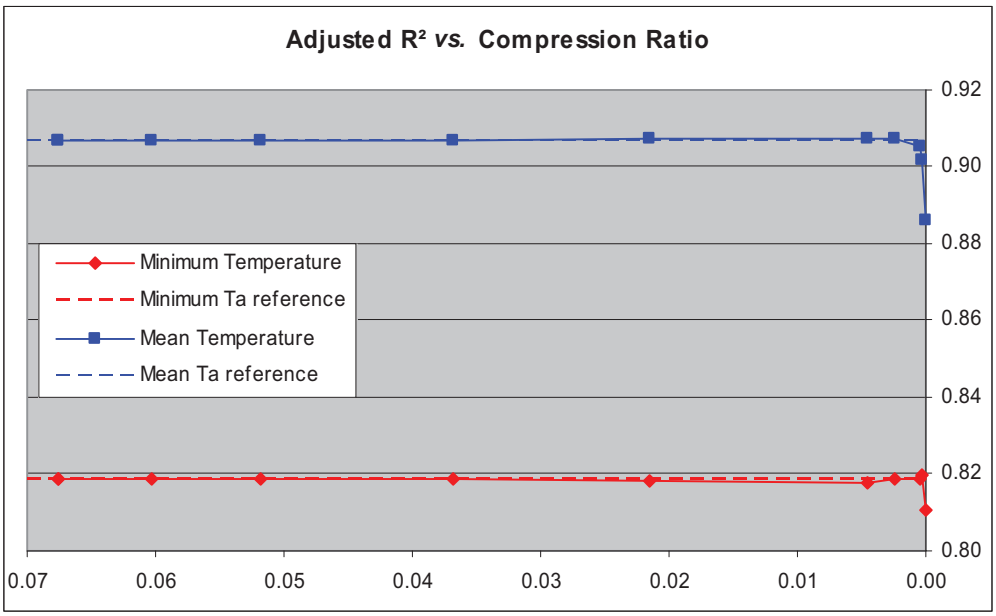

Fig. 4. Adjusted coefficient of determination, R^2, of the multiple regressions between dependent and independent variables related to compression ratio (CR) on G methods (only geographical variables) over the Iberian Peninsula.

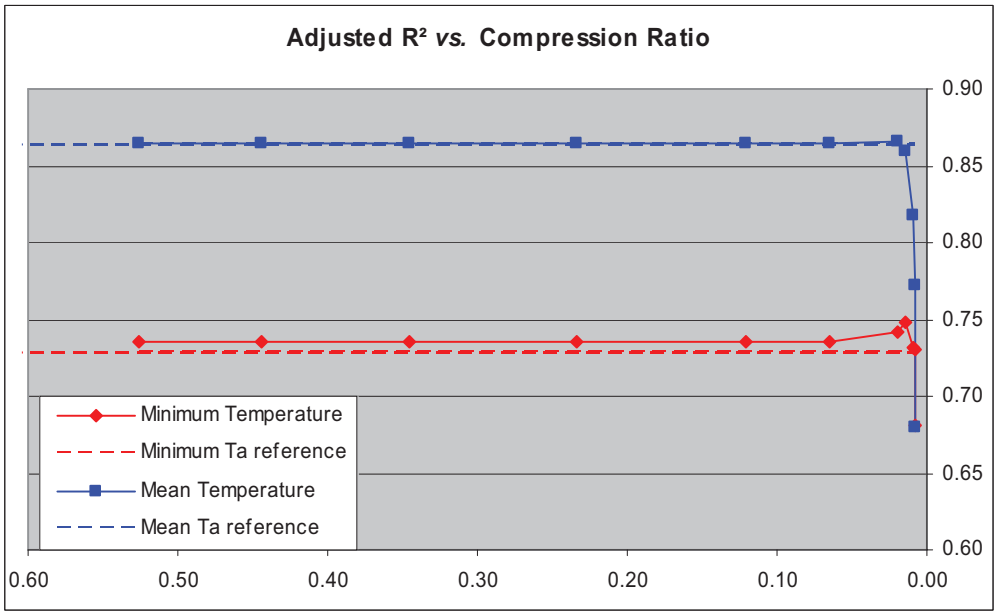

Fig. 5 Adjusted coefficient of determination, R^2, of the multiple regressions between dependent and independent variables related to compression ratio (CR) on GRS methods (geographical and remote sensing variables) over Catalonia.

Table I: Adjusted coefficient of determination, R^2, related to compression ratio on G methods over the Iberian Peninsula.

Intended CR	0.5	0.4	0.3	0.2	0.1	0.05	0.01	0.005	0.001	0.0005	0.0001
Obtained CR	0.0676	0.0676	0.0603	0.0519	0.0368	0.0215	0.0046	0.0025	0.0005	0.0003	0.0001
R^2 min. Ta	0.818552	0.818552	0.818552	0.818552	0.818549	0.818458	0.817757	0.818862	0.818674	0.819803	0.810875
R^2 mean Ta	0.907051	0.907051	0.907051	0.907051	0.907062	0.907129	0.907295	0.907170	0.905435	0.901710	0.886185

Table II: Adjusted coefficient of determination, R^2, related to compression ratio (CR) on GRS methods over Catalonia.

Intended CR	0.5	0.4	0.3	0.2	0.1	0.05	0.01	0.005	0.001	0.0005	0.0001
Obtained CR	0.5258	0.4448	0.3455	0.2333	0.1211	0.0651	0.0197	0.0139	0.0091	0.0084	0.0079
R^2 min. Ta	0.735604	0.735604	0.735602	0.735643	0.735888	0.735890	0.742403	0.748429	0.731826	0.730388	0.680678
R^2 mean Ta	0.864758	0.864763	0.864770	0.864776	0.865183	0.864801	0.866127	0.860027	0.817668	0.772123	0.680084

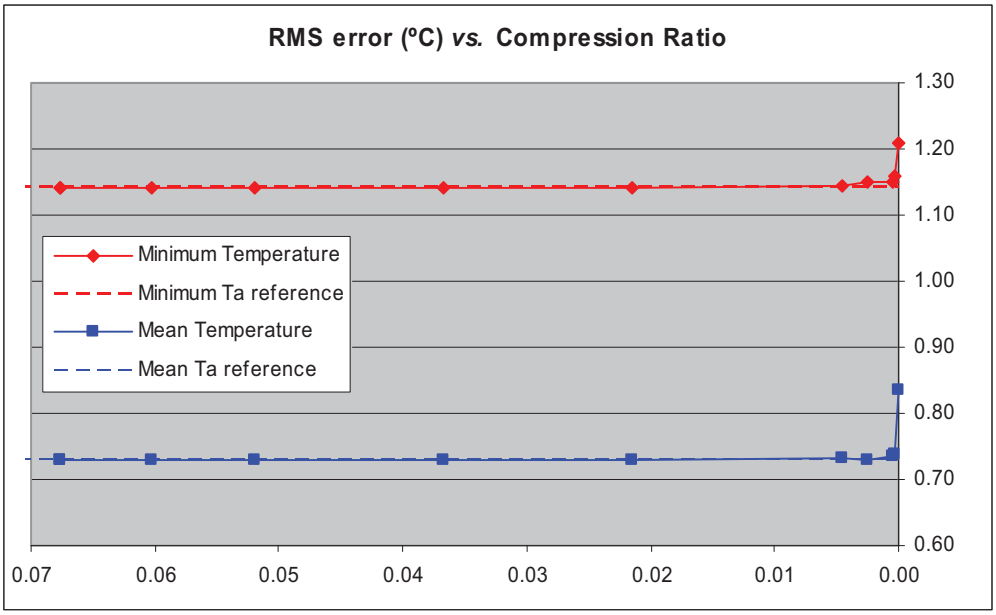

Fig. 6. Root mean square error (ºC) of the multiple regressions, obtained using independent points related to compression ratio (CR) on G methods (only geographical variables) over the Iberian Peninsula.

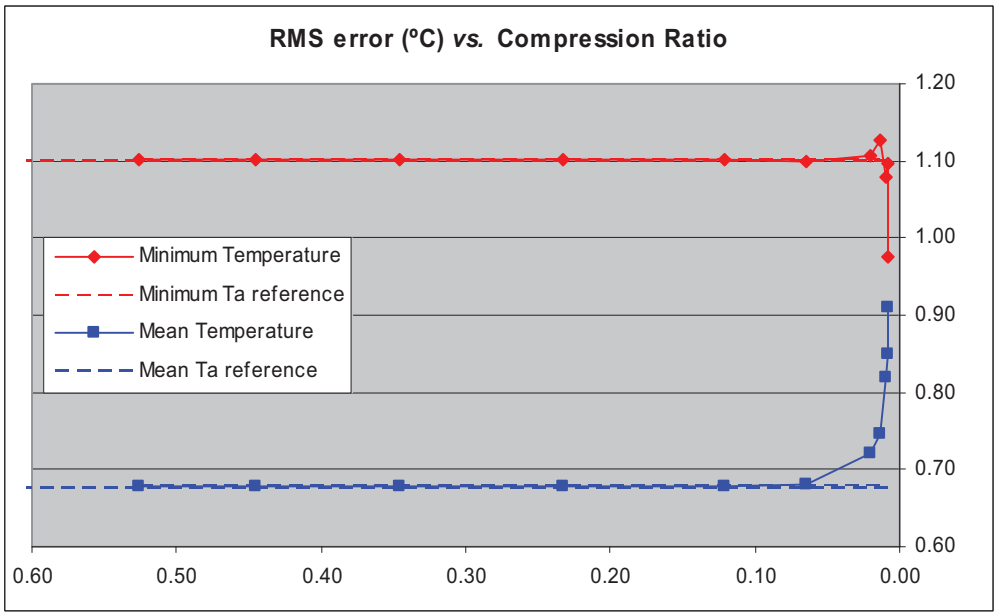

Fig. 7. Root mean square error (ºC) of the multiple regressions, obtained using independent points related to compression ratio (CR) on GRS methods (geographical and remote sensing variables) over Catalonia.

Table III: Root mean square error (ºC) of the multiple regressions, obtained using independent points related to compression ratio (CR) on G methods (only geographical variables) over the Iberian Peninsula.

Intended CR	0.5	0.4	0.3	0.2	0.1	0.05	0.01	0.005	0.001	0.0005	0.0001
Obtained CR	0.0676	0.0676	0.0603	0.0519	0.0368	0.0215	0.0046	0.0025	0.0005	0.0003	0.0001
RMS min. Ta	1.141481	1.141481	1.141481	1.141485	1.141472	1.140708	1.142690	1.151330	1.150313	1.159371	1.207469
RMS mean Ta	0.729801	0.729801	0.729801	0.729801	0.729855	0.729752	0.732098	0.730288	0.735204	0.737832	0.835376

Table IV: Root mean square error (ºC) of the multiple regressions, obtained using independent points related to compression ratio (CR) on GRS methods (geographical and remote sensing variables) over Catalonia.

Intended CR	0.5	0.4	0.3	0.2	0.1	0.05	0.01	0.005	0.001	0.0005	0.0001
Obtained CR	0.5258	0.4448	0.3455	0.2333	0.1211	0.0651	0.0197	0.0139	0.0091	0.0084	0.0079
RMS min. Ta	1.101868	1.101791	1.101728	1.101770	1.101447	1.100012	1.107691	1.126049	1.079567	1.096405	0.976040
RMS mean Ta	0.677340	0.677314	0.677269	0.677370	0.678906	0.680363	0.720106	0.746955	0.819340	0.850691	0.910243

When performing the regression model using compressed images as independent variables, R^2 is slightly affected. For G method, R^2 of minimum temperature regression using original variables is 0.818559 and for mean temperature regression is 0.9070770, thus the difference with the first compression level used is of only 0.000007 and 0.000026 respectively. For GRS method, R^2 of minimum temperature regression using original variables is 0.729708 and for mean temperature regression is 0.864767, thus the difference with the first compression level used is only -0.005896 and 0.000009 respectively. Regarding to R^2 determination, compression up to one thousandth of original file size (CR 0.001) does not produce significant variations neither on G nor GRS methods (see Fig. 4 and 5 and Table I and II).

RMS is also slightly affected when performing the regression model using compressed images as independent variables. For G method, RMS of minimum temperature regression using original variables is 1.141227 and for mean temperature regression is 0.729879, thus the difference with the first compression level used is only -0.000254 and 0.000078 respectively. For GRS method, RMS of minimum temperature regression using original variables is 0.101759 and for mean temperature regression is 0.677302, thus the difference with the first compression level used is only -0.000109 and -0.000038 respectively.

Regarding to RMS determination, compression has a more significant effect due to the fact that if third decimal of RMS (thousandth of ºC degree) wants to be preserved then the maximum compression that can be applied is a CR of 0.1 for minimum temperature (GRS method) and a CR of 0.2 for mean temperature (GRS method). If only the second decimal of RMS (hundredth of ºC degree) wants to be preserved then the maximum compression that can be applied is a 0.02 for minimum temperature (GRS method) and 0.1 for mean temperature. On fourth situations (min. Ta or mean Ta and two or three RMS decimals preservation) GRS method accepts less compression than G method. This is because geographical variables have a very high compression ratio even at the maximum bit-rate (refer to section 4.2c for details). Comparing both predicted values using GRS method, minimum temperature accepts more compression than mean temperature but for G method both accept the same compression.

5.2 Comparison with the maps obtained from the original images

Air temperature continuous surfaces are created from both original images and compressed images. Thus, each air temperature surface at given a CR can be compared to the original temperature surfaces to evaluate the error all over the study area. RMS error is computed from differences between these two air temperature surfaces. Results on air temperature surface comparison are shown on Fig. 8 and 9 and on Table V and VI. These figures show, for G and GRS methods respectively, the root mean square (RMS) error (ºC) of air temperature surface generated related to compression ratio (CR). In both of them, lines and squares on blue depict annual minimum temperature and lines and red rhombuses depict annual mean temperature. Table V and VI also display these RMS.

Cited figures and tables represent how temperature surface obtained from compressed images differs from temperature surface obtained from original images. The first interesting thing is that there are little differences between minimum and mean air temperature RMS, although modelling is better for mean temperature.

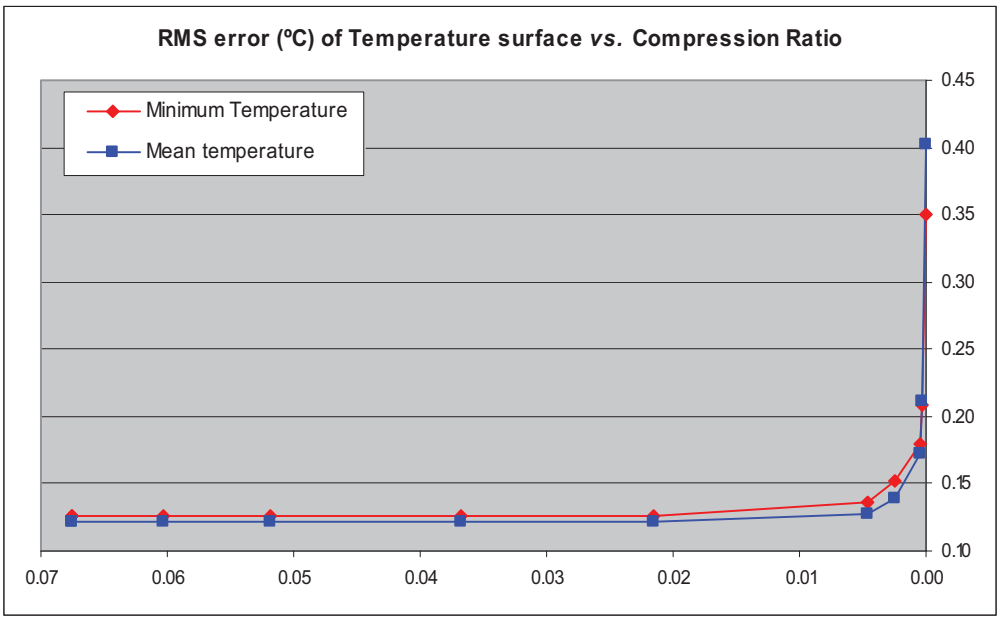

Fig. 8. Root mean square error (ºC) of the air temperature surface obtained from regressions using compressed images related to compression ratio (CR) on G methods (only geographical variables) over the Iberian Peninsula

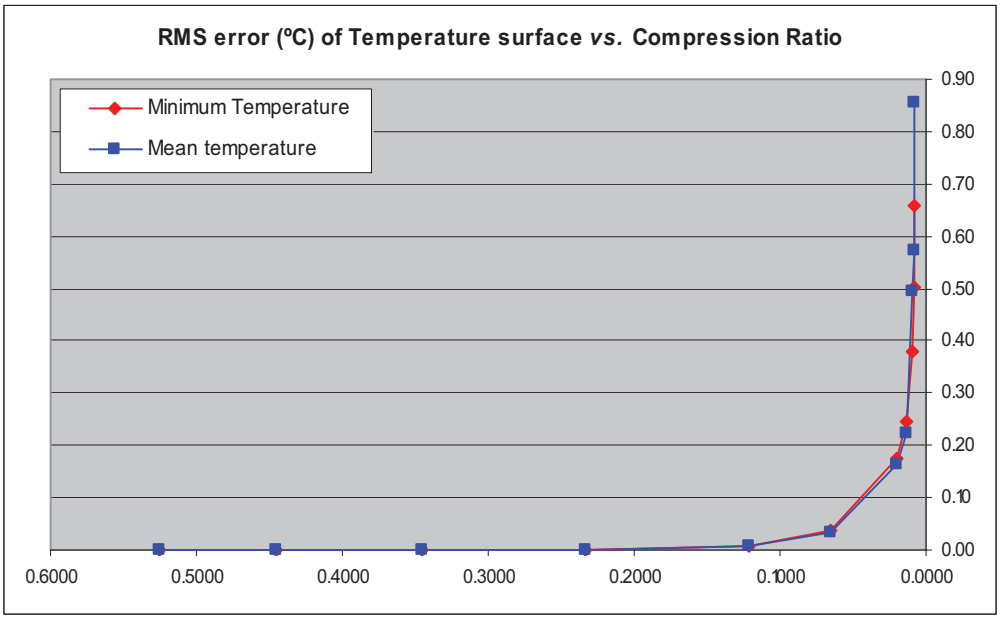

Fig. 9. Root mean square error (ºC) of the air temperature surface obtained from regressions using compressed images related to compression ratio (CR) on GRS methods (geographical and remote sensing variables) over Catalonia

Another interesting thing is that at lower compressions (higher CR), RMS on GRS method are very small, but these values increase rapidly at higher compression rations (lower CR). On the other hand G method is less influenced by compression than GRS method because compression produces a smaller increase on RMS. This can be explained also because geographical variables have a very high compression ratio even at the maximum bit-rate (refer to section 4.2c for details) and on the other hand remote sensing variables has a progressive compression but being more informational, at higher compression results are severely compromised. In fact, obtained CR for G methods are smaller than those

obtained with GRS methods for the same intended CR. In any case, RMS of air surface temperature is less than RMS of the regression validation, as could be expected.

Table V: Root mean square error (ºC) of the air temperature surface obtained from regressions using compressed images related to compression ratio (CR) on G methods (only geographical variables) over the Iberian Peninsula

Intended CR	0.5	0.4	0.3	0.2	0.1	0.05	0.01	0.005	0.001	0.0005	0.0001
Obtained CR	0.0676	0.0676	0.0603	0.0519	0.0368	0.0215	0.0046	0.0025	0.0005	0.0003	0.0001
RMS min. Ta	0.125576	0.125576	0.125576	0.125576	0.125610	0.126090	0.135670	0.152177	0.179961	0.208209	0.350665
RMS mean Ta	0.121510	0.121510	0.121510	0.121510	0.121543	0.121846	0.127672	0.138532	0.172515	0.211661	0.401825

Table VI: Root mean square error (ºC) of the air temperature surface obtained from regressions using compressed images related to compression ratio (CR) on GRS methods (geographical and remote sensing variables) over Catalonia

Intended CR	0.5	0.4	0.3	0.2	0.1	0.05	0.01	0.005	0.001	0.0005	0.0001
Obtained CR	0.5258	0.4448	0.3455	0.2333	0.1211	0.0651	0.0197	0.0139	0.0091	0.0084	0.0079
RMS min. Ta	0.000279	0.000267	0.000293	0.000480	0.005950	0.037085	0.174427	0.246180	0.378876	0.502222	0.659780
RMS mean Ta	0.000151	0.000095	0.000113	0.000357	0.006469	0.035243	0.162116	0.221735	0.494024	0.573359	0.856441

6. CONCLUSIONS

Results have revealed that, even at very high compression ratios, practically the same accuracy, measured with independent reference climatic stations, is obtained, so JPEG2000 seems an interesting technique not heavily affecting these common modelling approaches.

If regression using only geographical variables is intended, higher compression can be performed (up to 0.04 at the worst situation) than if a model with geographical and remote sensing variables is intended (up to 0.2 at the worst situation). Minimum air temperature is modelled with less accuracy (lower R^2 and higher RMS) but is also less affected by compression (up to 0.04 at worst situation) than mean air temperature modelling (up to 0.2 at worst situation).

According to air temperature surface RMS, regression using only geographical variables is less influenced by compression than a regression with geographical and remote sensing variables because compression produces a smaller increase on RMS.

ACKNOWLEDGEMENTS

This work was supported in part by the Ministry of Science and Technology and the FEDER funds through the research projects “Wavelet image compression for Remote Sensing and GIS applications” (TIC2003-08604-C04) and “Interactive coding and transmission of high-resolution images: applications in Remote Sensing, Geographic Information Systems and Telemedicine” (TSI2006-14005-C02-02).

We would like to express our gratitude to the Catalan Water Agency and to the Department of the Environment and Housing of the Generalitat (Autonomous Government) of Catalonia for their investment policy and the availability of Remote Sensing data, which has made it possible to conduct this study under optimal conditions. We would also like to thank our colleagues of the Department of Geography, CREAF and the dEIC of the UAB who have collaborated in any way in the treatment of the images, and INTA for its efficient image subscription service.

REFERENCES

1. G.K. Wallace, “The JPEG still picture compression standard”. *Communications of the ACM*, 34(4), 30-44, 1991.
2. ISO/IEC 10918-12, *Digital compressing and coding for continuous-tone still images*, Technical report, International Standard Organization / International Electrotechnical Commission, 1994.
3. ISO/IEC, *JPEG2000 image coding system. Part 1: Code coding system*, Technical report, International Standard Organization / International Electrotechnical Commission, 2000.

4. Z.L. Li, X.X. Yuan and W.K.K. Lam, "Effects of JPEG compression on the accuracy of photogrammetric point determination", *Photogrammetric Engineering and Remote Sensing*, 68(8), 847-853, 2002.
5. W.K.K. Lam, Z.L. Li and X.X. Yuan, "Effects of JPEG compression on the accuracy of digital terrain models automatically derived from digital aerial images", *Photogrammetric Record*, 17 (98), 331-342, 2001.
6. T.Y.Shih and J.K. Liu (2005), "Effects of JPEG 2000 compression on automated DSM extraction: Evidence from aerial photographs", *Photogrammetric Record*, 20 (112), 351-365, 2005.
7. J.D. Paola and R.A. Schowengerdt, "The effect of lossy image compression on image classification", *Geoscience and Remote Sensing Symposium, 1995. IGARSS '95. Quantitative Remote Sensing for Science and Applications*, IEEE International, 1, 118-120, 1995.
8. F. Tintrup, F. De Natale and D. Giusto, "Automatic land classification vs. data compression: a comparative evaluation". *Geoscience and Remote Sensing Symposium Proceedings, 1998. IGARSS '98*, IEEE International, 4, 1751 – 1753, 1998.
9. F. Tintrup, F. De Natale, and D. Giusto, "Compression algorithms for classification of remotely sensed images". *Acoustics, Speech, and Signal Processing, 1998. ICASSP '98. Proceedings of the 1998 IEEE International Conference*, IEEE International, 5, 565 –2568, 1998.
10. C. Pérez, D. Aguilera, A. Muñoz, "Estudio de viabilidad del uso de imágenes comprimidas en procesos de clasificación". In R. Pérez Utrero, P. Martínez Cobo. *Teledetección y desarrollo regional. X Congreso Nacional de Teledetección*, 309-312, 2003.
11. A. Zabala, X. Pons, R. Díaz-Delgado, F. García, F. Aulí-Llinàs and J. Serra-Sagristà, "Effects of JPEG and JPEG2000 Lossy Compression on Remote Sensing Image Classification for Mapping Crops and Forest Areas", *Geoscience and Remote Sensing Symposium, 2006. IGARSS 2006. IEEE International Conference on*, IEEE International, 790–793, Denver, 2006. Digital Object Identifier 10.1109/IGARSS.2006.203.
12. M. Ninyerola, X. Pons and J.M Roure, "A methodological approach of climatological modelling of air temperature and precipitation through GIS techniques", *International Journal of Climatology*, 20, 1823-1841, 2000.
13. M. Ninyerola, X. Pons and J.M Roure, "Objective air temperature mapping for the Iberian Peninsula using spatial interpolation and GIS", *International Journal of Climatology*, 27, 1231-1242, 2007.
14. L. Prihodko and S.N Goward, "Estimation of air temperature from remotely sensed surface observations", *Remote Sensing of Environment*, 60, 335-346, 1997.
15. C. Recondo y C.S. Pérez-Morandeiram, "Obtención de la temperatura del aire en Asturias a partir de la temperatura de la superficie terrestre calculada con imágenes NOAA-AVHRR", *Revista de Teledetección,* 17, 5-12, 2002.
16. Y.J. Sun, J.F. Wang, R.H. Zhang, R.R Gillies, Y. Xule and Y.C Bo, "Air temperature retrieval from remote sensing data based on thermodynamics", *Theoretical and applied climatology*, 80, 37-48, 2005.
17. J. Cristóbal, X. Pons and M. Ninyerola, "Modelling Actual Evapotranspiration in Catalonia (Spain) by means of Remote Sensing and Geographical Information Systems", *Göttinger Geographische Abhandlungen*, 113, 144-150, 2005.
18. J. Cristóbal, M. Ninyerola, X. Pons and M. Pla, "Mejoras en la modelización de la temperatura del aire mediante el uso de la Teledetección y de los Sistemas de Información Geográfica", *In*, *El acceso a la información espacial y las nuevas tecnologías geográfica*, M.T Camacho Olmedo, J.A. Cañete Pérez, and J.J. Lara Valle (Eds.), 93-103, 2006.
19. X. Pons, "Estimación de la Radiación Solar a partir de modelos digitales de elevaciones. Propuesta metodológica", *Proceedings VII Coloquio de Geografía Cuantitativa, Sistemas de Información Geográfica y Teledetección*. Vitoria-Gasteiz (Spain), 1996. Available at: http://magno.uab.es/atles-climatic/rad_pot.pdf.
20. C.D. Tomlin, *Geographic Information Systems and Cartographic Modelling*. Prentice Hall: New York, 1990
21. X. Pons, *MiraMon. Geographical Information System and Remote Sensing Software. Version 4.4*. Centre de Recerca Ecològica i Aplicacions Forestals, CREAF, 2002.
22. F. Aulí-Llinàs, J.R. Paton, J. Bartrina-Rapesta, J.L. Monteagudo-Pereira and J. Serra-Sagristà, "J2K: introducing a novel JPEG2000 coder". In: *SPIE, IST (Ed.) Visual Communications and Image Processing. Society of Photo-optical Instrumentation Engineers* (SPIE), Beijing, China, 2005.
23. ISO 19115, *International Standard: Geographic information – Metadata. ISO 19115:2003*. Technical Committee 211, 2003.
24. ISO 19139, *International Standard: Geographic information – Metadata – XML schema implementation*. ISO 19139:2007. Technical Committee 211, 2007.
25. A. Zabala and X. Pons, "Image Metadata: compiled proposal and implementation" In: Benes, T. (ed.) *Geoinformation for European-wide Integration*, Millpress, Rotterdam, 674-652, 2002.
26. N. Julià, J. Masó, A. Zabala and M. Vallès, "CaMM, Catálogo de Metadatos de MiraMon: Implementación en una corporación, el DMAH", *Revista Mapping*, 105, 2005.

4. EFFECTS OF LOSSY COMPRESSION ON REMOTE SENSING IMAGE CLASSIFICATION OF FOREST AREAS

International Journal of Applied Earth Observation and Geoinformation 13 (2011) 43–51

Contents lists available at ScienceDirect

International Journal of Applied Earth Observation and Geoinformation

journal homepage: www.elsevier.com/locate/jag

Effects of lossy compression on remote sensing image classification of forest areas

A. Zabala [a], X. Pons [a,b,*]

[a] Geography Department, Universitat Autònoma de Barcelona, 08193 Cerdanyola del Vallès, Spain
[b] Center for Ecological Research and Forestry Applications (CREAF), Universitat Autònoma de Barcelona, 08193 Cerdanyola del Vallès, Spain

ARTICLE INFO

Article history:
Received 7 August 2009
Accepted 4 June 2010

Keywords:
Image compression
Image classification
Forestry management
JPEG
JPEG 2000

ABSTRACT

Lossy compression is being increasingly used in remote sensing; however, its effects on classification have scarcely been studied. This paper studies the implications of JPEG (JPG) and JPEG 2000 (J2K) lossy compression for image classification of forests in Mediterranean areas. Results explore the impact of the compression on the images themselves as well as on the obtained classification. The results indicate that classifications made with previously compressed radiometrically corrected images and topoclimatic variables are not negatively affected by compression, even at quite high compression ratios. Indeed, JPG compression can be applied to images at a compression ratio (CR, ratio between the size of the original file and the size of the compressed file) of 10:1 or even 20:1 (for both JPG and J2K). Nevertheless, the fragmentation of the study area must be taken into account: in less fragmented zones, high CR are possible for both JPG and J2K, but in fragmented zones, JPG is not advisable, and when J2K is used, only a medium CR is recommended (3.33:1 to 5:1). Taking into account that J2K produces fewer artefacts at higher CR, the study not only contributes with optimum CR recommendations, but also found that the J2K compression standard (ISO 15444-1) is better than the JPG (ISO 10918-1) when applied to image classification. Although J2K is computationally more expensive, this is no longer a critical issue with current computer technology.

1. Introduction and objectives

Remote sensing (RS) images are used for many applications, including land cover mapping and analysis, disaster management, climate modelling and agricultural and forest management. In zones with fragmented landscapes, like the Mediterranean area, Landsat images are especially suitable for land cover maps due to their spatial, temporal and spectral resolution (Viñas and Baulies, 1995). In this direction, the recent release of the historical Landsat image archive (USGS, 2009) is potentially very beneficial for land cover studies. Moreover, it is now possible to work with long time series, something especially interesting in vegetation classification and studies of territorial dynamics. However, this implies managing large numbers of images, which, due to their temporal resolution (and even their medium spectral resolution), becomes a complex and difficult data handling, storing and processing task. The need for an efficient image compression technique becomes acute for the user that has to manage this enormous image volume.

The new Spatial Data Infrastructures (SDI) paradigm developed over recent years, promotes the establishment of web data services, usually in terms of Open Geospatial Consortium (OGC) standards like the Web Map Service (WMS) and the Web Coverage Service (WCS) (Maguire and Longley, 2005). Nevertheless, it is necessary to use compression and interactive transmission strategies in these web services in order to transfer very large images to environments with restricted bandwidth. It is also absolutely necessary to standardize data compression and transmission formats in SDI environments in order to achieve the desired interoperability. Thus, it is essential to use standard compression formats even if this implies a slightly worse compression than that obtained with new non-standard, recently published algorithms (Carvajal et al., 2008; Choi et al., 2008).

JPEG format, developed by the Joint Photographic Experts Group, first appeared in 1991 and revolutionized image compression, as it achieves very high compression ratios with no appreciable loss of image quality for file sizes up to a compression ratio of approximately 5:1 in the case of remotely sensed images. It was adopted as an ISO standard in 1994 (ISO/IEC, 1994) and is now used widely in everyday applications (photo cameras, Internet web pages, mobile phones, etc.) as well as in RS and Geographic

* Corresponding author at: Geography Department, Despatx B9-1094, Edicifi B, Facultat de Filosofia i Lletres, Campus de la Universitat Autònoma de Barcelona, 08193, Cerdanyola del Vallès, Barcelona, Spain. Tel.: +34 935 811 527; fax: +34 935 812 001.
E-mail addresses: Alaitz.Zabala@uab.cat (A. Zabala), Xavier.Pons@uab.cat (X. Pons).

0303-2434/$ – see front matter © 2010 Elsevier B.V. All rights reserved.
doi:10.1016/j.jag.2010.06.005

Information System (GIS) applications (quick looks, colour composites for visual analysis, etc.). Nowadays, one of the main sources of lossy compressed images (airborne or satellite) is the OGC-WMS and OGC-WCS servers, which mainly serve JPEG images because, among other reasons, Internet browsers hardly ever support other lossy formats, such as JPEG 2000. More recent compression techniques are based on wavelet transformations, which permit even higher compression ratios with similar or even better image quality. Indeed, in recent years, wavelet based formats, such as SID, ECW and JPEG 2000, have become particularly popular within the RS and GIS community for data visualization, but are still quite unusual in every day RS practices (classification, etc.). JPEG 2000 became an ISO standard in 2000 and was revised in 2004 (ISO/IEC, 2004). It is important to bear in mind that we are always dealing with lossy compression algorithms, which sacrifice part of the data in order to achieve a higher compression ratio. Both JPEG and JPEG 2000 have a lossless mode that will not be considered in this work because it does not achieve the same high compression ratios.

Outside Medicine, in which the implications of these compression strategies have recently been analyzed (López et al., 2008; Guarneri et al., 2008), in the fields of RS and GIS, and in spite of the increasing need for compression and the spectacular compression ratios that can be achieved, there are few studies that quantitatively approach the effect of this compression on image applications, especially in terms of long time series or relatively large images. If the information loss does not have negative effects on the resulting products, then lossy compression can be used more widely. The few studies on this subject have either used a low number of small images, or non-standard compression algorithms that are incompatible within SDI frameworks. Moreover, the results from these studies have generally not been very conclusive, suggesting that more research is necessary.

Paola and Schowengerdt (1995) obtained 83% agreement between classifications from compressed images and classifications from original images, using compressions of 7.1:1 or even more. Similar results were obtained by Tintrup et al. (1998a,b), who achieved 95% agreement using a compression ratio of 2.5:1. Kiema (2000) applied segmentation to obtain a classification of an urban area within a single Lansdat image and concluded that compression ratios up to 20:1 have no discernable effect on classification accuracy. Lau et al. (2003) classified a single SPOT image (two sub-scenes) into four categories, and concluded that the image can be compressed to 35:1 without affecting the classification accuracy. None of these studies used a multitemporal analysis and none used large images (the widest area was 512×512 pixels). They attempted to obtain classifications with only a few broad categories (eight categories at most) in the case of multispectral data, or more when hyperspectral data images were used (26 classes in Choi et al., 2008, 10 classes in Qian et al., 2005, 9 classes in Penna et al., 2007). Choi et al. (2008), using a single hyperspectral image of 256×256 pixels, concluded that compression has a positive effect on classification due to the removal of isolated error pixels, which therefore improves classification accuracy; although, this still cannot be considered as a general result.

However, Paola and Schowengerdt (1995) recognized that even though the overall appearance is maintained, most of the finer detail is lost. Pérez et al. (2003) recommended not using lossy compression in classification processes due to its negative effect on classification accuracy. Choi et al. (2008) advice against compression because, although compression might have some minor benefits for classification (removal of isolated pixels), the net effects may not be accurately controlled (*e.g.*, classification errors along the class boundaries) and similar results can be obtained using a classifier that uses spatial information. Moreover, Kiema (2000), Lau et al. (2003) and Liang et al. (2008) stated that their results varied according to image content and texture, and that experiments with larger images are necessary.

Recent studies have explored modifications of compression techniques (Qian et al., 2005; Penna et al., 2006, 2007; Du and Fowler, 2007; Wang et al., 2007; Carvajal et al., 2008; Choi et al., 2008; Chou and Liu, 2008), but only a few have considered the effect of compression on classification accuracy (Qian et al., 2005; Carvajal et al., 2008; Choi et al., 2008; Penna et al., 2007). Although the results of these studies seem to suggest that compression does not adversely affect classification accuracy, the compression ratios evaluated have usually been above those attempted in our study (softer), and, as noted above, non-standard compression algorithms outside the SDI framework have been employed.

This study aimed to assess the influence of lossy image compression on digital classification of forests in a real management environment, *i.e.*, a multitemporal set of images that covers a wide area, and obtain a detailed forest legend (14–15 forest categories). In order to provide more representative results, besides the multitemporal approach, the classification procedure also included non-radiometric variables, which is an increasingly common practice currently employed to improve mapping results (Moré et al., 2004; Moré and Pons, 2008; Serra et al., 2009).

2. Materials and methods

In order to measure the effect of compression on classification results, two scenarios were analyzed: JPG and JPEG 2000 (referred to as *J2K*) compression techniques. Compression was measured based on compression ratios (CR) and not on compression quality (common for JPG), since we considered CR to be more relevant given the practical applicability of our research. However, it should be kept in mind that the same compression ratio may produce different degrees of quality depending on the type of image, as will be shown in Section 3.1. In this paper, CR is computed as the ratio between the size of the original file and the size of the compressed file, and is generally expressed as, *e.g.*, 10:1 for a file that is compressed to a tenth of the original file size.

2.1. Zones and scenes used

Two zones, located in two different forest regions, were chosen: Garrotxa-Ripollès and Maresme-Vallès, both in Catalonia (northeastern Spain). The Garrotxa-Ripollès (GR) zone is less fragmented and mainly composed of *Quercus humilis* (26.07%), *Fagus sylvatica* (19.00%), *Quercus ilex* (16.92%) and *Pinus sylvestris* (16.57%). The Maresme-Vallès (MV) zone is more fragmented and is mainly composed of *Pinus halepensis* (24.09%), *Quercus suber* (19.78%), Mediterranean shrubs (16.96%) and *Quercus ilex* (13.00%). The forest legend is composed of 15 and 14 categories (at species or community level) for the GR and MV zones, respectively (see Fig. 8 for GR legend).

Landscape fragmentation was calculated with Monmonier's index (Monmonier, 1982), computed as the number of polygons (regardless of class) per unit area. These calculations were carried out on the classification obtained from the original images, and the obtained value was 2.1 polygons/ha for the GR zone and 2.9 polygons/ha for the MV area.

Both zones were analyzed using ETM+ and TM images (Landsat-7 and Landsat-5 satellites, respectively). The study area is located on path 197 and row 31 of the Landsat orbit. The spectral resolution of the two sensors is not identical because ETM+ has a panchromatic band and a high gain thermal infrared band. As panchromatic and thermal bands are not used in the classification method applied here, the two sensors are therefore equivalent. During geometric correction, with the method developed by Palà and Pons (1995), all Landsat images were resampled using their nearest neighbour to preserve the original image radiometry. The second step was radio-

metric correction to convert digital numbers into reflectance values using the sensor calibration parameters and other factors such as atmospheric effects and the solar incidence angle accounting for the relief (Pons and Solé-Sugrañes, 1994; Salvador et al., 1996).

The dimensions of Landsat scenes covering the GR zone were 1264×1264 pixels (50,176 ha of forests). This zone was analyzed using four images: 12-03-03, 26-04-02, 13-06-02 and 16-08-02 TM images. The Landsat scenes covering the MV zone were 3474×2323 pixels (146,687 ha of forests) and this zone was also analyzed using four images: 12-03-03 and 13-06-02 ETM+ images and 26-07-03 and 11-08-03 TM images. These images were selected from those available for 2002 and 2003 (without clouds) taking into account the annual vegetation dynamics in order to take advantage of the different spectral responses during the year as a result of the plant phenology, and assuming that inter-annual changes in the forests were negligible during the period 2002–2003. All the TM multitemporal bands were used to perform the classification, bearing in mind that the method used (described in the next section) works well despite the high correlation of some bands.

In addition to the above detailed images, other variables were used to improve classification accuracy. To consider photosynthetic activity and the climatic and terrain conditions, the NDVI vegetation index computed for each date, the climatic variables (mean precipitation, annual mean solar radiation, July maximum temperature, April minimum temperature, January minimum temperature) and topographic slope were also used in the classification method. Climatic variables were obtained from the Digital Climatic Atlas of Catalonia (http://magno.uab.es/atles-climatic/), according to the methodologies developed by Ninyerola et al. (2000) and Pons and Ninyerola (2008). The group of variables slope + climate will be referred as the "topoclimatic" variables.

2.2. Image compression and decompression

We used the classic JPEG compression/decompression algorithms based on the JPEG public libraries of the Independent JPEG Group (2008) (JPEGIMG module) implemented in the MiraMon v.6.4e software (Pons, 2008), and the JPEG 2000 implementation of the BOÍ software (Aulí-Llinàs et al., 2005) developed by the Group on Interactive Coding of Images (GICI) of the Autonomous University of Barcelona.

2.2.1. Image type transformations

JPEG compression uses byte images for each spectral component. Even though JPEG 2000 can compress both byte and integer data, to obtain comparable results for the two compression standards, we decided to apply a byte-type transformation to the original images before compressing them, even when JPEG 2000 compression was used.

Landsat TM and ETM+ images store each value band in bytes, but radiometric correction and slope computation produce float images. Original climatic variables from the Digital Climatic Atlas of Catalonia are integer images. Again, to obtain a comparable testbed, all float and integer images were converted into byte images before compression.

2.2.2. Nodata values

The original images include areas without data (NODATA) due to the radiometric corrections (for example, cast shadows) and the presence of a few clouds. Not all the compression/decompression programs used are currently able to consider these NODATA values properly. Using them as *bona-fida* values when images are compressed generates serious errors in the compressed images, especially when the NODATA value has been set to an extreme value of the available rank: 255. If this extreme value is used as a normal value in the compression it may affect neighbour pixels with low values inappropriately (*i.e.* a dark area surrounded by NODATA values). It is therefore necessary to eliminate these values from the original images before compression. Elimination was carried out using the MiraMon FagoVal module, which selectively eliminates a given value in raster files, replacing it with the arithmetical mean (in this case) of the adjacent values. Finally, it is necessary to create a mask with the NODATA areas in the original images in order to reapply it over the images after decompression.

2.2.3. JPEG and JPEG 2000 compression

The JPEG compression standard (ISO/IEC, 1994) allows one band to be compressed independently or three bands together (grey scale or real colour images, respectively). As our images have six bands per image date as well as other variables, we decided to compress each band (or variable) separately. Moreover, in the JPEG compression format, the quality of the resulting JPEG file is usually set. In general, and even after modifying the quality (an integer value), it is not possible to generate a JPEG file of a given size (in other words, an image whose compression ratio in relation to the original file is an exact, specific value). Therefore, all JPEG compressed files were created with a different JPEG quality; and we then chose the JPEG file with a CR value closest to the desired ratio(s) whose size was closest to the size necessary to obtain the appropriate compression ratio (CR) in each compression scenario.

One improvement of the JPEG 2000 compression standard is multiple-image transformation (ISO/IEC, 2004). However, to obtain comparable results from the two compression standards, we also decided to compress each image independently with JPEG 2000. Although multi-component transformation has some advantages, it is not entirely recommendable because each time an image is received the entire dataset needs to be recompressed. If compressing an entire set of images does not seem attractive, compressing all bands in the data set in a single JPEG 2000 file may be an alternative. As mentioned above, we chose band-by-band compression as it is more comparable with the JPEG scenario. Finally, it must be noted that the JPEG 2000 standard offers the possibility of obtaining an image with a specific CR.

2.2.4. Decompression and subsequent treatment

Images have to be decompressed to feed the classification process as this process is not able to deal with compressed images and the NODATA mask must be applied to images before classification. In some cases, after the decompression and due to the nature of the compression algorithms, some pixels had a value of "255" even though these pixels were not pixels without data (their original value before compression was not 255, but, for example, 254). As this value was reserved for the NODATA values, the value of these pixels had to be changed to "254". Next, the NODATA mask was applied to each image to recover areas not usable for classification.

During the image processing workflow, careful attention was taken to properly document image metadata in compliance with ISO standards 19115 (ISO, 2003) and ISO 19139 (ISO, 2007), and with the GeMM Profile (Zabala and Pons, 2002; Julià et al., 2005), which extends previously cited standards to cover some image metadata and other contributions not included in these standards.

2.3. Classification

In order to classify only the forest areas, a mask obtained from the Land Cover Map of Catalonia (LCMC, Ibáñez et al., 2002) was applied over the original and the compressed/decompressed images (the white areas in Figs. 5–7 are non-forest areas according to LCMC). The classification method used is a hybrid classification that combines satellite images and other variables in vegetation land cover maps. Hybrid classifiers are especially effective when cover types show complex variability in the spectral response. In

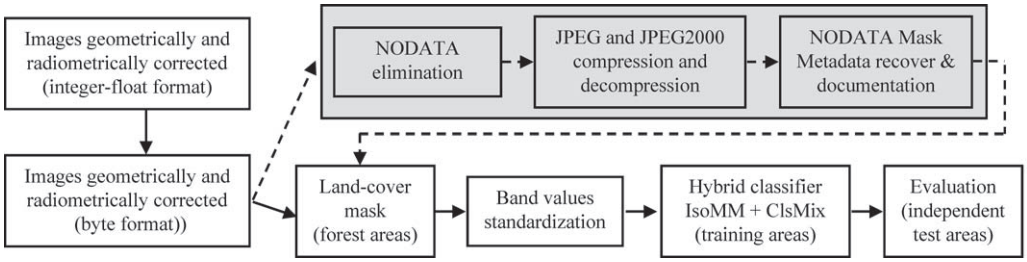

Fig. 1. Diagram of the methodology used. The general classification workflow is shown in the white boxes with continuous lines. The additional workflow relating to compression is shown in the grey boxes with dashed lines.

our case, the procedure works by starting with the unsupervised process to obtain a large number of statistical classes, while the supervised process is used to objectively assign these classes to the final categories. This method has been designed to improve the accuracy of the classifications (details can be found in Moré and Pons, 2008; Serra et al., 2009) and combines an unsupervised classifier (IsoMM) and a supervised one (ClsMix). The variables were standardized before the classification in order to avoid different ranges and variances that could affect the weight of the variables in the unsupervised stage of the classification. Classification using only radiometric variables was also tested, and worse results were obtained: when no ancillary data are used, both the overall accuracy and classified area are lower. Moreover, the behaviour of these classifications in relation to compression is the same (qualitatively) as that obtained when other variables are also used; thus, to simplify the paper, these results are not presented.

The classifications obtained (from images with or without compression) were evaluated using the confusion matrix based on test areas (ground-truth layer) which are independent of the training areas used in the supervised stage of the classification. The training and test areas were obtained from the Habitat Map of Catalonia (HMC), which is a map of Catalan habitats based on the interpretation and adaptation of habitat classification proposed by the European Union in the "CORINE Biotopes Manual".

These training and test areas were treated statistically to guarantee their quality (details can be found in Moré et al., 2004; Pons et al., 2006). Habitats with 80% or higher vegetation cover were selected from the HMC to guarantee that training areas had maximum thematic homogeneity. The selected habitats were eroded by 60 m on both sides of their polygon borders to reduce the potential effects of geographical positioning errors. This 60-m value was derived from the base map scale due to the unavoidable errors involved in delimiting natural habitats (fuzzy borders). The eroded polygons were fragmented into squares with 200 m sides. This allowed some pixels to be used as training areas and others to be reserved as test (ground-truth) areas. The following step is a depuration of the selected areas using the internal variability as a criterion (iterative process).

See Fig. 1 for a general overview of all the steps of the classification method and compression/decompression processes.

3. Results

The results investigate the effects of the different compression ratios applied and are grouped in three subsections: the first one (Section 3.1) explores differences on the images themselves after a compression/decompression cycle, the second one (Section 3.2) compares the metrics derived from the classifications (percentage of training pixels correctly classified) and the third one (Section 3.3) shows differences on overall accuracy and classified area. All subsections relate results to compression ratio and compression scenarios (JPG and J2K). In all graphics, the continuous line indicates JPG compression, and the dashed line shows the results for J2K; and both shape and colour of the symbols stands for the zone: red triangle for GR and blue circle for MV.

3.1. Image statistics

The first approach explores how the image itself is changed due to the compression process. Fig. 2 shows the mean percentage of pixels with unchanged value. This analysis is done for radiometric (including NDVI) variables. As expected, the number of pixels with unchanged value decreases with compression. For the same compression ratio, J2K compression preserves more pixels without changes than JPG.

Additionally to the proportion of changed/unchanged values, the magnitude of changes, for those pixels whose value has suffered a deviation from the original value, is also meaningful. To explore it, the maximum range of differences is computed for each band, compression scenario and ratio. The mean of all radiometric bands is then computed for each scenario, and results are shown in Fig. 3. It is clearly noticeable that J2K is able to keep compressed images more similar to the original ones than JPG.

3.2. Metrics derived from classifications

This subsection compares the percentage of training pixels correctly classified at different compression ratios. Training pixels are also compressed because the main aim of this study is to assess the effects of compression, regardless of when it is done. In other words, it is not possible to exclude from compression those pixels that will be used as training areas in a general workflow: if the compression, for example, is executed at the starting point of the image processing flow (receiving station), then it is clear that all the pixels must be equally treated because there is no way to know the interest of the final user (*e.g.*, forests, crops, urban areas, etc.) and which pixels will be used as training zones. As in many classification procedures, pixels used for training may be finally

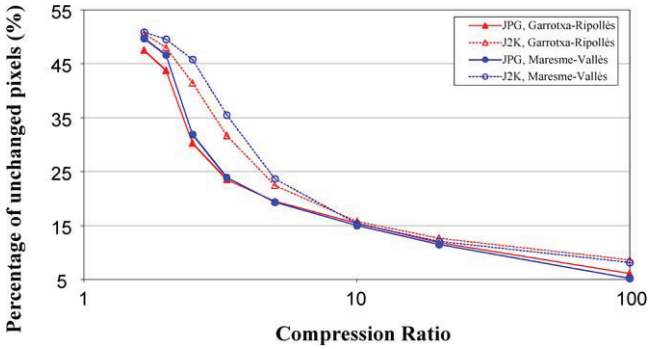

Fig. 2. Mean percentage of unchanged pixels between the original and compressed/decompressed radiometric images of the Garrotxa-Ripollès (GR) and Maresme-Vallès (MV) zones according to the compression ratio. The results for JPG and J2K compression algorithms are presented for the two areas.

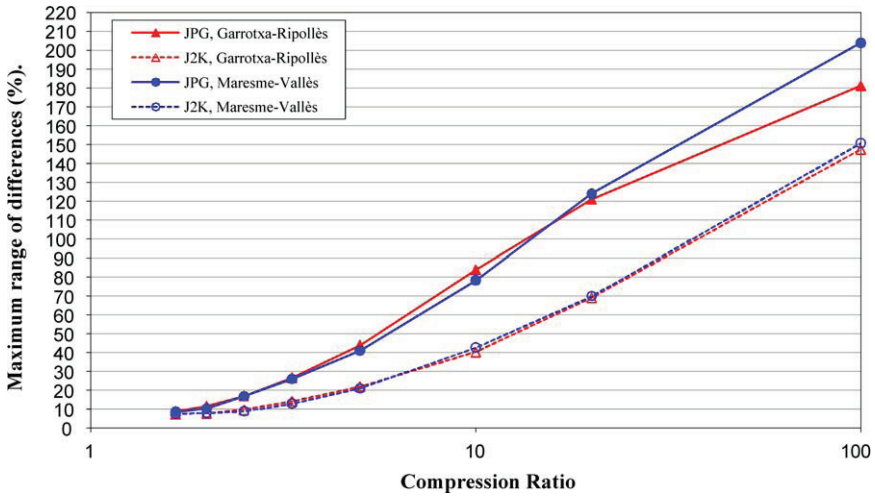

Fig. 3. Mean maximum range of differences between the original and compressed/decompressed radiometric images of the Garrotxa-Ripollès (GR) and Maresme-Vallès (MV) zones according to the compression ratio. The results for JPG and J2K compression algorithms are presented for the two areas.

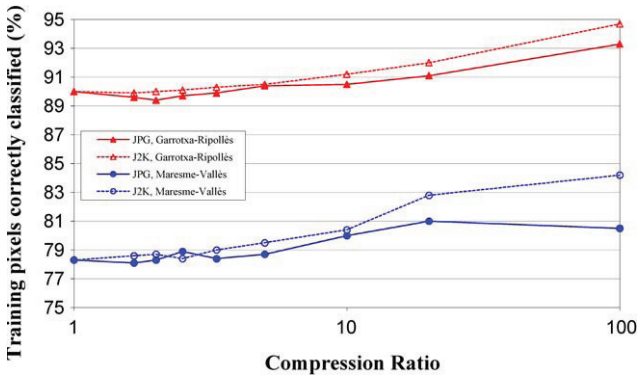

Fig. 4. Percentage of training pixels correctly classified of the Garrotxa-Ripollès (GR) and Maresme-Vallès (MV) zones in function of the compression ratio. The results for JPG and J2K compression algorithms are presented for the two areas.

assigned to a class different than expected, depending on the chosen classifier parameters. Developing this approach, Fig. 4 shows the percentage of training pixels correctly classified. Results show that at higher compression ratios a larger percentage of training pixels is classified to the "true" class. This maybe due to the homogenization effect of compression, that smoothes the image, removing differences on neighbour pixels. Accordingly, the similarity among training pixels of the same area increases and thus, become easier to classify because they are statistically closer and more similar to the class characterization. This does not imply a better classification; because the classifier may inadvertently err more frequently on pixels that are more difficult to classify.

3.3. Overall accuracy and classified area

Table 1 shows the percentage of the classified area and Table 2 the overall accuracy, both for the GR and MV zones and according to the different compression ratios (CR) applied. In these tables, the optimum CR recommended for each scenario is shown in bold type. To choose this optimum CR, the maximum loss accepted for the overall accuracy was set at −0.40 percentage points with respect to the original value. The maximum accepted loss in the classified area was −2.50 percentage points. These choices are conventional criteria, but useful to obtain clearer conclusions; they were set after some trials and accurately observing the results. Note that the classified area or the overall accuracy sometimes increased more than 0.40 or 2.50 percentage points respectively, due to the homogenization produced by compression. As such the results confirm those from the training pixels.

Table 1
Percentage of classified area with respect to the total forest area for the Garrotxa-Ripollès (GR) and Maresme-Vallès (MV) zones for different compression (JPG and J2K) scenarios. The difference in percentage points between the value obtained at each CR (each row) and the value obtained from the non-compressed image (first row) is shown in brackets. Optimum CR recommended for each scenario is shown in bold.

Classified area (%)	JPG		J2K	
	GR	MV	GR	MV
Original	88.00	69.17	88.00	69.17
CR 1.66:1	87.25 (−0.75)	69.67 (0.51)	88.44 (0.44)	70.60 (1.43)
CR 2:1	86.88 (−1.11)	**70.42 (1.25)**	88.31 (0.31)	70.09 (0.92)
CR 2.5:1	87.36 (−0.63)	70.17 (1.01)	88.88 (0.88)	69.66 (0.49)
CR 3.33:1	87.67 (−0.33)	69.59 (0.43)	88.32 (0.32)	**70.40 (1.23)**
CR 5:1	87.90 (−0.10)	68.86 (−0.30)	87.33 (−0.67)	70.25 (1.08)
CR 10:1	87.47 (−0.53)	68.79 (−0.38)	**87.46 (−0.54)**	69.16 (−0.01)
CR 20:1	**88.05 (0.06)**	69.55 (0.39)	**86.88 (−1.12)**	67.65 (−1.51)
CR 100:1	86.04 (−1.96)	63.97 (−5.19)	82.28 (−5.72)	61.33 (−7.84)

3.3.1. JPG compression scenario

The classified area obtained with compressed images of the GR zone was slightly smaller than that obtained with the original images; however, as a rule we observed the classified area increased with the compression ratio. With a CR of 20:1 the classified area obtained with compressed images was almost the same than the original (88.05% compared to 88.00%). The maximum loss of classified area as compression increased was 1.11 percentage points when the CR was 2:1. It is necessary to study the variation of classified area related to the overall accuracy behaviour. The overall

Table 2
Overall accuracy for the Garrotxa-Ripollès (GR) and Maresme-Vallès (MV) zones for different compression (JPG and J2K) scenarios. The difference in percentage points between the value obtained at each CR (each row) and the value obtained from the non-compressed image (first row) is shown in brackets. Optimum CR recommended for each scenario is shown in bold.

Overall accuracy (%)	JPG		J2K	
	GR	MV	GR	MV
Original	89.90	83.20	89.90	83.20
CR 1.66:1	89.90 (0.00)	83.10 (−0.10)	89.60 (−0.30)	83.10 (−0.10)
CR 2:1	89.90 (0.00)	**82.90 (−0.30)**	89.70 (−0.20)	83.10 (−0.10)
CR 2.5:1	90.00 (0.10)	82.70 (−0.50)	89.70 (−0.20)	83.70 (0.50)
CR 3.33:1	90.10 (0.20)	82.90 (−0.30)	89.80 (−0.10)	**83.80 (0.60)**
CR 5:1	90.30 (0.40)	82.90 (−0.30)	90.20 (0.30)	**83.40 (0.20)**
CR 10:1	90.10 (0.20)	83.00 (−0.20)	**90.70 (0.80)**	83.10 (−0.10)
CR 20:1	**90.40 (0.50)**	83.10 (−0.10)	**91.00 (1.10)**	83.30 (0.10)
CR 100:1	89.60 (−0.30)	83.20 (0.00)	92.40 (2.50)	84.00 (0.80)

accuracy of classifications obtained with compressed images was equal or higher to that obtained with the original images. Moreover, the overall accuracy increased as compression increased until it reached a maximum at CR 20:1; if compression was higher, the overall accuracy decreased sharply. This is the optimum compression ratio in this scenario for this zone (depicted in bold in Tables 1 and 2).

In the MV zone, the classified area was larger than that obtained with the original image for low CR and decreased if the images were compressed more than CR 3.33:1. The overall accuracy was lower than the original overall accuracy and had a minimum value at CR 2.5:1 (82.70% compared to 83.20%). As the criterion for selecting the optimum compression ratio was a maximum decrease in overall accuracy of 0.40 percentage points, the optimum CR of this scenario is CR 2:1.

3.3.2. J2K compression scenario

In the GR zone, the classified area was higher than the original classified area and increased until CR 2.5:1, when it started to decrease with the CR (at CR 5:1 it was smaller than the original). However, the overall accuracy was slightly lower than the original overall accuracy, but increased with compression. Therefore, the optimum CR is 10:1, or 20:1 when the classified area is slightly smaller than that of the original image, but the overall accuracy is higher.

Trends for the classified area and overall accuracy of the MV zone were similar to those obtained for the GR zone, but with different CR at which tendencies change. The classified area was higher than that obtained with the original image until CR 10:1, when it began to decrease with respect to the original value. The overall accuracy was slightly lower than the original at low compression ratios, and increased with CR until a maximum was reached at CR 3.33:1. Therefore, the optimum CR is 3.33:1, or 5:1 at which the classified area is larger and the overall accuracy is higher than the original.

4. Recommendations and discussion

Table 3 shows the maximum recommended CR for each scenario and the effects of this CR on the classifications carried out. The last column provides a recommendation of whether to use compression in the different studied scenarios.

4.1. Classification

Land cover classifications of forest areas from images, topoclimatic variables and NDVI values that have been compressed are greatly affected by the degree of landscape fragmentation. In less fragmented zones, both JPG and J2K at medium and high compressions (CR 10:1 or CR 20:1, ++ or +++ in the summary table) are possible as the effects of these compressions on the classification are negligible (=) or quite positive (+). This is the only situation in which JPG obtains slightly better results than J2K.

In fragmented zones it is not advisable to compress images using JPG as only very low compression is possible with practically negligible effects on classification. Moreover, as a JPEG 2000 lossless compression would achieve almost the same compression ratio without losing any information, it would be the recommended option to save space. However, J2K low (+) or medium (++) lossy compression is possible (CR 3.33:1 or CR 5:1) and the effects are quite positive (++).

Summarizing, it can be concluded that J2K can achieve higher compression ratios than JPG, and fragmented areas cannot be compressed as much as the less fragmented areas.

4.2. Other comments

It is clear then that compression does not generally have a negative effect on classification, but it is not true that images can always be compressed to ratios of CR 100:1 or more as has sometimes being

Table 3
Optimum compression ratio (CR) and effects of this compression on classification (classified area and overall accuracy) for each scenario. For each recommended CR, the difference between the values obtained using compressed images and original images is shown in percentage points.

	Less fragmented areas (*e.g.*, GR zone)			More fragmented areas (*e.g.*, MV zone)		
	Accepted compression[a]	Effects on classification[b]	Conclusion	Accepted compression[a]	Effects on classification[b]	Conclusion
JPG	+++ (CR 20:1)	+ Area: +0.06 Accuracy: +0.50	Yes	= (CR 2:1)	= Area: +1.25 Accuracy: −0.3	No
J2K	++ or +++ (CR 10:1 or 20:1)	= Area: −0.54 or −1.12 Accuracy: +0.8 or +1.1	Yes	+ or ++ (CR 3.33:1 or 5:1)	++ Area: +1.23 or +1.08 Accuracy: 0.6 or 0.2	Yes

[a] *Symbols regarding compression.* =: very low (equivalent to that obtained by lossless methods); +: low; ++: medium; +++: high.
[b] *Symbols regarding effects on classification.* =: the general effect is negligible; +: both overall accuracy and classified area are slightly higher than the original, or one is higher and the other equal to the original; ++: both overall accuracy and classified area are higher; +++: both overall accuracy and classified area are very high.

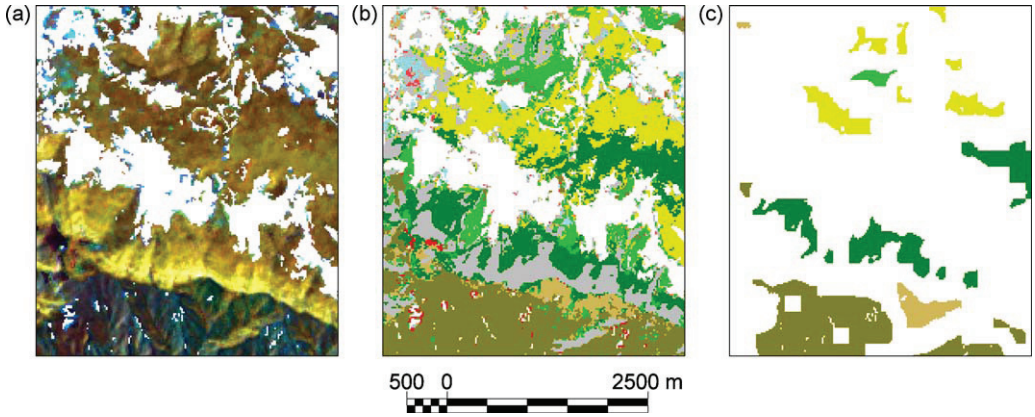

Fig. 5. (a) RGB composition (4,5,3) within the original 13-06-2002 image over the GR zone; (b) classification (see legend in Fig. 8) and (c) training and test areas.

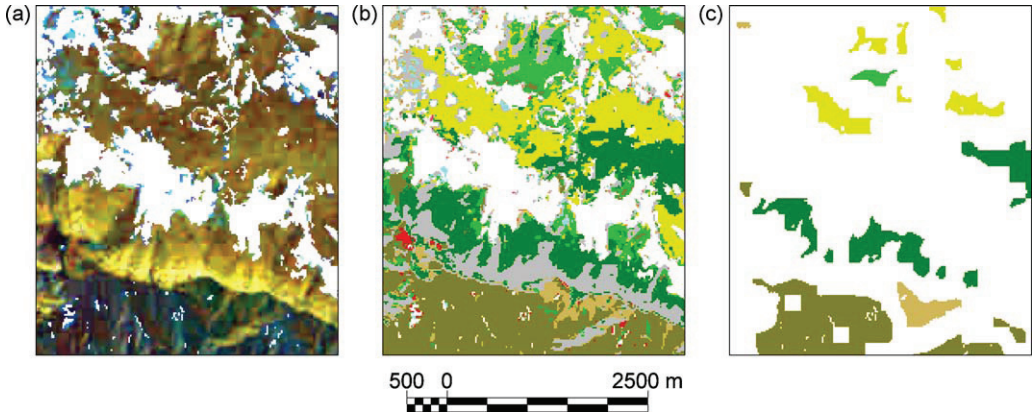

Fig. 6. (a) RGB composition (4,5,3) within the 13-06-2002 image over the GR zone after a JPG compression at CR 20:1; (b) JPG classification (see legend in Fig. 8); and (c) training and test areas.

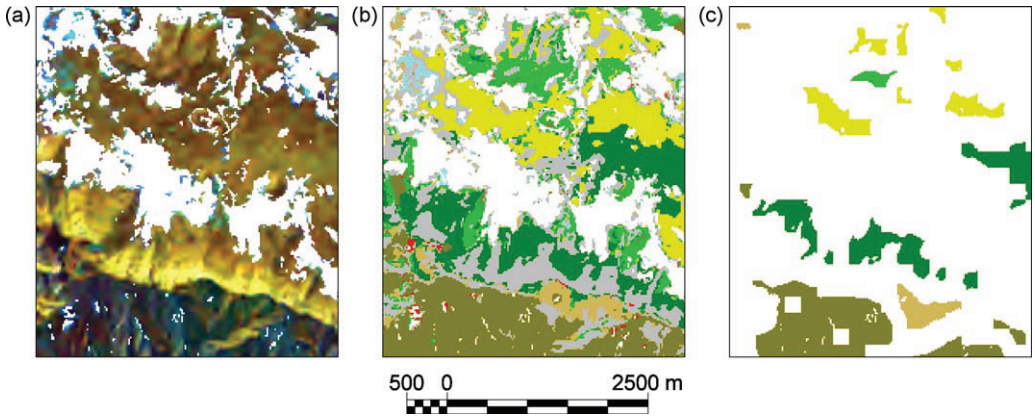

Fig. 7. (a) RGB composition (4,5,3) within the 13-06-2002 image over the GR zone after a J2K compression at CR 20:1; (b) J2K classification (see legend in Fig. 8); and (c) training and test areas. The less classified area of this scenario can be noticed if compared with the original one (Fig. 5).

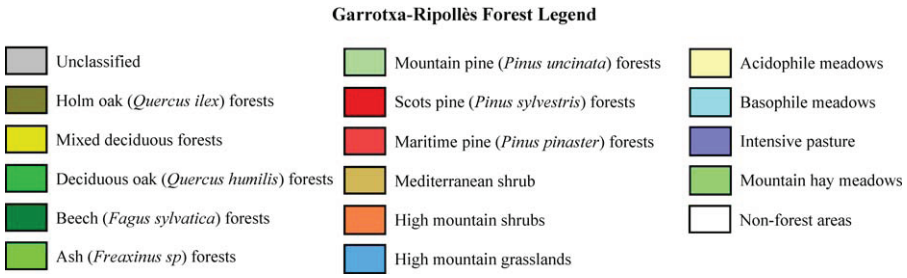

Fig. 8. Legend of forest categories obtained in the GR zone. White areas in Figs. 5–7 are non-forest areas.

claimed (Landgrebe, 2000), since a very high compression ratios may have an adverse effect on classification accuracy.

Besides the quantitative evaluations, other qualitative conclusions can be drawn from a visual assessment. It is very interesting to note that classifications obtained after J2K compression (Fig. 7) have less salt and pepper effect than those obtained with the original images (Fig. 5); thus, they are more convenient from a cartographic point of view. In this figure the loss of classified area obtained with this scenario can also be seen. Blocks appear when JPG compression is used at a high CR (*e.g.*, 100:1) and therefore heavy JPG compression should be avoided.

In the neighbouring areas between very differentiated spectral classes, compression frequently produces mixture effects that lead to misclassifications (Choi et al., 2008). Future studies on land use changes can be affected by this, producing erroneous conclusions in border areas.

The evaluation method may underestimate the classification errors due to the methodology used to obtain training and test areas (border erosion of HMC polygons). Paola and Schowengerdt (1995), Kiema (2000) and Pérez et al. (2003) consider the classification obtained from the original images as ground-truth terrain; however, this approach does not seem correct because the original classification also has errors and, in some cases, the classification obtained using compressed images is better than the original classification.

5. Conclusions

This paper studies the implications of lossy compression on image classification of forest areas. The results in more fragmented areas show that they support less compression when compared with more homogeneous zones (Figs. 6–8).

The classifications obtained after JPEG 2000 compression have less salt and pepper effect than those obtained with the original images. Furthermore, at high compression ratios (without surpassing the maximum compression recommended), the classification obtained using compressed images can produce better results than the classification obtained with the original images.

At high levels of compression, unwanted visual effects are produced; however, they do not appear to have a serious effect on the classification results. If the optimum compression level is exceeded, adverse affects on the classification accuracy must be expected. The inflection point is located at different CR depending on image fragmentation (more fragmented images accept less compression) and on the compression method (J2K makes it possible to obtain higher compression ratios with the same results).

In less fragmented zones, both JPG and J2K high compressions (CR 10:1 or CR 20:1) are possible. However, in fragmented zones, it is not advisable to compress images using JPG, and when J2K is used, only medium compression is possible (CR 3.33:1 or CR 5:1).

Provided that the JPEG 2000 compression standard has been confirmed to be better than the JPEG standard for image classification, future research can be focused on improving JPEG 2000 compression (taking advantage of other provided features such as integer or three dimensional compression), to obtain even fewer negative effects on classification with the possibility of other added benefits. It must be mentioned, however, that remote sensing general users do not have, in general, much compression expertise, and thus easily usable tools must be developed to bring compression knowledge near to them.

Acknowledgements

The authors wish to thank the Catalan Water Agency (ACA) and the Department of Environment and Housing (DMAH) of the Autonomous Government of Catalonia (*Generalitat de Catalunya*) for their investment policy regarding the availability of Remote Sensing data, which has made it possible to conduct this study under optimal conditions. The authors would also like to thank their colleagues in the Geography Department (especially Pere Serra, for his help with the study area and the training and test areas), the Center for Ecological Research and Forestry Applications (CREAF), and the Department of Information and Communications Engineering (especially Francesc Aulí-Llinàs for his advice on JPEG 2000 compression using BOÍ application) as well as all those at the Autonomous University of Barcelona (UAB) who have collaborated in any way in the treatment of the images. We would also like to express our gratitude to the Spanish National Institute for Aerospace Technology (INTA) for its efficient image subscription service. This work was supported in part by the Ministry of Education and Science and the FEDER funds through the research projects TSI2006-14005-C02-02 and TIN2009-14426-C02-02, as well as by the Catalan Government grant SGR2009-1511. Finally, two anonymous reviewers have greatly contributed to make this a better paper.

References

Aulí-Llinàs, F., Paton, J.R., Bartrina-Rapesta, J., Monteagudo-Pereira, J.L., Serra-Sagristà, J., 2005. J2K: introducing a novel JPEG 2000 coder. In: Proceedings of the SPIE, vol. 5960, pp. 1763–1773.

Carvajal, G., Penna, B., Magli, E., 2008. Unified lossy and near-lossless hyperspectral image compression based on JPEG 2000. IEEE Geosci. Remote Sens. Lett. 5 (4), 593–597.

Choi, E., Lee, S., Lee, C., 2008. Effects of compression on the classification of hyperspectral images. In: Mastorakis, N.E., Mladenov, V., Bojkovic, Z., Simian, D., Kartalopoulos, S., Varonides, A., Udriste, C., Kindler, E., Narayanan, S., Mauri, J.L., Parsiani, H., Man, K.L. (Eds.), Math. Comput. Sci. Eng. Heraklion, Greece, pp. 541–546.

Chou, C.H., Liu, K.C., 2008. Colour image compression based on the measure of just noticeable colour difference. IET Image Process 2 (6), 304–322.

Du, Q., Fowler, J.E., 2007. Hyperspectral Image Compression Using JPEG 2000 and Principal Component Analysis. IEEE Geosci. Remote Sens. Lett. 4 (2), 201–205.

Guarneri, F., Vaccaro, M., Guarneri, C., 2008. Digital image compression in dermatology: format comparison. Telemed. e-Health 14 (7), 666–670.

Ibáñez, J.J., Burriel, J.A., Pons, X., 2002. El Mapa de Cobertes del Sòl de Catalunya: Una eina per al coneixement, la planificació i la gestió del territori. Perspect. Territ. 3, 10–25.

Independent JPEG Group, 2008. Free library for JPEG image compression [Online]. More information and code available at: http://www.ijg.org/.

ISO/IEC, 1994. 10918-1:1994: Information Technology–Digital Compression and Coding of Continuous-tone Still Images: Requirements and Guidelines. Geneva, Switzerland, 182 pp.

ISO/IEC, 2004. 15444-1:2004: Information Technology–JPEG 2000 Image Coding System: Core Coding System. Geneva, Switzerland, 194 pp.

ISO, 2003. 19115:2003: Geographic Information–Metadata. Geneva, Switzerland, 140 pp.

ISO, 2007. 19139:2007: Geographic Information–Metadata–XML schema implementation. Geneva, Switzerland, 111 pp.

Julià, N., Masó, J., Zabala, A., Vallès, M., 2005. CaMM, Catálogo de Metadatos de MiraMon: Implementación en una corporación, el DMAH. Mapping (Madr.) 105, 24–31.

Kiema, J.B.K., 2000. Wavelet compression and the automatic classification of Landsat imagery. Photogramm. Rec. 16 (96), 997–1006.

Landgrebe, D., 2000. Information extraction principles and methods for multispectral and hyperspectral image data. In: Chen, C.H. (Ed.), Information Processing for Remote Sensing. World Scientific Publishing Co., USA, p. 2000.

Lau, W.L., Li, Z.L., Lam, K.W.K., 2003. Effects of JPEG compression on image classification. Int. J. Remote Sens. 24 (7), 1535–1544.

Liang, Z., Tang, X., Zhang, G., Wu, X., 2008. Effects of JPEG2000 and SPIHT compression on image classification. In: Int. Arch. Photogramm. Remote Sens. Spat. Inf. Sci., ISPRS Congress, vol. XXXVII, Beijing 2008, Part B7, Commission VII, pp. 541–544, ISSN: 1682-1750.

López, C., Lejeune, M., Escriva, P., Bosch, R., Salvado, M.T., Pions, L.E., Baugells, J., Cugat, X., Alvaro, R., Jaen, J., 2008. Effects of image compression on automatic count of immunohistochemically stained nuclei in digital images. J. Am. Med. Inform. Assoc. 15 (6), 794–798.

Maguire, D.J., Longley, P.A., 2005. The emergence of geoportals and their role in spatial data infrastructures. Comput. Environ. Urban Syst. 29, 13–14.

Monmonier, M.S., 1982. Computer-assisted Cartography: Principles and Prospects. Prentice-Hall, Englewood Cliffs, NJ, 214 pp.

Moré, G., Burriel, J.A., Castells, R., Ibáñez, J.J., Roijals, X., 2004. Tratamiento estadístico de variables radiométricas, orográficas y climáticas para la obtención de un mapa detallado de vegetación. In: Conesa, C., Álvarez, Y., Martínez, J.B. (Eds.),

Medio Ambiente, Recursos y Riesgos Naturales: Análisis mediante tecnología SIG y Teledetección, pp. 261–273.
Moré, G., Pons, X., 2008. Influencia del número de imágenes en la calidad de la cartografía detallada de vegetación forestal. Rev. Teledetec. 28, 61–68.
Ninyerola, M., Pons, X., Roure, J.M., 2000. A methodological approach of climatological modelling of air temperature and precipitation through GIS techniques. Int. J. Climatol. 20, 1823–1841.
Palà, V., Pons, X., 1995. Incorporation of relief into geometric corrections based on polynomials. Photogramm. Eng. Remote Sens. 61 (7), 935–944.
Paola, J.D., Schowengerdt, R.A., 1995. The effect of lossy image compression on image classification. In: Proceedings of the IGARSS '95, pp. 118–120.
Penna, B., Tillo, T., Magli, E., Olmo, G., 2006. Progressive 3-D coding of hyperspectral images based on JPEG 2000. IEEE Geosci. Remote Sens. Lett. 3 (1), 125–129.
Penna, B., Tillo, T., Magli, E., Olmo, G., 2007. Transform coding techniques for lossy hyperspectral data compression. IEEE Trans. Geosci. Remote Sens. 45 (5), 1408–1421.
Pérez, C., Aguilera, D., Muñoz, A., 2003. Estudio de viabilidad del uso de imágenes comprimidas en procesos de clasificación. In: Pérez Utrero, R., Martínez Cobo, P. (Eds.), Teledetección y desarrollo regional, pp. 309–312.
Pons, X., Solé-Sugrañes, Ll., 1994. A Simple Radiometric Correction Model to Improve Automatic Mapping of Vegetation from Multispectral Satellite Data. Remote Sens. Environ. 48 (2), 191–204.
Pons, X., Moré, G., Serra, P., 2006. Improvements on classification by tolerating nodata values. Application to a hybrid classifier to discriminate Mediterranean vegetation with a detailed legend using multitemporal series of images. In: Proceedings of the 26th International Geoscience and Remote Sensing Symposium, Denver, Colorado, USA, August 2006. IEEE Press, pp. 192–195.
Pons, X., 2008. MiraMon. Geographical Information System and Remote Sensing Software. Version 5 [Online], Available at: http://www.creaf.uab.es/miramon/.
Pons, X., Ninyerola, M., 2008. Mapping a topographic global solar radiation model implemented in a GIS and refined with ground data. Int. J. Climatol. 28, 1821–1834, doi:10.1002/joc.1676.
Qian, S.E., Hollinger, A., Bergeron, M., Cunningham, I., Nadeau, C., Jolly, G., Zwick, H., 2005. A multidisciplinary user acceptability study of hyperspectral data compressed using an on-board near lossless vector quantization algorithm. Int. J. Remote Sens. 26 (10), 2163–2195.
Salvador, R., Pons, X., Diego, F., 1996. Validación de un método de corrección radiométrica sobre diferentes áreas montañosas. Rev. Teledetec. 7, 21–25.
Serra, P., Moré, G., Pons, X., 2009. Thematic accuracy consequences in cadasterland-cover enrichment from a pixel and from a polygon perspective. Photogramm. Eng. Remote Sens. 75 (12), 1441–1449.
Tintrup, F., De Natale, F., Giusto, D., 1998a. Automatic land classification vs. data compression: a comparative evaluation. In: Proc. IGARSS '98, pp. 1751–1753.
Tintrup, F., De Natale, F., Giusto, D., 1998b. Compression algorithms for classification of remotely sensed images. In: Proc. ICASSP'98, pp. 2565–2568.
USGS, 2009. http://landsat.gsfc.nasa.gov/news/news-archive/news_0187.html.
Viñas, O., Baulies, X., 1995. 1:250000 land-use map of Catalonia (32000 km^2) using multi-temporal Landsat-TM data. Int. J. Remote Sens. 16 (1), 129–146.
Wang, H., Babacan, S.D., Sayood K, 2007. Lossless hyperspectral-image compression using context-based conditional average. IEEE Trans. Geosci. Remote Sens. 45 (12), 4187–4193.
Zabala, A., Pons, X., 2002. Image metadata: compiled proposal and implementation. In: Benes, T. (Ed.), Geoinformation for European-wide Integration. Millpress, Rotterdam, pp. 647–652.

Alaitz Zabala received her BS degree in Environmental Sciences in 2002 and her MS degree in Geography in 2006 at the Autonomous University of Barcelona. He is a researcher and associate professor at the Department of Geography of the Universitat Autònoma de Barcelona. Zabala research main interests are standardized metadata (following FGCD, CEN, ISO, and INSPIRE standards) and the study of the implications of extracting information from lossy compressed images and developing standardized servers. She was the main developer of the metadata profile and of the GeMM MiraMon tool that is a metadata tool for raster and vector layer.

Xavier Pons has done his main work in radiometric and geometric corrections of satellite imagery, in cartography of ecological and forest parameters from airborne sensors, in studies of the spectral response of Mediterranean vegetation and in GIS development (data structure, organization and software writing: MiraMon). He has recently worked in climatology models, in forest fire mapping and in analysis of landscape changes, water usage and snow coverage from long time series of images. He is currently working in the implications of image compression on Remote Sensing. Pons is full professor at the Geography Department of the UAB and coordinates research in GIS and RS at the CREAF.

5. JPEG 2000 ENCODING OF IMAGES WITH NODATA REGIONS FOR REMOTE SENSING APPLICATIONS

JPEG2000 encoding of images with NODATA regions for remote sensing applications

Alaitz Zabala,[a] Jorge González-Conejero,[b] Joan Serra-Sagristà,[b] and Xavier Pons[a,c]

[a]Department of Geography (DG),
Universitat Autònoma de Barcelona, 08209 Cerdanyola del Vallès, Spain
Alaitz.Zabala@uab.cat, Xavier.Pons@uab.cat
[b]Department of Information and Communications Engineering (DEIC),
Universitat Autònoma de Barcelona, 08209 Cerdanyola del Vallès, Spain
jgonzalez@deic.uab.cat, Joan.Serra@uab.cat
[c]Center for Ecological Research and Forestry Applications (CREAF),
Universitat Autònoma de Barcelona, 08209 Cerdanyola del Vallès, Spain

Abstract. The aim of this work is to, within the JPEG2000 framework, enhance the coding performance obtained for images that contain regions without useful information, or without information at all, here named as NODATA regions. In Geographic Information Systems (GIS) and in Remote Sensing (RS), NODATA regions arise due to several factors, such as geometric and radiometric corrections, atmospheric events, the overlapping of successive layers of information, etc. Most coding systems are not devised to consider these regions separately from the rest of the image, sometimes causing a loss in the coding efficiency and in the post-processing applications. We propose two approaches that address this issue; the first technique (Average Data Region, ADR) is carried out as simple pre-processing and the second technique (Shape-Adaptive JPEG2000, SA-JPEG2000) modifies the coding system to avoid the regions without information. Experimental results, performed on data from real applications and different scenarios, suggest that the proposed approaches can achieve, *e.g.*, for SA-JPEG2000, a Signal-to-Noise Ratio improvement of about 8 dB. Moreover, in a post-processing application such as a digital classification, the best classification results are obtained when the proposed approaches SA-JPEG2000 and ADR are applied.

Keywords: NODATA region coding, JPEG2000, shape-adaptive, digital image classification, remote sensing.

1 INTRODUCTION

Nowadays, the capabilities of modern sensors, which increase the size of images, as well as the growing number of Earth observation missions, mean an enormous demand for storage capacity. Also, the manipulation and interactive transmission of images is becoming an important issue for applications in many different fields, as in Geographic Information Systems (GIS) or in Remote Sensing (RS), where images are an important source of data. In these scenarios, a coding process may prove useful. Nevertheless, in some cases, images contain regions without useful data. In RS, for instance, either geometric and radiometric corrections [1–3], or atmospheric events (*e.g.*, clouds) may generate images containing regions with unavailable information. In GIS, the successive overlapping of layers of information produces images containing areas that should not be considered, especially on the Internet scenario. The number of Web Map Services (WMS) and of geoportal applications is raising on the last years [4]. Usually, WMS serve images combining raster and vector layers overlapped, thus, part of the images are always covered by vector entities (*e.g.*, buildings). Here, these regions without information are named as NODATA regions. Generally, on those samples where the value of the image is unknown, a

Received 30 Nov 2009; accepted 19 Apr 2010; published 14 Jul 2010 [CCC: 19313195/2010/$25.00]

particular value is used to mark it. The consideration of this value as a "normal" value has two main shortcomings for the coding process: first, the final coding performance could be penalized by the overhead produced by these NODATA regions, and second, it could generate errors on the post-processing applications, for instance, in a digital image classification process, or when computing a slope in digital elevation models.

In the literature, several approaches are available to encode images containing NODATA regions. On one hand, there are coding systems that are specifically devised to avoid the encoding of these NODATA regions. For instance, in [5] a set partitioning strategy is followed, and during the encoding process, NODATA samples are discarded. On the other hand, there are state-of-the-art coding systems extended to deal with these NODATA regions. As an example, in [6] the Embedded Block Coding with Optimized Truncation (EBCOT) [7] algorithm is modified to avoid the encoding of certain regions within the image, and in [8] the Set Partitioning in Hierarchical Trees (SPIHT) is revisited to deal with these useless regions. This type of approaches is also used to encode only a given region at a time. In [9] a multispectral image is segmented in different classes to jointly encode similar samples, thus only one class is encoded at a time, or, in [10], a scheme is proposed to encode only certain regions and components within a multispectral image to improve the capabilities of transmission, data mining, and retrieval applications.

JPEG2000 is one of the latest standards developed by the Joint Photographic Experts Group (JPEG) and is structured in 12 different parts, addressing the encoding, transmission, security, and manipulation of images and video. Part 1 [11] of the standard, is the basis of the other parts. JPEG2000 is a wavelet-based coding scheme with a two-tiered coding strategy built on the EBCOT paradigm. Among other features, the JPEG2000 core coding system provides scalability by quality, spatial location, resolution, and component. These different types of scalability fulfill most of the requirements of applications and scenarios where images are used. Nevertheless, approaches to handle and minimize the coding cost of NODATA regions have not been considered for the JPEG2000 standard. A complete review of JPEG2000 coding system is available in [12].

Traditionally, GIS and RS communities have been reluctant to lossy compression methods and its possible loss of information that might be relevant to posterior processes. Recent studies have demonstrated that, for the majority of applications, a certain degree of lossy compression might be applied without affecting the results of final applications: digital elevation model generation [13, 14], and digital image classification [15–17].

The aim of this work is to develop approaches within the JPEG2000 framework to reduce the penalization in the encoding process produced by the presence of NODATA regions. In addition, higher compression performance does not necessarily mean higher quality for a given remote sensing application [18], thus, the possible malicious effects on the post-processing stages –such as classification methods–, have to be carefully studied too.

This paper is structured as follows: Section 2 introduces the approaches developed for the encoding of images containing NODATA regions within the JPEG2000 framework; Section 3 presents how the NODATA regions arise and the datasets used to assess the performance achieved by the proposed approaches; Section 4 presents several experimental results and evaluates the impact in three post-processing digital classifications; and Section 5 draws some conclusions.

2 ENCODING OF IMAGES CONTAINING NODATA REGIONS

Most modern coding systems have four common main stages: Discrete Wavelet Transform (DWT), Quantization, Bit-plane Encoder (BPE), and Arithmetic Coder (AC). The DWT is devised to compact the energy of the image in some samples, and to de-correlate the information of the image detecting smooth areas and sharp edges. Quantization prepares the coefficients

from the DWT for the BPE. In the BPE, the image is encoded from the most to the least significant bit-plane. Finally, the AC is applied to reduce the total amount of bits generated by the encoding process.

Figure 1(a) depicts a section of a 1:5000 color orthoimage over Barcelona (Spain). In this image, the NODATA regions arise due to the successive overlapping of layers of information that produce areas that are permanently out of sight and, commonly, these regions are set by default to the highest or lowest value allowed by the bit-depth. Recalling the aim of the DWT, we can see in Fig. 1(b, c, d and e) that the separation between the data and NODATA regions (white areas in Fig. 1 a) is captured by the filter-bank and it is clearly noticeable in the subbands. These boundaries have a high coding cost, because they contain coefficients with a high magnitude. To ease the visualization in Fig. 1, a particular NODATA region is surrounded in red in the original image. Its corresponding coarse edges captured by the DWT filter-bank in the residual and detail subbands are also surrounded.

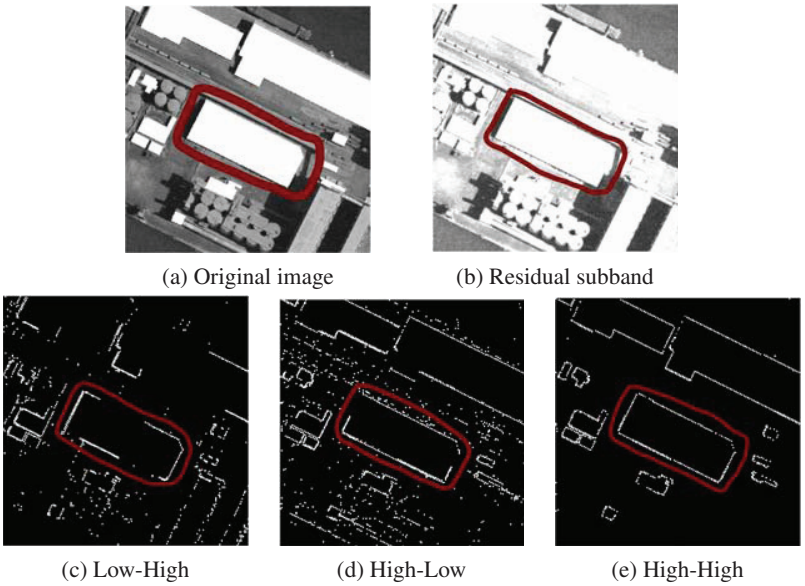

(a) Original image (b) Residual subband

(c) Low-High (d) High-Low (e) High-High

Fig. 1. Color orthoimage 1:5000 over Barcelona masked with overlapping layers. One level of DWT is applied to the original image using the common 9/7 filter-bank. To ease the visualization of the detail subbands in the DWT, they are separated and scaled. Low and High state the order of the low and high pass of the filter-bank, respectively.

There are two main reasons that explain the extra coding cost in the encoding process of images that contain NODATA regions: the cost of coding the sharp edges that arise after the DWT stage, and the cost of coding the coefficients belonging to the NODATA regions.

2.1 Encoding techniques

Figure 2 shows the main stages of JPEG2000 standard coding system and, in light gray, the two approaches proposed in this paper, which are devised to minimize, or even eliminate, the extra coding cost produced by the NODATA regions. The first approach, called *Average Data Region (ADR)*, is applied during the pre-processing stage of the JPEG2000, and consists of simple modifications of the image samples belonging to the NODATA region. The second approach, called *Shape-Adaptive JPEG2000 (SA-JPEG2000)*, modifies two important stages of the coding system: the DWT, and the BPE; however, this approach does not generate a compliant JPEG2000 code-stream. Another alternative approach could be based on the *MaxShift* Region

of Interest (ROI) Coding method (provided by the JPEG2000 standard). According to previous results [19, 20], the MaxShift approach obtains similar results than usual JPEG2000 –*i.e.*, without applying any of the proposed approaches–, with no particular advantage for NODATA coding; therefore, the MaxShift approach is not considered in this paper.

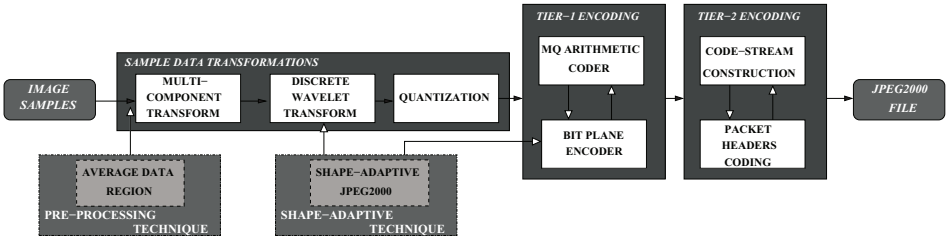

Fig. 2. Main stages of the JPEG2000 coding system. Light gray boxes depict the proposed approaches devised for the coding of images containing NODATA regions.

2.1.1 Average Data Region

The value selected to fill the NODATA region has an important effect in the final coding performance due to the coarse edges that arise after the DWT step. Figure 3 depicts three rate-distortion curves for an ASTER image (described in Section 3), applying the JPEG2000 coding system and obtaining the Signal-to-Noise Ratio (SNR) Energy computed only for the data regions. The NODATA samples are set to: 0, 100, and 200, and results suggest that the selection of this value must be accurate to maximize the coding performance achieved.

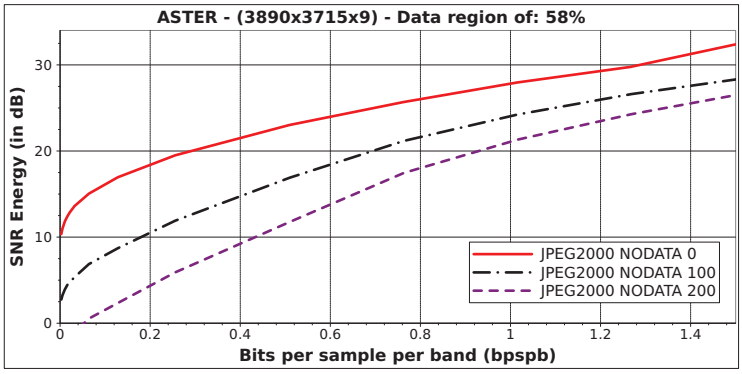

Fig. 3. Rate-distortion curves in SNR Energy (in dB) for an image from the tested datasets. JPEG2000 is applied when the NODATA samples are set to: 0, 100, and 200.

The aim of the ADR is to smooth the boundary between data and NODATA regions. ADR computes a single arithmetic mean from all the samples belonging to the data region, and sets each sample belonging to a NODATA region to the single computed arithmetic mean. Figure 4 shows an example of execution.

However, ADR does not consider local image variations since only one unique arithmetic mean is computed for the whole data region. In this sense, another pre-processing approach called Phagocyte, implemented in the commercial GIS application MiraMon [21], can be used. Phagocyte computes one arithmetic mean within a squared window that is shifted in iterative executions covering the entire image. Nevertheless, our experiments suggest that Phagocyte does not provide significant improvement in the final coding performance results, obtaining

similar SNR Energy results than ADR, and due to the computation of many different arithmetic means, the computational requirements are significantly increased.

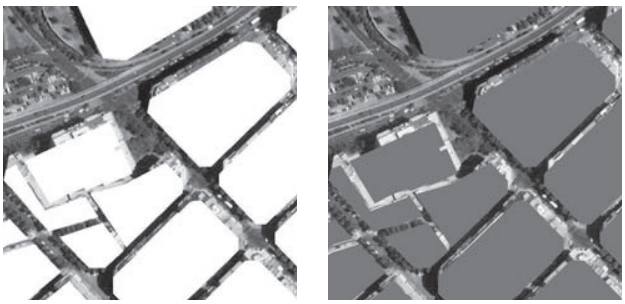

(a) Original Image (b) Image after ADR execution

Fig. 4. Section from an 1:5000 color orthoimage belonging to the tested sets. NODATA regions are depicted in white (highest value of the bit-depth) in the original image, and in gray (mean value of the data region) after ADR execution.

2.1.2 Shape-Adaptive JPEG2000

The main goal of the SA-JPEG2000 is to avoid the NODATA coefficients modifying two main stages within JPEG2000 coding system. The first stage modified is the DWT. An issue that comes up when applying the DWT to an image is what happens at the image boundaries, *i.e.*, how to deal with the non-existent samples –those samples outside the image– needed for the application of the filter-bank. This is commonly addressed carrying out a mirror effect that virtually extends the image boundaries. The main idea behind the shape-adaptive DWT (SA-DWT) is to apply a mirror effect at the boundaries of the data region, as shown in Fig. 5. The shape-adaptive approach of the DWT was introduced in the MPEG-4 [22] standard for video systems, and it was later proposed for still image compression [23].

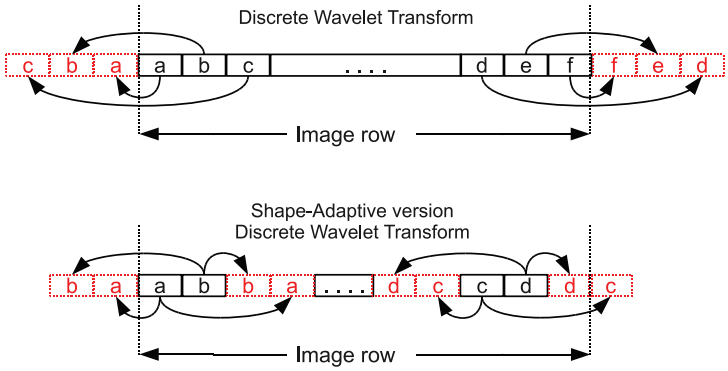

Fig. 5. Mirror effect applied to an image row. Top: classical DWT. Bottom: Shape-Adaptive version of the DWT.

In addition to the operations carried out by the SA-DWT, the BPE stage is also modified to skip the coefficients belonging to the NODATA regions. The JPEG2000 encoding process divides the subbands produced by the DWT into code-blocks that are encoded independently. The BPE encodes each code-block in stripes composed by four different rows within the code-block in a

predetermined order. The modifications carried out to the BPE, aimed to avoid the encoding of the NODATA coefficients, consist of adapting the scanning order such that coefficients without useful information are skipped, as shown in Fig. 6.

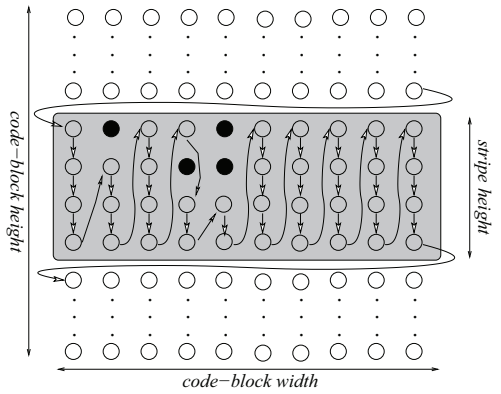

Fig. 6. Scanning order skipping the NODATA coefficients. Coefficients belonging to the NODATA regions are depicted in black.

Shape-adaptive coding has particular costs that do not appear in the conventional coding. First of all, the data and NODATA regions are separate entities, their shape must be described by a binary mask (bi-level image). The creation of the binary mask must be accurate to take advantage of the shape of the objects to improve the compaction of the energy of the SA-DWT, since due to the arbitrary shapes and sizes of data regions, the SA-DWT obtains, in general, a poorer compaction of the image information. The costs and advantages of the shape-adaptive encoding have been analyzed in [24].

2.2 Mask Encoding

For a clear distinction between the data and NODATA regions, the shape of the NODATA regions has to be transmitted. This shape information is associated with a binary mask specifying if the sample is inside the data region. In lossy compression, the encoded mask is placed at the beginning of the stored code-stream to ease the recovering without any loss of information at the start of the decoding process.

Several coding systems have been presented in the literature to encode bi-level images in a lossless mode. Coding systems able to deal with the binary mask could be divided into two different groups. On one hand, there are the contour-based methods, where the boundary information of the closed contour that contains the object represents the shape information [25, 26]. On the other hand, there are methods that encode the binary mask directly [9, 12, 27, 28]. Most coding systems designed to encode bi-level images are focused on object-based video coding. The contour-based methods encodes the contour-closed objects. So, they work properly in an object-based coding. The NODATA regions are not "natural" objects, as those found in a video sequence. Moreover, when the contour is recovered, a fill algorithm must be applied to obtain the complete binary mask needed by the proposed approaches. So, for the encoding of images that contain NODATA regions, a method that directly encodes the binary mask must be selected.

To ease the manipulation of code-streams obtained from the mask and the image, there is the possibility to combine both in a unique final code-stream through the JPEG2000 file format. JPEG2000 code-stream is entirely self-contained. However, many applications may find certain other information useful. Three JPEG2000 file formats are defined: 1) JP2 file format (minimal file format) [11], 2) JPX file format (compatible JP2 extensions, *e.g.*, allocate several codes-streams, metadata inclusion) [29], 3) JPM file format (for documents containing images and text) [30].

Software applications that implement approaches and coding systems evaluated in Section 4.1 perform the algorithm [28] for the encoding of binary masks. Approaches based on the JPEG2000 framework (ADR, MaxShift, and SA-JPEG2000) include the masks' code-stream produced in the final code-stream as metadata following the JPEG2000 Part 2 specifications.

3 DATASETS

In this section, six different datasets are introduced. They are employed to assess the coding performance and the digital classification results presented in Section 4. These datasets cover different situations and scenes used in RS and GIS real applications, *i.e.*, NODATA due to: 1) geometric corrections, 2) geometric and radiometric corrections, 3) geometric/radiometric corrections and masking of areas of interest, and 4) overlapping of RS images and GIS layers. In Fig. 7 the images and their corresponding binary masks are depicted. White and black areas on the binary masks represent the data and NODATA regions, respectively.

3.1 Geometrically corrected images

Full frame images geometrically corrected have NODATA regions distributed at their outer part. This is a very common situation in RS images, when they are corrected to a defined reference system to enrich the user GIS database and to be overlapped with other geographical information (as covered in Sect. 3.4). This special distribution of NODATA will have influence on compression performance results obtained among different coding techniques.

The first dataset is an image acquired through the Compact Airborne Spectrographic Imager (CASI), an airborne optic sensor that can be programmed to obtain a maximum of 288 bands from blue to near-infrared. Radiometric resolution of CASI images is unsigned 16 bits/pixel. The sensor flew on the airplane Cessna-Citation I of the Cartographic Institute of Catalonia (ICC). Lines captured by the sensor are affected by the movement of the airplane; therefore, it is necessary to geometrically correct the image line by line using a Global Positioning System (GPS) receiver and an Inertial Navigation System (INS). This geometric correction was made using the SISA system (developed by the ICC). This dataset is devised to capture the features of vegetation and farming for agricultural purposes, and is an image from Lleida (Spain) captured on 14th June 2004, with dimensions of $4058\times1073\times11$, hereafter CASI-1. Due to geometric corrections the data region of the image is 44%.

3.2 Geometrically and radiometrically corrected images

The second dataset is also devised for agriculture purposes and is composed by two images acquired through the *Satellite Pour l'Observation de la Terre* (SPOT). The region captured corresponds to the delta and adjacent regions of the Ebro river in Spain. Due to the geometric and radiometric corrections carried out on both images, to improve the accuracy of the information captured, samples are stored in real format with a bit-depth of 32 bits. Also, these corrections generate NODATA regions. The first image, SPOT_2008, was captured on 3rd October 2008 in the path-row 042-268 by the instrument *Haute Résolution Visible et Infrarouge* (HRVIR 2), boarded on the SPOT-4 satellite. This image has a dimensions of $1593\times1033\times4$, and the 79% of the samples contain information, while the rest are considered as NODATA. The second image, SPOT_2009, was captured on 14th January 2009 in the path-row 043-268 by the instrument *Haute Résolution Géométrique* (HRG 1), boarded on SPOT-5 satellite. Dimensions are $3186\times2066\times4$, and the 76% of the entire image is data. Both instruments provide four spectral bands (green, red, near-infrared, and short-wave infrared).

The Ebro delta, located in the northeast of Spain, is the third most important aquatic habitat of Western Mediterranean, after the Camargue (in France) and Doñana Park (in southern Spain). In the Ebro delta, rice farming only involves a period of six months every year (from April to September) remaining dry the rest of the year. Nevertheless this situation has changed from

the application of the agri-environmental measures of the European Union (Regulation CEE 1257/1999) of support for sustainable rural development, especially in areas with environmental restrictions. Two of these agri-environmental measures have been adopted in the Ebro delta: one is to maintain flooded the rice surface at least four months (in autumn-winter time) to favor aquatic fauna; the other measure is to eliminate spontaneous vegetation mixing soil and water by mechanic techniques in order to minimize pesticide contamination. Therefore, the objective of this classification is monitoring winter flooding of rice fields for identifying the application of these agri-environmental measures.

The third dataset is composed by one image from the Advanced Spaceborne Thermal Emission and Reflection Radiometer (ASTER) sensor, boarded on the Terra (EOS-AM) satellite, used to create maps of either temperature, reflectance, or elevation. The ASTER sensor can be programmed to acquire 15 different bands; however for our purposes only 9 are used (green, red, near-infrared, and 6 short-wave infrared). Area covered corresponds to a Mediterranean coast in Spain and was captured on 25th November 2007. In the image, named as ASTER, corrections generate NODATA regions, and samples are stored in real format with a bit-depth of 32 bits, like in the SPOT dataset. The dimensions are $3890\times3715\times9$ and the data region is the 58% of the whole image.

3.3 Land cover masking

The fourth covered situation is composed of five Thematic Mapper images (Landsat-5 satellite). Those images were used to obtain a 2004 crop map over Lleida (NE Spain), and were selected from those available (without clouds) taking into account its annual distribution to take advantage of the different spectral responses of crops along the year due to their phenological state. 6 optical bands (8 bits unsigned format) of each selected images (16-05-2004, 17-06-2004, 19-07-2004, 23-10-2004 and 08-11-2004) were used. Only a part of the whole Landsat scene is used (covering the area of interest) whose dimensions are $1517\times1311\times6$ (for each of the 5 dates). Radiometric corrections applied to the image produce NODATA regions. Moreover, in order to classify only the crop areas (to obtain the best results as suggested by [31]), a mask obtained from the Land Cover Map of Catalonia was applied, with a remaining 67% of data region.

The fifth dataset is an image from the Airborne Visible/Infrared Imaging Spectrometer (AVIRIS). This sensor acquires lines containing 614 pixels in 224 spectral bands (bit-depth of 16 bits/pixel), requiring hundreds of megabytes for storage. We used the Indian Pines scene (available at ftp://ftp.ecn.purdue.edu/biehl/MultiSpec/, Purdue University), over an area 6 miles west of West Lafayette, which is a subset of a significantly larger image file. This is a small image (145×145 pixels, 220 bands) but is selected for evaluation because ground truth is available for this image, and because is an usual one used on compression papers so results should be more comparable. This image has no originally NODATA regions, but, as they are needed to evaluate the proposed compression algorithms, we use the ground-truth image to set those areas with no ground truth information available as NODATA regions, with a remaining 49% of data region.

3.4 Images and vector overlapping

The last covered situation arise when different vector and raster layers are combined in a GIS application. The Overlapping dataset consists of two images composed by four different tiles of 1:5000 color orthoimages over Barcelona (Spain) masked with the buildings and block polygon layers from the 1:5000 Topographic Map (all produced by the ICC and available at http://www.icc.es). The image Overlapping-1 was acquired on May 2005, with dimensions of $3500\times2306\times3$ and 47% of samples are considered as data region. Overlapping-2, captured on June 2005, has a dimensions of $3500\times2306\times3$ and 35% of the whole image is data region. Both images have a bit-depth of 8 bits unsigned.

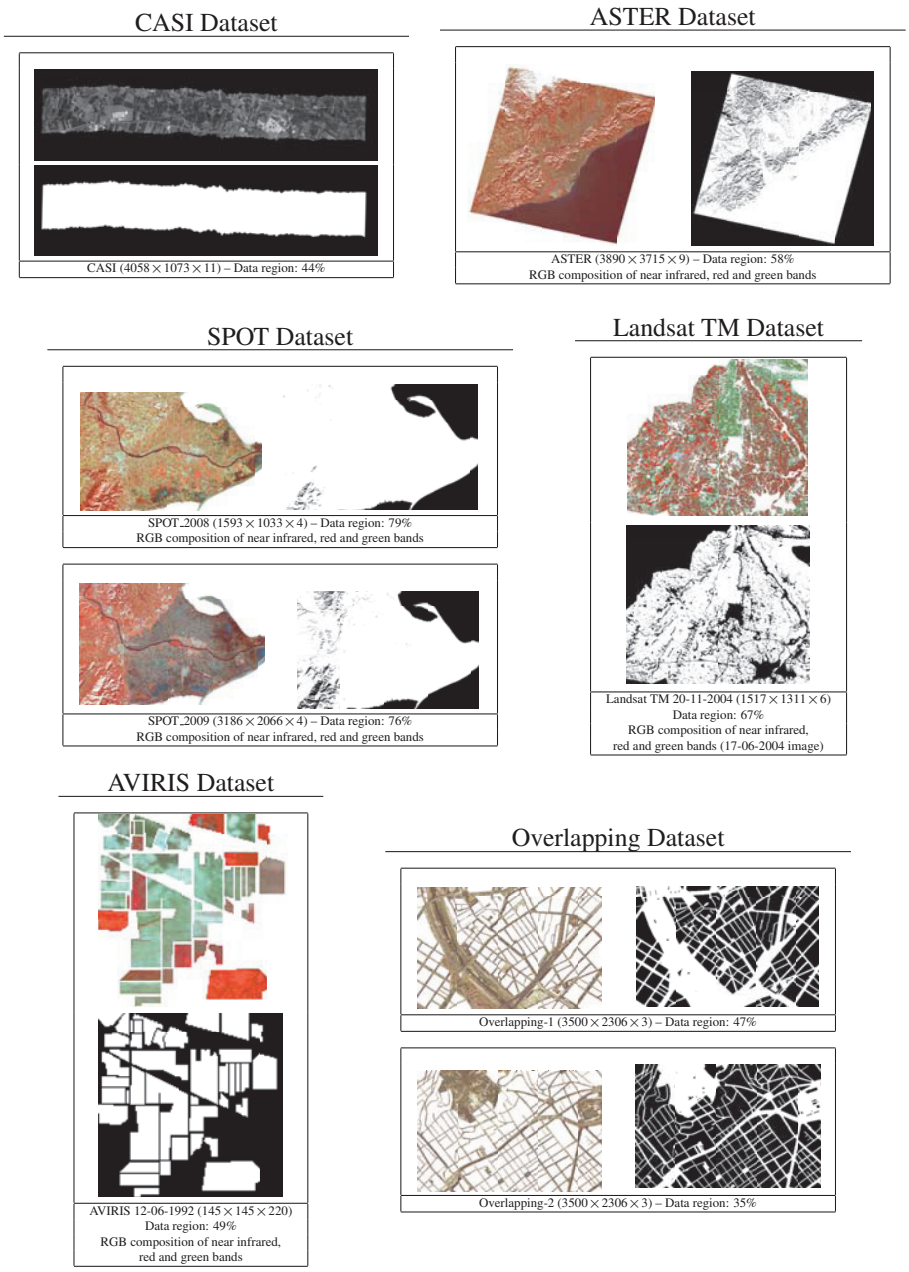

Fig. 7. Selected images with their corresponding data/NODATA regions. White areas depict data regions on the mask (the second image of the pair). The dimensions ($x \times y \times z$) and percentage of data region are given below the image.

4 RESULTS

This section provides results for two different types of experiments. First, the coding performance of the proposed approaches to encode images with NODATA regions is evaluated. Second, the impact of the NODATA images encoding is analyzed in three digital classification methodologies using three of the available datasets (described on Section 3) as example of post-processing application.

4.1 Coding Performance

The JPEG2000 approaches have been implemented in our JPEG2000 Part 1 and Part 2 implementation BOI (available at http://gici.uab.es/BOI, Group on Interactive Coding of Images -GICI-, DEIC, UAB). The proposed approaches are also evaluated against BISK [5], that is entirely devised to support shape-adaptive processing, and thus it is ideal for the coding of NODATA regions. Results are provided by our BISK software, that applies BISK to each component and builds the final code-stream following an interleaved rate-control process [32]. These tests have been carried out using 5 levels of DWT in all the cases. To evaluate the coding performance results over different images, *Signal-to-Noise Ratio (SNR) Energy* has been computed, only for data regions, at different bit-rates. The higher SNR Energy obtained, the most similarity between encoded and original images. The less bits per sample per band (bpspb) used, the more compressed the image is. All components were encoded jointly, and a unique JPEG2000 code-stream was generated. In addition to the two proposed approaches and BISK, we also report the results obtained when the original image is encoded without using any of the proposed approaches, referred to as JPEG2000. Due to the low number of spectral components, we have not applied any shape-adaptive spectral transform [33] to account for the spectral redundancy.

The first experiment assesses the coding performance provided by the proposed approaches (ADR and SA-JPEG2000), BISK, and JPEG2000. Figure 8, Table 1, Table 2 and Table 3 show the obtained results. Two important points are worth noting from these results. The first one is that SA-JPEG2000 yields the best coding performance, even outperforming BISK. Nevertheless, it does not generate a compliant code-stream. The second point is that the best compliant approach for all the experiments is the ADR, whose coding performance can be equivalent to the shape-adaptive approaches depending on the image, for instance for SPOT dataset, in Table 1.

The second evaluation is carried out among images with different percentage and distribution of data region. The main idea is to analyze the impact of these two issues in the final coding performance. The best approach and the best compliant approach, SA-JPEG2000 and ADR, respectively, are used to make the comparisons. For images with a high amount of data region the difference between the SA-JPEG2000 and ADR are meaningless, for instance, in Table 1 for image SPOT_2008, where the data region is a 79%, at 0.125 bpspb the difference is only 0.12 dB. However, when the data region decreases, the difference grows, in Fig. 8, for the image Overlapping-2 (with a 35% of data region), SA-JPEG2000 clearly outperforms ADR for all bit-rates. In addition to the amount of data region within the image, how these data is distributed is also important for the final coding performance. As an example, in Table 2 the three images have similar percentage of data region; however, the results provided by SA-JPEG2000 and ADR differ in function of the data distribution within the image. In Overlapping-1 and AVIRIS, most data regions are narrow and few connected. For this case, the non shape-adaptive approaches like ADR are penalized due to the application of the DWT to the whole image, since the filter-bank detects several boundaries between data and NODATA regions and, consequently, coarse edges arise. On the other hand, CASI image has only one fully connected data region, hence applying the DWT to the entire image has a minimal penalization. Moreover, as explained before, when data percentage on the image is higher, differences between ADR and SA-JPEG2000 become less important, and, therefore, the penalization of the ADR approach

due to the fragmentation of the nodata areas is also less prominent. For example for Landsat TM dataset (Table 3), results for ADR are comparable to those obtained by SA-JPEG2000 due to the higher proportion of data on the image (67%), in spite of the disconnected NODATA regions.

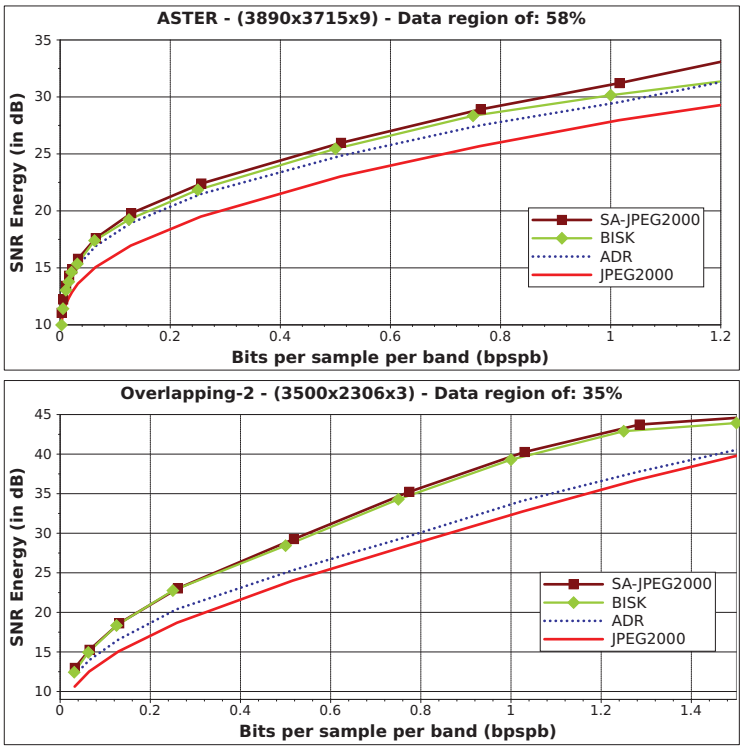

Fig. 8. Rate-distortion curves for ASTER and Overlapping-2 images. Coding performance for the two proposed approaches, BISK, and JPEG2000 is shown.

SPOT_2008 – (1593×1033×4) – Data region: 79%				
Bit-rate	BISK	SA-JPEG2000	ADR	JPEG2000
0.0625	16.14 (-0.60)	**16.74**	16.65 (-0.09)	13.79 (-2.95)
0.125	17.78 (-0.44)	**18.22**	18.10 (-0.12)	15.98 (-2.24)
0.25	19.84 (-0.39)	**20.23**	20.10 (-0.13)	18.62 (-1.61)
0.5	22.12 (-0.72)	**22.84**	22.67 (-0.17)	21.64 (-1.20)
1.0	26.06 (-0.78)	**26.84**	26.47 (-0.37)	25.66 (-1.18)
1.5	30.00 (-0.71)	**30.71**	29.69 (-1.02)	29.19 (-1.52)

SPOT_2009 – (3186×2066×4) – Data region: 76%				
Bit-rate	BISK	SA-JPEG2000	ADR	JPEG2000
0.0625	15.66 (-0.65)	**16.31**	16.16 (-0.15)	10.14 (-6.17)
0.125	17.64 (-0.68)	**18.32**	18.07 (-0.25)	12.86 (-5.46)
0.25	20.69 (-0.31)	**21.00**	20.67 (-0.33)	16.57 (-4.43)
0.5	24.44 (-0.27)	**24.71**	24.30 (-0.41)	21.32 (-3.39)
1.0	29.39 (-0.68)	**30.07**	28.95 (-1.12)	27.00 (-3.07)
1.5	32.26 (-1.73)	**33.99**	33.62 (-0.37)	30.72 (-3.27)

Table 1. Coding performance for SPOT images. Results report the SNR Energy (in dB) for different bit-rates (in bpspb). The best coding performance is printed in bold and the difference between this best coding approach and others is depicted in parenthesis.

CASI – (4058×1073×11) – Data region: 44%				
Bit-rate	BISK	SA-JPEG2000	ADR	JPEG2000
0.0625	20.52 (-0.80)	**21.32**	21.18 (-0.14)	20.70 (-0.62)
0.125	22.73 (-0.95)	**23.68**	23.52 (-0.16)	23.09 (-0.59)
0.25	25.97 (-0.96)	**26.93**	26.71 (-0.22)	26.28 (-0.65)
0.5	30.40 (-1.16)	**31.56**	31.26 (-0.30)	30.88 (-0.68)
1.0	37.62 (-0.82)	**38.44**	38.09 (-0.35)	37.80 (-0.64)
1.5	43.87 (-0.73)	**44.60**	44.13 (-0.47)	43.83 (-0.77)

AVIRIS – (145×145×220) – Data region: 49%				
Bit-rate	BISK	SA-JPEG2000	ADR	JPEG2000
0.0625	26.65 (-0.65)	27.29 (-0.01)	**27.30**	12.29 (-15.01)
0.125	30.62 (-0.46)	**31.08**	29.80 (-1.28)	14.16 (-16.92)
0.25	34.51 (-0.55)	**35.06**	32.85 (-2.21)	17.51 (-17.55)
0.50	39.82 (-0.64)	**40.46**	37.04 (-3.42)	21.66 (-18.80)
1.0	47.87 (-0.51)	**48.38**	43.24 (-5.14)	28.48 (-19.90)
1.5	53.95 (-0.27)	**54.22**	48.28 (-5.95)	33.85 (-20.37)

Overlapping-1 – (3500×2306×3) – Data region: 47%				
Bit-rate	BISK	SA-JPEG2000	ADR	JPEG2000
0.0625	16.35 (-0.51)	**16.86**	16.01 (-0.85)	15.15 (-1.71)
0.125	19.62 (-0.33)	**19.95**	18.93 (-1.02)	17.79 (-2.16)
0.25	23.42 (-0.30)	**23.72**	22.30 (-1.42)	21.12 (-2.60)
0.5	27.92 (-0.58)	**28.50**	26.55 (-1.95)	25.66 (-2.84)
1.0	34.52 (-0.81)	**35.33**	32.70 (-2.63)	32.08 (-3.25)
1.5	40.11 (-0.36)	**40.47**	37.68 (-2.79)	37.14 (-3.33)

Table 2. Coding performance for CASI, AVIRIS and Overlapping-1 images. Results report the SNR Energy (in dB) for different bit-rates (in bpspb). The best coding performance is printed in bold and the difference between this best coding approach and others is depicted in parenthesis.

Landsat TM (five dates) – (1517×1311×6) – Data region: 67%				
Bit-rate	BISK	SA-JPEG2000	ADR	JPEG2000
0.0625	17.16 (-1.09)	17.49 (-0.77)	**18.25**	6.56 (-11.70)
0.125	18.93 (-0.89)	19.59 (-0.24)	**19.82**	7.83 (-11.99)
0.25	21.00 (-0.82)	**21.82**	21.68 (-0.14)	9.65 (-12.17)
0.5	23.83 (-0.73)	**24.56**	24.02 (-0.54)	12.62 (-11.95)
1	27.95 (-0.59)	**28.54**	27.59 (-0.96)	18.11 (-10.43)
1.5	31.93 (-0.21)	**32.14**	30.68 (-1.45)	22.73 (-9.40)

Table 3. Coding performance for Landsat TM images. Results report the SNR Energy (in dB) for different bit-rates (in bpspb). The best coding performance is printed in bold and the difference between this best coding approach and others is depicted in parenthesis.

4.2 Digital Classification

In addition to coding performance, in RS and GIS scenarios it is necessary to evaluate the suitability of the images for the post-processing applications. As stated in [18], higher compression performance does not necessarily yield higher quality of a remote sensing image for a given application, and thus, it is necessary to evaluate encoding approaches not only according to their coding performance, but also according to the effects produced on the product obtained after image coding.

One of the most usual uses for RS images is to obtain thematic classifications. Several approaches can be developed to obtain them. Three approaches are here applied to classify one of the studied dataset for each classification methodology: discriminant analysis, multitemporal maximum likelihood and a hybrid classifier; they were applied to SPOT, Landsat TM and AVIRIS datasets.

4.2.1 Discriminant analysis classification

Discriminant Analysis (DA) is a statistical tool useful for classifying remote sensing data. A DA with canonical discriminant functions has been applied in order to separate nine categories: 1) deep water, 2) shallow water, 3) ploughed soil with water and residues of vegetation alternated, 4) mudflat with water, 5) mudflat without water, 6) dry soil, 7) unproductive land, 8) non-rice

crops and 9) active rice crops. Linear combinations of the independent variables (reflectance of SPOT images) are obtained and serve as the basis for classifying the nine groups. This methodology has been considered convenient for three reasons. Firstly, it reduces drastically the statistical dimensionality of data (there is a high correlation among spectral bands). Secondly, unlike other methods of reducing data dimensionality, as principal components analysis, the variables obtained by DA maximize the statistical differences among predefined groups. Finally, the estimated canonical coefficients are expected to have a significant meaning and to be suitable for using in other available dates, reducing the need of field work and obtaining a faster cartography. Therefore, in this work, the classifications functions were obtained from samples of both images with the objective to analyze flood dynamics [34].

Two SPOT images are available on the study area, presented both in Section 3. The first image, SPOT_2008, was captured on 3rd October 2008. At this moment, study area is mainly covered by rice before harvesting. The second studied image was captured on 14th January 2009, and, at this moment, the main present categories are ploughed soil, mudflat with water, deep water, dry soil and mudflat without water.

To evaluate the effect of compression on this classification method, it was applied to both SPOT available images without encoding and also after encoding these images with different approaches and at different bit-rates. A confusion matrix between these classifications was obtained to test the effect of the encoding process. Overall accuracy versus bit-rate of SPOT_2008 and SPOT_2009 images is shown on Table 4.

	SPOT_2008 – (1593×1033×4) – Data region: 79%				SPOT_2009 – (3186×2066×4) – Data region: 76%			
Bit-rate	BISK	SA-JPEG2000	ADR	JPEG2000	BISK	SA-JPEG2000	ADR	JPEG2000
0.0625	75.1%	**80.9%**	80.4%	77.0%	64.2%	**69.2%**	55.3%	55.3%
0.125	77.8%	**82.5%**	82.1%	78.8%	69.5%	**74.0%**	73.6%	61.8%
0.25	83.4%	**84.4%**	84.2%	82.5%	77.6%	**79.3%**	78.7%	70.4%
0.5	84.9%	**87.1%**	**87.1%**	85.9%	84.4%	**84.7%**	84.2%	79.9%
1.0	87.9%	**90.3%**	90.1%	89.3%	89.4%	**90.1%**	89.2%	87.4%
1.5	92.4%	**93.1%**	92.3%	91.7%	92.2%	**93.0%**	92.6%	90.5%

Table 4. Overall accuracy for SPOT dataset (Discriminant Analysis classifier) computed regarding classification obtained with non-compressed images. Results report the percentage (%) for different bit-rates (in bpspb). The best overall accuracy for each bit-rate is printed in bold. Classified area results are not presented because this DA methodology always classifies all pixels of the image.

Two important points are worth noting from these results. The first point is that SA-JPEG2000 obtains the best classification results; however, it does not generate a compliant code-stream. On the other hand, the best compliant approach is ADR, that provides similar classification results than a shape-adaptive coding system like BISK. The second point is that classification results provided by BISK vary in function on the features of the image. For instance, in SPOT_2008, despite that the coding performance provided by BISK for all the bit-rates is better than JPEG2000 (see Table 1), in the classification experiments, JPEG2000 produces better classification accuracy for several bit-rates. On the other hand, for the SPOT 2009 image, the classification accuracy provided by BISK and ADR is equivalent, outperforming that provided by JPEG2000. As a conclusion, results suggest that the application of the proposed approaches SA-JPEG2000 and ADR improves the classification results.

4.2.2 Multitemporal Maximum Likelihood classification

Monitoring crop areas is of wide importance not only because of their economic and human interest, but also because of the challenge it represents. As [31] mentions, to obtain the best results it is advisable to mask agricultural fields due to their heterogeneity. In line with current practice, it is also interesting to evaluate multitemporality to improve the classification. The Landsat legacy is so important in temporal coverage (from 1970's), spatial coverage (almost

all emerged lands), real availability of data, interesting coverage of the middle infrared spectral regions, etc, that the interest of Landsat becomes evident, without forgetting the current free access to all the USGS archive since December 2008. This is why those images are a very good solution to monitor wide areas with medium temporal and spatial resolution, such as the monitoring of crops areas along the year.

Five Landsat TM images are available to obtain a crop map over the Lleida area. The classification methodology used is a classical maximum likelihood supervised classifier, implemented on ENVI v4.3 software. To evaluate the effect of compression on classification, the classification method was applied over original images (without compression) and over encoding of these images with different approaches and at different bit-rates. The analysis of classification accuracy (obtained using original and compressed images) is based on a confusion matrix computed using test areas (ground-truth layer) which are independent from the training areas. Overall accuracy versus bit-rate of classifications is shown on Table 5.

	Landsat TM images 2004 – (1517×1311×6×5) – Data region: 67%							
	Overall accuracy				Classified area			
Bit-rate	BISK	SA-JPEG2000	ADR	JPEG2000	BISK	SA-JPEG2000	ADR	JPEG2000
0.0625	97.8%	98.4%	**98.5%**	93.8%	89.16%	88.41%	**92.78%**	81.00%
0.125	98.7%	98.8%	**99.1%**	96.3%	86.10%	85.86%	**88.90%**	80.17%
0.25	99.1%	**99.3%**	**99.3%**	97.8%	83.0%	83.06%	**86.08%**	80.03%
0.5	99.3%	**99.4%**	**99.4%**	98.1%	79.18%	78.68%	**80.82%**	79.72%
1	**99.6%**	**99.6%**	**99.6%**	99.1%	77.67%	77.37%	**77.65%**	79.28%
1.5	**99.6%**	**99.6%**	**99.6%**	99.3%	78.58%	78.46%	**78.53%**	78.06%

Table 5. Overall accuracy and classified area for Landsat TM images (Maximum Likelihood classifier) computed regarding independent test areas. Overall accuracy and classified area obtained with non-compresses images is 99.6% and 79.43% respectively. Results report the percentages (%) for different bit-rates (in bpspb). The best classification for each bit-rate is printed in bold.

As expected according to SNR Energy results for those images (see Table 2), ADR should provide similar (or even better at lower bit-rates) results than SA-JPEG2000. Both overall accuracy and classified area of obtained classifications confirm these expected tendencies. It is noticeable that ADR obtains, in general, similar results for overall accuracy but better result for classified areas than SA-JPEG2000 for the same bit-rates, even with a lower SNR Energy. For example, at 1 bpspb ADR obtains almost 1 dB less than SA-JPEG2000, but the same overall accuracy and higher classified area (77.7% versus to 77.4%). These similar results are due to the higher proportion of data on the image (67%), in spite of the disconnected NODATA regions.

4.2.3 Discriminant Analysis and Hybrid classification

AVIRIS image is also used to evaluate the effect of compression on classifications using this image. Discriminant Analysis is used with two purposes. First of all it is used to directly classify the original 220 images to obtain 16 categories: Alfalfa, Corn no-till, Corn min, Corn, Grass/Pasture, Grass/Trees, Grass/pasture mowed, Hay windrowed, Oats, Soybeans no-till, Soybeans min, Soybeans clean, Wheat, Woods, Bldg/Grass/Tree/Drives, Stone/steel/towers. These categories are those present on ground-truth available for the image. The second approach for Discriminant Analysis is to use it to obtain, from the original 220 bands, new 15 canonical discriminant functions that can be used to feed the classification process. The classification method is a hybrid classifier that combines an unsupervised classifier and a non parametric supervised one [35], implemented on MiraMon GIS and RS [21].

The analysis of classification accuracy (obtained using original and compressed images) is based on a confusion matrix computed using test areas (ground-truth layer) which are independent from the training areas. 70% of the ground-truth area (randomly selected) is used for training and the other 30% to test the results. Overall accuracy versus bit-rate of classifications

for the classifications methods (Discriminant analysis and the Hybrid classifier), are shown on Table 6.

	AVIRIS 12-06-1992 (145×145×220) – Data region: 49%							
	Discriminant Analysis classifier				Hybrid classifier			
Bit-rate	BISK	SA-JPEG2000	ADR	JPEG2000	BISK	SA-JPEG2000	ADR	JPEG2000
0.0625	96.7	**97.8**	96.3	91.1	96.2	**96.8**	91.0	91.5
0.125	96.5	**96.9**	95.8	93.1	88.6	86.9	85.4	**90.9**
0.25	96.7	**97.8**	93.9	91.5	79.6	82.8	81.8	**90.5**
0.5	94.9	**95.8**	82.0	85.8	74.6	75.2	75.7	**86.7**
1	**86.4**	85.1	56.4	82.3	78.0	**79.4**	77.6	74.7
1.5	**76.6**	65.6	29.6	75.9	77.6	**78.7**	78.1	72.5

Table 6. Overall accuracy for AVIRIS dataset computed regarding independent test areas. Overall accuracy obtained with non-compresses images is 77.5% for Discriminant Analysis and 78.9% for Hybrid classifier. Results report the percentage (%) for different bit-rates (in bpspb). The best overall accuracy for each bit-rate is printed in bold.

First aspect to be mentioned is that the Hybrid classifier obtains the best results over non-compressed images, followed by Discriminant Analysis. A Maximum likelihood classifier was also used to classify the new 15 canonical discriminant functions obtained by the DA, but the overall accuracy obtained was poorer (only 64.9%) and, thus, this classification method was not selected for evaluation for this image. Secondly, regarding compression algorithms that perform better, it depends on the ulterior classification approach to be used. If discriminant analysis is intended, SA-JPEG2000 is the best compression algorithm, because it increases the overall accuracy to very high values, especially at low compression ratios. If a Hybrid classifier is intended, SA-JPEG2000 or JPEG2000 can be used, depending on the desired compression ratio. In any case, compression on this image has very positive effects due to the noise reduction or smoothing, thus improving the classification results.

5 CONCLUSIONS

Digital images captured by sensors and devoted to Remote Sensing (RS) and Geographic Information Systems (GIS) applications may contain areas without useful information or without information at all, due to several factors such as geometric and radiometric corrections, atmospheric events, the successive overlapping of layers of information, etc. Usually, an arbitrary value is assigned to these regions without information. To consider this value as part of the image could penalize the encoding process and the post-processing applications. In this work, we propose two approaches to minimize, or even eliminate, the impact of these NODATA regions.

Experimental results suggest that the best approach to encode and classify images containing NODATA regions is SA-JPEG2000. Nevertheless, it does not provide a compliant JPEG2000 code-stream. The results provided by the SA-JPEG2000 are also compared against BISK, which is a coding system specifically devised to shape-adaptive encoding; SA-JPEG2000 yields better coding performance. Moreover, the JPEG2000 framework considers many features that are not available in BISK. The best JPEG2000 compliant approach is the ADR. The performance may vary due to the features of the encoded image; when data regions are small and low connected, the DWT is penalized instead of the SA-DWT; however, when data regions are large and fully connected, ADR achieves similar coding performance than SA-JPEG2000 and BISK. Regarding results of post-processing classification performed over encoded images, ADR and SA-JPEG2000 obtain similar results, especially if data region proportion is high or if NODATA regions are few and highly connected. Thus, SA-JPEG2000 would be the recommended approach both if image has a lower data proportion or if NODATA regions are small and disconnected (*e.g.*, for radiometrically corrected or land cover masked images). On the other hand, if data proportion is higher (*e.g.*, more than 70%) and/or NODATA regions are few and

highly connected (*e.g.*, geometrically corrected images), or if a JPE2000 compliant approach is required, ADR would be the best choice for encoding images.

Acknowledgments

This work has been partially supported by the Spanish Government, by FEDER, and by the Catalan Government, under Grants TSI2006-14005-C02, TIN2009-14426-C02, TIN2009-05-737-E, SGR2009-1224 and SGR2009-1511.

References

[1] X. Pons and L. Sole-Sugranes, "A simple radiometric correction model to improve automatic mapping of vegetation from multispectral satellite data," *Rem. Sens. Environ.* **48**, 191–204 (1994). [doi:10.1016/0034-4257(94)90141-4].

[2] H. Fujisada, "Aster level-1 data processing algorithm," *IEEE Trans. Geosci. Rem. Sens.* **36**, 1101–1112 (1998). [doi:10.1109/36.700994].

[3] F. Eugenio and F. Marques, "Automatic satellite image georeferencing using a contour-matching approach," *IEEE Trans. Geosci. Rem. Sens.* **41**, 2869–2880 (2003). [doi:10.1109/TGRS.2003.817226].

[4] M. G. Tait, "Implementing geoportals: applications of distributed GIS," *Computer, Environ. Urban Syst.* **29**, 33–47 (2005). [doi:10.1016/j.compenvurbsys.2004.05.011].

[5] J. Fowler, "Shape-adaptive coding using binary set splitting with K-D trees," in *IEEE Int. Conf. Image Proc.*, **2**, 1301–1304 (2004).

[6] J. Hua, Z. Liu, Z. Xiong, Q. Wu, and K. R. Castleman, "Microarray BASICA: background adjustment, segmentation, image compression and analysis of microarray images," *EURASIP J. Appl. Signal Proc.* **2004**(1), 92–107 (2004). [doi:10.1155/S1110865704309200].

[7] D. Taubman, "High performance scalable image compression with EBCOT," *IEEE Trans. Image Proc.* **7**, 1158–1170 (2000). [doi:10.1109/83.847830].

[8] M. Cagnazzo, G. Poggi, L. Verdoliva, and A. Zinicola, "Region Oriented compression of multispectral images by shape-adaptive wavelet transform and SPIHT," in *IEEE Int. Conf. Image Proc.*, **4**, 2459–2462 (2004).

[9] M. Cagnazzo, S. Parrilli, G. Poggi, and L. Verdoliva, "Improved class-based coding of multispectral images with shape-adaptive wavelet transform," *IEEE Geosci. Rem. Sens. Lett.* **4**, 566–570 (2007). [doi:10.1109/LGRS.2007.900696].

[10] M. Cagnazzo, G. Poggi, and L. Verdoliva, "Region-based transform coding of multispectral images," *IEEE Trans. Image Proc.* **16**, 2916–2926 (2007). [doi:10.1109/TIP.2007.909315].

[11] ISO/IEC 15444-1, *JPEG2000 image coding system. Part 1: Core coding system* (2000).

[12] D. Taubman and M. Marcellin, *JPEG2000: Image Compression Fundamentals, Standards, and Practice*, vol. 642, Kluwer International Series in Engineering and Computer Science, Kluwer, Norwell, MA (2002).

[13] W. Lam, Z. Li, and X. Yuan, "Effects of JPEG compression on the accuracy of digital terrain models automatically derived from digital aerial images," *Photogram. Record* **17**(98), 331–342 (2001). [doi:10.1111/0031-868X.00187].

[14] T. Shih and J. Liu, "Effects of JPEG 2000 compression on automated DSM extraction: Evidence from aerial photographs," *Photogram. Record* **20**(112), 331–342 (2005). [doi:10.1111/j.1477-9730.2005.00330.x].

[15] J. Paola and R. Schowengerdt, "The effect of lossy image compression on image classification," in *IEEE Int. Geosci. Rem. Sens. Symp*, **1**, 118–120 (1995). [doi: 10.1109/IGARSS.1995.519665].

[16] F. Tintrup, F. D. Natale, and D. Giusto, "Automatic land classification vs. data compression: a comparative evaluation," in *IEEE Int. Geosci. Rem. Sens. Symp*, **4**, 1751–1753 (1998). [doi:10.1109/IGARSS.1998.703640].

[17] A. Zabala, X. Pons, J. Maso, F. Garcia, F. Auli, and J. Serra, "Evaluation of JPEG and JPEG2000 effects on remote sensing image classification for mapping natural areas," *WSEAS Trans. Info. Sci. Appl.* **2**, 717–725 (2005).

[18] B. Penna, T. Tillo, E. Magli, and G. Olmo, "Transform coding techniques for lossy hyperspectral data compression," *IEEE Trans. Geosci. Rem. Sens.* **45**, 1408–1421 (2007). [doi:10.1109/TGRS.2007.894565].

[19] J. Gonzalez-Conejero, F. Auli-Llinas, J. Bartrina-Rapesta, and J. Serra-Sagrista, "JPEG2000 coding techniques addressed to images containing no-data regions," *Lect. Notes Comput. Sci.* **4678**, 1024–1036 (2007). [doi:10.1007/978-3-540-74607-2-93].

[20] J. Gonzalez-Conejero, J. Serra-Sagrista, C. Rubies-Feijoo, and L. Donoso-Bach, "Encoding of images containing no-data regions within JPEG2000 framework," in *IEEE Int. Conf. Image Proc.*, 1057–1060 (2008).

[21] X. Pons, *MiraMon, Geographic Information Systems and Remote Sensing software*, Center for Ecological Research and Forestry Applications, (CREAF). Bellaterra.

[22] ISO/IEC 14496-2, *Information Technology—Generic coding of audio-visual objects, Part 2: Visual* (1998).

[23] S. Li and W. Li, "Shape adaptive discrete wavelet transforms for arbitrarily shaped visual object coding," *IEEE Trans. Circuit. Syst. Video Tech.* **10**, 725–743 (2000). [doi:10.1109/76.856450].

[24] M. Cagnazzo, S. Parrilli, G. Poggi, and L. Verdoliva, "Costs and advantages of object-based image coding with shape-adaptive wavelet transform," *EURASIP J. Image Video Proc.* **2007**, 78323 (2007).

[25] S. M. Aghito and S. Forchhammer, "Context-based coding of bilevel images enhanced by digital straight line analysis," *IEEE Trans. Image Proc* **15**, 2120–2130 (2006). [doi:10.1109/TIP.2006.875168].

[26] A. Akimov, A. Kolesnikov, and P. Franti, "Lossless compression of map contours by context tree modeling of chain codes," *Pattern Recog.* **40**, 944–952 (2007). [doi:10.1016/j.patcog.2006.08.005].

[27] V. Ratnakar, "RAPP: lossless image compression with runs of adaptive pixel patterns," in *Proc. 32nd Asilomar Conf. Signal. Syst. Comput.*, 1251–1255 (1998).

[28] Z. Shen, M. R. Frater, and J. F. Arnold, "Quad-tree block-based binary shape coding," *IEEE Trans. Circuit. Syst. Video Tech.* **18**, 845–850 (2008). [doi:10.1109/TCSVT.2008.919086].

[29] ISO/IEC 15444-2, *JPEG2000 image coding system. Part 2: Extensions* (2004).

[30] ISO/IEC 15444-6, *JPEG2000 image coding system. Part 6: Compound image file format* (2003).

[31] J. G. H. Xie, Y.Q. Tian and G. Keller, "Suitable remote sensing method and data for mapping and measuring active crop fields," *Int. J. Rem. Sens.* **28**, 395–411 (2007). [doi:10.1080/01431160600702673].

[32] J. Gonzalez-Conejero, J. Bartrina-Rapesta, and J. Serra-Sagrista, "Encoding scheme for multi-component images containing no-data regions," in *IEEE Int. Conf. Image Proc.*, 1897–1900 (2009).

[33] J. Gonzalez-Conejero, J. Bartrina-Rapesta, and J. Serra-Sagrista, "JPEG2000 encoding of remote sensing multispectral images with no-data regions," *IEEE Geosc. Rem. Sens. Lett.* **7** (2010). [doi:10.1109/LGRS.2009.2032370].

[34] G. More, P. Serra, and X. Pons, "Multitemporal flooding dynamics of rice fields by means of discriminant analysis of radiometrically corrected remote sensing imagery," *Int. J. Rem.Sens.* **30**(In press) (2009).

[35] P. Serra, X. Pons, and D. Sauri, "Post-classification change detection with data from different sensors. some accuracy considerations," *Int. J. Rem.Sens.* **24**, 3311–3340 (2003). [doi:10.1080/0143116021000021189].

Alaitz Zabala: Alaitz Zabala received her BS degree in Environmental Sciences in 2002 and her MS degree in Geography in 2006 at the Autonomous University of Barcelona. She is a researcher and associate professor at the Department of Geography of the Universitat Autònoma de Barcelona (UAB). Zabala research main interests are standardized metadata (following FGCD, CEN, ISO, and INSPIRE standards) and the study of the implications of extracting information from lossy compressed images and developing standardized servers. She was the main developer of the metadata profile and of the GeMM MiraMon that is a metadata tool for raster and vector layers.

Jorge González-Conejero: Jorge González-Conejero received the B.S., M.S., and Ph.D. degrees in Computer Science from the Universitat Autònoma de Barcelona, Barcelona, Spain, in 2003, 2005, and 2009, respectively. Since 2003, he has been with the Department of Information and Communications Engineering, Universitat Autònoma de Barcelona. His current research interests include image coding and data compression, with special attention to remote sensing and telemedicine applications. He has coauthored several papers in these areas.

Joan Serra-Sagristà: Joan Serra-Sagristà received the Ph.D. degree in computer science from Universitat Autònoma de Barcelona (UAB), Spain, in 1999. Since 1992, he has been with the Department of Information and Communications Engineering, UAB, where he is currently an Associate Professor and the Director of the Group on Interactive Coding of Images. From September 1997 to December 1998, and from June to July 2000, he held a Deutscher Akademischer Austausch Dienst research grant at University of Bonn, Germany. His current research interests include image coding, data compression, and wavelet-based techniques, with special attention to remote sensing and telemedicine applications. He has coauthored several papers in these areas. He is also a Reviewer for the major international journals in his research field. He is a 2006 recipient of the Intensification Program Young Investigator Award. He has served on the steering committee and on technical program committees of several international conferences.

Xavier Pons: The main work of Xavier Pons has been done in radiometric and geometric corrections of satellite imagery, in cartography of ecological and forest parameters from airborne sensors, in studies of the spectral response of Mediterranean vegetation and in GIS development (data structure, organization and software writing: MiraMon). He has recently worked in climatology models, in forest fire mapping and in analysis of landscape changes, water usage and snow coverage from long time series of images. He is currently working in the implications of image compression on Remote Sensing. Dr. Pons is Full Professor at the Geography Department of the UAB and coordinates research in GIS and RS at the CREAF.

6. RESUM DE RESULTATS

6.1. INTRODUCCIÓ

El resum de resultats d'aquesta Tesi es realitzarà fent un repàs de les diverses publicacions que la formen (compendi de publicacions). Tal i com contempla la resolució de l'Escola de Postgrau a la sol·licitud de presentació de la Tesi amb aquesta modalitat, a l'apartat de resultats de la Tesi es poden comentar els resultats tant dels articles que formen la part fonamental (capítols 2 a 5) com els articles complementaris (annexos 1 a 3).

L'organització dels resultats s'ha realitzat principalment en funció del moment en què s'ha fet la compressió i del mètode emprat per a la obtenció de cartografia. En primer lloc es presenten els treballs que avaluen l'efecte de la compressió quan aquesta és realitzada a nivell d'usuari, i en segon lloc el treball realitzat quan la compressió és realitzada a bord. En tercer lloc es presentaran els resultats de l'article de codificació del NODATA en el marc de JPEG 2000. En aquest article també s'avalua l'efecte de les modificacions proposades en la generació de cartografia, però aquests resultats es presenten de manera independent (i no dins l'apartat de cartografia generada per classificació píxel a píxel) donada la seva especificitat. El primer apartat (compressió realitzada a nivell d'usuari) se subdividirà en diversos sub-apartats en funció del mètode de generació de cartografia.

6.2. COMPRESSIÓ A NIVELL D'USUARI

6.2.1 ANÀLISI VISUAL

El treball realitzat per avaluar els efectes de la compressió amb pèrdua d'imatges en el camp de l'anàlisi visual (capítol 2) utilitza un disseny experimental de dos factors amb interacció: el tipus de paisatge i la raó de compressió amb pèrdua. S'ha treballat sobre sis àrees de test, dues per cada tipus de paisatge: forestal, agrícola i urbà.

El material emprat per a cada àrea ha estat l'ortoimatge digital color a escala 1:5000 de l'Institut Cartogràfic de Catalunya (0.5 m de resolució). Les ortoimatges han estat sotmeses a una compressió amb pèrdua usant l'estàndard de compressió JPEG 2000 2D multibanda (amb transformada de color entre les tres component de l'ortoimatge en color), a diverses raons de compressió: 5:1, 10:1, 20:1 i 100:1.

Les imatges de les diverses zones d'estudi i resultants de diverses raons de compressió han estat objecte de fotointerpretació (llegenda de 24 categories, seguint el nivell 2 de llegenda del

Mapa de Cobertes del Sòl de Catalunya, Burriel *et al.* 2005), generant un total de 30 capes vectorials de polígons (una per cada zona i nivell de compressió, incloent les imatges sense compressió). A més, per a poder valorar l'efecte de variació introduït pel fotointèrpret s'ha realitzat (un temps després) una segona fotointerpretació sobre les imatges sense comprimir. La comparació de les dues fotointerpretacions sobre les imatges originals ha permès obtenir un indicador de les variacions degudes a la subjectivitat del fotointèrpret i que no han de ser atribuïdes a canvis a les imatges deguts a la compressió.

Els paràmetres analitzats per a comprovar l'efecte de la compressió es divideixen en dos grups. En primer lloc s'ha comprovat les variacions en la geometria i la topologia dels vectors generats a diverses raons de compressió. Els paràmetres escollits per a ser analitzats han estat el nombre de vèrtexs, el nombre de polígons i la longitud total dels arcs del vector digitalitzat. En segon lloc, s'ha avaluat l'efecte de la compressió sobre l'exactitud temàtica dels vectors obtinguts, calculant el percentatge d'encert respecte de la capa vectorial obtinguda sobre les imatges comprimides sense pèrdua (global i per categories).

Els resultats d'aquesta recerca ens mostren que a elevades raons de compressió els vectors obtinguts per fotointerpretació presenten diferències d'estructura geomètrica i topològica elevades respecte els vectors obtinguts amb les imatges originals. Els vectors obtinguts sobre imatges comprimides presenten un menor nombre de vèrtexs, nombre polígons i perímetre dels polígons. En tots els tipus de paisatges, la diferència respecte al valor dels vectors sense compressió és més acusada en les zones heterogènies. Respecte a l'estructura geomètrica i topològica, els vectors obtinguts amb la compressió 5:1 són només lleugerament diferents respecte la fotointerpretació original, però aquestes diferències semblen degudes a la subjectivitat del fotointèrpret. Aquesta raó de compressió sembla ser, per tant, òptima ja que implica una important reducció de la mida de les imatges i no té implicacions en els vectors resultants (ni quant a estructura ni quant a qualitat temàtica) quan es fotointerpreta una ortoimatge 1:5000 per generar una llegenda de 15 categories. És destacable que els efectes de la compressió també són diferents segons les categories per la capacitat del fotointèrpret de reconèixer-les. Així, per exemple, la fotointerpretació de la categoria de conreus és de les menys afectades per la compressió, a diferència de la categoria de matollars, més mal reconeguda a elevats nivells de compressió.

6.2.2 ANÀLISI DIGITAL

6.2.2.1 Regressió

La regressió múltiple és una tècnica comuna per obtenir variables quantitatives (temperatura, biomassa, índex d'àrea foliar) a partir de l'anàlisi digital d'imatges de teledetecció. Els píxels són tractats com a mostres pels quals es coneixen els valors de diverses variables independents i de variables dependents (només per alguns píxels) que es prediuen (per tots els píxels) a través de l'ajust d'una regressió. L'estudi de la compressió sobre aquests models de regressió ha estat tractat a l'article presentat al capítol 3.

La temperatura mínima anual i mitjana anual s'ha modelitzat usant dos mètodes en relació a les variables independents emprades: només variables geogràfiques, o variables geogràfiques i imatges de teledetecció conjuntament. Pels models amb variables geogràfiques (càlculs sobre la península Ibèrica, píxel 200*200 m) s'ha emprat dades d'altitud, latitud, continentalitat, radiació solar i curvatura del terreny. Els models amb les dues variables s'han calculat sobre Catalunya (zona per a la qual es disposa de dades de teledetecció) emprant els productes de temperatura terrestre diària i nocturna (producte compost per cada 8 dies: MOD11A2, 1 km de resolució) i l'NDVI (*Normalized Difference Vegetation Index*, producte compost per cada 16 dies: MOD13A1, 500 m de resolució) de TERRA-MODIS. En ambdós casos s'han emprat dades d'estacions meteorològiques (del *Instituto Nacional de Meteorología* i del Servei Català de Meteorologia per al primer i segon model respectivament).

Les diverses variables han estat sotmeses a una compressió amb pèrdua seguint l'estàndard de compressió JPEG 2000, usant l'aplicació BOÍ. Aquesta aplicació té un mètode no estàndard per a codificar imatges en format de reals, que facilita el treball amb les variables d'entrada (present en aquest format en algun dels casos). Les raons de compressió estudiades han variat des de 2:1 fins 10000:1.

Els resultats mostren que fins i tot a raons de compressió molt elevades, l'encert obtingut (mesurat amb les dades d'estacions meteorològiques independent reservades amb aquesta finalitat) és similar a l'encert obtingut amb les dades originals, per la qual cosa sembla que JPEG 2000 pot ser aplicar sens perjudici en aquest tipus de metodologies de modelització climàtica.

La raó de compressió màxima admissible és més gran per a models usant només variables geogràfiques (25:1) que per a models que també empren variables de teledetecció (5:1 en el

pitjor dels casos). A més, la regressió emprant només variables geogràfiques és menys influenciada per la compressió ja que el RMS de la capa obtinguda després de comprimir (en relació a la capa obtinguda amb les imatges originals) és menor per aquests models que pels que usen també variables de teledetecció.

6.2.2.2 Classificació

a) Classificació píxel a píxel

En estratègies de classificació píxel a píxel s'ha realitzat dos estudis de l'efecte de la compressió en funció del tipus de paisatge: forestal (article capítol 4) o agrícola (article annex 1). En ambdós casos, l'estudi s'emmarca en un context de classificació multitemporal (usant imatges de diverses dates per a poder recollir la variació fenològica de les espècies forestals o de conreus al llarg de l'any) i de gestió del territori, és a dir, classificant una zona àmplia del territori gràcies a la cobertura territorial d'un sensor de resolució mitjana com Landsat. El darrer aspecte que tots dos treballs han considerat és la definició de dues zones per a cada tipus de paisatge de diferent fragmentació, per a comprovar si l'efecte de la compressió pot ser dependent d'aquesta fragmentació.

a.1) *Zones forestals*

L'estudi sobre zones forestals utilitza dades radiomètriques (quatre imatges Landsat per cada zona) i altres variables (NDVI, precipitació mitjana, radiació solar mitjana anual, màxima temperatura al juliol, mínima temperatura a l'abril i mínima temperatura a l'abril) per tal de classificar una llegenda de 15 comunitats forestals (fins a nivell d'espècie) emprant el mètode de classificació híbrida HybCls descrit a l'apartat 1.3.2.4. de la introducció.

Les dades emprades han estat transformades a byte (per a poder ser comprimides amb JPEG clàssic) i comprimides amb pèrdua usant l'estàndard JPEG clàssic i JPEG 2000 banda a banda (per obtenir dades comparables amb JPEG clàssic), a diverses raons de compressió: 1.66:1, 2:1, 3.33:1, 5:1, 10:1, 20:1 i 100:1.

Els resultats mostren les classificacions sobre imatges comprimides usant JPEG 2000 tenen menys efecte de sal i pebre que les classificacions obtingudes amb les imatges originals. A més, a raons de compressió elevades (sense superar el màxim recomanable), poden obtenir fins i tot millors resultats que els obtinguts amb les imatges originals.

A elevats nivells de compressió, apareixen efectes visual indesitjats que no es reflecteixen encara als resultats de la classificació. Si el nivell de compressió màxim recomanat és superat, l'encert de la classificació es redueix. El nivell màxim de compressió admès depèn de la fragmentació de la imatge (més fragmentació accepta menys compressió) i del mètode de compressió (JPEG 2000 permet major compressió que JPEG amb els mateixos resultats).

Si la zona és poc fragmentada es pot comprimir fins a raons de compressió elevades (10:1 o 20:1) amb qualsevol dels dos estàndards de compressió. D'altra banda, en les zones més fragmentades, no és recomanable emprar JPEG clàssic (a cap nivell de compressió), i si s'usa JPEG 2000 només es pot arribar a raons de compressió mitjanes (3.33 a 5:1).

a.2) *Zones de conreus*

L'estudi sobre zones de conreus utilitza dades radiomètriques (cinc imatges Landsat per cada zona) per tal de classificar una llegenda de 6 tipus de conreus emprant el mètode de classificació híbrida (HybCls), així com els mètodes de classificació de mínima distància (MinDist) i màxima versemblança (MaxLike) descrits a l'apartat 1.3.2.4. de la introducció. Per a avaluar l'efecte de la compressió en relació al nombre d'imatges emprades en la classificació, s'han emprat dos escenaris de classificació: emprant totes les imatges disponibles o només una.

Les dades emprades han estat comprimides amb pèrdua usant l'estàndard JPEG clàssic (transformades a format byte), JPEG 2000 banda a banda i en format byte (per obtenir dades comparables amb JPEG clàssic) i JPEG 2000 3D (compressió multibanda emprant transformada *wavelet* en la dimensió espectral i usant les imatges en el format d'enters original), a diverses raons de compressió: 1.66:1, 2:1, 2:5:1, 3.33:1, 5:1, 10:1, 20:1, 100:1, 200:1 i 1000:1. En aquets cas l'avaluació de la classificació es realitza usant dos mètodes complementaris: emprant com a veritat terreny àrees de test independents o la classificació original.

De nou els resultats mostren que JPEG 2000 elimina els efecte de sal i pebre en les classificacions obtingudes, obtenint un millor resultat visual i eliminant aquest efecte que, d'acord amb la literatura prèvia, semblava inevitable a causa de l'heterogeneïtat dels camps de conreu (Yu *et al.* 2009).

La ubicació del punt de màxima compressió admesa està també en aquest cas relacionat amb el nivell de fragmentació de la imatge, el tipus de compressió (JPEG 2000 3D és el que accepta major compressió) i el nombre d'imatges emprades en la classificació (les classificacions

obtingudes usant un esquema multitemporal tenen un comportament més robust davant la compressió que si s'usa una sola imatge per a fer la classificació).

Si la classificació es realitza usant totes les dates disponibles sobre una zona poc fragmentada, és possible emprar una raó de compressió de 20:1 (usant JPEG) o 100:1 (usant JPEG 2000), i si la zona és més fragmentada la raó de compressió admesa amb els dos estàndards és 10:1. Si la classificació es realitza emprant una única data, només és recomanable usar JPEG 2000 3D (10:1 fins a 100:1 segons fragmentació de la zona).

Des del punt de vista del mètode de classificació, HybCls i MaxLike obtenen millors classificacions que MinDist, tot i que estan més afectats per la compressió, especialment a elevades raons de compressió i quan s'utilitza una aproximació multitemporal. En cas que s'utilitzi una sola data per a realitzar la classificació, IsoMM és menys afectat per compressió que els altres dos classificadors i per aquest motiu hauria de ser l'opció escollida.

b) Classificació per segments

Per avaluar els efectes de la compressió amb pèrdua en el camp de la classificació basada en objectes o segments (annex 2), s'ha escollit 4 àrees d'estudi (Sant Cugat del Vallès, Vallvidrera, Olot i Zizur Mayor) de les quals es disposa una ortoimatge color d'1 m de resolució. Les ortoimatges han estat sotmeses a una compressió amb pèrdua usant l'estàndard de compressió JPEG 2000 2D multibanda (amb transformada de color entre les tres component de la ortoimatge en color), a diverses raons de compressió: 5:1, 10:1, 20:1, 40:1, 100:1, 200:1 400:1 i 1000:1.

Les imatges de les diverses zones d'estudi i resultants de diverses raons de compressió han estat objecte de segmentació i classificació usant l'aplicació Definiens Professional v.5, seguint la metodologia explicada a l'apartat 1.3.2.4 de la introducció. Totes les àrees d'estudi es troben en zones de urbanització de tipus residencial, per la qual cosa les categories desitjades de la llegenda són: vegetació densa, zones herbàcies o de jardins, sòl nu, carreteres i zones asfaltades, edificacions i piscines.

La validació de la classificació es realitza amb dues aproximacions complementàries: sobre un mapa de veritat terreny absolut (obtingut per fotointerpretació d'un quart de cada escena) i sobre un conjunt d'àrees de test independents. Els resultats avaluen els efectes de la compressió sobre la segmentació i la classificació (encert global i encert per categories).

Els resultats de l'estudi demostren que a elevats nivells de compressió s'obtenen encerts baixos en la classificació obtinguda. Es comprova també que a les zones més fragmentades el descens de l'encert global degut a la compressió és més elevat que en zones menys fragmentades. La classificació obtinguda és similar a l'original si la raó de compressió és inferior o igual a 20:1.

Respecte a les diverses categories de la llegenda, el seu encert depèn de la mida dels elements de la coberta a la zona així com dels objectes que l'envolten i les diferències entre elles. En general es confirma que usant una ortoimatge en color, les categories de sòl nu, edificis, asfalt i zones herbàcies o de jardins són les més costoses de classificar. La vegetació densa i les piscines obtenen en general encerts elevat a tots els nivells de compressió: per sobre 65 % per la vegetació densa (excepte a la zona de Zizur Mayor on és minoritària) i per sobre del 70% per les piscines (excepte en la zona d'Olot, amb encert més baix a partir del segon nivell de compressió). Cal notar que la dificultat per diferenciar algunes d'aquestes cobertes ve donada per la limitació de l'ortoimatge d'entrada (amb només tres canals RGB), i seria més reduïda si es disposava d'imatges amb més informació espectral (per exemple amb una banda a l'infraroig proper), tot i que, malauradament, aquesta informació sovint no és disponible, especialment per a productes antics.

Els resultats també confirmen que cal ser molt curós amb la tria de les àrees de test independents, ja que una aproximació basada en polígons de test pot comportar avaluacions diferents que si es s'utilitza un mapa de veritat terreny absolut. Donat que aquest mètode de classificació és àmpliament utilitzat (sobretot pel seva petita relació cost/benefici) els resultats refermen l'avís als investigadors de ser curosos en la tria de les zones emprades amb aquesta finalitat.

6.3. COMPRESSIÓ A BORD

L'annex 3 presenta la recerca realitzada per avaluar l'impacte de la compressió a bord en la qualitat de la imatge i de les classificacions obtingudes emprant aquestes imatges.

La missió òptica Sentinel-2 formarà part del sistema *Global Monitoring for Environment and Security* (GMES), que és una iniciativa comuna de la Comissió Europea i de l'Agència Europea de l'Espai (ESA). Els dos satèl·lits bessons que formaran la petita constel·lació Sentinel-2 incorporaran un sensor òptic (MSI: *Multi Spectral Imager*) que adquirirà 13 bandes des del

visible (VIR) fins l'infraroig d'ona curta (SWIR) en tres resolucions simultànies (10, 20 i 60 m) i amb una adquisició d'uns 290 km de dallada.

EADS Astrium va desenvolupar el *Sentinel-2 Image Performance Simulator*, emprat per la ESA per a dissenyar i optimitzar els requeriments d'aquesta missió. Aquest simulador permet generar imatges Sentinel-2 simulades a partir d'imatges aeroportades de major resolució (espacial i espectral). Es va modificar el simulador (escrit en IDL) per a afegir els compressors estàndards CCSDS i JPEG 2000 (addicionalment al compressor propietari –CNES– que portava incorporat). El simulador permet escollir (entre molts paràmetres) si el sensor usa compressió a bord (i, després de la modificació, amb quin algorisme es fa aquesta compressió) i a quina raó de compressió.

Per tal avaluar l'impacte de la compressió a bord es calcula el canvi produït en les pròpies imatges per la compressió (calculant el PSNR) i també la variació de l'encert global de la classificació realitzada amb un classificador de màxima versemblança sobre les imatges simulades usant diversos estàndards i raons de compressió.

Els resultats mostren que l'estàndard CCSDS obté major fidelitat en la compressió a baixes raons de compressió (fins a 5:1), que són les raons de compressió desitjades en cas de fer compressió a bord. Per altra banda, a elevades raons de compressió, JPEG 2000 obté millor compressió que CCSDS. Cal notar que per tal i com és la cadena de processat, la compressió a bord s'aplica banda a banda, de manera que no és possible aprofitar tota la potència de JPEG 2000. Els resultats també permeten relacionar el rang dinàmic de la imatge a comprimir (valor màxim real de la imatge menys valor mínim real de la imatge) amb la diferència entre els dos estàndards: com gran és el rang dinàmic, més petita és la millora de CCSDS. Per exemple, amb una raó de compressió de 2:1, si el rang dinàmic és 349 (banda 2) la millora (en dB de PSNR) de CCSDS respecte JPEG 2000 és de 5.14902 i aquesta millora baixa fins a 1.34964 si el rang dinàmic és de 899 (banda 8). Aquesta observació és coherent amb el fet que en estudis amb imatges a nivell d'usuari (no presentats a l'article de l'annex 3), es demostra que JPEG 2000 obté millors resultats que CCSDS si és aplicat sobre imatges amb major rang dinàmic (per exemple en imatges corregides geomètrica i radiomètricament quan la compressió es realitza a nivell d'usuari). Els efectes sobre la classificació segueixen en la majoria de casos les tendències prèvies, però cal tenir en compte que els estudis sobre les aplicacions reals realitzades sobre les imatges són importants donat que no sempre una major fidelitat de compressió (o PSNR) implica un menor impacte en l'aplicació que l'usuari fa amb les imatges (Penna *et al.* 2007).

6.4. CODIFICACIÓ DEL NODATA

El capítol 5 presenta un mètode de codificació del NODATA dins el marc de l'estàndard JPEG 2000 que pretén millorar la codificació d'aquestes àrees, la importància de les quals és palesa tant en els altres treballs d'aquesta Tesi com en tots els àmbits de treball amb imatges de teledetecció. Els motius que fan aparèixer aquests zones de NODATA són diversos: correccions geomètriques, radiomètriques, presència de núvols, estudi d'una determinada àrea d'interès, solapament de diverses capes d'informació, etc.

Modificar el sistema de codificació permet adaptar-se millor a la presencia d'aquestes zones i evitar, en primer lloc, que el valor emprat per emmagatzemar aquestes zones tingui un important impacte en el valor de les zones adjacents (en la imatge recuperada), i, en segon lloc, que la compressió intenti emmagatzemar aquest valors a la imatge comprimida (utilitzant espai que podria ser emprat per codificar millor les zones de la imatge amb dades). L'article proposa dues tècniques noves per a solucionar aquesta situació i les avalua comparant-la amb altres tècniques existents. La primera tècnica proposada correspon a un simple pre-processat de la imatge per a substituir les zones de NODATA per la mitjana de la imatge (*average data region*, ADR), i la segona correspon a una modificació del mètode de compressió, per evitar que es codifiquin aquestes zones de NODATA (*shape-adaptative*, SA-JPEG 2000).

L'avaluació d'aquestes dues tècniques de compressió es realitza utilitzant un conjunt d'imatges que cobreix les diferents situacions i escenes presents en l'àmbit de la teledetecció i el SIG: imatges corregides geomètricament (una imatge CASI d'11 bandes sobre una zona de conreus), imatges corregides geomètricament i radiomètricament (dues imatges SPOT de 4 bandes cada una sobre la zona del Delta de l'Ebre i una imatge ASTER amb nou bandes sobre Barcelona), màscara d'usos del sòl (una imatge Landsat TM amb de 6 bandes –sense el tèrmic– i una imatge AVIRIS de 220 bandes, ambdues emmascarades amb un mapa d'usos del sòl per tal de deixar amb dades només les zones agrícoles) i superposició de vectors i ràsters (dues ortoimatges 1:5000 color amb zones de NODATA produïdes per un vector d'edificis superposat). La proporció i disposició de les àrees de NODATA en les diverses situacions comentades és variada i té implicacions en els resultats dels mètodes proposats. Els paràmetres emprats per avaluar els mètodes proposats consideren tant la millora en la fidelitat de la compressió com l'impacte en una aplicació posterior realitzada sobre un subconjunt de les imatges d'estudi (anàlisi discriminant, classificació de màxima versemblança i classificació híbrida).

Els resultats experimentals suggereixen que la millor aproximació per a codificar imatges contenint zones de NODATA és el SA-JPEG 2000. D'altra banda, aquesta codificació proporciona un fitxer JPEG 2000 no completament estàndard, i per aquest motiu en alguns contexts (p.ex. en servidors de cartografia) podria no ser adequat. Si es busca un mètode estàndard, la millor alternativa és la nova proposta ADR. Els resultats també confirmen que l'eficiència de cada mètode varia en funció de la ubicació i mida de les zones de NODATA: quan aquestes són petites i poc connectades SA-JPEG 2000 ofereix millors resultats, però si són grans i ben connectades, ADR obté resultats similars o fins i tot superiors a SA-JPEG 2000. Respecte als resultats de les aplicacions posteriors realitzades sobre les imatges, ambdues tècniques obtenen resultats similars. Així, SA-JPEG 2000 seria la tècnica recomanada si la zona de dades és petita o si les zones de NODATA són poques i mal connectades (per exemple per imatges corregides radiomètricament o per imatges emmascarades amb mapes d'usos del sòl) i ADR seria la millor opció si la proporció de NODATA és gran (més del 70%) i/o si les zones de NODATA són poques i ben connectades (per exemple a les vores de les imatges corregides geomètricament).

7. CONCLUSIONS

1. CONCLUSIONS (CATALÀ)

Aquesta Tesi doctoral estudia i quantifica els efectes de diferents tècniques de compressió amb pèrdua en la cartografia generada a través d'imatges de teledetecció, considerant diferents escenaris geogràfics i diferents nivells de compressió.

Entre les principals aportacions s'ha descobert que l'efecte de la compressió depèn de la metodologia emprada per a obtenir la cartografia desitjada així com del moment en què la compressió s'ha realitzat. Quan la compressió es realitza **a nivell d'usuari**:

1. Quan s'utilitza anàlisi visual (fotointerpretació) sobre ortoimatges per a obtenir un mapa categòric d'usos del sòl, una compressió JPEG 2000 de 5:1 pot ser aplicada sense obtenir efectes en la cartografia obtinguda, més enllà dels propis deguts a la subjectivitat del fotointèrpret.

2. Quan les tècniques emprades usen anàlisi digital amb models de regressió per a obtenir variables quantitatives com la temperatura mitjana o mínima anual, a partir de dades de teledetecció (temperatura de superfície terrestre i NDVI) i/o variables geogràfiques (altitud, latitud, continentalitat, etc.), la compressió JPEG 2000 no afecta la regressió fins a raons de compressió força elevades (25:1 o 5:1 segons si s'usen només variables geogràfiques o també variables de teledetecció).

3. Si l'objectiu és la classificació píxel a píxel multitemporal d'imatges de satèl·lit per a obtenir mapes de cobertes del sòl, la compressió aplicada pot ser diferent en funció del tipus de paisatge (zona de boscos o de conreus) i la fragmentació de la zona. El rang de compressions JPEG 2000 admeses varia des de 3.33:1 o 5:1 en el pitjor dels casos (zones de boscos fragmentades) fins el 100:1 (zones de conreus menys fragmentades). JPEG 2000 obté millors resultats que JPEG clàssic, especialment si s'utilitza compressió 3D.

4. Si el mètode és una classificació per objectes (grups de píxels obtinguts per segmentació), els resultats indiquen que fins a compressions del 20:1 (depenent de la fragmentació de la zona), la classificació obtinguda és similar a la classificació original.

Quan la compressió es realitza **a bord** de la plataforma, l'estàndard CCSDS obté major fidelitat en la compressió que JPEG 2000 a raons de compressió baixes (fins a 5:1), que són les raons de compressió desitjades en cas de fer compressió a bord, especialment si el rang dinàmic de la imatge és baix (fins a 1000).

Finalment, l'adaptació de l'estàndard JPEG 2000 per a **codificar el valor NODATA** és factible emprant les dues aproximacions proposades: ADR (pre-procés que assigna el valor mitjà de la imatge les zones de NODATA) i SA-JPEG 2000 (aproximació no estàndard que evita la codificació de les zones de NODATA). SA-JPEG 2000 seria la tècnica recomanada per imatges corregides radiomètricament (poques zones de NODATA i mal connectades) o per imatges emmascarades amb mapes d'usos del sòl o vectors que les solapen (zona de dades petita) i ADR seria la millor opció per a imatges corregides geomètricament (relativament poca zona de NODATA i ben connectada, generalment a l'exterior) o quan la proporció de NODATA és gran (més del 70%).

Treball de futur. La recerca plantejada a la Tesi és completa en el seu contingut però pot ser continuada en diversos aspectes. D'una banda, el treball sobre l'impacte de la compressió a bord pot ser ampliat considerant noves imatges i nous mètodes de classificació posterior, així com avaluar l'impacte de l'estàndard de CCSDS dedicat a dades multiespectrals (grup de treball MHDC) quan aquest sigui aprovat. D'altra banda, nous escenaris de generació de cartografia i noves tècniques de compressió poden ser objecte d'estudi en els futurs treballs. Una de les noves línies de recerca especialment actives haurà de ser l'àmbit de servidors de cartografia o imatges a Internet degut a la rellevància que aquests servidors estan prenent en els darrers anys, així com la necessitat de compressió que s'hi requereix quan el volum de dades a descarregar és gran o l'ample de banda de les connexions no és molt elevat (p.ex. en un context de situacions d'emergència on les connexions són sovint precàries).

2. CONCLUSIONS (ENGLISH)

This PhD dissertation assesses the effects of several lossy compression techniques on the cartography resulting from remote sensing images, covering several geographic scenarios and compression levels.

Among the main contributions of this thesis we found that the effects of compression depend on the methodology used to obtain the cartography as well as when the compression is applied. In terms of **user-level compression**:

1. If visual analysis is used on orthoimages to obtain a categorical land cover map, JPEG 2000 compression at 5:1 can be applied with fewer effects on the cartography than those introduced by the subjectivity of the photointerpreter.

2. If digital analysis using regression models is used to obtain quantitative variables, such as mean or minimum annual temperature, from remote sensing data (land surface temperature and NDVI) and/or geographical variables (altitude, latitude, continentality, solar radiation and terrain curvature), JPEG 2000 compression does not affect the regression if medium compression ratios are applied (25:1 or 5:1 depending on whether only geographical variables are used or if remote images are also used).

3. If the objective is pixel by pixel classification of a multitemporal remote sensing dataset, the appropriate compression depends on the main land cover (forest or crop areas) and on the area fragmentation. The JPEG 2000 compression ratio varies from 3.33:1 or 5:1 in the worst case (fragmented forest areas) to 100:1 (less fragmented crop areas). JPEG 2000 obtains better results than the classic JPEG, especially if a 3D compression is applied.

4. If object-based classification using image segmentation is the objective, the results show that when images are compressed up to a ratio of 20:1 (depending on the image fragmentation), the classification obtained is similar to the original classification.

If compression is implemented **on board** a platform, the CCSDS standard obtains better compression fidelity than JPEG 2000 at low compression ratios (up to 5:1), which are the compression ratios used in on board compression, especially if the dynamic range of the image is small (up to 1000).

Finally, it is possible to use a JPEG 2000 standard modification for **coding NODATA values** in both the proposed approaches: ADR (pre-processing that assigns a mean value from the image

to NODATA areas) and SA-JPEG 2000 (a non-standard approach that avoids coding NODATA areas). SA-JPEG 2000 is a better option for radiometrically corrected images, which have few, highly-disconnected NODATA areas, and ADR is the best option for geometrically corrected images, which have few, well-connected NODATA areas usually on the image boundaries, or also when the NODATA proportion of the image is large (more than 70%).

Future work. The research content in this PhD Thesis is complete, but it can be continued in several directions. On one hand, research into on-board compression can be extended to cover new images and new image classification methods, as well as evaluate the impact of the CCSDS standard devoted to multispectral data (MHDC working group) when it is approved. On the other hand, future research could cover new scenarios in cartography generation and new compression techniques. Research lines such as internet services, which are becoming increasingly important, and the compression required when the data downloaded is large or the band width is not very wide (for example in emergency management scenarios when connections are usually precarious) are especially interesting.

8. BIBLIOGRAFIA

(Aboufadel 2001): Aboufadel, E. (2001): *JPEG 2000: the next compression standard using wavelet technology*. [Online]. Available: http://faculty.gvsu.edu/aboufade/web/wavelets/student_work/EF/index.html, (accessed 25th October, 2010).

(Adams 2001): Adams, M. D. (2001): *The JPEG-2000 still image compression standard*, ISO/IEC JTC 1/SC 29/WG 1 N2412. 17.

(Aulí-Llinàs *et al.* 2005): Aulí-Llinàs, F.; J.R. Paton, J. Bartrina-Rapesta, J.L. Monteagudo-Pereira, J. Serra-Sagristà (2005): "J2K: introducing a novel JPEG2000 coder". *In*: SPIE, IST (Ed.) *Visual Communications and Image Processing. Society of Photo-optical Instrumentation Engineers (SPIE)*, Beijing, China.

(Baatz & Shäpe 2006): Baatz, M.; A. Shäpe (2006): "Multiresolution segmentation: an optimization for high quality multi-scale image segmentation". *In:* Strobl, J.; T. Blaschke, G. Griesebner (Ed.) *Angewandte Geograsphische Information-Verarbeitung XII*. Wichmann Verlag, Karlsruhe, pp. 12-23.

(Baatz *et al.* 2004): Baatz, M.; U. Benz, S. Dehghani, M. Heynen, A. Höltje, P. Hofmann, I. Lingenfelder, M. Mimler, M. Sohlbach, M. Weber, G. Willhauck (2004): *eCognition Professional: User Guide 4*, Definiens-Imaging, Munich.

(Blaschke 2010): Blaschke, T. (2010): "Object based image analysis for remote sensing". *ISPRS Journal of Photogrametry & Remote Sensing*, 65, pp. 2-16.

(Burriel *et al.* 2005): Burriel, J.A.; J.J. Ibáñez, X. Pons (2005): "Segunda edición del Mapa de Cubiertas del Suelo de Cataluña: herramienta para la gestión sostenible del territorio". *In:* Sociedad Española de Ciencias Forestales (Ed.) *La Ciencia Forestal: Respuestas para la sostenibilidad*. ISBN: 84-921265-7-4.

(Cabral 2009): Cabral, M. (2009): *WhiteDwarf compression tester user's manual*, European Space Agency, TEC-EDP, 3/12/2009.

(Campbell 2008): Campbell, J.B. (2008): *Introduction to Remote Sensing*, The Guilford Press. N.Y. 626 pàgs. 4ª edició.

(Carvajal *et al.* 2008): Carvajal, G.; B. Penna, E. Magli (2008): "Unified Lossy and Near-Lossless Hyperspectral Image Compression Based on JPEG 2000", *IEEE Geoscience Remote Sensing Letters*, 5, pp. 593-597.

(CCSDS 1997): CCSDS (1997): *Lossless Data Compression, CCSDS 121.0-B-1, Blue Book*. [Online]. Available: http://public.ccsds.org/publications/archive/121x0b1c2.pdf, (accessed 25th October, 2010).

(CCSDS 2005): CCSDS (2005): *Image Data Compression, CCSDS 122.0-B-1. Blue Book*. [Online]. Available: http://public.ccsds.org/publications/archive/122x0b1c2.pdf, (accessed 25th October, 2010).

(CCSDS 2007): CCSDS (2007): *Image Data Compression, CCSDS 120.1-G-1, Green Book*. [Online]. Available: http://public.ccsds.org/publications/archive/120x1g1e1.pdf, (accessed 25th October, 2010).

(CCSDS 2007b): CCSDS (2007b): *Multispectral Hyperspectral Data Compression Working Group*. [Online]. Information available: http://cwe.ccsds.org/sls/docs/Forms/AllItems.aspx.

(Choi *et al.* 2008): Choi, E.; S. Lee, C. Lee (2008): "Effects of Compression on the Classification of Hyperspectral Images". *In*: Mastorakis, N.E.; V. Mladenov, Z. Bojkovic, D. Simian, S. Kartalopoulos, A. Varonides, C. Udriste, E. Kindler, S. Narayanan, J.L. Mauri, H. Parsiani, K.L. Man (Ed.) *Mathematics and Computers in Science and Engineering*, Heraklion, Greece, pp. 541-546.

(Chou & Liu 2008): Chou, C.H.; K.C. Liu (2008): "Colour image compression based on the measure of just noticeable colour difference", *IET Image Processing*, 2 (6), pp. 304-322.

(Chuvieco 2010): Chuvieco, E. (2010): *Teledetección ambiental*. Ed. Ariel. Barcelona. 590 pp.

(Conchedda *et al.* 2008): Conchedda, G.; L. Durieux, P. Mayaux (2008): "An object–based method for mapping and change analysis in mangrove ecosystems", *ISPRS Journal of Photogrametry & Remote Sensing*, 63, pp. 578-589.

(Cristóbal *et al.* 2005): Cristóbal, J.; X. Pons, M. Ninyerola (2005): "Modelling Actual Evapotranspiration in Catalonia (Spain) by means of Remote Sensing and Geographical Information Systems", *Göttinger Geographische Abhandlungen*, 113, pp. 144-150.

(Cristóbal *et al.* 2006): Cristóbal, J.; M. Ninyerola, X. Pons, M. Pla (2006): "Mejoras en la modelización de la temperatura del aire mediante el uso de la Teledetección y de los Sistemas de Información Geográfica", *In:* , M.T. Camacho Olmedo, J.A. Cañete Pérez, J.J. Lara Valle (Eds.) *El acceso a la información espacial y las nuevas tecnologías geográfica*, pp. 93-103.

(Du & Fowler 2007): Du, Q.; J.E. Fowler (2007): "Hyperspectral Image Compression Using JPEG 2000 and Principal Component Analysis", *IEEE Geoscience Remote Sensing Letters*, 4, pp. 201-205.

(Duda & Hart 1973): Duda, R.D.; P.E. Hart (1973): *Pattern Classification an Scene Analysis*. John Wiley & sons. New York.

(Foody 2002): Foody, G.M. (2002): "Status of land cover classification accuracy assessment", *Remote Sensing of Environment*, 80, pp. 185-201.

(García-Vílchez & Serra-Sagristà 2009): García-Vílchez, F.; J. Serra-Sagristà (2009): "Extending the CCSDS Recommendation for Image Data Compression for Remote Sensing Scenarios", *IEEE Transactions on Geoscience and Remote Sensing*, 47, pp. 3431-3445.

(ISO JTC 1/SC 29 1994): ISO JTC 1/SC 29 (1994): *Information technology -- Digital compression and coding of continuous-tone still images: Requirements and guidelines*. 182 pp.

(ISO JTC 1/SC 29 2004): ISO JTC 1/SC 29 (2004): *Information technology -- JPEG 2000 image coding system: Core coding system*. 194 pp.

(ISO TC 211 2003): ISO TC 211 (2003): *International Standard: Geographic information – Metadata. ISO 19115:2003*. Technical Committee 211. 140 pp.

(ITTVIS 2006): ITTVIS (2006): *ENVI software version 4.3*. [Online]. Information available: http://www.ittvis.com/ProductServices/ENVI.aspx, (accessed 25th October 2010).

(Jensen 2004): Jensen, J.R. (2004): *Introductory Digital Image Processing. A Remote Sensing Perspective*. Prentice Hall. Englewood Cliffs. 3rd edition. 544 pp.

(Julià *et al.* 2005): Julià, N.; J. Masó, A. Zabala, M. Vallès (2005): "CaMM, Catálogo de Metadatos de MiraMon: Implementación en una corporación, el DMAH". *Revista Mapping*. 105, pp. 24-30. ISSN: 1131-9100.

(Ke *et al.* 2010): Ke, Y.; L.J. Quackenbush, J. Im (2010): "Synergistic use of QuickBird multispectral imagery and LIDAR data for object-based", *Remote Sensing of Environment*, 114, pp. 1141–1154.

(Kettig & Landgrebe 1975): Kettig, R.L.; D.A. Landgrebe (1975): "Classification of multispectral image data by extraction and classification of homogeneous objects." *In: Proceedings of the Symposium on Machine Classification of Remotely Sensed Data*. West Lafayette. Lab for Applications in Remote Sensing, pp. 2A-1-2A-11.

(Kiema 2000): Kiema, J.B.K. (2000): "Wavelet Compression and the Automatic Classification of Landsat Imagery", *Photogrammetric Record*, 16 (96), pp. 997-1006.

(Lam *et al.* 2001): Lam, W.K.K; Z.L. Li, X.X. Yuan (2001): "Effects of JPEG compression on the accuracy of digital terrain models automatically derived from digital aerial images", *Photogrammetric Record*, 17 (98), pp. 331-342.

(Lee *et al.* 1990): Lee, J.B.; A.S. Woodyatt, M. Berman (1990): "Enhancement of high spectral resolution remote sensing data by a noise-adjusted principal components transform", *IEEE Transactions on Geoscience and Remote Sensing*, 28, pp. 295-304.

(Li *et al.* 2002): Li, Z.L.; X.X. Yuan, W.K.K. Lam (2002): "Effects of JPEG compression on the accuracy of photogrammetric point determination", *Photogrammetric Engineering and Remote Sensing*, 68 (8), pp. 847-853.

(Magli & Taubman 2003): Magli, E.; D. Taubman (2003): "Image compression practices and standards for geospatial information systems", *Geoscience and Remote Sensing Symposium, 2003. IGARSS '03. Proceedings*, 1, pp. 654-656.

(Maguire & Longley 2005): Maguire, D.J.; P.A. Longley (2005): "The Emergence of Geoportals and Their Role in Spatial Data Infrastructures", *Computers, Environment and Urban Systems*, 29, pp. 3-14.

(Mann & Rothley 2006): Mann, S.; K.D. Rothley (2006): "Sensitivity of Lansat/IKONOS accuracy comparison to errors in photointerpreted reference data and variations in test point sets". *International Journal of Remote Sensing*, 27 (20), pp. 5027-5036.

(Masó *et al.* 2010): Masó J.; K. Pomakis, N. Julià (2010): *OpenGIS® Web Map Tile Service Implementation Standard, v.1.0.0*. - 07-057r7. Open Geospatial Consortium Inc. [Online]. Available: http://www.opengeospatial.org/standards/wmts (accessed 25th October, 2010).

(Ninyerola *et al.* 2007): Ninyerola, M.; X. Pons, J.M. Roure (2007): "Objective air temperature mapping for the Iberian Peninsula using spatial interpolation and GIS", *International Journal of Climatology*, 27, pp. 1231-1242.

(Paola & Schowengerdt 1995): Paola, J.D.; R.A. Schowengerdt (1995): "The effect of lossy image compression on image classification". *Geoscience and Remote Sensing Symposium, 1995. IGARSS '95. 'Quantitative Remote Sensing for Science and Applications'*, 1, pp.118-120.

(Penna *et al.* 2006): Penna, B.; T. Tillo, E. Magli, G. Olmo (2006); "Progressive 3-D coding of hyperspectral images based on JPEG 2000", *IEEE Geoscience Remote Sensing Letters*, 3, pp. 125-129.

(Penna *et al.* 2007): Penna, B.; T. Tillo, E. Magli, G. Olmo (2007): "Transform coding techniques for lossy hyperspectral data compression", *IEEE Transactions on Geoscience and Remote Sensing*, 45, pp. 1408-1421.

(Pennebaker & Mitchell 1993): Pennebaker, W.B.; J.L. Mitchell (1993): *JPEG still image data compression standard*. Van Nostrand. New York, NY. 638 pp.

(Pérez *et al.* 2003): Pérez, C.; D. Aguilera, A. Muñoz (2003): "Estudio de viabilidad del uso de imágenes comprimidas en procesos de clasificación". *In*: Perez Utrero, R.; P. Martínez Cobo (Ed.) *Teledetección y desarrollo regional. X Congreso Nacional de Teledetección*, pp 309-312. ISBN: 84-607-8649-8.

(Pons 2008): Pons, X. (2008): *MiraMon. Sistema d'Informació Geogràfica i Teledetecció. Versió 7*, [Online]. Information available: http://www.creaf.uab.cat/miramon/ (accessed 25th October, 2010).

(Prihodko & Goward 1997): Prihodko, L.; S.N Goward (1997): "Estimation of air temperature from remotely sensed surface observations", *Remote Sensing of Environment*, 60, 335-346.

(Qian *et al.* 2005): Qian, S.E.; A. Hollinger, M. Bergeron, I. Cunningham, C. Nadeau, G. Jolly, H. Zwick (2005): "A multidisciplinary user acceptability study of hyperspectral data compressed using an on-board near lossless vector quantization algorithm", *International Journal of Remote Sensing*, 26, pp. 2163-2195.

(Recondo & Pérez-Morandeiram 2002): Recondo, C.; C.S. Pérez-Morandeiram (2002): "Obtención de la temperatura del aire en Asturias a partir de la temperatura de la superficie terrestre calculada con imágenes NOAA-AVHRR", *Revista de Teledetección*, 17, 5-12.

(Richards & Xia 2005): Richards, J.A.; X. Xia (2005): *Remote Sensing Digital Image Analysis. An Introduction*, Berlin, Springer-Verlag. 439 pp. 4ª edition.

(Sentinel-2 2007): Sentinel-2 team (2007): *GMES Sentinel-2 Image Performance Simulator Description*, S2-TN-ASG-SY-2002, Issue 1 Rev. 1, 09/02/2007. [ESA confidential].

(Sentinel-2 2010): Sentinel-2 team (2010): *GMES Sentinel-2 Mission Requirements Document, EOP-SM/1163/MR-dr*, Issue 2 Rev. 1, 08/03/2010. [Online]. Available: http://esamultimedia.esa.int/docs/GMES/Sentinel-2_MRD.pdf (accessed 25th October, 2010).

(Serra *et al.* 2003): Serra, P.; X. Pons, D. Saurí (2003): "Post-classification change detection with data from different sensors. Some accuracy considerations", *International Journal of Remote Sensing*, 24, pp. 3311-3340.

(Serra *et al.* 2009): Serra, P.; G. Moré, X. Pons (2009): "Thematic Accuracy Consequences in Cadastre Landcover Enrichment from a Pixel and from a Polygon Perspective", *Photogrammetric Engineering & Remote Sensing*, 75, pp.1441-1449.

(Shih & Liu, 2005): Shih, T.Y.; J.K. Liu (2005): "Effects of JPEG 2000 compression on automated DSM extraction: Evidence from aerial photographs", *Photogrammetric Record*, 20 (112), pp. 351–365.

(Sun *et al.* 2005): Sun, Y.J.; J.F. Wang, R.H. Zhang, R.R. Gillies, Y. Xule, Y.C. Bo (2005): "Air temperature retrieval from remote sensing data based on thermodynamics", *Theoretical and applied climatology*, 80, pp. 37-48.

(Taubman & Marcellin 2002): Taubman, D.S.; M.W. Marcellin (2002): *JPEG 2000: Image compression fundamentals, standards and practice*. Kluwer Academic Publishers.

(Taubman 2008): Taubman, D. (2008): *Kakadu software*. [Online]. Information and software available: http://www.kakadusoftware.com/ (accessed 25th October, 2010).

(Tintrup *et al.* 1998): Tintrup, F., F. De Natale, D. Giusto (1998): "Automatic land classification vs. data compression: a comparative evaluation". *Geoscience and Remote Sensing Symposium Proceedings, 1998. IGARSS '98*, 4, pp.1751-1753.

(Wallace 1991): Wallace, G.K. (1991): "The JPEG still picture compression Standard". *Communications of the ACM*, 34(4), pp. 30-44.

(Wang 2008): Wang, H. (2008): *An implementation of CCSDS 122.0-B-1 Recommended Standard*, 18/03/2008. [Online]. Information and software available: http://hyperspectral.unl.edu/ (accessed 25th October, 2010).

(Wang *et al.* 2007): Wang, H.; S.D. Babacan, K. Sayood (2007): "Lossless hyperspectral-image compression using context-based conditional average", *IEEE Transactions on Geoscience and Remote Sensing*, 45 (12), pp. 4187-4193.

(Xiaoxia *et al.* 2005): Xiaoxia, S.; Z. Jixian, L. Zhengjun (2005): "A comparison of object-oriented and pixel-based classification approaches using quickbird imagery". *ISPRS STM, Beijing*, pp. 281-284.

(Xu *et al.* 2003): Xu, B.; P. Gong, E. Seto, R. Spear (2003): "Comparison of gray-level reduction and different texture Spectrum encoding methods for land-use classification using a panchromatic Ikonos image". *Photogrammetric Engineering and Remote Sensing*, 69(5): 529-536.

(Yu *et al.* 2009): Yu, G.; T. Vladimirova, M.N. Sweeting (2009): "Image compression systems on board satellites", *Acta Astronautica*, 64 (9-10), pp. 988-1005.

(Zabala & Masó 2005): Zabala, A.; J. Masó (2005): "Integrated hierarchical metadata proposal: series, layer, entity and attribute metadata". *In*: XXII International Cartographic Conference (Ed.) *Mapping approaches into a changing world* (CD-ROM edition). ISBN: 0-958-46093-0.

(Zabala & Pons 2002): Zabala, A.; X. Pons (2002): "Image Metadata: compiled proposal and implementation" *In*: Benes, T. (Ed.) *Geoinformation for European-wide Integration*. Millpress, Rotterdam, pp. 674-652. ISBN: 90-77017-71-2.

(Zabala & Pons 2010): Zabala, A.; X. Pons (2010): "Effects of lossy compression on remote sensing image classification of forest areas", *International Journal of Applied Earth Observation and Geoinformation (JAG)*, doi:10.1016/j.jag.2010.06.005, ISSN: 0303-2434.

(Zabala & Pons 2010b): Zabala, A.; X. Pons (2010): "Impact of lossy compression on mapping crop areas from remote sensing", *International Journal of Remote Sensing*. Submitted.

(Zabala *et al.* 2007): Zabala, A.; X. Pons, F. Aulí-Llinàs, J. Serra-Sagristà (2007): "Implications of JPEG2000 lossy compression on multiple regression modelling", *In*: Ehlers M.; U. Michel (Ed.) *Remote Sensing for Environmental Monitoring, GIS Applications, and Geology VII. Book series: Proceedings of*

the Society of Photo-optical Instrumentation Engineers (SPIE), 6749, pp. 674918-1–674918-12. ISBN: 978-0-8194-6907-6, Florence, Italy, September 2007. Publisher: SPIE-Int Soc Optical Engineering, 1000 20th St, Po Box 10, Bellingham, WA 98227-0010 USA.

(Zabala *et al.* 2008): Zabala, A.; X. Pons, F. Aulí-Llinàs, J. Serra-Sagristà (2008): "Image compression effects in visual analysis", *In*: Huang B.; R.W. Heymann, J. Serra-Sagristà (Ed.) *Satellite Data Compression, Communication, and Processing IV. Book series: Proceedings of the Society of Photo-optical Instrumentation Engineers (SPIE)*, 7084, pp. 70840I-1–70840I-12.ISBN: 978-0-8194-7304-2, San Diego, California, USA, September 2008. Publisher: SPIE-Int Soc Optical Engineering, 1000 20th St, Po Box 10, Bellingham, WA 98227-0010 USA.

(Zabala *et al.* 2010): Zabala, A.; J. González-Conejero, J. Serra-Sagristà, X. Pons (2010): "JPEG2000 encoding of images with NODATA regions for Remote Sensing applications", *Journal of Applied Remote Sensing (JARS)*, 4 (041793), ISSN: 1931-3195.

(Zabala *et al.* 2010b): Zabala, A.; C. Cea, X. Pons (2010): "Segmentation and thematic classification of color orthophotos over non-compressed and jpeg 2000 compressed images", *International Journal of Applied Earth Observation and Geoinformation (JAG) – Special Issue: Geobia'10.* Submitted.

(Zabala *et al.* 2010c): Zabala, A.; R. Vitulli, R. Duca, F. Ramoino, X. Pons (2010): "Impact of CCSDS and JPEG 2000 on-board compression on image quality and classification", 2nd Int. WS on On-Board Payload Data Compression (OBPDC), *in press*.

ANNEX 1: IMPACT OF LOSSY COMPRESSION ON MAPPING CROP AREAS FROM REMOTE SENSING[2]

[2] Segons la normativa de la UAB a què s'acull aquesta Tesi per compendi de publicacions, a part dels articles acceptats per a format la part fonamental de la mateixa (i inclosos en els capítols 2 a 5 d'aquesta Tesi), es pot adjuntar altres articles com a annexos (o part no fonamental). Segons la mateixa normativa, els treballs fets en aquestes publicacions poden ser comentats a la discussió de resultats. Aquest és el primer article dels tres presentats com a annexos i que pretenen completar l'aportació de la Tesi en el camp dels efectes de la compressió amb pèrdua d'imatges de teledetecció aplicades a l'obtenció de cartografia.

Impact of lossy compression on mapping crop areas from remote sensing

ALAITZ ZABALA† and XAVIER PONS*†,‡
† Geography Department
‡ Centre for Ecological Research and Forestry Applications (CREAF)
Autonomous University of Barcelona, 08193, Cerdanyola del Vallès, Spain

This study measures the effect of lossy image compression (JPEG2000 and JPG) on the digital classification of crop areas. The results provide new insights into the influence of compression on the quality of the cartography produced. Both a multitemporal and a single-date classification approach were analyzed. With the multitemporal approach it is possible to use high compression ratios (CR), up to 20:1 or even 100:1, and the overall accuracy of the classification is similar to that obtained with the original images. Moreover, the classified area is similar or even greater (less pixels are uncertain). For a single-date approach it is only advisable to use 3D-JPEG2000 at CRs up to 20:1. The optimum CR is also affected by landscape fragmentation (fragmented images tolerate less compression) and the classification method (hybrid classifiers are affected less than the maximum likelihood and minimum distance classifiers). Finally, classifications from compressed images have less "salt and pepper" effect than those obtained from the originals, especially when JPEG2000 (3D or not) is used.

1. Introduction and objectives

Remote Sensing (RS) images are used for many applications, including land cover mapping and analysis, disaster management, climate modelling and agricultural and forest management. In zones with quite fragmented landscapes, like the Mediterranean area, Landsat images are especially suitable for producing land cover maps due to their spatial, temporal and spectral resolution (Chirici et al. 2003). The recent release of the historical Landsat image archive by the USGS (December 2008) is potentially very beneficial for land cover studies. Indeed, it is now possible to work at practically no cost with long time series, which is especially interesting for vegetation classification and studies of territorial dynamics. However, this implies managing an enormous amount of images, which, due to their temporal resolution and spatial coverage (and even to their medium spectral resolution), is a volume of data that is difficult to store, transmit, handle and process. Therefore, image compression is necessary for users that manage this huge volume of images.

On the other hand, the new Spatial Data Infrastructures (SDI) paradigm developed over recent years, promotes the establishment of web data services, usually in terms of Open Geospatial Consortium standards like the Web Map Service (WMS), the Web Coverage Service (WCS) (Maguire and Longley 2005) or the recent Web Map Tile Service (WMTS, Masó et al. 2010). However, it is necessary to use compression and interactive transmission strategies for these web services in order to transfer images (which may be very large in the case of WCS) repetitively to environments with restricted bandwidth. It is also necessary to standardize data compression and transmission formats in SDI environments in order to achieve the desired interoperability. Thus, the use of standard compression formats is unavoidable even if it implies slightly worse compression than that obtained with new but non-standard algorithms published recently.

Previous research on image compression (usually without taking into account the effects on the user's application) concluded that wavelet based algorithms, such as JPEG 2000 (ISO standard since 2000, revised in 2004: ISO/IEC 15444-1:2004), obtain better results than those based on discrete cosine transform (DCT), such as JPEG (ISO standard since 1994: ISO/IEC 10918-1:1994). Thus, JPEG 2000 seems the option to be studied further in terms of the effect of compression on the final user application, such as crop classification. However, taking into account that JPEG is widely used in daily applications, and also that it is currently used by many Web Map Services (which are becoming one of the most used data sources), it would be an interesting additional approach to obtain results using not only JPEG2000 but also JPEG.

*Corresponding author. Email: xavier.pons@uab.cat

It is important to bear in mind that we are always dealing with lossy compression algorithms, which sacrifice part of the data information in order to achieve higher compression ratios. Both JPEG and JPEG 2000 have lossless modes that will not be considered in this work because these modes do not achieve such high compression ratios (for example 100:1).

In the RS and GIS fields, and in spite of the spectacular compression ratios reached, there has been little quantitative analysis on the implications of these compressions for classification, especially in real-environment applications. Indeed, previous research has generally focused on compression, and explored modifications to compression techniques in order to improve them (Qian et al. 2005, Penna et al. 2006, Penna et al. 2007, Du and Fowler 2007, Carvajal et al. 2008, Choi et al. 2008); however, only some of these studies regard the effect of this compression on classification (Qian et al. 2005, Penna et al. 2007, Carvajal et al. 2008, Choi et al. 2008, Zabala and Pons 2010). Moreover, and with the exception of the last reference, none of these papers used multitemporal analyses and they all used small images (the widest area was 512x512 pixels).

This study aims to assess the influence of lossy image compression on digital classification in a real agricultural management environment (i.e., multitemporal analysis to take advantage of the crop dynamics (Lo et al. 1986), and also a unitemporal analysis for the reasons explained in Section 2.2.3) with a regional approach (using images that cover a wide area). Multitemporal analysis is very important for crop analysis because it allows the overall accuracy to be increased (Wolter et al. 1995, Shriever and Congalton 1993, Moré and Pons 2007).

The regional approach (using images that are bigger than those used in previous literature) allows us to obtain more general results due to the wider area covered and thus the larger number of different landscape structures studied. Authors agree that not only is the total area covered by the images important but also the pixel size of the sensor used because the landscape is captured differently depending on the pixel size (e.g., landscape patch size). A multiresolution (or multisensor) study would be of great interest but is out of the scope of this paper due to the availability of images. Nevertheless, Landsat provides a reasonable pixel size for Mediterranean areas (Chirici et al. 2003) and is widely used, so it is very interesting as test material.

As compression technology progresses, and the best compression methods are selected and used as part of standard Remote Sensing software packages and on-board sensor platforms (Garcia-Vilchez and Serra-Sagrista 2009, Delaunay et al. 2010), it is important for the end-users of these images (experts in RS but not compression) to know the degree of compression they can apply to their images. This, therefore, is another objective of this paper: to bring compression closer to those who are not experts in data compression, giving them some rules to decide which compression ratio and compression standard should be applied to their classification scenario.

2. Material and methods

2.1. The zones and scenes used

We chose two medium-sized zones located in two different agricultural regions: Segrià and Pla d'Urgell. The Segrià zone is richer in fruit trees and slightly less fragmented. The Pla d'Urgell zone is richer in maize and somewhat more fragmented; it is a zone in which irrigated herbaceous crops and dry permanent crops predominate.

Both zones are in Catalonia (NE Spain, see figure 1) and were analyzed by using TM images (Landsat-5 satellite). The images were geometrically corrected, resampled (using nearest neighbour to preserve the original radiometry) and processed to convert digital numbers into reflectance values.

The dimensions of the fragment of the TM scenes covering the study zones were 1517x1311 pixels (53585 ha of crops) for Segrià and 1307x1059 (50099 ha) for Pla d'Urgell. Both were analyzed using the images 16-05-2004, 17-06-2004, 19-07-2004, 23-10-2004 and 08-11-2004. They were selected from those available for 2004 (without clouds) to take advantage of the different spectral responses over the year due to their phenological state.

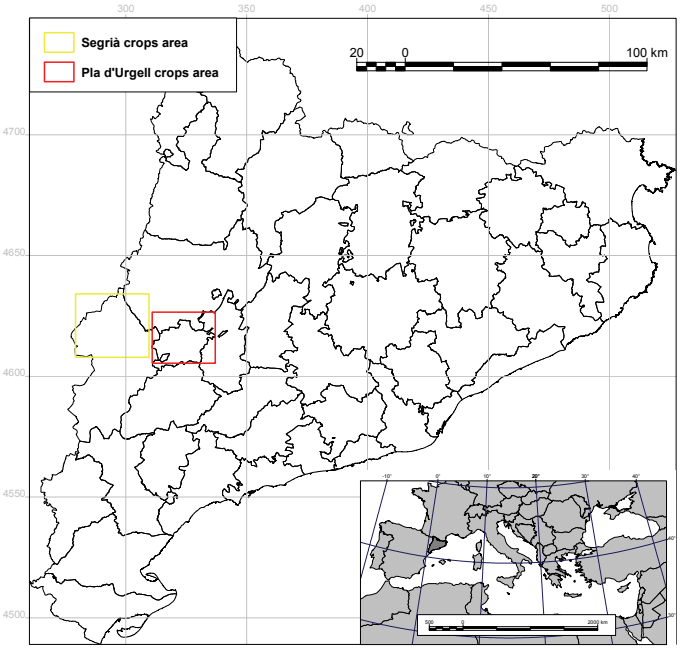

Figure 1. Zones used in the study, located in Catalonia (northeast Spain). Two zones were selected: Segrià and Pla d'Urgell.

2.2. Image compression

Both JPEG 2000 and JPEG were considered in order to measure the effect of compression on the classification results. The compression algorithms used were the JPEG 2000 implementations of Kakadu (Taubman 2008) and BOÍ (Aulí-Llinàs *et al.* 2005), and the JPEGIMG module implemented in the MiraMon v.6 software (Pons 2008) based on the JPEG public libraries (Independent JPEG group 2008).

In this paper, the compression ratio (CR) is computed as the ratio between the size of the original file and the size of the compressed file, and is expressed as, *e.g.*, 10:1 for a file that is compressed to a tenth of the original file size.

2.2.1 Image type transformations: Landsat TM images store each value band in bytes, but radiometric correction using a Digital Elevation Model can produce short integer images (reflectances*10000). JPEG 2000 allows the compression of both byte and integer data types. However, JPEG compression usually uses byte-type images for each spectral component, and for this reason radiometrically corrected images have to be converted into bytes before compression by means of linear stretch. The main advantage of this transformation method is that each output image band uses the whole available rank to describe the rank of the original image. This maximum exploitation of the output rank is very important in order to penalize this necessary transformation as little as possible.

2.2.2 JPEG 2000 and JPEG compression scenarios: Two improvements of the JPEG 2000 compression standard are the multiple-component and the third dimension decorrelation transformation. The first compression scenario makes full use of the JPEG 2000 capabilities, *i.e.*, 3D compression of integer images (hereafter J2Km) using the Kakadu software.

The JPEG compression standard allows the user to compress one band independently or three bands together (grey scale or colour images respectively). As the images we are dealing with have six bands (the TM thermal band was not used), we decided to compress each byte-scaled band separately to the desired compression ratios (hereafter JPG) using MiraMon software. Moreover, to obtain comparable results between the two compression standards, a second JPEG 2000 approach (hereafter J2K) was used to compress each byte-scaled component independently using BOÍ.

2.3. Classification

In order to classify only the crop areas and to obtain the best results (Xie *et al.* 2007) a mask obtained from the Land Cover Map of Catalonia was applied. Three classification methods were used. The first one (hereafter HybCls) is a hybrid classifier that combines an unsupervised classifier and a non-parametric supervised classifier (Serra *et al.* 2003, Serra *et al.* 2009) implemented in MiraMon software. Moreover, classic Minimum Distance and Maximum Likelihood general classifiers were also used (hereafter MinDist and MaxLike respectively) implemented in the ENVI software (ITTVIS, 2006). We considered both supervised and non-supervised methods based on the spectral information of the pixels. Classification methods that use contextual information are out of the scope of this study; although we are currently researching these methods.

The classifications obtained (from images with or without compression) were evaluated using the confusion matrix (Foody 2002) based on ground-truth test areas that are independent of the training areas used in the supervised classification stage. Moreover, the confusion matrix was also obtained using the classification of non-compressed integer images as the ground truth (instead of test areas), to compute the agreement of the maps obtained. The two complementary evaluation approaches enhance the comparability of this study with those published earlier (using the first or the second evaluation method, *e.g.*, Qian *et al.* 2005 and Choi *et al.* 2008 respectively).

Due to the classification methods and depending on the parameters used, some pixels remain unclassified. This parameter adjustment allows the expert to produce the best possible classification. For the three classification methods some parameters (or thresholds) can be used to prevent all the pixels from being classified if they are not similar enough to the spectral characteristics of the trained categories. This is a common, and usually desirable, practice when land cover maps are produced so that pixels that represent other categories are not artificially set to one of the trained ones even though they are very different from the category characteristics (Richards 2006, p.197). Thus, the classified area (number of classified pixels in relation to the number of pixels to be classified) is another interesting parameter for evaluating the quality of the maps obtained.

The number of images used in the classification also needs to be considered. Multitemporality and adjusted classification methods allow the best classification possible to be obtained with the images, usually with high classification accuracies (Wolter et al. 1995, Shriever and Congalton 1993, Moré and Pons 2007). However, sometimes only one or a small number of images is available for a specific area during a crop season. This is especially important in areas with high cloud cover or when a map is needed with one single image (e.g., for crisis management or retrospective studies with few available data, usually only one per year, or simply for economic reasons when imagery that is not free is used). As expected, when fewer images are used, the classifications obtain lower overall accuracies. Two classification scenarios were used to asses the effects of multitemporality and compression on classification scenarios with different overall accuracies (on non-compressed images): with all five images and with only one of the available images (17-06-2004).

During the whole image processing workflow, careful attention was given to documenting image metadata properly and complying with ISO standards (19115, 19115-2 and 19139).

3. Results

3.1. Overall accuracy computed using independent test areas

Table 1 shows the overall accuracy (without taking into account unclassified pixels) and the percentage of the classified area according to the compression ratio (CR) for each of the two studied areas, the three classification methods and three compression scenarios. These were computed in relation to independent test areas using the full set of dates (left) or only one date (right). Columns entitled “1” for CR show the results obtained for non-compressed integer (J2Km) or byte-scaled (JPG and J2K) images. The differences shown in the other CR columns always refer to the difference regarding the value obtained using non-compressed integer images (scenario J2Km) in order to be able to discuss not only differences due to

compression but also due to byte scaling. Colour shaded scenarios will be discussed here and shaded in grey in the next section.

Table 1. Overall accuracy (without taking into account unclassified pixels) computed using independent test areas, and the classified area of classifications obtained using the full set of images (on the left) and only one image (on the right). The results for the three classification and compression algorithms are shown.

5 Landsat images

HybCls

		CR	1	1.66	2	2.5	3.33	5	10	20	100	200	1000
Overall Accur.	S	J2Km	99.1	0.1	0.0	0.0	0.0	0.3	0.4	0.1	0.3	0.1	1.4
		J2K	99.0	0.2	0.2	0.3	0.1	0.2	0.2	0.1	0.2	1.0	4.8
		JPG	99.0	0.4	0.1	0.3	0.5	0.2	0.3	0.4	1.6	5.2	11.4
	PU	J2Km	99.7	0.0	0.0	0.0	0.1	0.0	0.5	0.2	0.1	0.4	2.2
		J2K	99.5	0.2	0.2	0.1	0.2	0.1	0.0	0.3	1.0	2.0	14.7
		JPG	99.5	0.1	0.3	0.1	0.1	0.2	0.0	0.1	2.6	12.1	15.9
Classified Area	S	J2Km	81.13	0.15	0.15	0.21	0.61	0.17	0.32	1.00	0.29	1.23	4.90
		J2K	79.42	2.85	1.17	1.80	2.89	1.72	3.30	2.45	4.34	3.39	8.39
		JPG	79.42	0.66	2.95	0.52	1.86	1.78	0.04	0.57	1.28	8.86	13.04
	PU	J2Km	72.09	0.01	0.07	0.19	0.41	0.87	0.59	0.74	1.34	0.18	6.84
		J2K	70.45	1.51	1.97	0.70	0.98	1.39	1.57	3.18	3.46	7.97	11.11
		JPG	70.45	1.66	1.19	0.68	2.94	0.51	1.82	1.73	6.52	18.91	25.66

1 Landsat image

HybCls

		CR	1	1.66	2	2.5	3.33	5	10	20	100	200	1000
Overall Accur.	S	J2Km	86.1	0.0	0.1	0.0	0.1	0.8	0.5	0.6	0.2	2.6	5.2
		J2K	87.0	0.1	1.0	0.3	1.0	0.1	0.3	0.8	1.3	2.3	10.2
		JPG	87.0	0.8	0.8	0.7	0.1	0.9	0.5	1.2	5.7	9.4	30.3
	PU	J2Km	79.2	0.1	0.2	0.5	0.4	0.3	0.8	0.3	3.4	6.0	14.2
		J2K	80.5	0.1	1.0	0.2	0.3	0.0	0.8	3.0	6.1	9.4	19.0
		JPG	80.5	0.7	0.5	0.3	0.5	0.1	1.7	2.4	13.4	29.6	36.8
Classified Area	S	J2Km	97.40	0.25	0.25	0.55	0.67	0.66	1.18	0.34	0.93	0.54	0.83
		J2K	97.11	0.43	0.21	0.46	0.28	0.02	0.22	0.64	0.21	0.44	1.16
		JPG	97.11	0.59	0.64	0.50	0.75	0.69	1.01	0.06	0.37	2.11	2.41
	PU	J2Km	97.07	0.13	0.09	0.05	0.22	0.38	0.21	1.21	0.60	1.74	2.00
		J2K	96.95	0.36	0.34	0.30	0.30	0.38	0.17	0.86	0.35	1.18	0.99
		JPG	96.95	0.76	0.12	0.67	1.28	0.61	1.61	1.68	0.20	2.29	2.75

MaxLike

		CR	1	1.66	2	2.5	3.33	5	10	20	100	200	1000
Overall Accur.	S	J2Km	99.5	0.0	0.0	0.0	0.0	0.0	0.0	0.1	0.7	1.3	4.9
		J2K	99.6	0.1	0.1	0.1	0.1	0.1	0.0	0.2	1.3	2.5	7.9
		JPG	99.6	0.1	0.1	0.1	0.0	0.0	0.1	0.1	14.4	95.9	95.9
	PU	J2Km	99.9	0.0	0.0	0.0	0.1	0.1	0.1	0.2	0.7	0.9	6.1
		J2K	99.9	0.0	0.0	0.0	0.1	0.1	0.2	0.2	1.2	2.6	14.4
		JPG	99.9	0.0	0.0	0.1	0.1	0.1	0.1	0.2	99.8	99.8	99.8
Classified Area	S	J2Km	81.50	0.00	0.00	0.01	0.14	0.03	1.73	0.95	10.52	12.12	13.49
		J2K	79.43	1.93	1.35	0.90	1.53	3.07	2.80	1.19	9.63	11.45	13.11
		JPG	79.43	0.24	0.26	0.39	0.54	1.00	3.43	5.84	10.23	18.50	18.50
	PU	J2Km	72.12	0.00	0.01	0.02	0.19	0.15	0.37	4.53	19.34	22.36	26.91
		J2K	70.99	0.88	0.16	0.06	0.45	0.53	0.44	5.42	18.80	20.07	23.18
		JPG	70.99	0.63	1.59	2.34	2.92	3.90	7.88	12.49	27.88	27.88	27.88

MaxLike

		CR	1	1.66	2	2.5	3.33	5	10	20	100	200	1000
Overall Accur.	S	J2Km	85.5	0.0	0.0	0.1	0.3	0.2	0.6	1.1	0.7	0.4	6.8
		J2K	85.4	0.3	0.7	1.1	1.3	1.4	1.3	1.4	2.0	5.9	12.0
		JPG	85.4	0.9	1.7	1.7	1.7	1.8	1.7	2.7	42.4	81.9	81.9
	PU	J2Km	74.0	0.1	0.0	0.1	0.1	0.2	0.8	1.2	1.5	5.0	13.8
		J2K	74.0	0.4	0.7	0.9	1.9	2.1	2.3	2.5	4.7	5.0	15.1
		JPG	74.0	1.2	1.8	2.4	2.4	2.6	2.2	4.2	73.9	73.9	73.9
Classified Area	S	J2Km	97.09	0.00	0.00	0.00	0.03	0.09	0.47	0.33	2.05	2.53	2.65
		J2K	96.79	0.24	0.09	0.05	0.09	0.11	0.39	0.29	1.72	1.80	2.29
		JPG	96.79	0.08	0.36	0.34	0.27	0.18	0.76	1.25	2.07	2.91	2.91
	PU	J2Km	97.09	0.00	0.00	0.01	0.05	0.06	0.14	0.76	2.29	2.64	2.80
		J2K	96.75	0.26	0.14	0.05	0.02	0.01	0.26	0.48	1.97	1.89	2.16
		JPG	96.75	0.11	0.29	0.34	0.40	0.52	1.11	1.77	2.91	2.91	2.91

MinDist

		CR	1	1.66	2	2.5	3.33	5	10	20	100	200	1000
Overall Accur.	S	J2Km	98.4	0.0	0.0	0.0	0.0	0.0	0.0	0.0	0.0	0.1	2.1
		J2K	98.1	0.2	0.2	0.2	0.3	0.2	0.2	0.2	0.8	2.4	7.4
		JPG	98.1	0.3	0.2	0.2	0.2	0.2	0.2	0.3	2.7	5.3	14.9
	PU	J2Km	99.4	0.0	0.0	0.0	0.1	0.1	0.1	0.0	0.0	0.2	2.7
		J2K	99.5	0.0	0.0	0.1	0.1	0.1	0.2	0.1	0.5	2.1	16.0
		JPG	99.5	0.1	0.1	0.1	0.0	0.1	0.2	0.0	2.0	20.2	39.4
Classified Area	S	J2Km	80.80	0.00	0.00	0.00	0.01	0.01	0.25	0.11	2.73	4.29	8.51
		J2K	80.03	0.80	0.70	0.66	0.85	1.11	0.78	0.37	4.17	5.96	10.44
		JPG	80.03	0.59	0.61	0.62	0.63	0.36	0.41	1.44	6.22	9.24	8.02
	PU	J2Km	72.64	0.00	0.00	0.00	0.01	0.05	0.02	0.61	4.53	7.06	14.88
		J2K	69.72	2.99	2.86	2.85	2.95	2.98	2.13	0.27	5.67	9.69	19.46
		JPG	69.72	2.74	2.63	2.54	2.39	1.94	0.95	0.61	6.98	2.62	6.39

MinDist

		CR	1	1.66	2	2.5	3.33	5	10	20	100	200	1000
Overall Accur.	S	J2Km	70.1	0.0	0.1	0.1	0.0	0.0	0.2	0.7	2.6	1.5	4.4
		J2K	69.4	0.5	1.0	1.3	1.3	1.4	0.0	1.8	0.1	2.1	5.2
		JPG	69.4	1.3	1.6	1.0	0.6	0.3	1.1	1.0	1.1	4.1	65.6
	PU	J2Km	53.2	0.0	0.0	0.1	0.1	0.1	0.1	0.1	0.1	0.2	1.9
		J2K	52.5	0.9	1.0	1.0	1.1	1.2	0.7	0.7	0.7	0.6	5.0
		JPG	52.5	1.0	1.0	1.0	1.4	1.1	1.3	1.3	8.5	32.9	41.2
Classified Area	S	J2Km	97.39	0.00	0.01	0.01	0.00	0.02	0.03	0.03	0.39	0.22	0.44
		J2K	97.18	0.28	0.15	0.05	0.01	0.09	0.42	1.21	0.55	1.53	1.25
		JPG	97.18	0.11	0.00	0.19	0.39	0.48	0.80	1.27	2.72	1.64	9.33
	PU	J2Km	97.17	0.00	0.00	0.00	0.00	0.00	0.04	0.06	0.32	0.63	1.09
		J2K	96.81	0.36	0.37	0.36	0.36	0.36	0.28	0.09	0.58	0.58	0.61
		JPG	96.81	0.34	0.32	0.34	0.36	0.37	0.17	0.07	0.81	7.28	8.68

Overall Accuracy and Classified Area for each studied area (S for Segrià and PU for Pla d'Urgell), classification method (IsoMM, MaxLike and MinDist) and compression scenario (J2Km, J2K and JPG). First column shows the value obtained with images without compression (CR=1) for integer (J2Km) and byte (JPG, J2K) scenarios. Other columns show the difference between integer reference value and those obtained for each CR (red values are negative).

When the full set of images is used for both areas the overall accuracies obtained are very high, especially when the HybCls and MaxLike classifiers are used. These high accuracies are due to the use of multitemporal images and the suitability of the classifiers (Serra et al. 2003, Serra et al. 2009). Moreover, medium compression barely seems to affect this accuracy, the value of which almost always remains very close to the original value, except for the most extreme compressions where the accuracy significantly decreases. A CR of 20:1 could be used in almost all cases, taking into account the general considerations stated below.

If only one image is used, the overall accuracy is lower (and classified areas are larger), especially when the MinDist classifier is used. Compression has a different affect depending on the classification method used. When HybCls is used, medium compressions can be applied, but at a slightly lower CR than when the full set of images is used. The MaxLike and MinDist classifiers using a single image are highly affected by compression and are only recommendable if J2Km is used.

Byte-scaling (needed to compress images using JPG or J2K) has an effect in all cases: for almost all situations both the overall accuracy and classified area obtained using byte-scaled images are lower than those obtained with integer images. Only in a few cases the overall accuracy of integer images is slightly

lower than when byte images are used; however, a larger classified area is always obtained with integer images.

The general tendencies show that the overall accuracy decreases with CR in all cases. The size of the decrease depends on the compression standard, fragmentation of the area and initial overall accuracy, as is discussed in the next section. However, the classified area generally increases with the compression ratio in relation to the initial (integer or byte) value. Sometimes it seems to decrease, but the difference is due to integer-to-byte scaling more than to the compression itself. As an example, the Pla d'Urgell zone using all dates and the MinDist classifier at CR 1.66 using JPG (shaded blue) loses 2.74 percentage points of the classified area in relation to the classified area obtained with non-compressed integer images (72.64%); however, as the classified area of non-compressed byte-scaled images is 69.72%, the difference regarding non-compressed byte-scaled images is +0.78.

It is interesting to note that smooth compression seems to be beneficial for the classification due to the homogenization effect on the radiometric values of neighbour pixels. The same overall accuracy compared to the original images and an increased classified area is obtained. Two examples of this behaviour are (shaded in green in table 1): the Pla d'Urgell zone using all dates, J2Km or JPG compression and the MaxLike classifier; and the Segrià zone using one date, J2Km compression and the HybCls classifier.

Moreover, landscape fragmentation influences how compression affects classification. It can be clearly seen that in the most fragmented zone (Pla d'Urgell) the decrease in the overall accuracy is more apparent at lower CRs than in the least fragmented zone using any of the compression and classification methods with one or all images. For example, using MaxLike, the maximum CRs that obtained the same overall accuracy as the original integer classification were (Segrià vs. Pla d'Urgell values, shaded yellow in table 1) 10:1 vs. 2.5:1 (J2Km and J2K) and 5:1 vs. 2:1 (JPG).

Finally, and as pointed out previously, MaxLike (and in a few cases MinDist and HybCls) obtains very bad results at higher CRs (the scenarios shaded pink in table 1) when JPG is used. These values are not an error in the confusion matrix computation, but rather they are due to the fact that the entire study area is classified to a single category or to a few categories (and thus these classifications are unacceptable); they usually show the blocking effect produced by JPG compression. MaxLike is the only classifier among those studied that uses dispersion measures to characterize classes. For the extremely compressed images, the histogram is highly quantified (only a few values are used), and training areas include pixels with very different values; thus, one or a few classes act as a sink class.

Does compression affect class separability? Our initial classes were very separable thanks to the multitemporal approach, which compiles enough information to easily discriminate them. For example, computing the Jeffries-Matusita (JM) index for the Segrià area using the ENVI software (over integer original images) reveals that the lowest separability is as high as 1.9902, and that 12 of the 15 class pairs have a separability of 2.0000. Compression does not change this situation very much: at a CR of 5:1, 12 class pairs also have a JM index of 2.0000, and at 100:1 the number of class pairs with a JM index value of 2.0000 is 11 and 13 (J2K and J2Km scenarios respectively). Additional research with classes that are not so separable (using a single date from the five available dates from the entire year) obtained similar results.

3.2. Overall accuracy computed using the original classification as reference

Figure 2 shows the overall accuracy according to the compression ratio (CR), presented for each of the two areas studied (continuous lines for Segrià and dashed lines for Pla d'Urgell), three classification methods (one graphic per method) and three compression scenarios (green for J2Km, blue for J2K and red/orange for JPG), when computed in relation to the original integer classification and using the full set of dates (left) or only one of them (right).

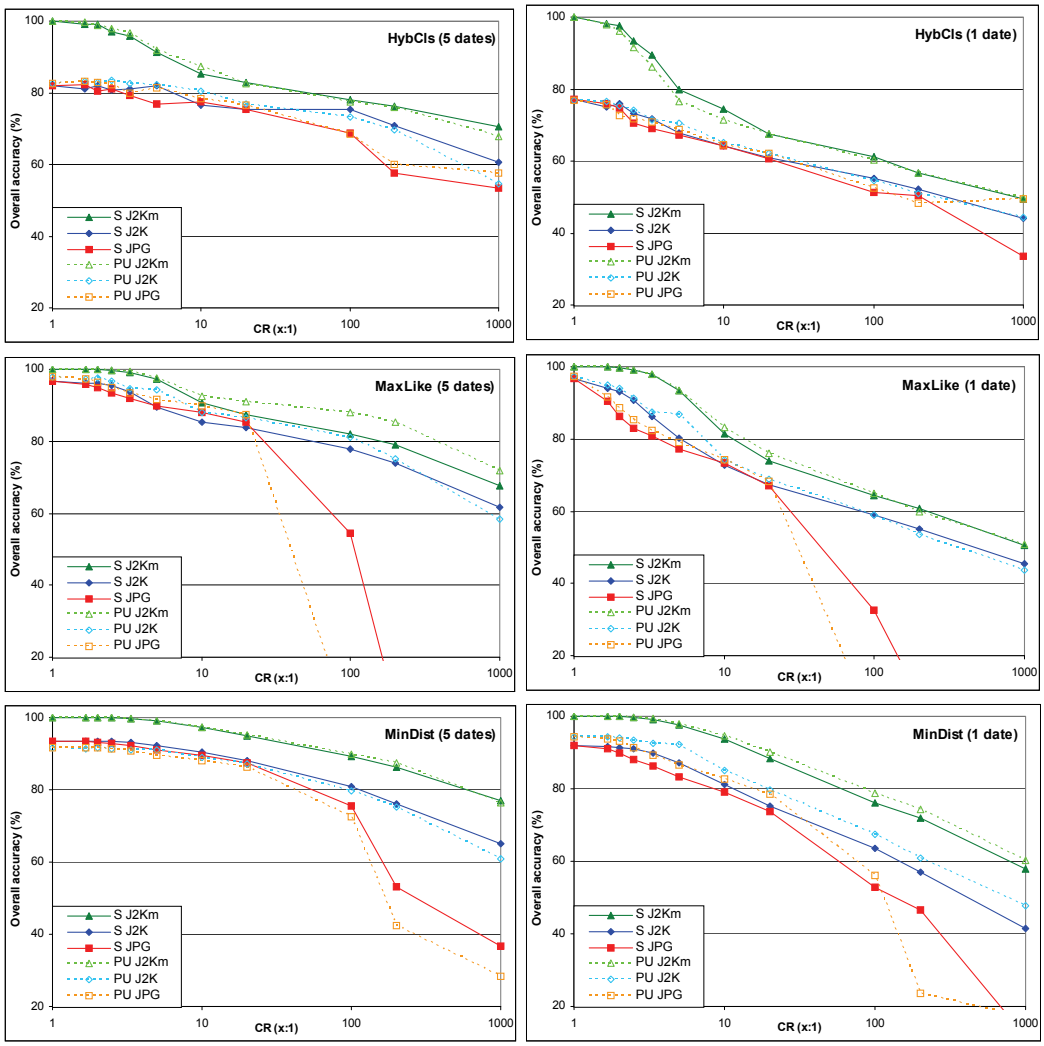

Figure 2. Overall accuracy in relation to the original classification of the classifications obtained using the full set of images (on the left) and only one image (on the right). Results for the two study zones, three classification methods and three compression algorithms are shown.

First we should mention the differences obtained when non-compressed integer or byte images are used. In all the graphics, the first point of each line corresponds to the non-compressed image results. For each compression scenario, the reference value is the one obtained using integer or byte-scaled images, depending on each case. The J2Km scenarios (green lines) use integer images and the J2K/JPG scenarios (blue and red/orange lines) use byte-scaled images. The overall accuracy computed for these graphics uses classification over non-compressed integer images as the ground-truth and this is why there is 100% overall accuracy in the J2Km scenarios. However, up to 20% of the differences (depending on the classification method and scenario) are found between non-compressed integer and byte-scaled images. These differences are mainly due to border effects (98 to 99% of the polygons of change are small polygons of less than 9 pixels that are visually located on the edges of fields). It is clearly understandable that in these areas the radiometry of the pixels is produced by a certain mixture of two or more categories, and thus these pixels are often classified with a higher degree of uncertainty. The rank reduction produced by byte-scaling can make this decision even harder, and thus differences arise in these areas. These differences between integer and byte-scaled classifications are not reflected in the overall accuracy computed using test areas because they are produced in the border areas where neither training nor test areas are selected.

Among compression standards, J2Km is the least affected by compression, followed by J2K and JPG. The last compression standard obtains very bad results at high compression ratios, especially when MaxLike and MinDist classifiers are used. HybCls is the classifier that is most affected by the byte-scaling (especially in scenarios with only 1 date). The three classification methods are affected similarly by compression (the same decrease in the overall accuracy) except for high JPG compression which can only really be used when HybCls is used.

Finally, it can also be clearly seen that the more difficult the classification is (the lowest overall accuracy computed using independent test areas, see previous section), the more it is affected by compression. All the graphics clearly show that, when 1 single date is used, less compression can be applied (no matter which compression scenario or classification method is used).

4. Discussion

Table 2 shows the maximum CR recommended for each scenario and the effects of this CR on the classifications. To choose these CRs, the maximum variation accepted for the overall accuracy was ±0.50 percentage points. This is a conventional criterion which is useful for obtaining clearer conclusions. These scenarios are shown on a grey background in table 1.

4.1. J2Km scenario

When a multitemporal approach is used, the maximum CR recommended is from 20:1 to 200:1 depending on the fragmentation of the zone and on the classification method used. The results of the compression on the classification have equal effects in almost all situations (indicated with "=" in table 2).

If only one date is used, the maximum CR recommended depends on the classification method and the fragmentation of the area. When HybCls is used more compression can be applied (up to 100:1 or 20:1 depending on the fragmentation of the zone). If MaxLike is used, medium compression can be used (10:1 or 20:1), and if MinDist is used, a CR of 20:1 can be used for less fragmented areas; however, compression is not advisable if the area is more fragmented. The impact of this compression on classification (when advised) is positive (++ or +++ in table 2) in most cases.

4.2. J2K scenario

When five Landsat images are used, the maximum CR recommended is from 10:1 to 100:1 depending on the fragmentation of the zone and on the classifier. For fragmented zones with the HybCls classifier, less compression should be applied. The results of this compression on the classification have equal or low negative effects in almost all situations (indicated with "=" or "-" in table 2).

If a single-date approach is used, the maximum CR recommended is not very high. Only when HybCls is used can a medium CR of 10:1 to 5:1 be used (for less and more fragmented areas respectively). If MaxLike or MinDist are used on less fragmented areas, a slight compression of 1.66:1 can be employed. If MinDist is used on more fragmented areas, lossy compression is not recommended. The impact of this compression on the classification obtained is equal or quite negative (= or --- in table 2). Thus, when classifying from a single image, we advise using J2K compression and the MaxLike or MinDist classifiers with lossless compression (obtaining CRs of 1.69:1 and 1.6:1 for the Segrià and Pla d'Urgell areas respectively).

4.3. JPG scenario

If a multitemporal approach is used, the maximum recommended CR is 10:1 or 20:1. This low (+) or medium (++) compression has different effects on the classification depending on the classification method employed. In almost all situations, compression has a low positive effect on classification (+), except when HybCls is used, as it obtains more fluctuating results. This slightly higher variation may be

due to the less-parametric approach of HybCls, which is more affected by changes in values due to the compression.

On the other hand, when only one image is used, JPG compression is only advised when HybCls is used, especially for less fragmented areas. As the optimum CR is not very high (CR 10:1 for the Segrià zone), it is not recommended to use the JPG compression standard when only one image is used for classification.

Table 1. Optimum CR and effects on overall accuracy and classified area

5 Landsat images

		Hybrid Classifier		Maximum Likelihood		Minimum Distance	
		Optimum CR [a]	Effects [b]	Optimum CR [a]	Effects [b]	Optimum CR [a]	Effects [b]
J2km	Less fragmented areas (*e.g.*, Segrià area)	+++ CR 200:1	= Accuracy: -0.1 (-) Area: +1.23 (+)	++ CR 20:1	= Accuracy: -0.1 (-) Area: +0.95 (+)	+++ CR 100:1 to 200:1	+ to = Accuracy: 0.0 (=) to -0.1 (-) Area: +2.73 to +4.29 (+)
	More fragmented areas (*e.g.*, Pla d'Urgell area)	++ CR 20:1	– Accuracy: -0.2 (--) Area: +0.74 (=)	++ CR 20:1	- Accuracy: -0.2 (–) Area: +4.53 (+)	+++ CR 100:1 to 200:1	+ to = Accuracy: 0.0 (=) to -0.2 (--) Area: +4.53 (+) to +7.06 (++)
J2K	Less fragmented areas (*e.g.*, Segrià area)	+++ CR 100:1	- Accuracy: -0.2 (–) Area: +4.34 (+)	++ CR 20:1	- Area: +1.19 (+) Accuracy: -0.2 (–)	++ CR 20:1	-- Accuracy: -0.2 (--) Area: +0.37 (=)
	More fragmented areas (*e.g.*, Pla d'Urgell area)	+ CR 10:1	Accuracy: 0.0 (=) Area: -1.57 (-)	++ CR 20:1	= Accuracy: -0.2 (–) Area: +5.42 (++)	++ CR 20:1	+ Accuracy: +0.1 (+) Area: -0.27 (=)
JPG	Less fragmented areas (*e.g.*, Segrià area)	+ to ++ CR 10:1 to 20:1	--- Accuracy:-0.3 to -0.4 (---) Area: +0.04 to +0.57 (=)	++ CR 20:1	+ Accuracy: -0.1 (-) Area: +5.84 (++)	++ CR 20:1	-- Accuracy: -0.3 (--) Area: +1.44 (+)
	More fragmented areas (*e.g.*, Pla d'Urgell area)	+ CR 10:1	- Accuracy: 0.0 (=) Area: -1.82 (-)	++ CR 20:1	+ Accuracy: -0.2 (–) Area: +12.49 (+++)	++ CR 20:1	= Accuracy: 0.0 (=) Area: +0.61 (=)

1 Landsat images

		Hybrid Classifier		Maximum Likelihood		Minimum Distance	
		Optimum CR [a]	Effects [b]	Optimum CR [a]	Effects [b]	Optimum CR [a]	Effects [b]
J2km	Less fragmented areas (*e.g.*, Segrià area)	++ to +++ CR 20:1 to 100:1	– Accuracy:-0.3 to -0.4 (---) Area: +0.34 (=) to +0.93 (+)	+ CR 10:1	+++ Accuracy: +0.6 (+++) Area: -0.47 (=)	++ CR 20:1	+++ Accuracy: 0.7 (+++) Area: +0.03 (=)
	More fragmented areas (*e.g.*, Pla d'Urgell area)	+ to ++ CR 10:1 to 20:1	+++ Accuracy: 0.8 to 0.3 (+++) Area: +0.21 (=) to + 1.21 (+)	++ CR 20:1	+ ++ Accuracy: +1.2 (+++) Area: -0,.76 (=)	- CR 1:1	-
J2K	Less fragmented areas (*e.g.*, Segrià area)	+ CR 10:1	--- Accuracy: -0.3 (---) Area: +0.22 (=)	- CR 1.66:1	--- Accuracy: -0.3 (---) Area: +-0.24 (=)	- CR 1.66:1	-- Accuracy: -0.5 (---) Area: -0-21 to -0.28 (=)
	More fragmented areas (*e.g.*, Pla d'Urgell area)	= to + CR 5:1 to 10:1	= Accuracy: 0.0 (=) Area: ±0.30 (=)	- CR 1.66:1	-- Accuracy: -0.4 (---) Area: +-0.26 (=)	- CR 1.:1	-
JPG	Less fragmented areas (*e.g.*, Segrià area)	+ CR 10:1	+++ Accuracy: +0.5 (++) Area: +1.01 (+)	- CR 1:1	-	- CR 1.:1	-
	More fragmented areas (*e.g.*, Pla d'Urgell area)	- CR 1.66	-- Accuracy: -0.7 (--) Area: +0.76 (=)	- CR 1.:1	-	- CR 1.:1	-

[a] *Symbols regarding compression* . -: no compression (CR 1.0 or 1.66); =: very low (CR 2 to 3.33); +: low (CR 5 or 10:1); ++: medium (CR 20:1) or +++: high (CR 100:1 or 200:1). [b] *Symbols regarding effects on classification.* = : similar (equal accuracy, area

4.4. General comments

In both scenarios, fragmented images (Pla d'Urgell zone) accept less compression than other images (Segrià zone) and the effects of this compression are more damaging. Furthermore, the more difficult the original classification (*e.g.* using only one date) the more the impact of compression (five-date classification is less affected than the one-date scenario). When a multitemporal approach is used, the classifications obtained reach very high overall accuracies, and since high CRs are applied the effects of these compressions are not conspicuous. However, if a single-image approach is used, compression is more damaging.

J2Km and J2K affect the classification less than JPG, especially with regard to the smaller decrease in overall accuracy when images are compressed. For example, at a CR of 100:1 for the Segrià zone (multitemporal scenario), the overall accuracy for JPG (using HybCls) is reduced by 1.6 percentage points and for J2K by only 0.2 percentage points (0.3 percentage points for J2Km). For the Pla d'Urgell zone at the same CR, the overall accuracy for the JPG scenario is reduced by 2.6 percentage points, by 1.0

percentage points for J2K and by 0.1 percentage points for J2Km. This smaller reduction in the overall accuracy is related to a similar or even greater increase in the classified area.

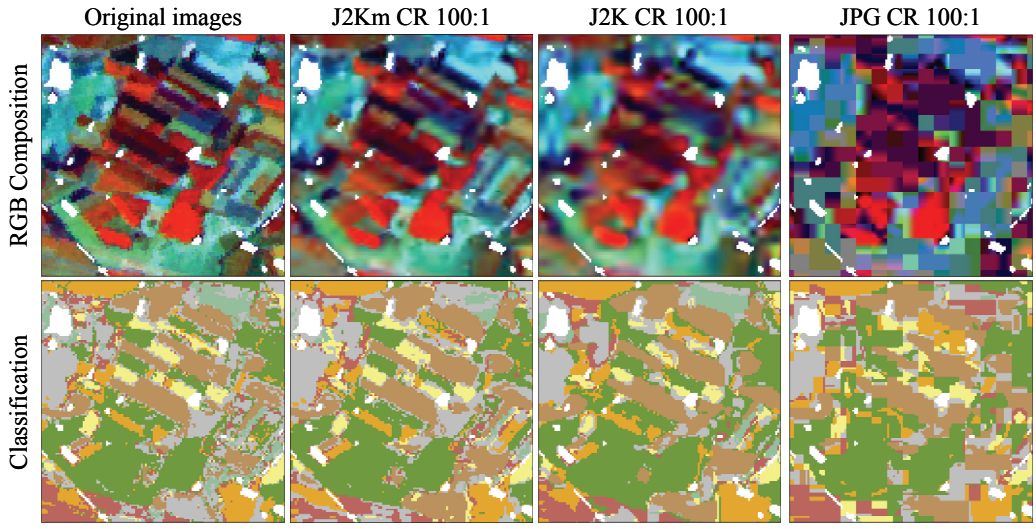

Figure 3: RGB composites (using near-infrared (4), medium-infrared (5) and red (3) bands of a 17-06-2004 image) and the resulting multitemporal classifications of the original, J2K at CR 100:1, J2K at CR 100:1 and JPG at CR 100:1. White indicates non-crop areas, grey indicates unclassified areas and other colours indicate different crops.

Spatial regularization that is introduced by using compression methods may be beneficial for the classification methods used in the sense that these classification methods exploit the spectral information of pixels; thus, the small differences that usually produce a "salt and pepper" effect are smoothed by compression. This effect is common in digital classifications, and is due to spectral differences among neighbour pixels that are classified by the algorithm as different classes although they occupy only one or a few pixels (see this effect on classification in the original images in figure 3). Final users generally do not want to keep these isolated pixels; thus, users may prefer the classification obtained after a J2Km or J2K compression considering the reduction in the "salt and pepper" effect. However, JPEG used to compress images at reduced compression ratios (high compression level) shows the visible effect of blocks (resulting from the compression algorithm) both in the compressed images and the classifications (see figure 3). These tendencies may not be applicable to classification methods that use contextual information.

As Choi et al. (2008) also found, in the neighbour areas between very contrasted spectral classes, compression produces mixture effects that lead to misclassifications. These border effects will have a particular impact on future studies of land use changes because study results could be compromised by this erroneous classification in the polygon edges.

The usual evaluation methods may underestimate the classification errors due to the ways in which the test areas are obtained. One option might be to evaluate all classifications against another reference map ("spatially full") that could be considered as a ground truth; however, such a reference is not usually available. If the classification obtained using original images is used as the ground-truth (as we have also evaluated), it obscures the beneficial effects of using compressed images (for example, due to the cited visual homogenization).

5. Conclusions

We conclude that JPEG 2000 compression eliminates the "salt and pepper" effect, and the result is always visually better when the images are compressed (without going over certain compression limits). This is an interesting finding because previous papers (Yu *et al.* 2006, Xie *et al.* 2007) seemed to find these "salt and pepper" effects unavoidable when high resolution images are used because of the heterogeneity of agricultural fields.

When compressing in excess, unwanted visual effects are initially produced which do not have quantitatively serious effects on the classification results. If this first limit is also exceeded, then the influence of compression clearly reduces the overall accuracy of the classifications. This inflection point is located at different CRs depending on image fragmentation (more fragmented images accept less compression), the compression procedure (JPEG 2000 makes it possible to use higher compression ratios with very similar cartographic results) and the number of images used for the classification (the multitemporal approach is more robust against compression effects, and a single-date classification may be highly affected by medium compressions).

When images are used to obtain crop maps through multitemporal classification, and when the JPEG compression standard is used, it is advisable to compress images up to a compression ratio of 10:1 or 20:1, depending on image fragmentation. If JPEG 2000 is used, the maximum compression ratios for more fragmented images are the same as when JPEG is used. For less fragmented images the maximum compression ratios are similar or even higher (up to 100:1) than those recommended for JPEG, especially if 3D JPEG 2000 compression is used. JPEG 2000 compression leads to fewer harmful effects on the classification than JPEG compression. When a single-date classification approach is used, however, only a 3D JPEG 2000 compression is advisable, especially when HybCls and MaxLike are used.

In terms of the classification method used, HybCls and MaxLike obtain better results than MinDist. However, MinDist is less affected by compression and MaxLike is the most affected by compression, especially at higher CRs, due to its class characterization that uses deviation measures. If a single-date classification scenario is used, both MaxLike and MinDist are highly affected by compression; thus, HybCls should be the selected option.

The JPEG 2000 compression standard has been shown to be better than the JPEG standard when applied to images for agricultural classification, especially if 3D images are used. Consequently, standard servers offering geoservices (WMS, WMTS, WCS, etc.) should consider including JPEG 2000 among their format capabilities more frequently.

Acknowledgements

The authors wish to thank the Catalan Water Agency (ACA) and the Department of Environment and Housing (DMAH) of the Autonomous Government of Catalonia (Generalitat de Catalunya) for their investment policy regarding the availability of Remote Sensing data, which has made it possible to conduct this study under optimal conditions. The authors would also like to thank their colleagues in the Geography Department, the Centre for Ecological Research and Forestry Applications (CREAF), and the Department of Information and Communications Engineering as well as all those at the Autonomous University of Barcelona (UAB) who collaborated in the treatment of the images. We would also like to express our gratitude to the Spanish National Institute for Aerospace Technology (INTA) for its efficient image subscription service. This work was supported in part by the Ministry of Education and Science and the FEDER funds through the research project TIN2009-14426-C02-02, as well as by the Catalan Government grant SGR2009-1511.

References

Aulí-Llinàs, F; J.R. Paton, J. Bartrina-Rapesta, J.L. Monteagudo-Pereira, J. Serra-Sagristà, 2005, J2K: introducing a novel JPEG 2000 coder, In *Proceedings SPIE*, **5960**, pp. 1763-1773.

Carvajal, G.; B. Penna, E. Magli, 2008, Unified Lossy and Near-Lossless Hyperspectral Image Compression Based on JPEG 2000, *IEEE Geoscience Remote Sensing Letters*, **5**, pp. 593-597.

Chirici, G.; P. Corona, M. Marchetti, D. Travaglini, 2003, Testing Ikonos and Landsat 7 ETM+ potential for stand-level forest type mapping by soft supervised approaches. In *Advances in Forest Inventory for Sustainable Forest Management and Biodiversity Monitoring*. P. Corona, M. Köhl, M. Marchetti, (Ed.) pp. 71-86 (The Netherlands: Kluwer Forestry Series).

Choi, E.; S. Lee, C. Lee, 2008, Effects of Compression on the Classification of Hyperspectral Images. In *Mathematics and Computers in Science and Engineering*, N.E. Mastorakis, V. Mladenov, Z. Bojkovic, D.

Simian, S. Kartalopoulos, A. Varonides, C. Udriste, E. Kindler, S. Narayanan, J.L. Mauri, H. Parsiani, K.L. Man (Ed.), pp. 541-546 (Greece: Heraklion).

Delaunay, X.; M. Chabert, V. Charvillat, G. Morin, 2010, "Satellite image compression by post-transforms in the wavelet domain", *Signal Processing*, **90**, pp. 599-610.

Delaunay, X.; M. Chabert, V. Charvillat, G. Morin, 2010, "Satellite image compression by post-transforms in the wavelet domain", Signal Processing, 90, pp. 599-610.

Du, Q.; J.E. Fowler, 2007, Hyperspectral Image Compression Using JPEG 2000 and Principal Component Analysis, *IEEE Geoscience Remote Sensing Letters*, **4**, pp. 201-205.

Foody, G.M., 2002, Status of land cover classification accuracy assessment, *Remote Sensing of Environment*, **80**, pp. 185-201.

Garcia-Vilchez, F; J. Serra-Sagrista, 2009, "Extending the CCSDS Recommendation for Image Data Compression for Remote Sensing Scenarios", *IEEE Transactions on Geoscience and Remote Sensing*, **47**, pp. 3431-3445.

Independent JPEG Group, 2008, *Free library for JPEG image compression*, Available online at: http://www.ijg.org/ (accessed 20 August 2010).

ITTVIS, 2006, *ENVI software version 4.3*, Information available online at: http://www.ittvis.com/ProductServices/ENVI.aspx (accessed 20 August 2010).

Lo, T.H.C.; Scarpace, F.L.; Lillesand, T.M., 1986, "Use of multitemporal spectral profiles in agricultural land-cover classification", *Photogrammetric Engineering & Remote Sensing*, **52**, pp. 535-544.

Maguire, D.J.; P.A. Longley, 2005, The Emergence of Geoportals and Their Role in Spatial Data Infrastructures, *Computers, Environment and Urban Systems*, **29**, pp. 3-14.

Masó J, Pomakis K, Julià N., 2010, *OpenGIS® Web Map Tile Service Implementation Standard, v. 1.0.0* Open Geospatial Consortium Inc. Document reference number 07-057r7, Available online at: http://www.opengeospatial.org/standards/wmts (accessed 20 August 2010).

Moré, G.; X. Pons, 2007, "Influencia del número de imágenes en la calidad de la cartografía detallada de vegetación forestal", *Revista de Teledetección*, **28**, pp. 61-68.

Penna, B; T. Tillo, E. Magli, G. Olmo, 2006, Progressive 3-D coding of hyperspectral images based on JPEG 2000", *IEEE Geoscience Remote Sensing Letters*, **3**, pp. 125-129.

Penna, B; T. Tillo, E. Magli, G. Olmo, 2007, Transform coding techniques for lossy hyperspectral data compression", *IEEE Transactions Geoscience Remote Sensing*, **45**, pp. 1408-1421.

Pons, X., 2008, *MiraMon. Geographical Information System and Remote Sensing Software. Version 6*, Available online at: http://www.creaf.uab.es/miramon/ (accessed 20 August 2010).

Qian, SE; A. Hollinger, M. Bergeron, I. Cunningham, C. Nadeau, G. Jolly, H. Zwick, 2005, A multidisciplinary user acceptability study of hyperspectral data compressed using an on-board near lossless vector quantization algorithm, *International Journal of Remote Sensing*, **26**, pp. 2163-2195.

Richards, J.A., J. Xiuping, 2006, Remote Sensing Digital Image Analysis. An Introduction, p. 197 (Berlin-Heidelberg: Springer-Verlag).

Serra, P.; X. Pons, D. Saurí, 2003, Post-classification change detection with data from different sensors. Some accuracy considerations, *International Journal of Remote Sensing*, **24**, pp. 3311-3340.

Serra, P.; G. Moré, X. Pons, 2009, Thematic Accuracy Consequences in Cadastre Landcover Enrichment from a Pixel and from a Polygon Perspective, *Photogrammetric Engineering & Remote Sensing*, **75**, pp.1441-1449.

Shriever, J. R.; Congalton, R. G., 1993, "Mapping forest cover types in New Hampshire using multi-temporal Landsat Thematic Mapper data". *ASPRS/ACSM Ann. Conv. Exp*., New Orleáns. pp. 333-342.

Taubman, D., 2008, *Kakadu software*, Available online at: http://www.kakadusoftware.com/ (accessed 20 August 2010).

Wolter, P. T.; Mladenoff, D. J.; Host, G. E. Y Crow, T. R., 1995, "Improved forest classification in the northern Lake States using multitemporal Landsat imagery", *Photogrammetric Engineering & Remote Sensing*, **61**, pp. 1129-1143.

Xie, H; Y.Q. Tian, J.A. Granillo, G.R. Keller, 2007, "Suitable remote sensing method and data for mapping and measuring active crop fields", *International Journal of Remote Sensing*, **28**, pp. 395-411.

Yu, Q.; P. Gong, N. Clinton, M. Kelly, D. Schirokauer, 2006, "Object-based detailed vegetation classification with airborne high spatial resolution remote sensing imagery", *Photogrammetric Engineering & Remote Sensing*, **72**, pp. 799–811.

Zabala, A.; X. Pons, 2010, "Effects of lossy compression on remote sensing image classification of forest areas", *International Journal of Applied Earth Observation and Geoinformation*, doi:10.1016/j.jag.2010.06.005, *in press*.

ANNEX 2: SEGMENTATION AND THEMATIC CLASSIFICATION OF COLOR ORTHOPHOTOS OVER NON-COMPRESSED AND JPEG 2000 COMPRESSED IMAGES[3]

[3] Segons la normativa de la UAB a què s'acull aquesta Tesi per compendi de publicacions, a part dels articles acceptats per a format la part fonamental de la mateixa (i inclosos en els capítols 2 a 5 d'aquesta Tesi), es pot adjuntar altres articles com a annexos (o part no fonamental). Segons la mateixa normativa, els treballs fets en aquestes publicacions poden ser comentats a la discussió de resultats. Aquest és el segon article dels tres presentats com a annexos i que pretenen completar l'aportació de la Tesi en el camp dels efectes de la compressió amb pèrdua d'imatges de teledetecció aplicades a l'obtenció de cartografia.

Segmentation and thematic classification of color orthophotos over non-compressed and JPEG 2000 compressed images

A. Zabala [a,*], C. Cea [a], X. Pons [a, b]

a Dept. of Geography. Autonomous University of Barcelona, 08193 Cerdanyola del Vallès, Spain

b Centre for Ecological Research and Forestry Applications (CREAF), 08193 Cerdanyola del Vallès, Spain

Abstract: Lossy compression is now increasingly used due to the enormous amount of images gathered by airborne and satellite sensors. Nevertheless, the implications of these compression procedures have been scarcely assessed. Segmentation before digital image classification is also a technique increasingly used in GEOBIA (GEOgraphic Object-Based Image Analysis). This paper presents an object-oriented application for image analysis using color orthophotos. We use different compression levels in order to study the effects of the data loss on the segmentation-based classification results. A set of 4 color orthophotos with 1 m spatial resolution and each covering an area of about 1200*1200 m^2 (144 ha) was chosen for the experiment. Those scenes were compressed at 8 compression ratios (between 5:1 and 1000:1) using the JPEG 2000 standard.

There were 7 thematic categories: dense vegetation, herbaceous, bare lands, road and asphalt areas, building areas, swimming pools and rivers (if necessary). The best category classification was obtained using a hierarchical classification algorithm over the second segmentation level. The same segmentation and classification methods were applied in order to establish a semi-automatic technique for all 36 images.

To estimate the overall accuracy, a confusion matrix was calculated using a photointerpreted ground-truth map (fully covering 25% of each ortophoto). The mean accuracy over non-compressed images was 66%. It is interesting to obtain this medium overall accuracy to be able to properly assess the compression effects (if the initial overall accuracy is very high, the possible positive effects of compression would not be noticeable). The first and second compression levels (up to 10:1) obtain results similar to the reference ones. Differences in the third to fifth levels (20:1 to 100:1) were moderate to large (accuracies 61%-58%), while more compressed images obtained the worst results (accuracies lower than 55%). As a comparison, the usual independent test areas (covering a small percentage of the classified area) were also used. The results show that this classification evaluation approach must be used with caution because it may underestimate the classification errors.

KEY WORDS: Segmentation, Mapping, Lossy compression, Orthophotos, Wavelets, JPEG 2000.

1. Introduction and objectives

The total amount of data generated by remote sensing (RS) platforms is increasing every day. Even though the commercial providers have a large structure to store all this information, users do not often have access to this structure, and thus data management problems arise. Moreover, some softwares have significant difficulties in working with large images. The new paradigm of Spatial Data Infrastructures (SDIs) promotes the establishment of web data services, usually in terms of Open Geospatial Consortium standards like the Web Map Service (WMS), the Web Coverage Service (WCS) (Maguire and Longley, 2005) or the recent Web Map Tile Service (WMTS, Masó et al., 2010). However, it is necessary to use compression and interactive transmission strategies in these web services in order to transfer images (which may be very large in the case of WCS) repetitively to environments with restricted bandwidth. In disaster or emergency management environments, and especially in a crisis situation, image compression techniques are crucial for sending this very important data efficiently and quickly to the reaction teams, who normally use laptop computers and mobile devices. In this context, high-resolution satellites like GeoEye and QuickBird, and medium resolution satellites, such as the two generations of the Disaster Monitoring Constellation (DMC) (DMC International Imaging, 2005-7), are able to capture images anywhere in the world and quickly provide imagery for disaster emergencies. Using semi-automatic or automatic classification methods of images could allow users to assess the damage and act quickly.

In recent years, a set of lossy compression techniques based on different algorithms has appeared (discrete cosine transform, DCT, discrete wavelet transform, DWT,…). JPEG was one of the first formats based on lossy compression to appear. Later wavelet based specifications, such as SID, ECW and JPEG 2000,

appeared and became particularly popular within the RS community (Magli and Taubman, 2003; Zabala et al., 2006; Zabala and Pons, 2010). JPEG 2000 became an ISO standard in 2000 and was revised in 2004 (ISO/IEC 2004). In this paper we study this widely used compression standard and aim to evaluate the implication of image lossy compression on object based classifications, as there are few quantitative analyses of this approach for compressing data. It is important to bear in mind that we are always dealing with lossy compression algorithms, which sacrifice part of the data in order to achieve a higher compression ratio but sometimes with no appreciable loss of image quality (Kiema, 2000; Zabala et al., 2007).

Image classification has traditionally employed pixel-based methods based on statistical measurements of individual pixel values to classify each pixel with supervised or unsupervised classifiers (Xiaoxia et al., 2005; West et al., 2009). Nevertheless, with the improvement in spatial resolution of the image (such as aerial or high resolution satellite sensors), the number of articles on GEOBIA (GEOgraphic Object-Based Image Analysis) techniques has increased (Blaschke, 2010). In fact, a sign of the growing importance of this area is that, since 2006, there have been biennial international conferences covering this topic. In this case, image classification needs groups of pixels selected as objects, and therefore the segmentation process is needed to obtain these objects, and is the first step in the classification process (Conchedda et al., 2008; Ke et al., 2010). There are many different approaches to segmentation and classification. In this study we use Definiens algorithms (Baatz et al., 2005).

The main aim of this paper is to assess the impact of compression on the segmentation-based classification results. Therefore, the conclusions of this study show how compression affects the segmentation and classification processes. Moreover, we will also discuss the feasibility of this approach (segmentation over compressed images) in an emergency management environment, and the different conclusions obtained when ground-truth layers or independent test sites in a reduced area percentage are used. See figure 1 for a general overview of the experimental design.

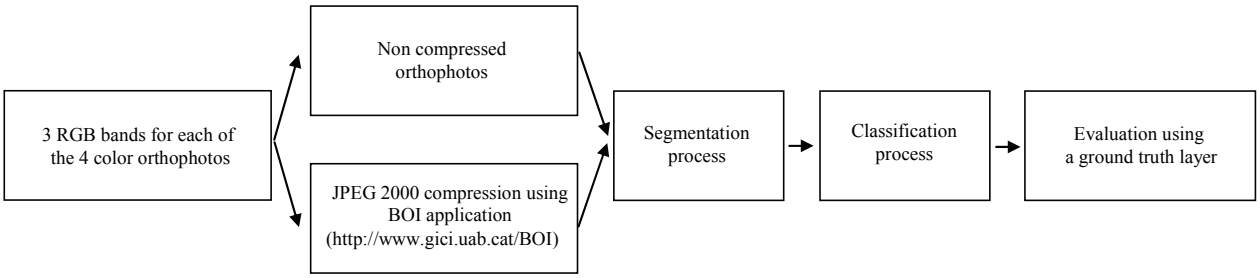

Figure 1: Overview of the experimental design.

2. Methods

2.2. Study area and material

A set of 4 aerial RGB orthophotos was selected: 3 orthophotos over Catalonia (NE Spain) and the other one over Navarre (N Spain) (see figure 2). More specifically, in Catalonia we selected areas in Sant Cugat del Vallès, Vallvidrera and Olot, and in Navarre, we selected an area in Zizur Mayor. These 4 orthophotos (see figure 3) were selected because of their similar urban landscape, characterized by low density urban areas with a significant number of swimming pools, gardens, forested areas and field crops. However, there are some differences among the images: in two of them (Vallvidrera and Sant Cugat) the predominant urban structure is detached houses, while in the other two more semi-detached and multi-family houses are present.

A working spatial resolution of 1 meter was selected. In some cases, the original spatial resolution was 0.5 m, and in these cases the pixel size was changed to 1 m using a mean filter. A sub-scene of approximately 1200*1200 m^2 was selected over each area to speed up the process.

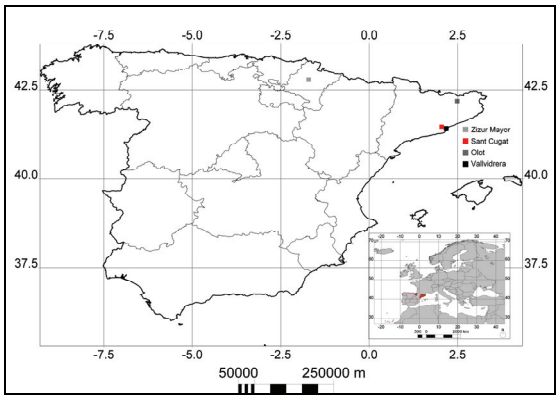

Figure 2: Location of the 4 studied areas in Spain.

Figure 3: Ortophotos of the 4 studied areas. From left to right and top to bottom: Vallvidrera, Olot, Sant Cugat and Zizur Mayor.

2.3. Image compression

The compression and decompression application used was BOÍ, an implementation of JPEG 2000 standard Part 1, developed by the GICI team of the Autonomous University of Barcelona (Aulí-Llinàs et al., 2005).

The 3 RGB bands of the color orthophoto of each area were compressed to a single JPEG 2000 compressed file. This joint compression is beneficial as it preserves as much detail as possible from the three bands together, and allows more information of the color components to be kept if necessary. A lossy compression was computed over the original images, at eight compression ratios (CR), 5:1, 10:1, 20:1, 40:1, 100:1, 200:1, 400:1 and 1000:1, in which the first number on the ratio defines the size of the original image related to a compressed file size equal to 1.

Compressed images are then decompressed to feed the segmentation and classification process. A total of 36 images was used in this study (1 non-compressed and 8 compressed for each of the 4 study areas).

2.4. Image segmentation

Definiens professional 5 has 4 segmentation algorithms. A large part of the literature suggests using a multiresolution algorithm (for example, Baatz et al., 2007) as the first step for obtaining highly homogeneous image objects in the first level of segmentation for aerial orthophotos and satellite images.

This algorithm allows several parameters to be defined. The first one is the weight of the different layers; the same weight was chosen for each of the RGB components. The second one is the scale parameter, which defines the desired object size and determines the maximum allowable heterogeneity of the objects, which also depend on the size of the objects found in the image (a value of 10 was selected for the scale parameter). Finally, the parameters of shape/color and compactness/smoothness, which define the total relative homogeneity for the resulting image objects (Baatz et al., 2005), require more attention because of the difficulty in applying an appropriate value.

Different tests were performed using different shape and color, and compactness and smoothness parameter values, which were chosen empirically based on visual inspection. The higher the value for the shape or color parameter, the more optimized for spectral or spatial homogeneity the resulting objects will be. The default values for shape and color offered by the software were used in the first try (10% for shape and 90% for color). However, giving most of the weight to the digital values (or digital numbers, DN) is not the best option when the process is using only 3 visible bands. In this scenario, the shape of objects is also significant for the segmentation because digital values are not enough to define the categories. In a second try, a weight of 50% for each variable was selected, so each variable has an equal influence on the segmentation outcome. In the case of the compactness and smoothness, the default values were 50% in both cases; however, it was found that the higher values of compactness resulted in better discrimination of the edges of different objects. With the final selected values (90% for compactness and 10% for smoothness), little objects such as private pools were identified as individual objects, as well as isolated trees and some building roofs.

After an initial segmentation level had been established, a second segmentation was carried out using the Difference Spectral Segmentation algorithm to collect some objects belonging to the same class. This algorithm creates a new level from an existing level because the objective is to join neighboring objects according to the mean DN of the different layers (Definiens, 2005). The most important parameter is the total spectral difference among the objects generated in the previous segmentation. If the spectral difference between neighbors is less than the selected value, neighbor objects join together. Different values were tested. With a spectral value of 5 no important changes occurred between the two segmentation levels. With a value of 15, objects of different classes were confused, for example bare soil and asphalt. The optimal value was finally set at 10.

Different segmentation levels are important in order to extract the boundaries of the objects at the corresponding scales.

The same parameters were always applied to all original and compressed orthophotos.

2.5. Image classification

The segmented image was classified using a user-defined fuzzy classification. The first step was to assign classes, the semantic meaning of image objects in the Definiens network. Each class was selected based on its visual appearance in the true color image. To create the classification scheme, six dominant object classes (land-cover types) were identified in each orthophoto, including dense vegetation, herbaceous, bare lands, road and asphalt areas, building areas, swimming pools and rivers (see Table 1).

	Orthophotos			
Class	**Olot**	**Sant Cugat**	**Vallvidrera**	**Zizur Mayor**
Dense vegetation	Yes	Yes	Yes	Yes
Herbaceous	Yes	Yes	Yes	Yes
Bare lands	No	Yes	Yes	Yes
Road and asphalt areas	Yes	Yes	Yes	Yes
Building areas	Yes	Yes	Yes	Yes
Swimming pools	Yes	Yes	Yes	Yes
Rivers	Yes	No	No	No

Table 1: Classes defined for each orthophoto.

Some classes were divided into subclasses due to the spectral and textural differences among them. This division helps the classifier and improves the classification results because each subclass has its own features. Thus, the bare lands class was then divided into two sub-classes as fallow fields and abandoned

agriculture lands. Buildings were separated into different sub-classes depending on the roof color, light and dark. Herbaceous was divided into garden and agriculture.

The different methods offered by the software were used to perform the classification. In the first attempt each class and subclass was classified separately using simple conditions or using feature description classes. In the second attempt the classes and subclasses in the class hierarchy were classified simultaneously based on their feature description. Finally, the last attempt was an automatic classification based on the nearest neighbor algorithm, defining training areas.

The best results were obtained with the classification based on class hierarchy and fuzzy functions defined for selected features, because it gave more control over the classification process and could be more easily adapted to other orthophotos (Kressler, 2005). Using only simple conditions resulted in confusion between classes. Using the Nearest Neighbor algorithm (NN) was not considered appropriate because the training areas in each image must be defined, and therefore the classification cannot be automated.

Table 2 shows the features used for each class. The values of these features were adapted, changing this value or activating or disabling expressions in the class description for each orthophoto and each compression level.

Class	Features
Dense vegetation	Ratio green, Brightness, Max. Difference
Herbaceous	Brightness, Standard Deviation Green
Bare lands	Brightness, Area, Mean red, Ratio red
Building areas	Brightness, Ratio RGB, Area
Road and asphalt areas	Max. Difference, length, brightness
Swimming pools	Area, Mean blue, Distance to edifications
Rivers	Topographic map mask

Table 2: Features used for classification.

It is important to note that working with only 3 bands from the visible spectrum makes it difficult to obtain an optimal classification due to the limited input information. However, this kind of orthophoto is widely used because most of the institutional map servers offer free RGB orthophoto download or WMS geoservices. In addition, it must be taken into account that every institution distributes these orthophotos in different compression formats and compression ratios, and unfortunately, this information is often not specified in the image metadata. Although in recent years the amount of infrared orthophotos has increased, they are not yet generally freely available.

2.6. Validation/accuracy assessment

The accuracy assessment of all classifications was computed by generating confusion matrices (Foody, 2002) in relation to ground-truth information using MiraMon Software (Pons, 2008). The accuracy reports overall accuracy, describing the percentage of the well classified pixels and the total amount of classified pixels, as well as the overall kappa index for each classification (Campbell, 2002). The user's and producer's accuracy for each class were also obtained.

It is very important for studies that assess compression effects (as well as for most land cover change studies) to be able to evaluate classifications with the highest possible reliability. The best option is to analyze the obtained maps with an "absolute" ground-truth layer. This approach is not widely used (in fact, if there is a large and absolute ground truth layer, why would we need the result obtained by the classification process?) but it allows us to evaluate the appropriateness of the proposed methodology to be confident in applying it to other areas with similar characteristics. Therefore, this paper evaluates the overall accuracy of the obtained classifications regarding a ground-truth layer obtained by means of the photointerpretation of a quarter scene (north-east) of each study area. The criterion for selecting a quarter of each scene was the large time investment of a highly accurate photointerpretation. This photointerpretation was carried out by an experienced (8 years), independent photointerpreter, mainly using the vectors obtained during the segmentation process with the aim of reducing border effect errors. However, and of course if the photointerpreter considered that segmentation was not correct somewhere, the polygons were corrected.

Moreover, a set of independent test areas was selected by an external operator to assess the classification accuracy. For each of the four study areas a set of about 100 polygons was selected, covering an area of between 5 m^2 and 600 m^2. The use of test areas is a common approach in the evaluation of classifications because it employs independent information not used on the classification, and is not very time consuming. By comparing the two evaluation approaches we can determine some recommendations on how classifications coming from segmentation processes should be evaluated.

3. Results

The results are presented in three main sections. The first one discusses the effects of compression on the images themselves in order to provide a numerical overview. The second is a detailed description of the generated segmentation for all compression ratios. The last section presents the classification results for each orthophoto and compression ratio.

3.1. Images

The effect of compression on the images themselves can be studied in several ways. The most common approach is to compute the differences between the original and the compressed images. There are several indices to quantify the fidelity of the compression (i.e. the more differences, the less compression fidelity) related to the compression ratio. One of the most common approaches is the definition of the Signal-to-Noise ratio (SNR) energy, which is widely used on papers researching compression modifications (for example, Penna et al., 2007, Carvajal et al., 2008 and Zabala et al., 2010). SNR energy is computed in dB, and the higher SNR energy obtained, the most similarity there is between the encoded and original images.

Figure 4 shows the SNR of each studied area in relation to the compression ratio. The decrease in SNR related to compression is clearly noticeable in the figure. The more fragmented the image is, the more difficult it is to compress it; thus, a lower SNR is obtained at the same compression ratio. This can be seen in the figure, in which the Sant Cugat and Vallvidrera areas obtain the lowest SNR at all compression ratios due to their higher complexity (see figure 3). On the other hand, Olot and Zizur Mayor obtain better SNR due to their less fragmented landscape. The larger impact of compression on more fragmented images can be seen not only in the lower SNR that is obtained, but also in the highest decrease in the SNR of these images in relation to compression. As an example, at a compression ratio of 1000:1, the SNR of the Sant Cugat image (10.53 dB) is only 32% of the SNR of the same image at 5:1 (32.47 dB), and for the Olot area, the SNR at 1000:1 (18.71 dB) is 52.95% of the SNR of that area at 5:1 (35.33 dB).

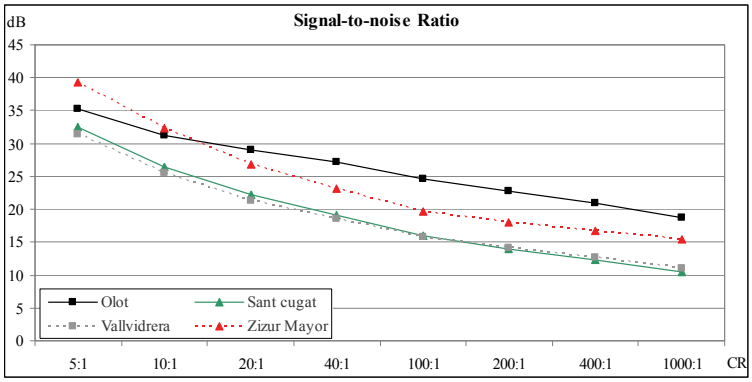

Figure 4: Signal-to-noise ratio (SNR) of each of the studied areas at several compression ratios.

3.2. Segmentation

As described in section 2.3, segmentation was performed at two levels for all original and compressed images. In the first step, the image was divided into numerous objects as a previous step to merging these into larger ones. Figure 5 shows a detail of the Zizur Mayor uncompressed orthophoto with the first (upper image) and second (lower image) segmentation levels overlaid in black. At the first segmentation level, different land covers are well separated, but larger objects such as roofs, public swimming pools, green areas and roads are divided into numerous objects. To reduce the number of objects, a second level of

segmentation was necessary (see the image below in figure 5). Roofs, green areas and swimming pools were well merged into one or two objects, except roads.

Figure 5: Level 1 (left) and level 2 (right) segmentation over a part of the uncompressed Zizur Mayor image.

Figure 6 and figure 7 show the relation in a percentage between the number of objects of each compressed image and the number of objects of the original image (all of them obtained using the same segmentation parameters) for the first and second segmentation levels respectively. The four studied areas show a similar trend. The first three compressed levels have a very similar number of objects with respect to the original images; however, after the fourth compression level, the number of objects decreases with the increase in compression. This occurs because at high compression ratios images are homogenized, i.e., small objects tend to merge into one influenced by close covers.

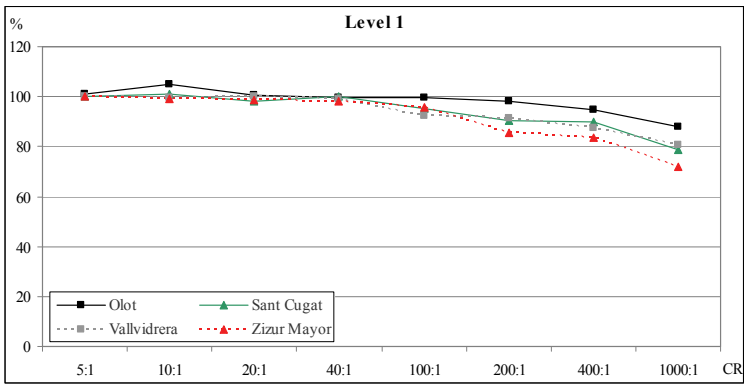

Figure 6: Percentage of the number of objects obtained over compressed images at several compression ratios in relation to the number of objects obtained with the uncompressed images, in Level 1.

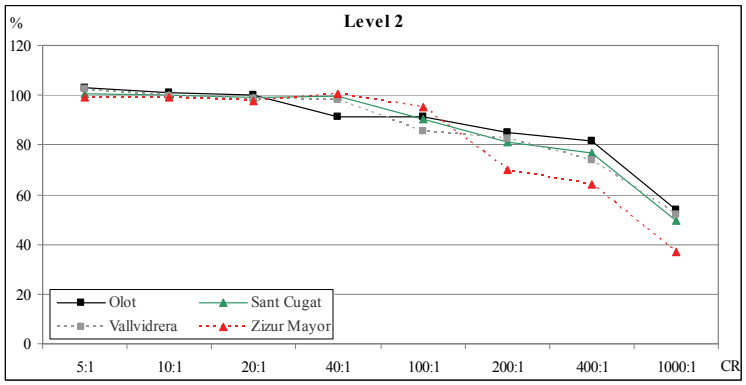

Figure 7: Percentage of number of objects obtained over compressed images at several compression ratios regarding to the number of objects obtained with the uncompressed images, in Level 2.

Generally, segmentation processes have a reduced computing time, between 30 to 60 seconds in our case (Intel(R) Core(TM)2 Duo CPU 3.00GHz 2.99 GHz, RAM 1.98GB). However, choosing the scale parameters as well as setting the weights for the input data sources has to be carried out by the user to

adapt the previous values (defined over non-compressed images of each area) to each classification performed (at each compression ratio). This parameter modification requires a large time investment to obtain the optimal values for each classification.

3.3. Classification

One of the aims of this study was to create a semi-automatic fuzzy user-defined classification process (Baatz et al., 2005) that could be applied to all orthophotos using the same object features in order to discriminate the different categories. After different attempts, as explained in section 2.4, it was proved that it can be achieved; however, it is important to note that it is necessary to adapt the values of these object features to each RGB orthophoto, and that, in some cases, another new object feature is also needed. However, it is important to note that establishing a semi-automatic methodology allows users to reduce the processing time because it is not necessary to define all the process steps.

Unlike segmentation processes, classification processes take several minutes of computing time, as in our case. This is because there are fewer segmentation parameters than classification ones; however, it is important to note that it depends on the selected variables. For instance, using a large number of features or using texture parameters can increase the computing time to several hours. Moreover, it needs to be mentioned that the classification method has several software options (classifying methods), variables to choose and parameters to optimize, and this selection procedure (even if executed only once) is quite time consuming. Therefore, users must select the optimal value for each category and variable, which takes a long time. In our case, the time spent was higher in the first classified image, and less for the other images because it was not necessary to choose the variables, only to change the values.

Due to the large number of classifications carried out, it is not possible to show all of them here. Figure 8 shows a detail of the recovered images (on the left) and the classifications (on the right) obtained for the three compression levels and over the same area.

Figure 8: Detail of the images (on the left) and of the classifications (on the right) of original, 10:1, 20:1 and 200:1 compression ratios over the Zizur Mayor area.

As explained in section 2.5, it is very important to be able to evaluate classifications with the highest possible reliability; thus, an "absolute" ground-truth layer obtained by expert photointerpretation was used. The following subsections explain and discuss the accuracy results (overall accuracy and user's accuracy per category) obtained using a ground-truth layer to evaluate the classifications obtained through a confusion matrix. The last subsection briefly describes the results obtained using the common approach

of evaluating classifications with independent test areas, and shows the differences between the two evaluation approaches.

3.3.1. Overall accuracy

Figure 9 shows the overall accuracy for each classification and each compression ratio obtained by the confusion matrix between the classification results and the ground truth layer. As in the case of segmentation, the four areas follow the same trend: better overall accuracy was obtained in the three first compression levels, but if more compression was applied, this value decreased considerably. This decrease is less prominent for the Olot area, because this orthophoto has a large area of dense vegetation, which is less problematic to classify at any compression level. In the case of the Zizur Mayor area, this decrease is more significant because roofs are an important cover. Roofs are difficult to classify well due to the significant confusion with bright bare soil and asphalt.

As explained in section 2, the Sant Cugat and Vallvidrera areas are fragmented areas characterized by single semi-detached and detached houses with private swimming pools surrounded by dense vegetation. This type of fragmented landscape implies that at high levels of compression, there is a trend to homogenize and blur small objects with the objects situated around them, which reduces the overall accuracies obtained.

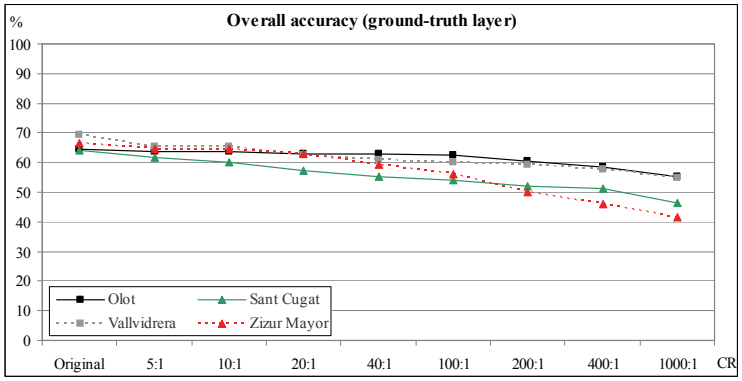

Figure 9: Overall accuracy of each classification area for different compression ratios, obtained in relation to a ground-truth layer (photointerpretation).

3.3.2. User's accuracies

Figure 10 shows the user's accuracy for dense vegetation. Except in one case, high accuracy is maintained for the areas at all compression levels, but a decrease in the category accuracy in relation to compression can be clearly seen. In the Olot area this decrease is less significant, which may be because the vegetation type is more dense and spatially defined, and thus less affected by compression effects. Only the Zizur Mayor area shows a large decrease in the user's accuracy due to the fact that the dense vegetation area is minimal. This implies that at high compression levels this class is homogenized with the surrounding covers. This category was not included in this figure due to its low representation cover.

Figure 11 shows the user's accuracy for the herbaceous class. This cover has important confusion errors with dense vegetation and bare soil covers. When multispectral classification methods are used, it is not difficult to discriminate vegetation from other covers; however, precise discrimination between dense and herbaceous vegetation in unitemporal RGB orthophotos is sometimes not feasible. This confusion implies that there are different accuracy values among different compression levels.

Although this cover mostly includes gardens, some bare soil covered with the first stages of vegetation is also present. This is highly dependent on the photointerpretation because there are differences between the land use and the land cover. The Zizur Mayor area obtained the best accuracy at the first compression ratio because most of the vegetation corresponds to herbaceous. The other areas have lower accuracies for all compression levels due to the difficulty in discriminating this cover (mainly small private gardens) from dense vegetation or bright covers.

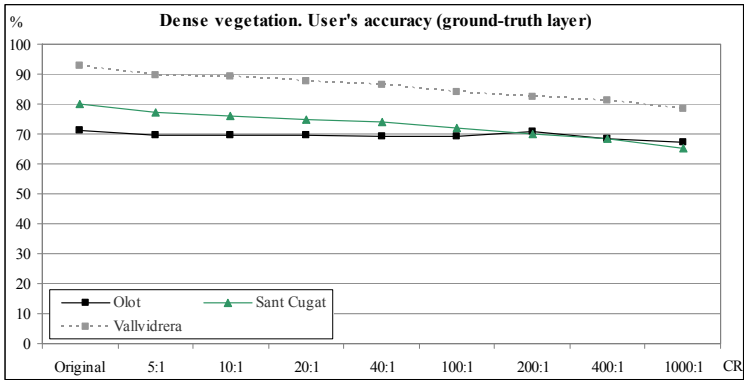

Figure 10: Dense vegetation user's accuracy, obtained in relation to a ground-truth layer (photointerpretation).

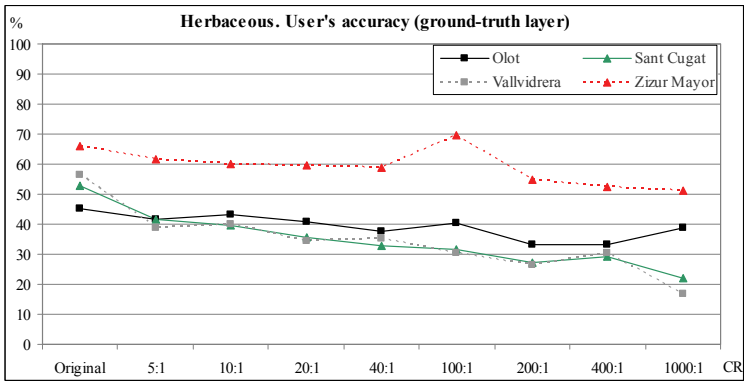

Figure 11: Herbaceous user's accuracy, obtained in relation to a ground-truth layer (photointerpretation).

Building area cover is heavily dependant on the color and type of roof, which increases the confusion with fallow lands and asphalt areas. Better user's accuracies, shown in figure 12, were obtained in the areas with dense edification, such as Olot. The effect of compression on this area is smaller than in other areas. In other areas, the impact of compression is higher (especially if high compression, 100:1 or more is applied) because the heterogeneous landscape is homogenized by compression.

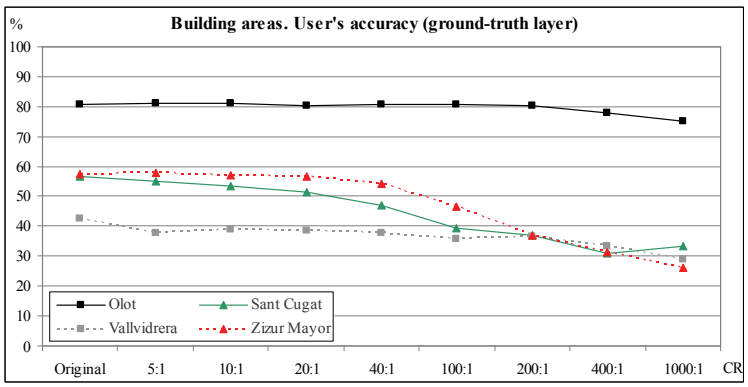

Figure 12: Building area user's accuracy, obtained in relation to a ground-truth layer (photointerpretation).

In the case of road and asphalt areas, as shown in figure 13, better user's accuracies were obtained in the Zizur Mayor area, where there are large roads. The worst results were obtained in other areas (especially Vallvidrera) because there are few large roads and these are located in low density residential zones. In addition, many of the narrow roads are covered by canopy trees.

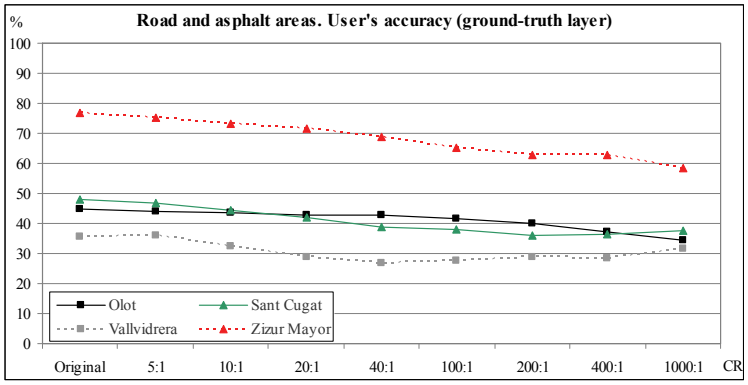

Figure 13: Road and asphalt area user's accuracy, obtained in relation to a ground-truth layer (photointerpretation).

The user's accuracy for swimming pools is shown in figure 14. Unlike the independent test validation method, this cover shows a lot of differences between areas and compression ratios. The small area covered by this cover in the studied areas is the reason for the variation in the accuracy (if there are few pixels in a category, a small variation in the classification implies a high variation in classification accuracy in percentage).

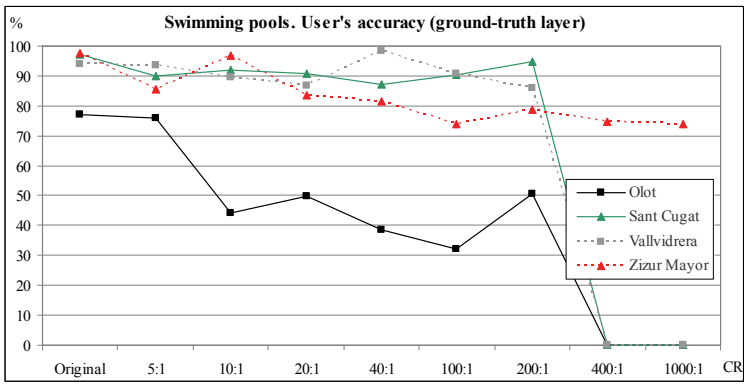

Figure 14: Swimming pool user's accuracy, obtained in relation to a ground-truth layer (photointerpretation).

These five covers are in all four areas, and bare soil and rivers are in some of them. Bare soil was classified in three of the four areas. This cover is often confused with other covers, especially at high compression levels, because of the different types of bare soil (future building, fallow land, etc.). In addition, it is highly dependant on the photointerpretation, as mentioned above. The last class, rivers, was well classified because a topographic map was introduced in the classifier.

3.3.3. Evaluation using independent test areas

A set of independent test areas was also used to obtain the ground truth layer for the evaluation. This is a common approach widely used in evaluation of classifications because it is not very time consuming.

A set of independent test areas (about 100 polygons) was selected by an external operator for each of the four study areas, covering an area between 5 m^2 and 600 m^2.

Figure 15 shows the overall accuracy for each classification and each compression ratio obtained by confusion matrices computed considering the classification results and the independent test areas. The four areas follow the same trend: better overall accuracy was obtained in the non-compressed and the three first compression levels, but if more compression is applied, this value decreases considerably. Moreover, in the Olot and Sant Cugat areas, the best results were obtained in the first compression, which were even better than the process with non-compressed images. This effect is also shown for example in building areas (see figure 16) and has been reported in other cases in which moderate lossy compression can improve the classification results (Choi et al., 2008).

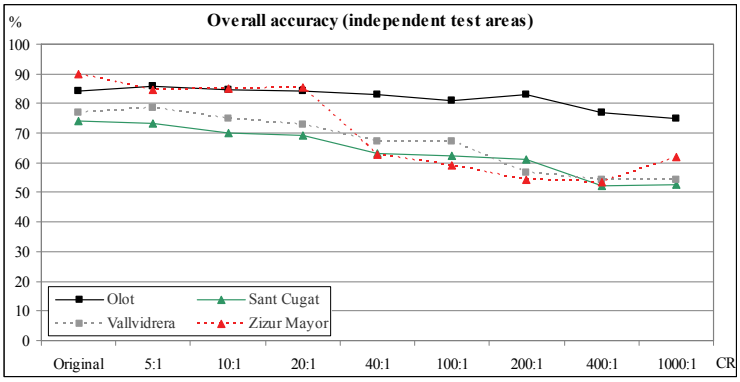

Figure 15: Overall accuracy of each classification area for different compression ratios, obtained in relation to independent test areas.

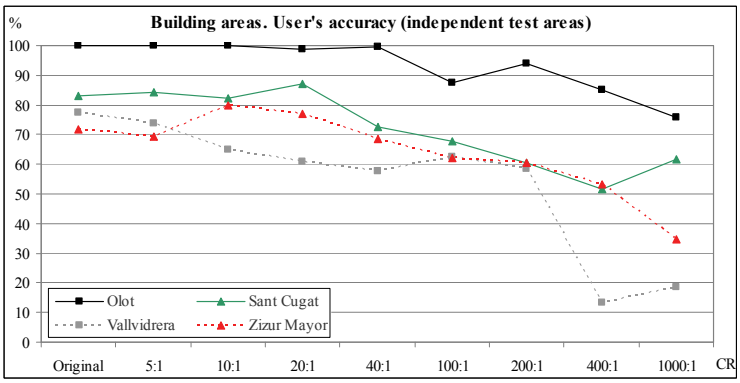

Figure 16: Building area user's accuracy, obtained in relation to independent test areas.

If we focus on the different overall accuracies among areas, Vallvidrera and Sant Cugat have the lowest accuracies. This is because these areas are characterized by single semi-detached and detached houses with private swimming pools surrounded by dense vegetation. This means that they are fragmented areas and high levels of compression tend to homogenize the area, which blurs small objects with the objects surrounding them. The Olot area it is the most homogeneous zone, with well differentiated classes, which means that high compression does not produce significant effects on the classification. Although the Zizur Mayor area is also a homogeneous zone, the large confusion between bare soil and asphalt, white roofs and herbaceous vegetation means that classification with high compression levels obtains low accuracy.

Although pointing to qualitatively similar conclusions, these results are clearly more optimistic quantitatively than those obtained when the analysis uses a ground-truth layer. Assuming that the ground-truth layer is fully representative, this illustrates the importance of selecting the independent areas and outlines the risk of not to succeed when trying to obtain a representative set of test polygons for all the study area. In other words, underestimating or overestimating the accuracy, and therefore obtaining unstable results, is a large risk when the effect of compression on GEOBIA is evaluated.

4. Conclusions

The main conclusion of this study is that at high compression levels, poor accuracies are obtained when image segmentation is applied to obtain categorical maps. Although for all uncompressed images similar overall accuracies were obtained, in more fragmented areas the decrease in accuracy at the first compression level was more significant than in the less fragmented areas. Similar overall accuracies were obtained for classifications for less fragmented areas in the uncompressed and the first three compression levels (up to 20:1), and this decreases more significantly if more compression (40:1 or higher) is applied.

For each cover type, the accuracy depends on the size of this cover in each orthophoto, the objects that surround this cover and the heterogeneity with respect to the other covers. It is important to note that there are also some differences between validation approaches, but the results show that bare soils, buildings,

asphalt and herbaceous categories are more difficult to classify. Dense vegetation obtains user's accuracies above 65 % at all compression levels, except in the case of Zizur Mayor. Finally, swimming pools obtain user's accuracies above 70% at all compression levels, except in the case of Olot, where results are below this from the second compression level on.

With these two validation approaches, we have also proved that using 100 independent test areas to evaluate the classifications results can generate important quantitative discrepancies; therefore, in order to rigorously estimate the effects of compression on GEOBIA, a complete (or at least more complete than 100 test areas) ground truth layer is necessary.

It is important to note that classifying using 3 visible bands and using object-based methods produces acceptably stable results even when lossy compression is applied; however, adding an infrared band could reduce confusion errors among categories and improve discrimination, especially in classes such as bare soil, vegetation and water bodies. Nevertheless, it is also true that currently, most aerial information available does not have these infrared components, especially in older dates.

5. Emergency management applicability

The last aim of this study was to assess if segmentation processes applied to lossy compressed images could be usefully applied to emergency management scenarios. In such situations, a quick response also implies quick analysis, and the time needed to define segmentation and classification variables and parameters makes it impossible to achieve this goal. The research carried out shows that the segmentation and classification processes are not faster for the compressed images than for the original images. Furthermore, with significant compression ratios it is more difficult to define the categories covering the study area. Thus, the only advantage of compressed images would be that they can be transferred faster, but they are not analyzed quicker or better. Therefore, in an emergency environment the best option would be to use lossless or low-compression-ratio lossy compressed images.

Acknowledgements

This work has been partially supported by the Spanish Government, by FEDER, and by the Catalan Government, under Grants TIN2009-14426-C02-02 and SGR2009-1511, and also by the European Commission through the FP7-242390-GEO-PICTURES project (FP7-SPACE-2009-1). The authors would also like to thank their colleagues in the Centre for Ecological Research and Forestry Applications (CREAF), especially Charo Guerro, for their excellent work in the photointerpretation of the studied areas to use the produced maps as ground truth layers.

References

Aulí-Llinàs, F., Bartrina-Rapesta, J.L., Paton-Martín, J.R.., Monteagudo-Pereira, J.L., Serra-Sagristà, J., 2005. "J2K: introducing a novel JPEG 2000 coder", In. *Proc. SPIE*, vol. 5960, 2005, pp. 1763-1773.

Baatz, M., Benz, U., Dehghani, S., Heynen, M., Höltje, A., Hofmann, P., Lingenfelder, I., Mimler, M., Sohlbach, M., Weber, M. and Willhauck, G. (2004) eCognition Professional: User Guide 4, Definiens-Imaging, Munich

Baatz, M., Shäpe, A., 2000. Multiresolution segmentation: an optimization for high quality multi-scale image segmentation. Strobl, J., Blaschke, T., Griesebner, G (Eds.). 2006. *Angewandte Geograsphische Information-Verarbeitung* XII. Wichmann Verlag, Karlsruhe, pp. 12-23.

Blaschke, T., 2010. Object based image analysis for remote sensing. *ISPRS Journal of Photogrametry & Remote Sensing*, 65, pp. 2-16.

Campbell, J.B., 2002. *Introduction to Remote Sensing*, 3rd ed. (Book Review) -. Guilford Press, 2002. ISBN 1-57290-640-8.

Carvajal, G.; B. Penna, E. Magli, 2008, Unified Lossy and Near-Lossless Hyperspectral Image Compression Based on JPEG 2000, *IEEE Geoscience Remote Sensing Letters*, 5, pp. 593-597.

Choi, E., S. Lee, C. Lee (2008). Effects of Compression on the Classification of Hyperspectral Images. In Mastorakis NE; Mladenov V; Bojkovic Z; Simian D; Kartalopoulos S; Varonides A; Udriste C; Kindler E; Narayanan S; Mauri JL; Parsiani H; Man KL (Ed.), *Math. Comput. Sci. Eng.* (pp. 541-546). Greece: Heraklion.

Conchedda, G., Durieux, L., and Mayaux, P., 2008. An object–based method for mapping and change analysis in mangrove ecosystems. *ISPRS Journal of Photogrametry & Remote Sensing*, 63, pp. 578-589.

DMC International Imaging Ltd. 2005-7. Earth observations solutions. http://www.dmcii.com/about_us_constellation.htm (accessed 20.09.10).

Foody, G.M., 2002, Status of land cover classification accuracy assessment, *Remote Sensing of Environment*, 80, pp. 185-201.

ISO/IEC, 2004, 15444-1:2004, Information technology – JPEG 2000 image coding system: Core coding system. Geneva, Switzerland, 2004, 194 pp.

Ke, Y., Quackenbush, L.J., Im, J. 2010. Synergistic use of QuickBird multispectral imagery and LIDAR data for object-based. *Remote Sensing of Environment*. 114, pp. 1141–1154.

Kiema, J.B.K., 2000. Wavelet compression and the automatic classification of Landsat imagery. *Photogrammetric Record*, 16 (96), pp 997-1006.

Kressler, F. P., Franzen, M., and Steinnocher, K., 2005. Segmentation based classification of aerial images and its potential to support the update of existing land use data bases, *Proceeding ISPRS Hannover Workshop 2005, High Resolution Earth Imaging for Geospatial Information,* Heipke C., Jacobsen K., Gerke M. (Eds.), Hannover, Germany.

Magli, E.; D. Taubman, 2003, Image compression practices and standards for geospatial information systems. In Proceedings of the 2003 *IEEE International Geoscience & Remote Sensing Symposium Geoscience and Remote Sensing Symposium (IGARSS'03)*. 1, pp. 654-656.

Maguire, D.J.; P.A. Longley, 2005, The Emergence of Geoportals and Their Role in Spatial Data Infrastructures, *Computers, Environment and Urban Systems*, 29, pp. 3-14.

Masó J, Pomakis K, Julià N., 2010, *OpenGIS® Web Map Tile Service Implementation Standard, v. 1.0.0* Open Geospatial Consortium Inc. Document reference number 07-057r7, Available online at: http://www.opengeospatial.org/standards/wmts (accessed 20 August 2010).

Penna, B; T. Tillo, E. Magli, G. Olmo, 2007, Transform coding techniques for lossy hyperspectral data compression", *IEEE Transactions Geoscience Remote Sensing*, 45, pp. 1408-1421.

Pons, X., 2008, *MiraMon. Geographical Information System and Remote Sensing Software*. Version 7, Available online at: http://www.creaf.uab.cat/miramon/ (accessed 20 September 2010).

Xiaoxia, S., Jixian Z., Zhengjun, L., 2005. A comparison of object-oriented and pixel-based classification approaches using quickbird imagery. *ISPRS STM*, Beijing, pp.281-284.

Zabala, A., Pons, X., Díaz-Delgado, R., García, F., Aulí-Llinàs, F. and Serra-Sagristà, J., 2006. Effects of JPEG and JPEG 2000 Lossy Compression on Remote Sensing Image Classification for Mapping Crops and Forest areas. In Proceedings of the 2006 *IEEE International Geoscience & Remote Sensing Symposium & 27th Canadian Symposium on Remote Sensing (IGARSS2006)*. Denver, Colorado, EE.UU. ISBN: 0-7803-9510-7. pp790-793. 10.1109/IGARSS.2006.203 PDF Document

Zabala, A., Pons, X., Aulí-Llinàs, F., Serra-Sagristà, J., 2007. Implications of JPEG 2000 lossy compression on multiple regression modelling. *Remote Sensing for Environmental Monitoring, GIS Applications, and Geology VII*. Ehlers M, Michel U (ed.). ISBN: 9780819469076 (DOI: 10.1117/12.738028)

Zabala, A; X. Pons, 2010, Effects of lossy compression on remote sensing image classification of forest areas, *International Journal of Applied Earth Observation and Geoinformation* (JAG), doi:10.1016/j.jag.2010.06.005, ISSN: 0303-2434.

Zabala, A; J. González-Conejero, J. Serra-Sagristà, X. Pons, 2010, JPEG2000 encoding of images with NODATA regions for Remote Sensing applications, *Journal of Applied Remote Sensing*, 4 (041793), ISSN: 1931-3195.

ANNEX 3: IMPACT OF CCSDS AND JPEG 2000 ON-BOARD COMPRESSION ON IMAGE QUALITY AND CLASSIFICATION[4]

[4] Segons la normativa de la UAB a què s'acull aquesta Tesi per compendi de publicacions, a part dels articles acceptats per a format la part fonamental de la mateixa (i inclosos en els capítols 2 a 5 d'aquesta Tesi), es pot adjuntar altres articles com a annexos (o part no fonamental). Segons la mateixa normativa, els treballs fets en aquestes publicacions poden ser comentats a la discussió de resultats. Aquest és el darrer article dels tres presentats com a annexos i que pretenen completar l'aportació de la Tesi en el camp dels efectes de la compressió amb pèrdua d'imatges de teledetecció aplicades a l'obtenció de cartografia.

IMPACT OF CCSDS AND JPEG 2000 ON-BOARD COMPRESSION ON IMAGE QUALITY AND CLASSIFICATION

Alaitz Zabala[1,2], Raffaele Vitulli[2], Riccardo Duca[2], Fabrizio Ramoino[2] and Xavier Pons[1,3]

[1] Geography Department, Autonomous University of Barcelona.
Despatx B9-1092, Facultat de Filosofia i Lletres, Edifici B, Universitat Autònoma de Barcelona.
08193, Cerdanyola del Vallès, Barcelona, Spain.
Email: alaitz.zabala@uab.cat, xavier.pons@uab.cat

[2] European Space Agency
European Space Agency, ESTEC, Noordwijk, The Netherlands
Email: Raffaele.Vitulli@esa.int, Riccardo.Duca@esa.int, Fabrizio.Ramoino@esa.int

[3] Centre de Recerca Ecològica i Aplicacions Forestals (CREAF)
CREAF, Edifici C, Universitat Autònoma de Barcelona.
08193, Cerdanyola del Vallès, Barcelona, Spain.

Abstract: This study measures the impact of lossy on-board image compression (CCSDS and JPEG 2000) on image quality and classification. The Sentinel-2 Image Performance Simulator (developed to assess mission requirements) is modified to allow these compression algorithms and used to produce Sentinel-2 simulated images using on-board lossy compression. The performance of several compressors is evaluated using PSNR computation of compressed images (regarding to simulated image without compression) and also evaluated computing the overall accuracy of land-cover classifications over two of these images. From the compression point of view is worth to mention that two strategies has been used to share compression ratio among bands. The first one uses the same aimed compression ratio for all the bands. The second one applies more compression on 10 m bands and less compression on 20 m and 60 m bands, in order to obtain the same aimed compression ratio. Results show that CCSDS performs better than JPEG 2000 in terms of compression fidelity especially at lower compression ratios (from CR 2:1 up to CR 4:1). On the other hand, and regarding to the effect of this compression of a land cover classification, it mainly follows the previous tendencies. But it still have to be kept in mind than compression fidelity may not be enough to asses the impact of compression on end-user applications. Differences among compression algorithms and compression ratio distributions are lower than in compression fidelity.

INTRODUCTION

The recent trend in Remote Sensing satellites is characterized by an increase of resolution (spatial, spectral and temporal) of the new satellite sensors. This improve on the sensors is highly appreciated by remote sensing users who can easily exploit these big amount of data. Unfortunately, this increase has to be kept inside the downlink capacity of the mission, or apply on-board compression instead. Lossless compression has been applied but also lossy compression is being considered as a possible solution when lossless compression is not enough.

The main aim of this study is to assess the usability of CCSDS, JPEG 2000 and the embedded CNES compressors to be applied on-board. The assessment will consider both the compression fidelity and an applied approach regarding the effect of this compression on a user final application such as image classification.

METHODS AND SCENES USED

Overview of the Sentinel-2 Mission and the Sentinel-2 Image Performance Simulator

To be able to assess the effect of a possible on-board image compression, we can profit the instruments simulators developed to assess mission requirements. The Sentinel-2 optical mission [1] is part of the Global Monitoring for Environment and Security (GMES) system, which is a joint initiative of the European Commission (EC) and the European Space Agency (ESA), designed to establish a European capacity for the provision and use of operational monitoring information for environment and security applications. Sentinel-2 polar-orbiting satellites will provide systematic global acquisitions of high-resolution multispectral imagery with a high revisit frequency. The optical payload, the MSI (Multi Spectral Imager), which acquires scenes at three simultaneous resolution (10 m, 20 m and 60 m) in the VNIR and SWIR ranges over a wide swath around 290 km.

The Sentinel-2 Image Performance Simulator [2] has been developed by EADS Astrium. It produces simulated Sentinel-2 images starting from hyperspectral images with an adequate spectral configuration (covering all bands of MSI instrument) which pixels represent bottom of atmosphere's reflectance. The simulator had the feature of simulate Sentinel-2 images using on-board compression at several compression ratios. The simulator had an internal compressor developed by CNES. The simulator is written in IDL, and has a graphical interface where the user can define all the parameters of the scenario. It can be compiled and executed from inside IDL.

The compression and decompression during the image simulation is performed calling to external executables from the IDL routine to perform the steps of both processes. As our main concern is to compute the performance of the CNES, CCSDS and JPEG 2000 compressors when used on-board, the simulator is modified to allow the user using among these three choices. The same compression algorithm is applied to all simulated bands.

Compression

The Image Data Compression (IDC) recommendation (CCSDS 122.0-B-1 [3]) is a lossy compression standard defined by the Consultative Committee for Space Data Systems (CCSDS) specially designed for use on-board a space platform, since this standard has sought a balance between the complexity of the algorithm and its performance, so it can be more easily implemented by hardware or software. However, it is necessary to consider also the highly extended JPEG 2000 compression standard [4], because its broadly use in remote sensing and GIS community, even though its computational requirements is bigger and the usability of this standard has to be carefully asses in an on-board application.

The ESA CCSDS compression implementation·[5] is used to compress the images using CCSDS standard. The ESA implementation has two main applications: the WhiteDwarf (GUI application to compress and decompress images) and the imageComp executable to be used on command line calls. This executable is used on the simulator. The ESA CCSDS compression implementation does not have a command line application to decompress the images. Thus, the University of Nebraska-Lincoln implementation [6] is used for decompression. In fact this code is the same embedded on whiteDwarf for decompression. The JPEG 2000 compression implementation of Autonomous University of Barcelona (GICI group) [7], called BOÍ, is used to compress and decompressed images using JPEG 2000 standard. The Java executable files BOICode.jar and BOIDecode.jar are used for compression and decompression. Moreover, the CNES internal compressor (a non-standard compression algorithm, included in the original Sentinel-2 Image Performance Simulator) is used to compare its results to those obtained with previous standardized options.

Scenes: CEFLES-2 Campaign

CEFLES2 (CarboEurope, FLEX and Sentinel-2) was conceived as a collective multi-objective campaign exploiting synergies between the three experiments to be collocated in the Les Landes region of France during the period April to September 2007 [8]. It focused on various landscape types, including urban, agricultural, water and forested areas. That campaign is mainly based on optical airborne and satellite acquisitions and this dataset has been completed with several on-ground observations and measurement. The airborne hyperspectral acquisitions have been considered as main input for the simulation phase, giving continuity to the similar activity already done with the Agrisar campaign. The Airborne Hyperspectral Scanner (AHS) is an 80-bands airborne imaging radiometer, developed and built by SensyTech Inc. (currently Argon ST, and formerly Daedalus Ent. Inc.) and is operated by the Spanish Institute for Aerospace Technology (INTA) in different remote sensing projects. It has 63 bands in the reflective part of the electromagnetic spectrum, 7 bands in the 3 to 5 microns range and 10 bands in the 8 to 13 microns region.

The study uses four AHS images coming from the third mission of the CEFLES campaign (September 2007), covering areas with different landscape (urban, crops, forest and mixed area. Les Landes is characterized by an agricultural environment with different crops and fields located around very small urban centres. Two images of this area are selected, the first one covering a trees crop area (P01BS) and the second one covering a non-trees crop area (P01BS) for which available ground truth is available. Images over Toulouse have been sensed over very urbanized parts, including also outskirts principally characterized by the presence of asphalted areas and industrial zones, and also a forested area (F01BS). On the urban selected area (T01BS) ground truth can be digitized by means of photo-interpretation.

The co-registration is the first operation to do over the AHS images contained in the CEFLES-2 Campaign Database. The ortho-rectification of all images has been done by IDL-ENVI using as base the .BSQ files provided with the CEFLES-2 Campaign Dataset. The Cubic Convolution method with a re-sampling kernel size 3x3 has been used. During the ortho-rectification, the proposed rotation angle is maintained to obtain smaller files, minimize radiometric variations due to interpolation and obtain images with less NODATA areas. After the geometric correction several

NODATA areas arise on the edges of the images. These areas need to be removed (to prevent them to affect the simulation process) by means of a resize of the geometrically corrected image.

Sentinel-2 Simulation Adjustments

To obtain the simulated Sentinel-2 images for each of the four scenes used, several parameters on the Sentinel-2 Image Performance Simulator have to be adjusted. Most of the parameters on the simulator remain constant to their best option on the whole set of tests, but they have to be correctly defined or optimized. The parameters to be adjusted are included in the next sections: Observation parameters (geographical and temporal parameters of the test image along the orbit and within the swath), Atmosphere parameters (atmospheric conditions independent of the observation parameters), Instrument parameters (optical parameters, detector parameters and scanning geometry) and Ground segment (calibration) parameters (typical residual errors to be expected from level 1a to level 1c data processing).

On instrument parameters section you can also define the bands to be simulated, their main characteristics (centre wavelength, wavelength wide, Modulation Transfer Function –MTF– and pixel size –or GSD: ground sampling distance–) as well as whether to apply lossless or lossy compression and at which compression ratio (for lossy compression). The selected bands are the 13 bands defined on Sentinel-2 Mission Requirement Document [1].

Two strategies have been used to distribute compression ratio (defined for each band) among bands. The first one uses the same aimed compression ratio (CR) for all the bands. The second one applies more compression on 10 m bands and less compression on 20 m and 60 m bands, in order to obtain the same aimed compression ratio. The proportion of compression ratio applied to each band follows the proportion usually used on Earth Observation scenarios of CR 4.0 for 10 m bands and CR 2.2 for other bands. Taking into account these values and the spatial and spectral configuration of Sentinel-2, a proportion is set to 0.67761194 and 1.23202171 of the desired CR to be applied to 20-60 m and 10 m bands respectively. The compression ratio applied to each band at several compression ratios is shown on Table 1. First CRs are those studied for Sentinel-2 mission and CR 10 and 20 are out of scope for Sentinel-2 but are also chosen to see results over classification. For these higher compression ratios only the equally distributed CR is selected because they are out of the scope for on-board Earth Observation missions and, then, the previous rule does not need to be applied.

Performance of Simulated images

The performance of several compressors and compression ratios is evaluated using noise evaluation and a final application assessment. On one hand, PSNR of compressed images (regarding to simulated image without compression) is computed and, on the other hand, the overall accuracy of land-cover classifications over two of these images is used.

Noise evaluation method

To evaluate compression noise, L1B bands simulated using both compression and instrument noises are compared to those L1B bands simulated with instrument noise but without compression (for each scene). Gcomp application (developed by GICI group of the Autonomous University of Barcelona) is used to compute PSNR.

Classification method and evaluation method

After image simulation and before image classification, some processing needs to be done. Simulated bands to be used on the classification (10 m and 20 m bands for “Les Landes - P03BS” and “Toulouse - Urban - T01BS” scenes) need to be registered to desired projection system, they need to be stacked on one file and finally they are used to perform classification on them. All these processes are included in an IDL routine to easily apply them to each of the desired scenario (different scenes, compression ratios and compression algorithms).

Table 1. Compression ratios and distribution among bands: two approaches are used.

Aimed CR	2	2.39	3	3.25	4	4.79	5	10	20
10 m unequally.	2.46404	2.94453	3.69607	4	4.92809	5.90138	6.16011	-	-
20-60 m unequally.	1.35522	1.61949	2.03284	2.2	2.71045	3.24576	3.38806	-	-
10 m equally	2	2.39	3	3.25	4	4.79	5	10	20
20-60 m equally	2	2.39	3	3.25	4	4.79	5	10	20

Simulated images have to be registered to the desired reference system to combine them with ground-truth georeferenced information. Ground control points (GCP) are defined on each set of images (10 m and 20 m) and MiraMon software [9] was used to perform georegistration of all the bands. This registration can be embedded inside IDL routine using MiraMon batch processing tools. For each scenario, four bands have a 10 m pixel size and six have 20 m pixel size. All the bands need to have the same pixel size and be part of a single BSQ file to be classified using ENVI routines. ENVI Layer Stacking basic tool (inside the IDL routine) is used to create a single BSQ file with all bands at 20 m pixel size, with a cubic convolution resampling method.

Training and test areas are needed to execute the supervised classification and to evaluate it. For "Les Landes - P03BS" scene, on CEFLES campaign there was information available (not in a GIS format but still) of crops on the area. Using this information, the whole set of ground truth information was manually digitized over the AHS original image. 165 polygons were digitized as ground truth, covering a total area of 218 ha (more than 10% of the area covered by the image). Aimed legend for this area includes: corn, trees, plastic foils, wheat, wild grass, fruit trees, beans, wheat mixture, water and bare soil. On the other hand, for "Toulouse - Urban - T01BS" scene, any ground truth information was available. Thus, a general classification was intended, by manually digitizing the categories to be classified over the original AHS image. 165 polygons were digitized as ground truth, covering a total area of 135 ha (about 4% of the area covered by the image). Aimed legend for Tolouse scene covers: water, trees, gardens, soil, agricultural fields, asphalt and buildings. The ground-truth information (of each scene) was randomly split on two sets, one to train the classifier and the other to make and independent evaluation test. This split was done in a way that approximately 70% of ground truth was used to train and remaining 30% to test the classification.

Supervised classification is an automatic process that based on each pixel characterization (i.e. its value on all the bands) and on some train pixels (for which preferred class is known), assigns the pixels of the image to one of the predefined classes or, if a threshold is used, to a new "unclassified" category. Among supervised classification techniques (such as Parallelepiped, Minimum Distance, Mahalanobis Distance, Maximum Likelihood, Spectral Angle Mapper (SAM), Binary Encoding, etc.), one of the most used ones is the Maximum Likelihood method. Maximum likelihood classification assumes that the statistics for each class in each band are normally distributed and calculates the probability that a given pixel belongs to a specific class. Unless you select a probability threshold, all pixels are classified. Each pixel is assigned to the class that has the highest probability (i.e., the maximum likelihood). For technical details, refer to a remote sensing manual (for example [10]). The supervised classification methods in ENVI differentiate masked pixels from unclassified pixels. Masked pixels do not have the classification algorithm applied because they are already masked out. If a mask band is chosen upon input, ENVI creates a class called Masked Pixels. In our processing routine, a mask is created and used to avoid the classification of surrounding areas with a value of 0 (that appear due to image registration).

Obtained classifications (from images with or without compression) are evaluated using the confusion matrix ([11]) based on ground-truth test areas. Moreover, confusion matrix is also obtained using the classification over non compressed images as ground truth (instead of test areas). By computing this contingency matrix several parameters are obtained: an overall accuracy, producer and user accuracies, kappa coefficient, confusion matrix, and errors of commission and omission are reported.

RESULTS

Noise evaluation results

Compression noise is assessed computing PSNR between L1B bands simulated with lossy compression with L1B bands simulated with lossless compression (both using instrument noise). Several compression ratios are studied and two approaches to distribute it among bands.

Only some values are available for the CNES compressor. This is why results are presented in two different sets. First of all, Fig. 1 and Table 2 show the mean PSNR obtained by all the bands of each simulated images using CCSDS and JPEG 2000 compression at several compression ratios. On the figure (showing compression ratios up to CR 5), line colour indicates the compression algorithm (red or orange for CCSDS and blue for JPEG 2000) while line style depicts unequally or equally distribution of CR among bands (continuous and dashed respectively). The table shows results for the higher studied compression ratios (CR 5 to 20). CR 5 appears both in the figure and the table to easily relate them.
Results regarding CCSDS and JPEG 2000 compressors clearly indicate that CCSDS performs better than JPEG 2000 at lower compression ratios (up to CR 5:1, see Fig. 1). JPEG 2000 overcomes CCSDS if higher CRs are used (10 or 20,

see Table 2). This tendency is found both in scenarios with unequally and equally CR distribution among bands. Regarding comparison of the two approaches of CR distribution among bands, unequally distributed scenarios clearly obtain higher all-band mean PSNR. To quantify the CCSDS improvement, the PSNR difference between the two compression standards is shown in for the four scenes and the two CR distribution approaches.

It is difficult to compare CNES compressor to CCSDS and JPEG 2000 because only some values for the mean of all bands are available for CNES scenarios. Thus, the presented comparison is based on 10 m bands, which are the subset of bands with more available CNES results. PSNR of 10 m bands for all compression algorithms is presented in Fig. 2. As expected, in this case equally distribution of CR obtains better results because it implies less compression applied to these bands (*i.e.* for CR 2 when unequally distributed CR is used, actual CR applied to 10 m bands is 2.464, see Table 1). Regarding CNES compression it obtains in most of the cases lower compression fidelity than both of the other compression standards. Moreover, as this is not a standardized algorithm, its use should be avoided on-board.

Another interesting thing to mention is that depending on the compression standard and ratio applied, results are the same up to medium compression. Table 3 shows the PSNR results for "Toulouse - Urban - T01BS" scene for each band at all compression ratios when CCSDS and JPEG 2000 using unequally distributed CR are applied. When unequally distributed compression is applied, 20-60 m bands are less compressed and thus, it is expected that higher PSNR are obtained. Band 1 (60 m) can be compressed up to CR 2.710 (mean CR 4, see Table 1) with the same PSNR. This is due to that the whole compressed bit stream is using fewer bits than needed to achieve this compression ratio. This tendency is also observed in band 9 (60 m) and, with less cases, with 20 m bands. This is easily explained taking into account both the spatial resolution and the dynamic range of the original images to compressed (L0 bands). The number of scenarios with the same PSNR (grey shadowed) can be explained taking into account spatial size and dynamic range of each band (the larger pixel size or lower dynamic range, the more compression ratios with the same PSNR). It is interesting to mention that this order is also related to the difference between JPEG 2000 and CCCSD PSNR values. Thus, for the same spatial resolution, the higher the dynamic range is, the lower the difference between the two compression standards (as can be seen looking at the last column of the table).

Table 2. PSNR regarding compression ratio (CR) of CCSDS and JPEG 2000 for all scenes at high compression ratios. At such compression ratios only equally distributed CR among bands is studied.

	P01BS		P03BS		F01BS		T01BS	
CR	CCSDS	JPEG 2000	CCSDS	JPEG 2000	CCSDS	JPEG 2000	CCSDS	JPEG 2000
5	91.8644	92.9457	91.6408	93.4645	90.9775	92.6525	88.32	90.48
10	86.308	87.9672	85.7116	88.5405	84.7609	87.6026	81.8719	84.538
20	83.0789	85.4968	81.7035	85.6847	80.8974	84.2873	78.3234	80.5292

Table 3. PSNR results for "Toulouse - Urban - T01BS" scene for each band at lower compression ratios when CCSDS and JPEG 2000 using unequally distributed CR are applied. Blue color depicts 10 m bands (those with higher CR applied), and gray shadowing depicts bands at several compression ratios obtaining the same PSNR value.

	CR 10m/other	B1	B2	B3	B4	B5	B6	B7	B8	B8a	B9	B11	B12
CCSDS	2.464/1.355	104.61	108.06	102.54	99.568	108.21	110.85	110.88	103.21	112.74	103.25	109.58	107.48
	2.945/1.619	104.61	103.40	98.233	95.259	108.21	110.85	110.88	98.834	112.74	103.25	109.58	107.48
	3.696/2.033	104.61	98.621	93.526	90.375	108.21	107.85	107.50	93.995	108.05	103.25	102.56	101.89
	4.004/2.202	104.61	97.340	92.022	89.003	104.28	105.13	105.00	92.829	106.30	103.25	99.978	99.042
	4.928/2.710	104.61	94.450	89.079	86.174	98.710	99.802	99.796	89.784	100.51	97.629	94.289	93.282
	CR 10m/other	B1	B2	B3	B4	B5	B6	B7	B8	B8a	B9	B11	B12
JPEG2000	2.464/1.355	97.144	102.91	99.395	97.604	100.90	103.68	103.82	101.86	105.54	96.288	102.64	100.43
	2.945/1.619	97.144	101.09	96.941	95.015	100.90	103.68	103.82	98.985	105.54	96.288	102.64	100.43
	3.696/2.033	97.144	98.354	93.546	91.042	100.90	102.64	102.69	95.270	103.96	96.288	99.258	97.848
	4.004/2.202	97.144	97.063	92.440	89.644	99.727	101.40	101.53	93.678	103.07	96.288	97.917	96.230
	4.928/2.710	97.144	94.820	89.402	86.987	96.956	98.451	98.527	91.294	99.553	94.194	93.594	92.273

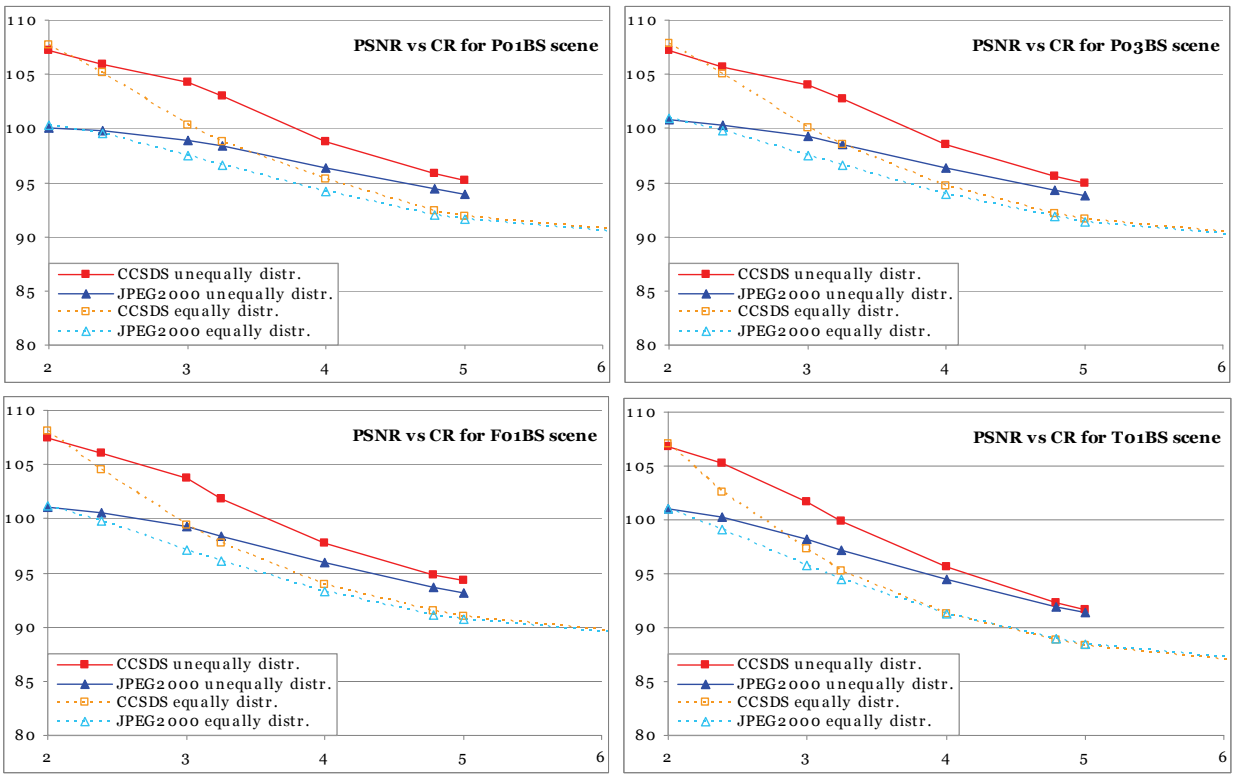

Fig. 1. PSNR regarding compression ratio (CR) of CCSDS and JPEG 2000 for all scenes at low compression ratios. Two strategies are used to split CR among bands (at each compression ratio): unequally or equally distributed.

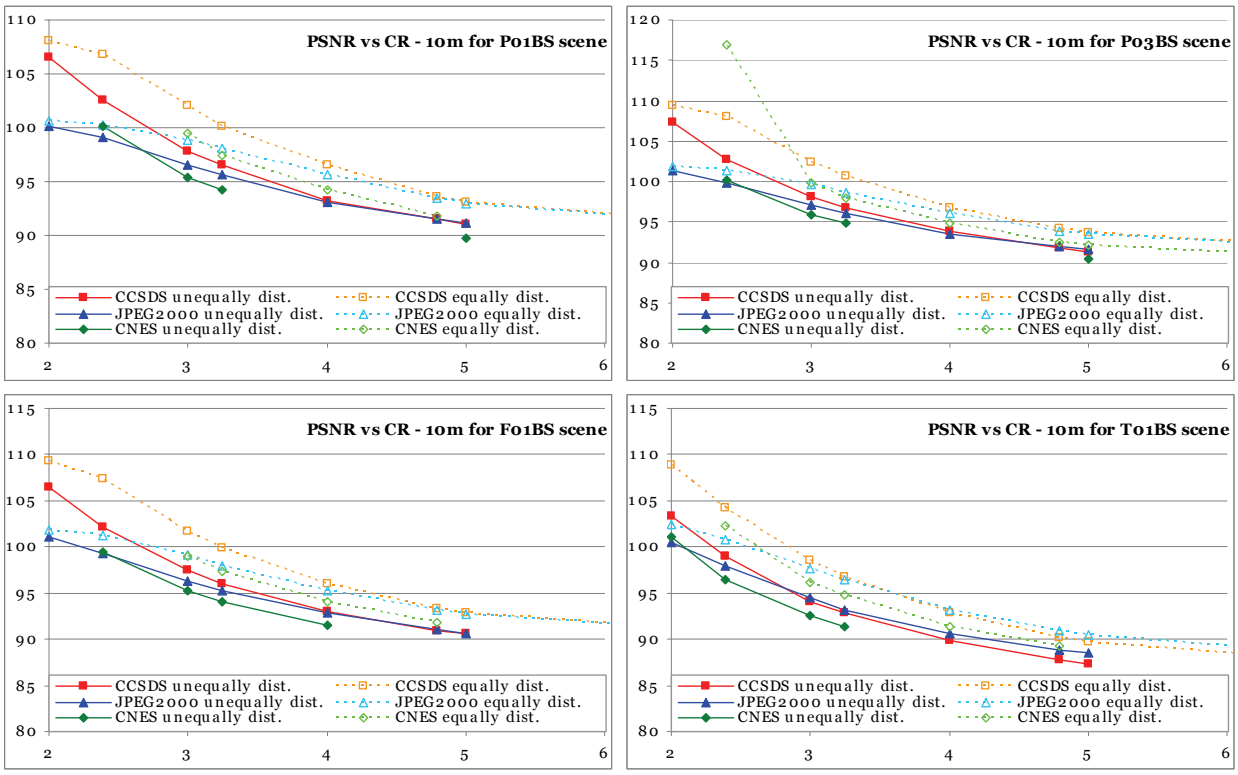

Fig. 2. PSNR of 10 m bands regarding compression ratio (CR) of all the compression algorithms for all scenes at low compression ratios. Two strategies are used to split CR among bands (at each compression ratio): unequally or equally distributed.

Classification results

"Les Landes - P03BS" and "Toulouse - Urban - T01BS" scenes have been used to assess the impact of on-board compression on image classification. To evaluate each classification the overall accurracy of each classification is computed using a confusion matrix using independent ground-truth areas. Only CCSDS and JPEG 2000 standards have been studied because CNES compressors have only a very few scenarios with results available.

Results of the two scenes (see Fig. 3, upper graphics) are quite different and the tendencies are not always in line with previous PSNR results. This is interesting because remembers us the need to use applied approaches, and not only noise or fidelity approaches to evaluate the impact of on-board compression on end-uses of the images.

On one hand, for "Les Landes - P03BS" scene, JPEG 2000 impact on overall accuracy is less important than CCSDS. Moreover, and at low compression ratios, equally distribution of CR among bands give similar or even better results than unequally distribution of CR. These tendencies are contrary to those obtained with PSNR estimations. On the other hand, for "Toulouse - Urban - T01BS" scene tendencies show that CCSDS improves JPEG 2000 results and that unequally distributed CR is better from the applied approach as well. The reason of the diferent behaviour of "Les Landes" scene may be the ease classification of test areas that produce lower variations on overall accuracy regarding CR distribution or compression algorithm.

To deep in this question another aproach to asses the classsification is carried out. Is also a comon practice to consider classification over non compressed images as ground-truth, instead of using independent test areas. A confusion matrix can be also computed in this case to obtain the overall accuracy regarding original classification. Results are presented in Fig. 3 (lower graphics). Using this approach, both areas have the same behaviour than the observed before, *i.e.* unequally distributed areas preserves more valuable information for the classification, obtaining higher overall accuraccy. From this point of view, differences between the two compression standard are small but sligtlhy better for CCSDS.

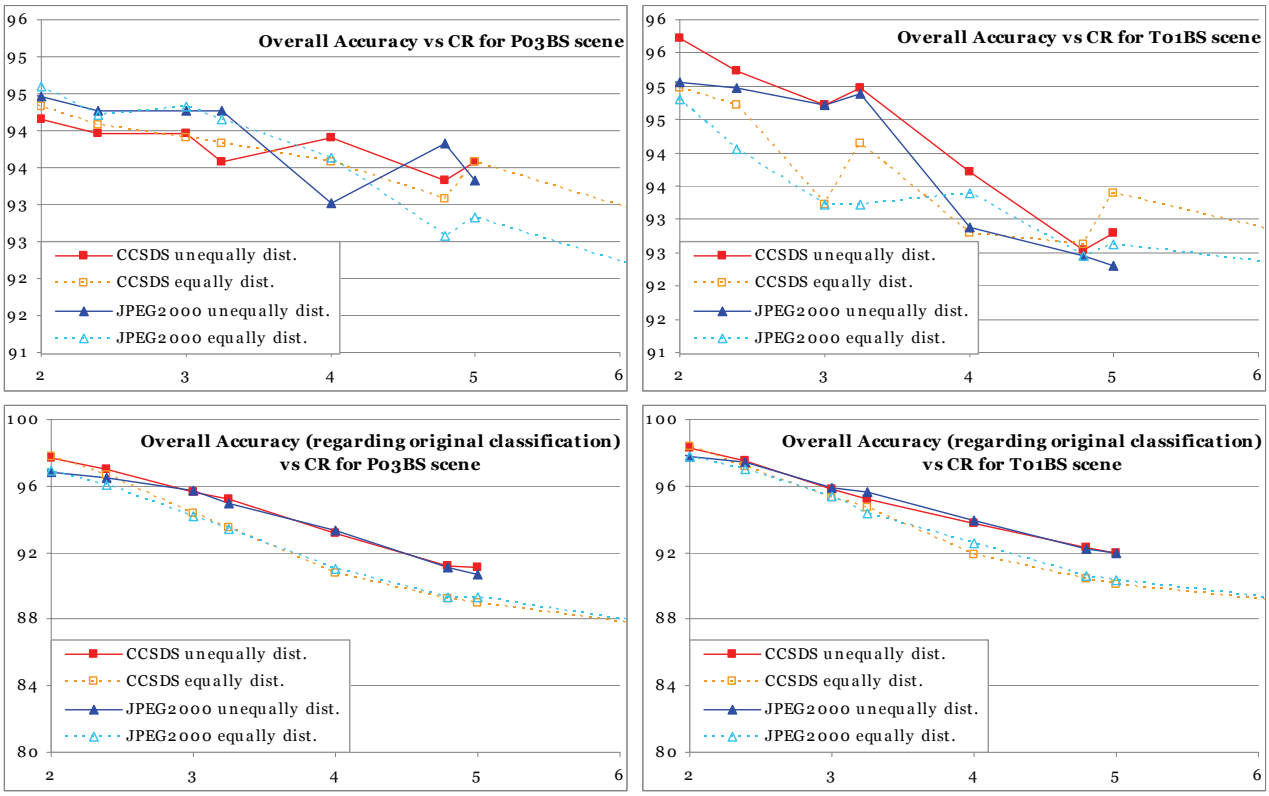

Fig. 3. Overall accuracy of classifications regarding compression ratio (CR) of CCSDS and JPEG 2000 compression standards for "Les Landes - P03BS" and "Toulouse - Urban - T01BS" scenes. As ground-truth, upper graphics use independent test areas while lower graphics use classification obtained without compression.

CONCLUSIONS

Regarding the impact of on-board compression using the Sentinel-2 Image Performance Simulator and testing CNES, CCSDS and JPEG 2000 compressors it can be concluded that CCSDS obtains higher compression fidelity than JPEG 2000 at lower compression ratios (up to CR 5:1). This improvement is up 7.15 or 7.46 dB in the best case ("Les Landes - P03BS" scene compressed at CR 2:1 with unequally or equally CR distribution respectively). On the other hand, at higher compression ratios (out of scope for Earth Observation on-board missions), JPEG 2000 overcomes CCSDS. It is also interesting to take into account that the higher the dynamic range is, the lower the difference between the two compression standards. Using a unequal distribution of CR among bands (for example 4.0 for 10 m bands and 2.2 for 20-60 m bands) improves the global obtained compression fidelity (using any of the compression algorithms used). CNES compressor obtains in most of the cases lower compression fidelity than both of the other compression standards. Moreover, taking into account that it is not a standardized algorithm, its use should be avoided for on Earth Observation on-board missions. In most of the cases the impact of compression on image classification follows the previous tendencies. But it still have to be kept in mind than compression fidelity may not be enough to asses the impact of compression on end-user applications. Differences among compression algorithms and compression ratio distributions are lower than in compression fidelity.

ACKNOWLEDGEMENTS

The authors wish to thank to Sentinel-2 team at ESA-ESTEC and to EADS Astrium who provide and allow us using and extending Sentinel-2 Image Performance Simulator which is the pillar of this paper. The authors would also like to thank their colleagues at the Department of Information and Communications Engineering (Autonomous University of Barcelona, UAB) who helped with compression, decompression and metric computation tools. On the other hand, this work was supported in part by the Ministry of Education and Science and the FEDER funds through the research project TIN2009-14426-C02-02, as well as by the Commission for Universities and Research (CUR) at the Department of Innovation, Universities and Enterprise (DIUE) of the Catalan Government (SGR2009-1511 and BE2009-2-00426).

REFERENCES

[1] Sentinel-2 team, *GMES Sentinel-2 Mission Requirements Document*, EOP-SM/1163/MR-dr, Issue 2 Rev. 1, 08/03/2010. [Online]. Available: http://esamultimedia.esa.int/docs/GMES/Sentinel-2_MRD.pdf.

[2] Sentinel-2 team, *GMES Sentinel-2 Image Performance Simulator Description*, S2-TN-ASG-SY-2002, Issue 1 Rev. 1, 09/02/2007. [ESA confidential].

[3] *Image Data Compression*, Nov. 2005. ser. Blue Book, CCSDS 122.0-B-1. [Online]. Available: http://public.ccsds.org/publications/archive/122x0b1c2.pdf.

[4] ISO/IEC (2004). 15444-1:2004: Information technology – JPEG 2000 image coding system: Core coding system. Geneva, Switzerland, 2004, 194 pp.

[5] M. Cabral, *WhiteDwarf compression tester user's manual*, European Space Agency, TEC-EDP, 3/12/2009.

[6] H. Wang, *An implementation of CCSDS 122.0-B-1 Recommended Standard*, 18/03/2008. Software download and more information in: http://hyperspectral.unl.edu/.

[7] GICI group, *BOI user manual*, Department Group on Interactive Coding of Images (GICI) at the Autonomous University of Barcelona (UAB), Sept. 2005. Software download and more information in: http://www.gici.uab.cat/BOI/.

[8] CEFLES team, *CEFLES2 Final Report (Contract nº: 20801/07/I-LG and 20802/07/I-LG)*. 12/06/2009. More information in: http://www.fz-juelich.de/icg/icg-3/cefles, final report in: http://earth.esa.int/campaigns/index.htm.

[9] Pons, X., 2008, *MiraMon. Geographical Information System and Remote Sensing Software*. Version 6, Available online at: http://www.creaf.uab.es/miramon/ (accessed 20 August 2010).

[10] J.A.Richards, 1999, *Remote Sensing Digital Image Analysis*, Springer-Verlag, Berlin, p. 240.

[11] G.M. Foody, "Status of land cover classification accuracy assessment", *Remote Sens. Environ.*, vol. 80(1), pp. 185-201, April 2002.